APPENDIX B

TIME TRENDS ANALYSIS (MOUNTAIN-WHISPER-LIGHT, 2002)

Time Trends in PCB Concentrations in Sediment and Fish

Lower Fox River and Green Bay, Wisconsin

Prepared by:

The Mountain-Whisper-Light Statistical Consulting
1827 – 23rd Avenue E.
Seattle, Washington 98112

and

The RETEC Group, Inc.
1011 S.W. Klickitat Way, Suite #207
Seattle, Washington 98134

RETEC Project No.: WISCN-14414-215

Prepared for:

Wisconsin Department of Natural Resources
101 S. Webster Street
Madison, Wisconsin 53707

December 2002

Time Trends in PCB Concentrations in Sediment and Fish

Lower Fox River and Green Bay, Wisconsin

Prepared by:

The Mountain-Whisper-Light Statistical Consulting
1827 – 23rd Avenue E.
Seattle, Washington 98112

and

The RETEC Group, Inc.
1011 S.W. Klickitat Way, Suite #207
Seattle, Washington 98134

RETEC Project No.: WISCN-14414-215

Prepared for:

Wisconsin Department of Natural Resources
101 S. Webster Street
Madison, Wisconsin 53707

Prepared by:

Nayak L. Polissar, Ph.D., The Mountain-Whisper-Light Statistical Consulting
Steven McKinney, Ph.D., The Mountain-Whisper-Light Statistical Consulting
Kevin Cain, Ph.D., The Mountain-Whisper-Light Statistical Consulting
Thomas Lumley, Ph.D., The Mountain-Whisper-Light Statistical Consulting
Paul Sampson, Ph.D., The Mountain-Whisper-Light Statistical Consulting
Shiquan Liao, Ph.D., The Mountain-Whisper-Light Statistical Consulting

Technical Review by:

Alessandro Battaglia, The RETEC Group, Inc.
David Morgan, The RETEC Group, Inc.
Paul Putzier, The RETEC Group, Inc.
Timothy A. Thompson, The RETEC Group, Inc.

December 2002

Executive Summary

Introduction

PCBs were introduced into the Fox River, Wisconsin, from the manufacture and recycling of carbonless, multi-copy paper. PCBs were deposited in river sediments and were also passed along the food chain to fish and other wildlife. The fate of the PCBs is an important issue. This report presents rates of change of PCB concentrations in sediment and fish over time.

Methods

Sediment

Sediment samples were grouped into 23 newly designated geographic deposits that were spatially relatively compact within each river reach (see Figure 5 through Figure 8). Depth strata within each deposit were defined consistent with earlier studies: 0 to 10, 10 to 30, 30 to 50, 50 to 100, and 100+ cm. A total of 1,618 observations in 46 combinations of deposit and depth were included in the sediment time trends analysis. PCBs were analyzed as the logarithm of PCB concentration (in ppb) due to the approximately lognormal distribution of these values.

Samples were determined to be spatially correlated, and a method was used which spatially clusters observations into groups that are then approximately independent, and the statistical significance of time trends can be appropriately calculated (Lumley and Heagerty, 1999; Heagerty and Lumley, 2000).

Regression models for log PCB concentration in sediment versus time, depth, and spatial coordinates were fitted using the method of maximum likelihood, which readily incorporates the observations below detection limit. A meta-analysis was performed to yield an average time trend of PCB concentrations in surface deposits (0 to 10 cm) in each reach.

Fish

There were 19 combinations of reach, species, and sample type (whole body or fillet with skin) that had a sufficient sample size and a sufficient time spread for analysis of time trends. These 19 combinations included 867 samples. Carp and walleye provided the largest number of observations of any species.

Regression models for log PCB concentrations versus time were fitted using the logarithm of percent lipid content and time as independent variables. A linear spline function was included in some time trends analyses to accommodate a "breakpoint" and different rates of change in PCB concentrations during earlier versus later periods. The maximum likelihood method was used to accommodate observations below detection limit.

The differences in fish PCB concentrations between De Pere to Green Bay Reach and Green Bay Zone 2 were analyzed using cross-sectional data (1989–1991, five analyses) and data over time (1989–1998, four time trends analyses).

Results and Conclusions

Concentrations of PCBs in fish tissue and surface sediments have generally declined following the elimination of PCB point source discharges. However, there are statistically significant breakpoints in the decline for most of the fish species examined, suggesting that the decline has slowed down or, in some cases, that tissue concentrations of PCBs have increased. The time trends appear to be quite changeable and confidence intervals for rates are quite wide so that it is not possible to project PCB concentrations into the future for fish or sediment with much confidence.

Data on PCBs in surface sediment samples suggest that PCB concentrations have generally declined over time. Trends in concentrations of PCBs in subsurface sediments are mixed—some deposits show declining trends, while others show trends either close to zero or not significantly different from zero and yet others show increasing trends.

Specific conclusions of the time trends analysis include:

- **Fish tissue concentrations have generally declined over the period of time for which there are data in the Lower Fox River and Green Bay Zone 2.** Fish tissue PCB concentrations generally showed a slow rate of decline throughout the Lower Fox River and Green Bay Zone 2. Most time trend slopes were negative, and all statistically significant slopes for the most recent period were negative except one.

- **Significant "breakpoints" in the decline were identified for some of the fish species examined, suggesting that rates of decline in PCB tissue concentrations are changeable and may be slowing and, in some cases, tissue concentrations may be increasing.** Fish tissue concentrations have not declined at a constant rate since the 1970s. Among fish time trends analyzed, seven out of 19 combinations of reach, species, and sample type showed a statistically significant change in trend between earlier and later periods. In Little Lake Butte des Morts, De Pere Reach, and in Green Bay Zone 2, there were steep declines in fish tissue PCB concentrations from the 1970s, but with significant breakpoints in declines for some species beginning around 1980. A meta-analysis of the most recent time trends was carried out for three reaches, yielding 5 to 7 percent rates of decline per year averaged across species. Six species showed an increasing rate in their final slope, but only two of these rates were statistically significant. The existence of breakpoints and an additional analysis showing non-constant rates suggests that rates of change are not stable and could be different in the future.

- **PCBs in surface sediment samples have generally declined over the period of time for which there are data for the Lower Fox River.** Surface sediment PCB concentrations combined within each reach by meta-analysis showed statistically significant decreasing trends in all reaches (10 to 15 percent decline per year) except Appleton to Little Rapids (1 percent increase per year). Surface sediments of individual deposits within the reaches included a mixture of positive and negative slopes. Among the 16 negative slopes, six were statistically significant; and neither of the two positive slopes was statistically significant. There were wide confidence intervals for rates of change, both for individual deposits and combined deposits, indicating that rate estimates are not precise. This imprecision and other uncertainties associated with the data prevent truly accurate future projections of sediment PCB concentrations.

- **Time trends in PCB concentrations in sediments below the surface sediment are quite varied—some indicate a decline, others indicate no change, others indicate an increase.** There is a strong trend toward fewer and weaker negative slopes at increasing depths. For Little Lake Butte des Morts, subsurface trends are mixed. The only statistically significant subsurface trend shows an increase and the other trends are a mixture of positive and negative trends. In the Appleton and De Pere reaches, there are both positive and negative trends that, taken together, are not clearly distinguishable from an overall zero trend. For Little Rapids to De Pere, there are consistently negative trends in the 10- to 30-cm strata, but in the lower strata, the data are consistent with either a zero trend (30 to 50 cm), or an increasing trend (50 to 100 cm and 100+ cm).

- **Projection of PCB concentrations into the future for fish or sediments are speculative because of imprecision and other uncertainties identified in the analysis.** The analyses carried out cannot assure a continued decline in PCB concentrations in fish and sediments over time. Even though there are a number of negative time trends that suggest PCB declines, future projection is speculative. Increases in PCB concentrations in some deeper sediments and breakpoints and other indications of changing rates in fish PCB time trends suggest that the river, its sediment, and its fish species could experience an arrest or reversal of such a decline at some time in the future.

- **PCB concentrations may increase or decrease in the future.** Some, perhaps all, of the changes in slope from before to after a breakpoint in the fish time trends may be genuine, due to unpredictable events, such as floods accompanied by scouring and deposition. As discussed in the RI, sediment bed elevations have been altered historically and may also undergo changes in the future due to scouring and redistribution of sediments. The occurrence of these breakpoints in the past suggests that the river may change again in the future. The presence of non-constant rates of change in the post-breakpoint period also suggests unpredictability. These findings support the notion of a dynamic process, liable to change, rather than a steady state with future constant rates of change. Thus, the data do not provide assurance of a continuing future decline in PCB concentrations.

- **PCB concentrations in fish in the De Pere Reach differ from concentrations from the same species in Green Bay Zone 2.** Comparison of samples from the De Pere to Green Bay Reach (Green Bay Zone 1) and Green Bay Zone 2 showed statistically significant differences between alewife, carp, gizzard shad, and walleye in the two reaches in seven out of eight analyses. A given species and sample type differed between the reaches in one or more ways: 1) average PCB concentration differed, 2) time trend in PCB concentration differed, or 3) the relationship of PCB concentration to lipid content differed.

Discussion

Some of the considerable variability observed in the data may be accounted for by changes in river profile, burial, scour by flood or ice, and propeller wash in the lower reaches of the river during the period of data collection. Changes in sediment bed elevations have been documented and are discussed in Technical Memorandum 2g (WDNR, 1999a) and in the Remedial Investigation (ThermoRetec, 2001a). These potential mechanisms could not be introduced into the statistical analysis and could not be controlled. The time trends analysis is dependent upon the existing hydraulic conditions in the Lower Fox River. Any changes in those conditions might result in exposure of underlying PCB-laden sediments or burying of such sediments, and lead to new trends that may not be similar to the trends from the present analysis.

The conclusions of a general decrease in PCB burdens in sediments and fish of the Lower Fox River and in Zone 2 of Green Bay are consistent with findings from other research on PCBs in the Great Lakes (Offenberg and Baker, 2000; DeVault *et al.*, 1996; Lamon *et al.*, 1998; Gobas *et al.*, 1995; Smith, 2000). Some of these reports have also noted slowing of trends. Based on the present and previous studies, there may continue to be slow, gradual declines, or a steady state in PCB concentrations in fish and sediment in the future. The possibility of some increases cannot be ruled out.

Controlling for lipid content of fish samples distinctly helped in calculating more accurate time trends. The lipid content is best used as an independent variable in regression analysis rather than as the denominator of a ratio (*PCB concentration ÷ percent lipid content*) used in traditional "lipid normalization."

Some strengths of the study include the methods used to handle data below a detection limit, methods used to detect and handle spatial correlation of sediment samples, approaches to quantifying and testing for non-constant rates of change in fish time trends, data-driven modeling of lipid content as a factor in PCB concentrations, and meta-analysis of rates to increase precision and power. The inherent very great variability of the PCB concentrations has been thoroughly described quantitatively and graphically, and clear statements about confidence in and statistical significance of the various quantitative trends have been provided to guide the reader in the use of the trends.

Sources of Uncertainty

The data used for both sediment and fish time trends analyses are inherently quite variable. Of the 46 sediment deposit group analyses and four surface sediment meta-analyses, only 16 of the analyses can offer us a reasonably firm conclusion that PCB concentrations are changing. Two of the 16 analyses indicate increasing trends and 14 indicate decreasing trends. The remaining 34 analyses show trends with wide confidence intervals. Among the 19 analyses of individual fish species and three meta-analyses, 17 clearly demonstrate a non-zero trend. The other five analyses or meta-analyses do not support a solid "no change," zero-slope conclusion, but yield an uncertain rate, consistent with a fairly wide range of plausible increasing or decreasing trends.

Relative depth was used rather than absolute depth. Depth of sediment is closely related to PCB concentration. We used depth defined as the distance of a sample to the sediment-water interface. Some of the time trends noted here may possibly be due to a change in the depth due to deposition or scouring over time, so that different parcels of sediment are identified with the same depth label at different times. Some changes that have occurred in sediment or fish tissue concentrations may be due to flooding, ice scouring, propeller wash, or other mechanisms that would have caused changes to the hydraulic conditions in the river or may have changed the relative depth of a deposit or a sample.

Age of fish may be related to their PCB concentrations, due to different feeding habits and locations during the lifecycle. Incorporating age proxy variables (either length or mass, unavailable in this study) might reduce unexplained variance and increase power to detect trends.

A "laboratory effect," whereby different laboratories would produce a different mean PCB concentration on split samples, is possible. In addition, analytical techniques may have changed over the 1989-through-1998 period of sediment sample collection and both the laboratory and analytical variation may have introduced spurious positive or negative trends, or masked real trends.

Table of Contents

Table of Contents

List of Figures

List of Figures

List of Figures

List of Figures

List of Tables

List of Tables

1 Introduction

PCBs are toxic chemicals that may pass through the food chain via fish, birds, and other wildlife to ultimately reach humans. PCBs were introduced into the Fox River, Wisconsin, from the manufacture and recycling of carbonless, multi-copy paper between 1954 and 1971. A number of studies have been carried out on the burden of PCBs in sediment, wildlife, water, and other media. The issue of time trends in PCB concentrations motivates our analysis. Carbonless paper manufacturing no longer introduces PCBs into the river, and other sources negligibly add to the PCB burden. Therefore, one can determine the rate at which the original store of PCBs is changing over time in fish and sediments.

In this report, therefore, we analyze the trends of PCB concentrations in sediment and fish over time. We provide quantitative estimates of rates of change of PCBs concentrations in sediments for:

- River reaches,
- Deposits within those reaches,
- Depth strata within the deposits, and
- Surface sediments combined within each reach.

We also provide quantitative estimates of time trends of PCBs in fish tissue for:

- Individual species, by reach, and
- Estimates combined across species, by reach.

In addition, we compare time trends in PCB concentrations in fish between the De Pere to Green Bay Reach and Green Bay Zone 2.

The analysis proves challenging due to the following features of the data:

- Concentrations below detection limits (both in sediment and fish),
- Spatial correlation of observations in sediment (due to the proximity of many of the samples in space),
- Potentially confounding spatial trends in sediment concentrations,
- A decline in fish PCB concentrations that, for several cases, is neither linear on the original scale of concentration per unit mass nor on a logarithmic scale,
- A limited number of sampling episodes for sediment and fish, typically leading to just a few distinct points in time for each analysis,

- Limited sample sizes for some deposits and some fish species, and

- Generally wide confidence intervals for estimates of rates of change.

Our methodology attempts to address each of the issues noted above. Despite the somewhat daunting methodology (a discussion of our methodology occupies more space in this report than our findings), the key results boil down to some fairly simple values: slope coefficients that represent the rate of change of the logarithm of PCB concentrations in sediment or fish over time. From the slope coefficients we calculated the following items of interest:

- The annual percent rate of decrease (or increase) of PCB concentrations in fish and sediments, and

- The statistical significance of the rate of change over time compared to a zero rate of change over time.

The last item refers to a "hypothesis test." Specifically, we test the null hypothesis that a given rate of change (of sediment or fish) is zero (no change over time) versus the alternative hypothesis that the PCB concentration is either decreasing or increasing over time.

2 Methods for Sediment Analysis

2.1 Sediment Data

Sediment data were obtained from EcoChem, the contractor responsible for maintaining the Fox River database. An initial selection from the Fox River Database (FRDB) yielded 2,776 observations for the following restrictions: analyte = total PCBs; matrix = sediment; and location = Little Lake Butte des Morts, Appleton, Little Rapids, or De Pere reaches.

2.1.1 Variables of Interest

Each sediment sample was described by a number of variables, of which the following variables were used in this study:

- Sample ID (used to identify records in case of unusual values or problems),
- Location (reach designation),
- Deposit (traditional deposit designations supplied with each record within the FRDB and used in other reports on the Fox River),
- "Depth from" and "depth to" (minimum and maximum depth of a sample),
- Sample date (date sample was obtained),
- Analyte (we used only total PCB concentration),
- Qualifier (indicates whether PCBs were detected or were below detection limits, and, also, data quality),
- Northing and easting (geographic location in meters), and
- "Result," which, in this case, gives the PCB concentration or the detection limit in µg/kg (or parts per billion, ppb).

2.1.2 Preliminary Data Handling

We excluded the following types of data:

- Ninety-four (94) samples with northing and easting coordinates outside the river boundaries, or with no northing or easting coordinates. These were typically side samples from creeks and tributaries, unusual samples such as bottled samples collected by divers with no exact location specified, or samples with sediment type indicated as coal composite, coarse-screened material, sand, stockpile, or non-TSCA pile;

- Thirty-four (34) samples from Appleton Deposit N, collected after January 1, 1999 (after dredging operations, which would have disturbed the natural action of the river); and

- Thirty (30) duplicated records, samples the data from which were present in more than one record in the database.

After these initial exclusions, a total of 2,618 observations were available. Any samples with a quality qualifier of R (rejected value—do not use) were ineligible for inclusion, but no samples were excluded on this basis alone.

Some data were missing the month and day, or just the day of the sample acquisition. Samples missing the day, but including month and year, were assigned to the midpoint of the month (i.e., day set to 15). Samples missing both day and month were set to the midpoint of the year (July 1). Because the time trends span data covering several years, these date imputations have a minor impact on the trend analysis.

To handle the fairly dramatic differences in concentrations and potential trends by depth, we incorporated the framework for stratifying observations by depth used in many other Fox River studies. The depth strata were right-endpoint inclusive (e.g., the interval 10 to 30 cm includes all samples with a depth greater than 10 cm and less than or equal to 30 cm): 0 to 10 cm, 10 to 30 cm, 30 to 50 cm, 50 to 100 cm, and 100+ cm). Samples were placed into a stratum based on their average depth (the mean of the minimum and maximum depth of the sample).

2.1.3 Logarithmic Transformation

We analyzed sediment and fish concentrations of PCBs after a logarithmic transformation. We implemented the $\log_{10}$ transform for two main reasons. First, plotting the logarithm of the concentrations generated a far more normally distributed (bell-shaped) curve than plotting values on the original scale.

Second, an analysis on the log scale corresponds to modeling percent change. Expressing the rate of change as percent change per year rather than absolute change in concentration is generally more meaningful. Percentages are a common way to express rates of change (e.g., "3 percent per year"). A fixed percentage rate of change per year (analogous to compound interest) corresponds to an exponentially increasing or decreasing curve. Such a curve on the natural scale transforms to an easily modeled straight line on the logarithmic scale.

Stated another way, fixed multiplicative increments on the natural scale (as in compound interest) become fixed additive increments on the log scale.

We note, also, that the logarithmic transform is consistent with the analysis of halving and doubling times for a PCB concentration. Like the percentage rate of change, the halving (or doubling) time can readily be calculated from a model for the logarithm of PCB concentration versus time. However, throughout this report, we favor the use of the percentage rate of change over halving and doubling times. The reported percentage estimates the actual rate of change during the period when the data were collected. The halving and doubling times, however, refer to a halving or doubling of concentration that would occur only if the rate of change of log concentration remains constant over the stated halving or doubling period. For example, suppose the coefficient of time (in years) for a model of $\log_{10}$ PCB concentration versus time is –0.01 per year during the period 1989 through 1998. The average rate of change of the PCB concentration during that period is, then, –2.3 percent per year $\left[=100\%\left(10^{-0.01}-1\right)\right]$ and the calculated halving time is 30.1 years $\left[=\left(\log_{10} 0.5\right)\div\left(-0.01\right)\right]$. On the one hand, the –2.3 percent per year is a confident statement about a real period of time, 1989 through 1998. On the other hand, the 30.1 years for halving assumes a steady state that may not occur in a changeable river during a speculative 30.1 years. There is a one-to-one correspondence between the percentage rate of change, *P*, and the halving time, *T* (–*T* for doubling): $P=100\left(0.5^{1/T}-1\right)$. Both bear the same information. We avoid, however, the connotation of possible long-term stability implied by the "doubling" and "halving" terms.

Figure 1 provides an example of a distribution of PCB concentrations plotted on the original scale (ppb, left plot), which can be compared to a plot on a logarithmic scale ($\log_{10}$ ppb, right plot). The *X*-axis is an arbitrary scale for each plot, expressed as positive or negative deviations from the mean. The *Y*-axis shows the number of cases in each bin. A bell-shaped curve has been superimposed on each plot. The logarithmic plot shows a more symmetrical distribution and no outliers, compared to the plot on the natural scale. Generally speaking, for the hypothesis tests used in this study, such as those used to detect non-zero time trends, a more normal or "bell-shaped" distribution is less likely to lead to biased results. An exact or approximate normal distribution is desirable because the hypothesis tests used in our study assume a normal distribution. Moderate departures from this assumption are acceptable.

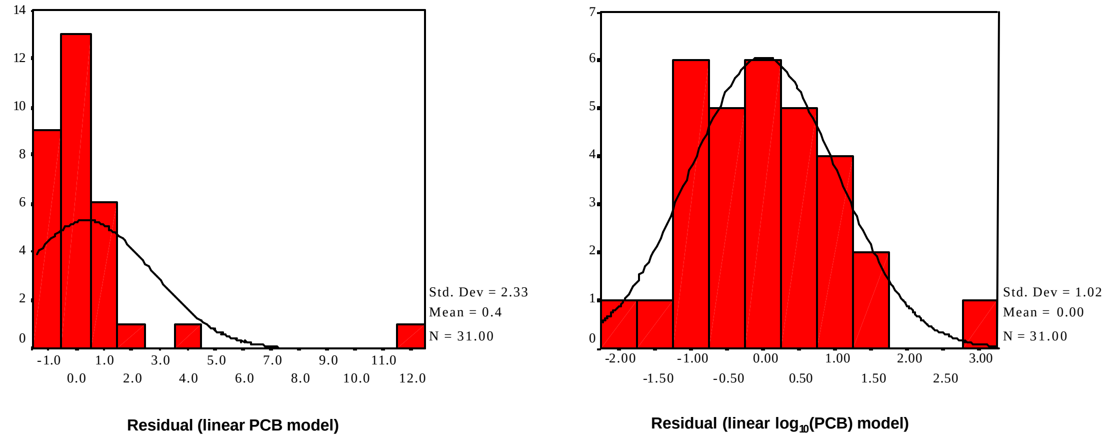

Figure 1 Example of PCB Concentration Distribution on Natural and Logarithmic Scales

Time trend estimates based on less skewed, more normal distributions are less likely to be influenced by extreme observations. A measure of skewness is the classical skewness coefficient, which is zero for symmetrical distributions and increasingly positive or negative for distributions that are increasingly stretched toward large values or small values, respectively. The normal distribution has a skewness coefficient of zero. The Appendix contains the skewness coefficients for the PCB concentrations and $\log_{10}$ (PCB concentration). Almost all distributions of sediment PCB concentrations had smaller skewness coefficients (closer to zero) on the logarithmic scale than on the natural scale. In addition, use of the logarithmic transformation passed an important visual test for the bell-shaped normality, based on "residuals." A residual here is defined as an observed value of log PCB concentration minus the corresponding predicted value from the fitted regression model. If the residuals have a bell-shaped distribution, then estimates from the fitted model are more likely to be correct. To check the bell shape, we commonly use a visual display called the QQ, or "cum-cum" plot. One plots the cumulative distribution of residuals against the corresponding cumulative normal distribution. If the residuals are normally distributed, the points will all huddle along the 45 degree line. If the residuals are not normally distributed, the points will stray therefrom.

Figure 2 shows an example of a cum-cum plot. The log PCB data (right plot) lie closer to the straight line representing the normal distribution than the PCB data on the original scale (left plot).

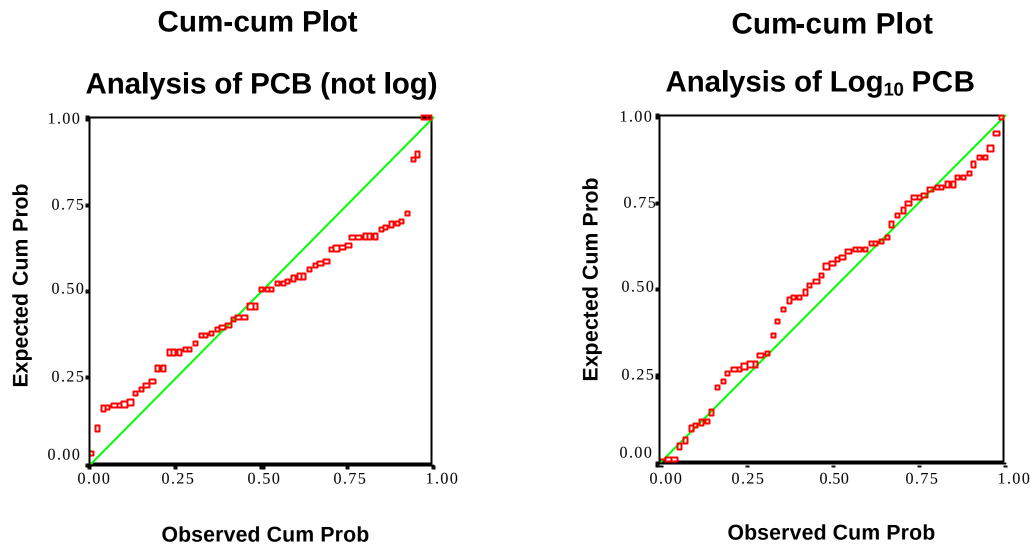

Figure 2 Comparison of Cum-cum Plots Based on Untransformed and Log-transformed Data

We have not carried out a formal hypothesis test that the distributions of $\log_{10}$ PCB concentrations are normal. With the sample sizes used in this study (both for sediment and fish), the visual checks noted here are adequate and consistent with good statistical practice. Formal tests for normality, such as that of Kolmogorov and Smirnov, have low power for these sample sizes. In addition, regression and other procedures used in this study are robust, even if distributions are only approximately normal.

Given the good fit of the lognormal distribution to most of the observed distributions of PCB concentrations, we analyzed PCBs as the logarithm to base 10 of the PCB concentration in parts per billion. Throughout the report, our reference to PCB concentrations denotes this logarithm, unless stated otherwise. In plots and tables, the log carries the usual, easily interpreted quantification: a log value equal to 0 means an untransformed value of 1, a value of 1 represents 10, 2 represents 100, and so on.

Later, we develop models for log PCB concentration over time, i.e., "time trends" models. Given a correct model for time trend in a particular deposit, the predicted value of log PCB concentration at a specific time from the model is an unbiased estimate of the corresponding true mean log concentration at that time. The anti-logarithm of this predicted mean is an unbiased estimate of the geometric mean (GM_{est}) of PCB concentrations on the natural scale at the specified time. Because of the skewness toward large values on the natural scale, however, the geometric mean underestimates the arithmetic mean at the specified time. The arithmetic mean PCB concentration is a value of particular interest. Equation 1 provides an estimate of the arithmetic mean (AM_{est}) that can be calculated from the geometric mean.

Equation 1

$$AM_{est} = GM_{est} \exp(s^2 \cdot 5.302 / 2).$$

where *GM* is the geometric mean and s^2 is the estimated variance on the $\log_{10}$ scale, calculated from a regression model. The quantity 5.302 comes from use of a $\log_{10}$ scale rather than a $\log_e$ scale. If a $\log_e$ scale is used, the 5.302 can be dropped.

2.1.4 Core Averaging

We refer to the combination of some samples from the same vertical core sample as "core averaging." As described below, proximate samples were correlated (showed similar PCB values). Thus, we replaced the log PCB concentrations of multiple samples from the same core in a given depth range with their mean (on the log scale), yielding one core-averaged sample per core per depth stratum. Twenty-five (25) percent of the sediment observations included in the analysis resulted from core averaging. A mean of 2.4 single observations contributed to a core-averaged observation. After core averaging, there were 1,980 observations.

Core averaging offers several advantages. Samples taken from exactly the same location constitute a distinct spatial sampling pattern with, possibly, different correlations than may be found among samples taken at distinct locations. Spatial correlation typically varies inversely with distance, so that samples taken close together possess stronger correlations than samples taken far apart. A distance of zero, and its infinite inverse, arising from samples taken at exactly the same location may not fit into the spatial correlation pattern present among samples collected from dispersed locations. Specifically, if $r(d)$ is the correlation between samples separated by distance d, the value of $r(0)$ may not equal the limit of $r(d)$ as d approaches zero; i.e., $r(0)$ may be an isolated discrete value. Taking the average of multiple samples from a single location will likely yield a concentration that fits better with the spatial correlation pattern from other, spatially dispersed samples. Also, multiple samples from a single location would weight that location more heavily in subsequent analyses than locations represented by a single sample. Core averaging equally weights each location.

Other than addressing an unusual correlation scenario and a statistical weighting issue, core averaging probably has little influence on the calculated time trends. A scatter plot of $\log_{10}$ PCB concentration (Y-axis) versus time (X-axis) would spread the multiple PCB concentrations from the single location vertically around the core-averaged value at the same value for time, $X = t_0$. If the individual sample concentrations are given the same total statistical weight as the single core-averaged value, then a least-squares regression analysis of log PCB concentration versus time would yield identical slopes for either representation of the samples—core-averaged or individual. This simplified example ignores the spatial variables that we used in our regression analysis. However, the point is that core averaging is unlikely to influence the slope of a time trend.

Core averaging probably does not affect statistical significance because of two offsetting factors:

1. Heightened precision of a core-averaged log PCB concentration (compared to the less precise individual concentrations) would tend to add power to detect a non-zero slope and designate it as statistically significant.

2. Reduced sample size from core averaging would tend to subtract power to detect non-zero slopes, and would then be less likely to designate a real non-zero slope as statistically significant.

These two factors may balance out.

Core averaging imputes the mean log PCB concentration to the mean depth of the samples (all within the same stratum). Thus, core averaging reduces the information available to determine and control spatial trends. This is probably a small effect, because 75 percent of $\log_{10}$ PCB concentrations used in the time trends analysis did not result from core averaging.

In summary, core averaging protects against a mixture of two possibly distinct spatial correlation patterns, offers equal statistical weight to each location sampled, and likely will have little influence on both estimated time trend slopes and statistical significance. It may result in slightly less precise estimates of spatial trends.

In subsequent calculations, a core-averaged value counted as one observation, on par with other single observations that had not been core averaged.

2.1.5 Observations Below Detection Limit

A number of observations dropped below detection limits. We used the maximum likelihood method (see next section) to handle these observations. In statistical parlance, observations below detection limits are designated as "censored," which simply refers to truncated observations. Note that "censored" does not mean that observations have been excluded from the analysis. Observations both above and below detection limits contribute to the analysis. By using the maximum likelihood methodology, an observation below the detection limit brings all the information that it contains to the analysis—namely, a concentration observed as not exceeding a certain limit—and obviates the need to impute a replacement value, such as half the detection limit.

2.2 Maximum Likelihood Method

Maximum likelihood (ML) is a method very commonly used in statistics to estimate parameters such as coefficients in a regression model or in other types of models (Lawless, 1982). The precision of an estimated parameter depends on the size of the dataset, the complexity of the model, and other factors. One expresses the precision as the standard error. In many situations, adding and subtracting twice the standard error to the estimated parameter value, as obtained from the sample, provide a 95 percent confidence interval for the true population value. That is, we are 95 percent confident that the interval includes the true population parameter. Like other estimation methods, including normal-based least-squares, ML yields: 1) an estimate of the parameter; 2) a standard error of the parameter, which indicates the precision of the estimate; and 3) a statement of statistical significant (*p*-value), which tells us the strength of evidence that the true parameter is not zero. One can conduct tests for statistical significance using either: 1) the parameter compared to its standard error (the ratio would be approximately normally distributed with an expected mean of zero if the true value of the parameter, such as a slope, is zero), or 2) a likelihood ratio test (LRT).

Specifying some distribution for the data is integral to the ML method. This assumption of a particular distribution is part of our model for the observed data. The models used in the current study, both for sediment and fish PCB concentrations, assume that the PCB concentration depends on some known variables. For PCB in sediments, the variables are spatial dimensions and time. For PCB concentrations in fish tissue, the variables are time, position within the annual seasonal cycle, and lipid content of the tissue. For specified values of these other variables (e.g., specified time, sediment depth, and northing and easting coordinates), the observations are assumed to occur randomly above or below an expected value. This random variation constitutes "noise." As part of the maximum likelihood approach, one must specify the distribution of this "noise." In our analysis, we have assumed a normal distribution for log PCB concentrations and, equivalently, a lognormal distribution for the original data. As noted earlier (Section 2.1.3), this assumption fit the distribution of log-transformed sediment concentrations exceptionally well. The normal distribution then was assumed when using the ML method with log PCB concentrations.

Data analysis customarily assumes a model, such as that noted here, for generating observations: random variation generates observations scattered around the "truth." In this study, "the truth" of sediment time trends has been modeled as a straight line (logarithm of PCB concentration versus time) corresponding to an exponential decay of the actual PCB concentration, with appropriate adjustment for spatial coordinates. The "noise" has been modeled as the normal distribution—a bell-shaped curve.

The idea behind maximum likelihood estimation for the coefficients in a model can be illustrated by a simple example. We can visualize a scatter plot of a dependent variable (y) versus time (t) with some apparent linear trend to the scatter of points. When attempting to fit a straight line to the data, we can imagine taking the line and shifting it around the plot until we see a "best fit." We can get residuals from this line of predicted values to the observed data points. For a given point, the residual is the observed value minus the predicted value. Generally large residuals imply a poorer fit than generally small residuals. Given the assumption of a normal distribution of points around the line (a bell-shaped curve) at each time t and an estimate of the "width" or variance of the normal distribution around the straight line, we then can calculate the probability of getting a particular collection of residuals around the line. (The reader should note that this simplified example of PCB concentration versus time does not include spatial coordinates. The actual models developed later do include spatial coordinates.)

A straight line that does not pass through most of the data would produce a very unlikely collection of residuals. As such, the probability of such a line being a good fit would be low. Similarly, a straight line driving right through the data would produce a far more likely collection of residuals. The "best fit" line is the one with the most probable collection of residuals.

The maximum likelihood method lets us actually calculate the probability, given a particular straight line, that we would get a certain set of residuals scattered around the straight line. Each residual would contribute to that probability. For a concentration below the detection limit, we can calculate the probability, given the line, that an observation would occur at or below the specified detection limit. By multiplying together the probabilities for all residuals, we would calculate one overall probability that the given configuration of residuals would occur around this line.

We can think of the maximum likelihood method as calculating probabilities for infinitely many lines, with infinitely many values of noise around the line. The method allows one to identify the line and the value of the noise around the line with the maximum probability for the data. (The maximizing and probability concepts lead to the name "maximum likelihood.")

One can then find the statistical significance of the slope of the line—the probability that the non-zero slope could have arisen randomly when the "truth" is a zero, or horizontal, slope. The statistical significance (or of lack thereof) of the departure of a fitted line from zero slope involves comparing a model with that slope set to zero (in this simple example a horizontal, straight line) to the model with a sloping straight line. A small change in the likelihood from the horizontal, straight line to the sloping line suggests a non-statistically significant difference, and, similarly, a non-statistically significant non-zero slope. That is, random variation could easily generate a line with this magnitude of slope.

Conversely, if we have to tilt the line quite a bit in order to get a better representation of the data, and the likelihood of that fit increases dramatically compared to the horizontal, zero-slope line, then we would probably declare the slope "statistically significant." Such an impressively sloping line probably could not have arisen by chance if "the truth" had a zero slope. So, we would reject the hypothesis of zero slope.

The typical output from the maximum likelihood method includes:

- The estimate for each parameter,
- The standard error of the parameter estimate, and
- The statistical significance (*p*-value) for the null hypothesis that the true parameter is zero.

One can extend the ML method to more complex models including spatial coordinates with relative ease. Either simple or complex models will have residuals. As in the simple linear case, the more complex models also involve multiplying probabilities together and adjusting parameters in the model to get the largest overall probability of producing the observed set of residuals.

Throughout the report, significance levels of $p < 0.05$, from regression analysis or from any other analyses, have been designated as "statistically significant." "$p < 0.05$" means that there is less than 5 percent probability that an observed non-zero slope could arise randomly and differ from zero to the extent observed, if the true slope were zero.

2.3 Spatial Dependence

Analysis of sediment PCB concentrations for the Fox River data revealed a close-range spatial dependence. As will be shown later, measured total PCB concentration from samples obtained within a few centimeters or meters of one another tended to have similar values. Samples located hundreds of meters apart were more dissimilar. Thus, PCB concentrations appear to be spatially correlated.

Standard statistical methods typically assume independent observations. When data show spatial correlation, standard statistical methods may provide an unbiased parameter estimate, but they will also underestimate the standard error of the estimate, generate anticonservative *p*-values and confidence intervals, and overstate claims of statistical significance. This occurs because two observations that show spatial correlation do not produce as much information as two independent observations. Hence, standard statistical methods overestimate effective sample size.

Consider the following illustration of dependence, polling voters on their choice of a presidential candidate: asking five people in each of two households to choose the next president will yield 10 answers, but the true sample size will be closer to two, not 10, as people within households tend to vote more similarly than people in separate households. Asking the same question of 10 individuals from separate households in different neighborhoods across the country will yield much more information than asking five individuals within two households. As an extreme example, we cannot obtain a precise percentage estimate of the popular vote by asking one person repeatedly 10,000 times how they expect to vote.

We investigated spatial correlation using semivariogram analysis (Cressie, 1993), a method developed in the field of mining geostatistics for assessing close-range correlation of mineral concentrations in soil samples. In our context, the semivariogram vertical axis shows the average squared difference in $\log_{10}$ (PCB concentration) between pairs of observations, and the horizontal axis shows the distance between the observation pairs. If the observed difference in PCB concentrations is smaller for pairs close together, this curve will rise from zero up to a "sill" level, where the curve flattens out, as in Figure 3. Beyond the sill level, the approximately constant difference in concentration indicates independence between data pairs at that level of separation. The semivariogram in Figure 3 also sports a smooth curve, added to aid in assessing the sill level; these smoothed curves do not always accurately show the initial rise to the sill (as in Figure 4), due to the particular algorithm used for smoothing. The leftmost data values help to visually assess the "rise to the sill." The leftmost point(s) are lower on the *Y*-axis than other points, indicating that points close together have more similar PCB concentrations than the concentrations of points farther apart. Around any trend, however, one finds considerable scatter.

The log of core-averaged concentrations was used in calculating and plotting the semivariograms. Because most observations (75 percent) did not arise from core averaging, semivariogram plots based on the original concentrations (not core averaged) would be expected to differ little from plots based on core averaging. Without core averaging, points on the plot would tend to shift upward (toward larger variances).

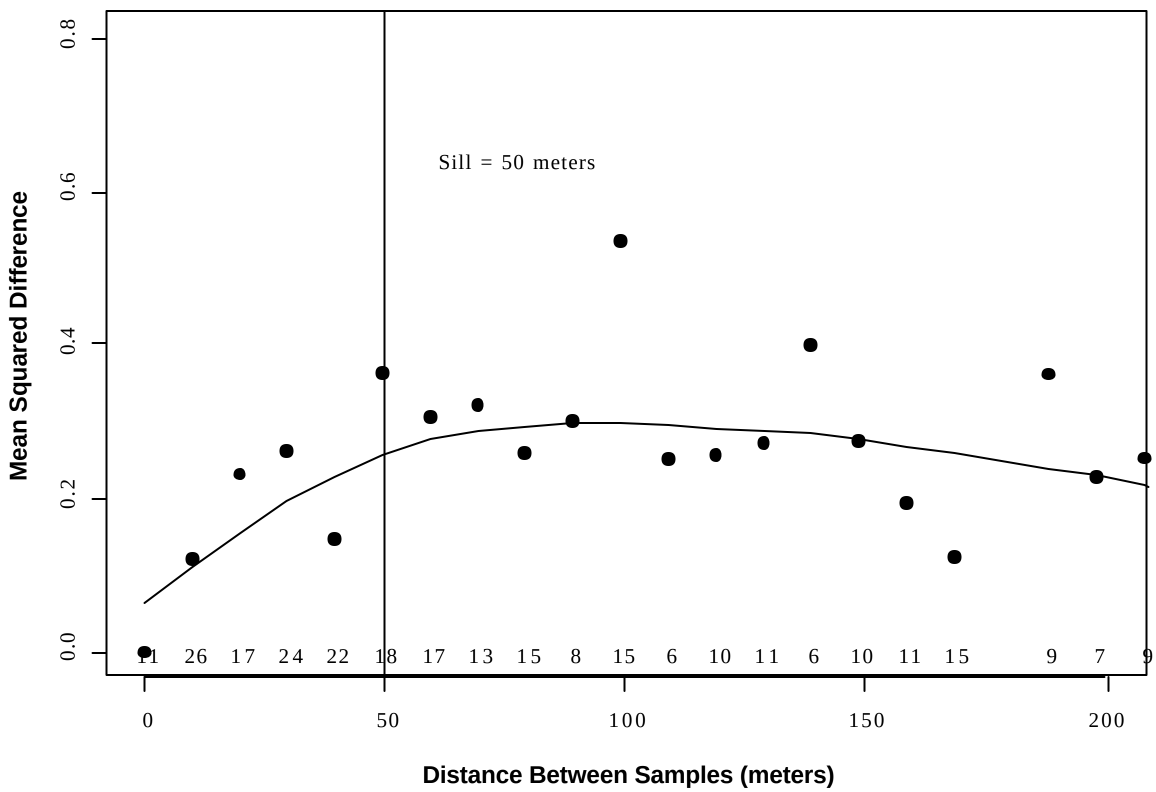

Figure 3 Semivariogram Plot of Appleton Deposit Group N Pre-dredge, 10+–30 cm Depth

The semivariogram considers all possible pairs of *n* samples. That is, sample #1 and sample #2 are a pair, sample #1 and sample #3 are a pair, and so on, up to the last pair, sample #*n* and #(*n* – 1). There are *n* (*n* – 1) ÷ 2 total pairs. The vertical axis shows the mean squared difference in $\log_{10}$ (PCB concentration) between a pair of samples, and the horizontal axis shows the distance between the pair. The distance between pairs of samples binned (i.e., all pairs of samples closer than about 10 meters are pooled into one bin). For each sample pair in this bin, the squared difference of their $\log_{10}$ PCB concentration is calculated and the mean of the squared values is plotted above the bin location on the *X*-axis. The next bin represents pairs of samples separated by about 10 to 20 meters. Again, the mean squared difference is calculated and plotted. A similar process of calculation and plotting is carried out for all possible pairs of samples. Note that a given sample will appear in (*n* – 1) pairs (once with each other sample). Moreover, it may occur in multiple bins as a member of some pairs that are close together and other pairs that are far apart. A smooth curve has been added to represent the trend of increasing mean squared difference with increasing distance between pairs of samples. The number of sample pairs in each bin shows just above the horizontal axis, directly beneath the estimated mean squared difference point for that bin. Samples obtained very close together show small differences, as their measured PCB values tend to be quite similar; i.e., samples obtained close together are not statistically independent. The average squared difference rises from zero as distance between points increases, up to the "sill" value (marked as 50 meters in the plot), where the average squared difference levels off and reflects the distance beyond which points are effectively independent. Semivariogram plots were used to detect spatial dependence, but no quantitative results from the semivariograms entered calculation of time trends.

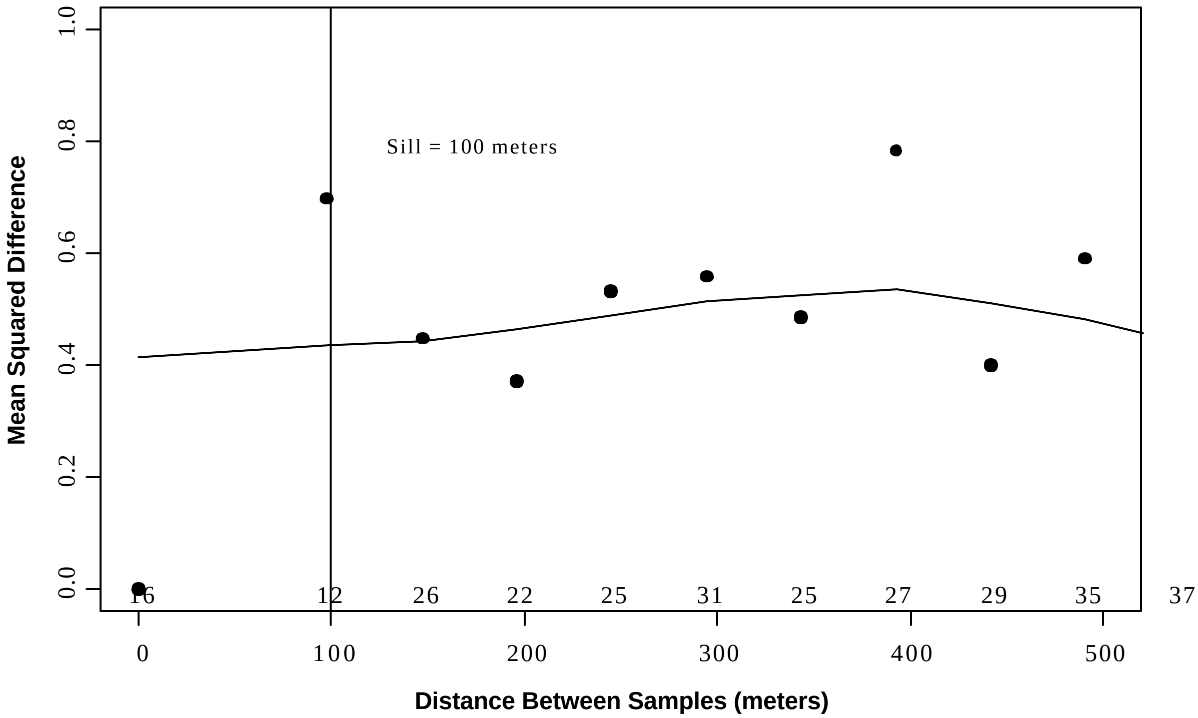

Figure 4 Semivariogram Plot of De Pere to Green Bay Deposit Group 2025, 10–30 cm Depth

(See explanation in legend of Figure 3.) Semivariogram plot portraying a case where smoother curve shows the "sill" level adequately, but does not curve up from zero due to lack of sample pairs close together. The leftmost data point indicates a very low mean squared difference for sample pairs located closer than about 25 meters. Beyond 100 meters, the average squared difference is fairly constant, indicating that samples separated by at least 100 meters are effectively independent.

Semivariograms were plotted for each of the many combinations of deposit and depth that were ultimately analyzed. The plots showed that short-range spatial dependence was pervasive in these data. Semivariogram analysis was used only to visually display spatial dependence. No quantitative results from the semivariogram analysis were used in subsequent time trends calculations. Spatial dependence was handled through the WSEV estimate, discussed below.

2.4 Addressing Spatial Dependence Using the WSEV Method

Lumley and Heagerty (1999) and Heagerty and Lumley (2000) have developed a method for more accurately assessing variability in the presence of spatial correlation using Window Subsampling Empirical Variance (WSEV) estimation. The problem being addressed is that the effective sample size is smaller than the total sample size because correlated observations do not contain as much total information as totally independent, uncorrelated observations. The WSEV method tends to lump correlated observations together into groups that are then approximately uncorrelated. In the WSEV method, one divides up the geographic region over which the data values are obtained into a collection of windows, or subregions. We can think of the subregions being defined by a rectangular grid (with rectangular grid cells) placed over the map of sample locations. With a grid of the right spacing, the observations in different subregions of the grid will tend to be independent. The mean of the observations in a subregion can represent that subregion. The WSEV method works with means of regions, though one actually uses a more complex function than the mean. The WSEV method is analogous to using a sample size that is more closely related to the number of independent regions, rather than the number of samples available. This smaller effective sample size yields a more accurate estimate of the standard error of a parameter, more accurate confidence intervals, and a more accurate statement of statistical significance.

The ML method discussed earlier provides estimates of regression coefficients, such as a time trend slope, that do not need any adjustment. Only the standard error of these regression coefficients is adjusted by the WSEV method. In turn, the standard error is used to calculate statistical significance (a *p*-value).

Implementing Lumley's WSEV method involves dividing the spatial region using a coarse mesh grid, then averaging particular functions of the data within grid cells and using the averages to obtain standard error estimates for the regression model parameters. One repeats the procedure with decreasing grid mesh sizes (i.e., decreasing size of subregions), typically investigating five to ten mesh sizes. As the mesh size decreases, parameter standard errors initially increase and then decrease.

Inordinately large grid sizes result in too much averaging and subregions exhibit too little variation among themselves. As the grid size initially decreases, the estimated standard error will increase. As the grid size continues to decrease, at some point the estimated standard error will now stop increasing and begin to decrease. This occurs because neighboring cells will show too little variation due to their correlation with one another. The WSEV method uses the standard error of the regression model intercept as an aid in determining the proper grid size. We fit all of our regression models with an intercept (constant term). The WSEV standard error of the intercept will show the increasing-then-decreasing magnitude with increasing grid size as just described. In the WSEV method, the grid size that yields the largest standard error for the intercept term of the regression model is selected. From this grid size, we then calculate the WSEV standard error for the coefficient of time (the time trend slope). This standard error fully accounts for spatial dependence and is selected in an objective way.

In each analysis, we used ML estimation S-PLUS functions "SurvReg" and "CensorReg" to fit regression models and calculate the time trend slope coefficients. (The two S-PLUS functions SurvReg and CensorReg provide the same estimates of slope, but each generates different quantities used in the WSEV analyses.) Using the WSEV method, we then calculated the standard error of the time trend slope coefficient. We wrote our own software routines (in S-PLUS) to calculate the WSEV estimates of standard error, based on output from SurvReg and CensorReg (S-PLUS 2000, Release 2, MathSoft, Seattle).

We calculated the statistical significance (*p*-value) of each time trend slope using the *t*-distribution; i.e., a "*t*-test." The *t*-statistic was calculated as the ratio of: 1) the time trend slope coefficient (the coefficient of time, *t*, in Equation 1); and 2) the WSEV standard error. The degrees of freedom for the *t*-statistic was the number of grid cells, at the chosen grid mesh size, which contained at least one sample. This is analogous to the number of independent groups of observations. The Appendix includes this number of non-empty grid cells.

2.5 Geographic Grouping of Data

Our need for geographically grouping samples for statistical analysis led to the creation of new "deposit groups." The sample deposit designations in the FRDB were unsuited to defining spatially cohesive subsets, as many samples fell outside the original deposits (and had no deposit designation). Furthermore, some deposit designations spanned stretches of a river reach too long to allow adequate control of spatial variation in PCB concentration. We examined the spatial layout of all samples in each river reach. Based on this plotting and mapping exercise, we defined new "Deposit Groups," forming data subsets with spatial variation far more amenable to statistical analysis. We named the deposit groups to reflect, to some extent, the original deposit designations already in place, with the added benefit that these groups designated non-overlapping spatial sets that included all samples. The geographic size of deposit groups is a compromise between a desire for large sample sizes in each group and a desire for tiny areas with homogeneity (i.e., relatively similar PCB concentrations within each depth stratum).

There was an isolated sample, labeled as "POG," located by Wrightstown in the Appleton to Little Rapids Reach. The sample was located at least 2 miles from upstream samples and at least 3 miles from downstream samples. The sample was excluded.

Table 1 through Table 4 show how the original sample designations (identified in table rows) correspond to our "deposit group" designations (positioned in table columns). For example, the new "Little Lake Butte des Morts Deposit **Group** E" primarily contains samples from the original Little Lake Butte des Morts Deposit E (40 samples), but also includes four samples from the original Little Lake Butte des Morts Deposit D and nine from Deposit POG. Samples with no deposit designation in the FRDB constitute from 5 to 70 percent of samples within each of the four reaches (Table 1 through Table 4). Little Lake Butte des Morts had 5 percent of samples with no deposit designation (presumably samples located spatially outside the original deposit designations). The corresponding percentages of samples without designations in other reaches were 7 percent for Appleton Reach, 12 percent for Little Rapids Reach, and 72 percent for the De

Pere Reach. The large percentage for De Pere Reach arises because the original deposit designations were noted only for SMU Deposits 50–67. Our new "deposit group" designation includes all samples and thus increases sample sizes available for trend estimates and hypothesis tests. In any case, having an original deposit designation became irrelevant with the formation of our new deposit groups. Furthermore, the lack of an original deposit designation had no role in disqualifying a sample from inclusion in our time trends analysis. Finally, not having an original deposit designation does not suggest poor data quality.

Table 1 Little Lake Butte des Morts Deposit Groups Defined for Time Trends Analysis

Original Deposit Designation	Time Trends Analysis: Deposit Group Designation							Total
	LLBdM Deposit Group AB	LLBdM Deposit Group C	LLBdM Deposit Group POG	LLBdM Deposit Group D	LLBdM Deposit Group E	LLBdM Deposit Group F	LLBdM Deposit Group GH	
Deposit A	281	0	0	0	0	0	0	281
Deposit B	5	0	0	0	0	0	0	5
Deposit C	0	52	0	0	0	0	0	52
Deposit D	0	0	1	49	4	8	0	62
Deposit E	0	0	2	1	40	68	32	143
Deposit F	0	0	0	0	0	12	0	12
Deposit G	0	0	0	0	0	0	3	3
Deposit H	0	0	0	0	0	0	3	3
Deposit POG	0	0	27	0	9	0	0	36
No Designation	13	2	4	5	0	10	0	34
Total:	**299**	**54**	**34**	**55**	**53**	**98**	**38**	**631**

Note:

Column entries show number of samples from original deposits included in each time trends deposit group.

Table 2 Appleton Deposit Groups Defined for Time Trends Analysis

Original Deposit Designation	Time Trends Analysis: Deposit Group Designation					Total
	Appleton Deposit Group IMOR	Appleton Deposit Group N	Appleton Deposit Group VCC	Appleton Deposit Group SU	Appleton Deposit Group DD	
Deposit AA	0	0	1	0	0	1
Deposit BB	0	0	3	0	0	3
Deposit CC	0	0	9	0	0	9
Deposit DD	0	0	0	0	20	20
Deposit I	4	0	0	0	0	4
Deposit J	2	0	0	0	0	2
Deposit K	3	0	0	0	0	3
Deposit L	3	0	0	0	0	3
Deposit M	2	0	0	0	0	2
Deposit N	0	136	0	0	0	136
Deposit O	7	0	0	0	0	7
Deposit P	12	0	0	0	0	12
Deposit Q	12	0	0	0	0	12
Deposit R	2	0	0	0	0	2
Deposit S	0	0	0	7	0	7
Deposit T	0	0	0	15	0	15
Deposit U	0	0	0	3	0	3
Deposit V	0	0	7	0	0	7
Deposit W	0	0	39	0	0	39
Deposit X	0	0	46	0	0	46
Deposit Y	0	0	3	0	0	3
Deposit Z	0	0	2	0	0	2
No Designation	9	0	15	0	0	24
Total:	**56**	**136**	**125**	**25**	**20**	**362**

Note:

Column entries show number of samples from original deposits included in each time trend deposit group.

Table 3 Little Rapids Deposit Groups Defined for Time Trends Analysis

Original Deposit Designation	Time Trends Analysis: Deposit Group Designation				Total
	Little Rapids Deposit Group Upper EE	Little Rapids Deposit Group Lower EE	Little Rapids Deposit Group FF	Little Rapids Deposit Group GGHH	
Deposit EE	100	96	94	145	435
Deposit FF	0	0	3	5	8
Deposit GG	0	0	0	75	75
Deposit HH	0	0	0	49	49
No Designation	4	22	0	52	78
Total:	**104**	**118**	**97**	**326**	**645**

Note:

Column entries show number of samples from original deposits included in each time trend deposit group.

Table 4 De Pere SMU Groups Defined for Time Trends Analysis

Original Deposit Designation	Time Trends Analysis: Deposit Group Designation					Total
	De Pere SMU Group 2025	De Pere SMU Group 2649	De Pere SMU Group 5067	De Pere SMU Group 6891	De Pere SMU Group 92115	
SMU56/57	0	0	282	0	0	282
No Designation	201	284	97	88	61	731
Total:	**201**	**284**	**379**	**88**	**61**	**1,013**

Note:

Column entries show number of samples from original deposits included in the time trends SMU group.

Figure 5 through Figure 8 map the location of samples and our deposit groups in the four river reaches. The boundaries separating the deposits were approximations drawn by eye, as formal definitions were unnecessary. Figure 8 breaks our SMU groups into smaller units than actually used, showing some of the original SMU designations. Our SMU Group 2025 aggregated (approximately) the original SMU designations 20–25; our SMU Group 2649 aggregated the original SMU designations 26–49; and so on for our SMU groups 5067 (aggregating 50–67), 6891 (aggregating 68–91), and 92115 (aggregating 92–115).

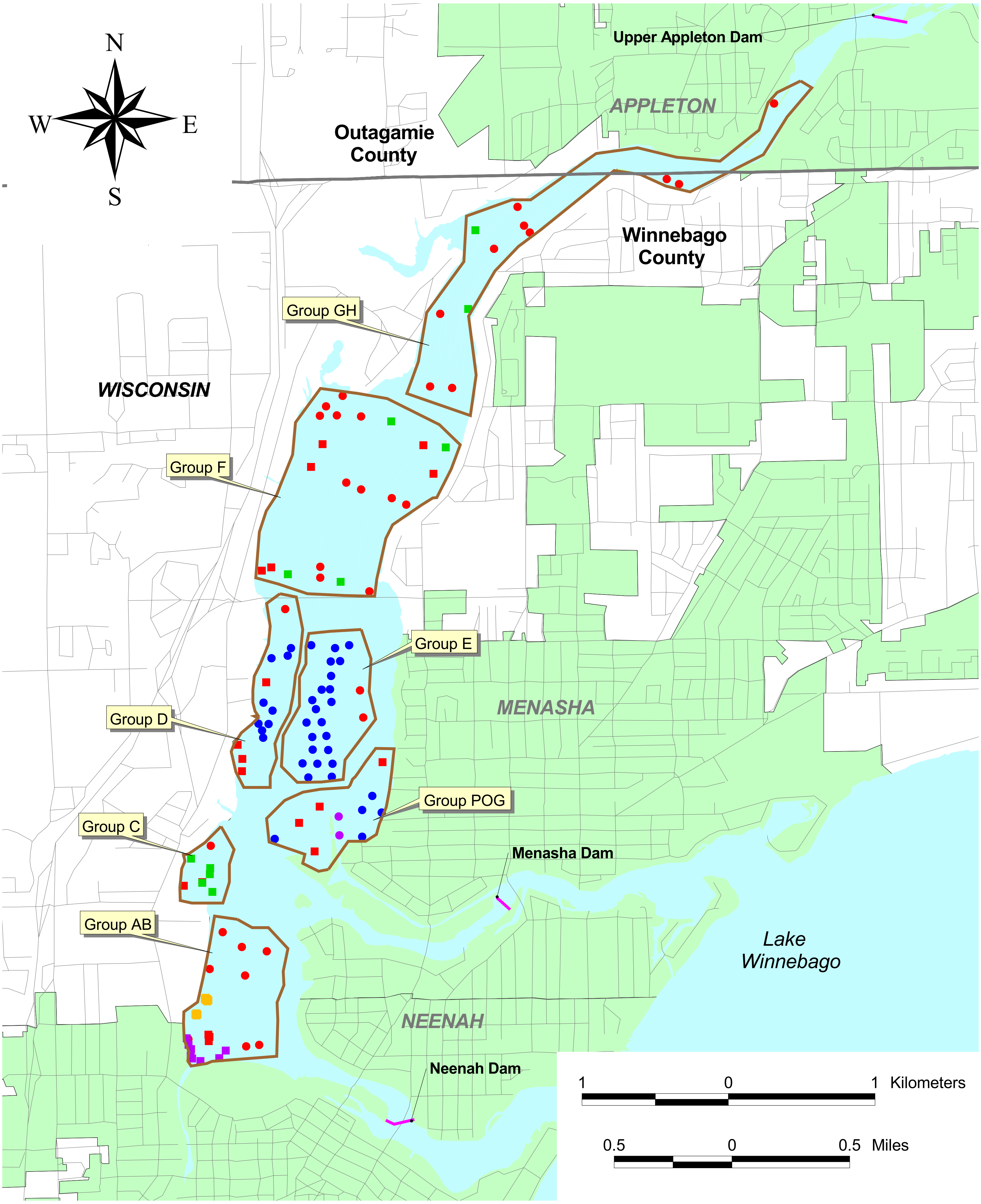

Revised Deposit Outlines
Sediment Sample Data Collection Points
- 1989/90 Mass Balance sediment data study
- 1994 SAIC and GAS study
- 1995 WDNR
- 1996 BBL data study
- 1997 SMU 56/57 Demonstration Project
- 1998 BBL data study
- 1998 Deposit N Post-Dredge sediment Demonstration Project
- 1998 RI/FS Supplemental data
- 1992/1993 LLBDM RI/FS Deposit A
- 1994 Woodward Clyde Deposit A sediment sample

Dam Locations
Roads
County Boundary
Water

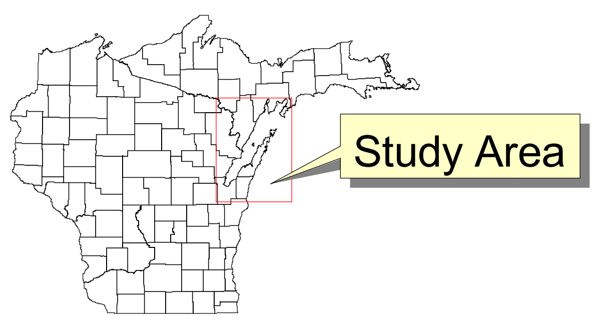

NOTES:
1. Basemap generated in ArcView GIS, version 3.2 , 1998, and TIGER census data, 1995.
2. Sediment sample point data obtained from Wisconsin Dept. of Natural Resources, 1999. and are included in the Fox River database.
3. Revised deposit outlines created by Nayak Polissar, Mountain-Whisper-Light Statistical Consulting, and Stephen Jesse, ThermoRetec Engineering Consultants, 2000.

ThermoRetec	Natural Resource Technology	Risk Assessment	Sample Point Groups for Sediment Time Trend Analysis: Little Lake Butte des Morts	FIGURE NO: RA-14414-425-1
				PRINT DATE: 1/23/01
				CREATED BY: SCJ
			FIGURE 5	APPROVED: AGF

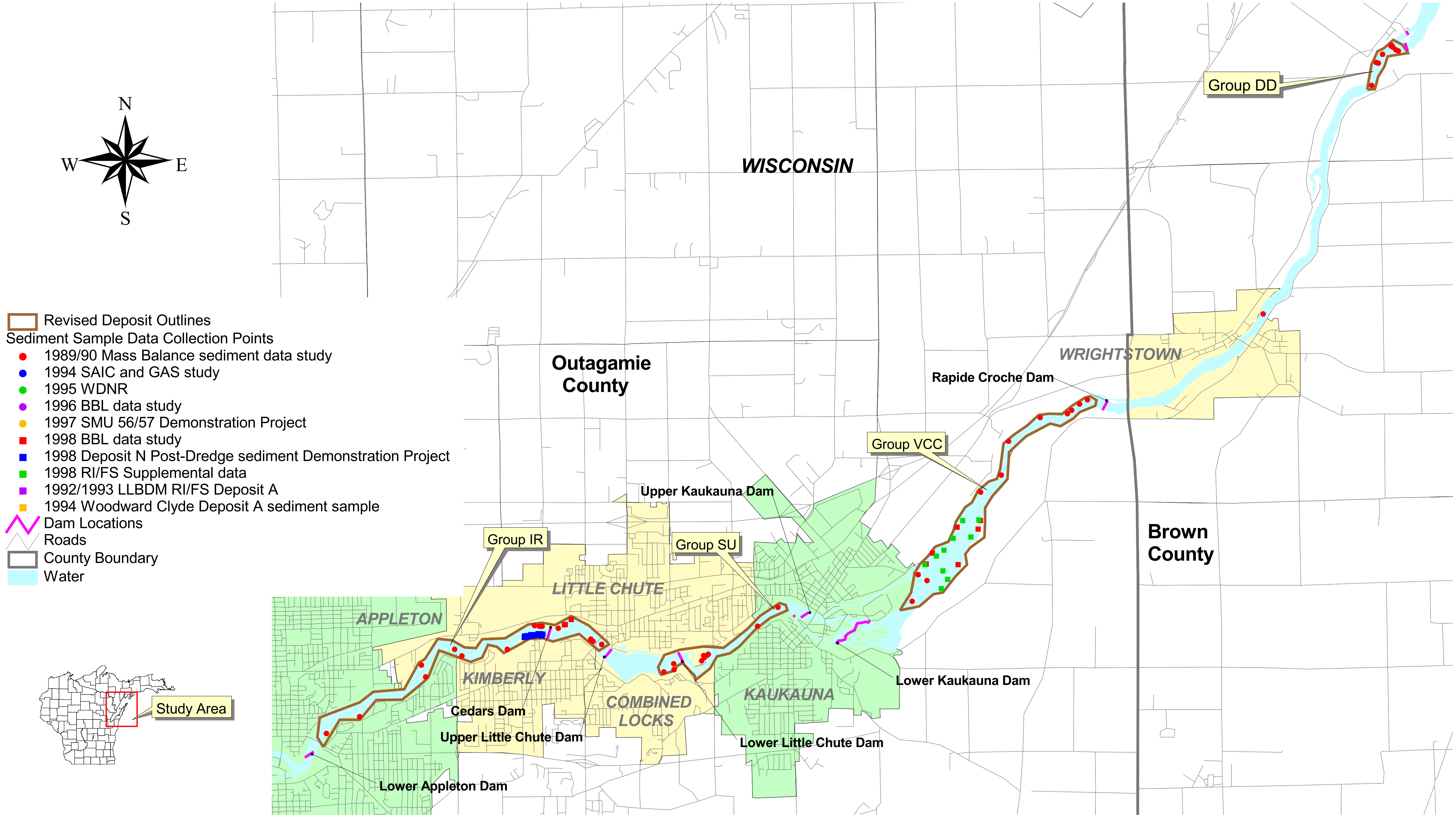

NOTES:
1. Basemap generated in ArcView GIS, version 3.2 , 1998, and TIGER census data, 1995.
2. Sediment sample point data obtained from Wisconsin Dept. of Natural Resources, 1999, and are included in the Fox River database.
3. Revised deposit outlines created by Nayak Polissar, Mountain-Whisper-Light Statistical Consulting, and Stephen Jesse, ThermoRetec Engineering Consultants, 2000.

1 0 1 2 3 Kilometers

1 0 1 2 Miles

ThermoRetec	Natural Resource Technology	Risk Assessment	Sample Point Groups for Sediment Time Trend Analysis: Appleton to Little Rapids	FIGURE NO: RA-14414-425-2
				PRINT DATE: 1/23/01
				CREATED BY: SCJ
			FIGURE 6	APPROVED: AGF

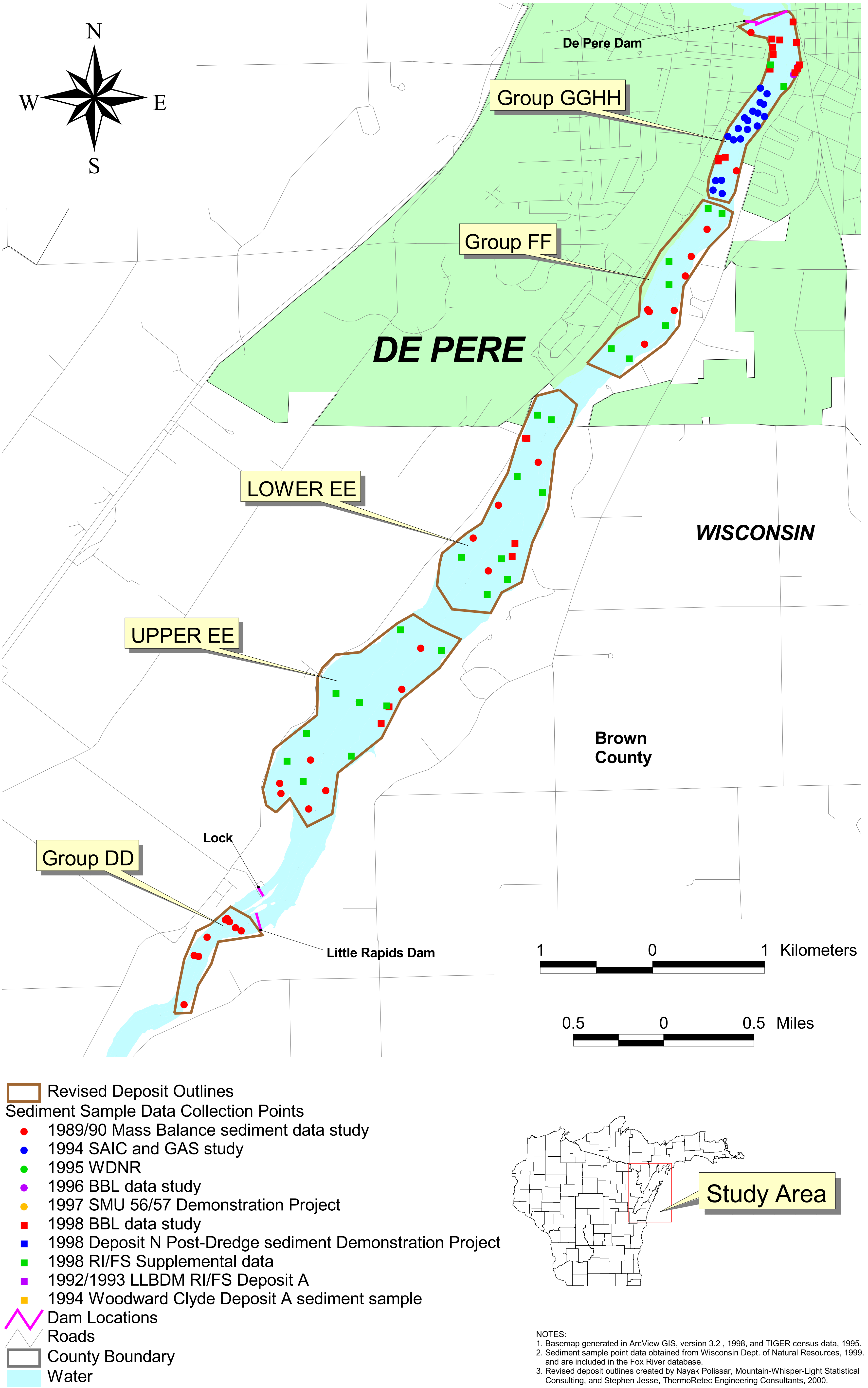

NOTES:
1. Basemap generated in ArcView GIS, version 3.2 , 1998, and TIGER census data, 1995.
2. Sediment sample point data obtained from Wisconsin Dept. of Natural Resources, 1999. and are included in the Fox River database.
3. Revised deposit outlines created by Nayak Polissar, Mountain-Whisper-Light Statistical Consulting, and Stephen Jesse, ThermoRetec Engineering Consultants, 2000.

ThermoRetec Smart Solutions. Positive Outcomes.	Natural Resource Technology	Risk Assessment	Sample Point Groups for Sediment Time Trend Analysis: Little Rapids to De Pere	FIGURE NO: RA-14414-425-3
				PRINT DATE: 1/23/01
				CREATED BY: SCJ
			FIGURE 7	APPROVED: AGF

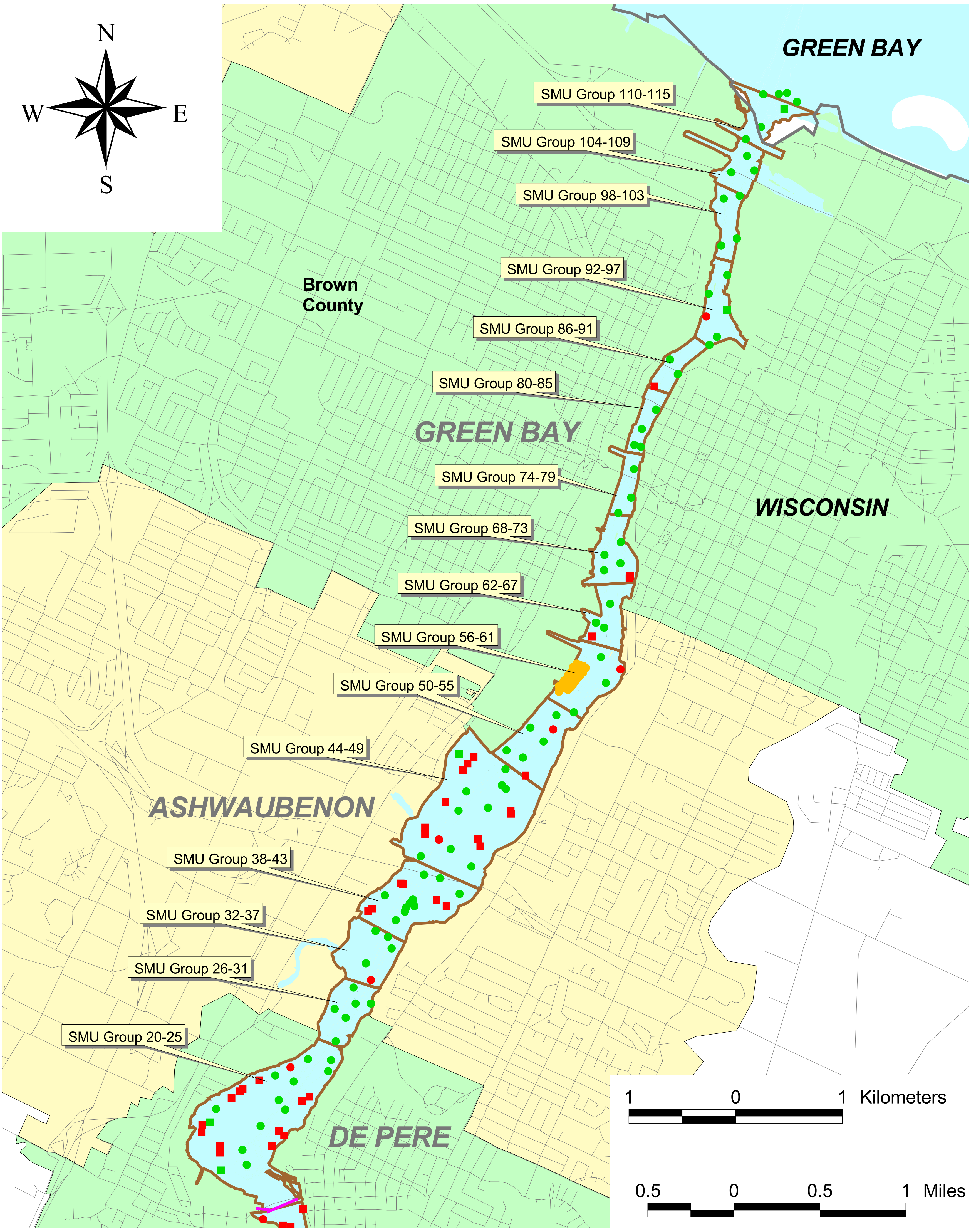

SMU Deposits

Sediment Sample Data Collection Points

- 1989/90 Mass Balance sediment data study
- 1994 SAIC and GAS study
- 1995 WDNR
- 1996 BBL data study
- 1997 SMU 56/57 Demonstration Project
- 1998 BBL data study
- 1998 Deposit N Post-Dredge sediment Demonstration Project
- 1998 RI/FS Supplemental data
- 1992/1993 LLBDM RI/FS Deposit A
- 1994 Woodward Clyde Deposit A sediment sample

Roads

County Boundary

Water

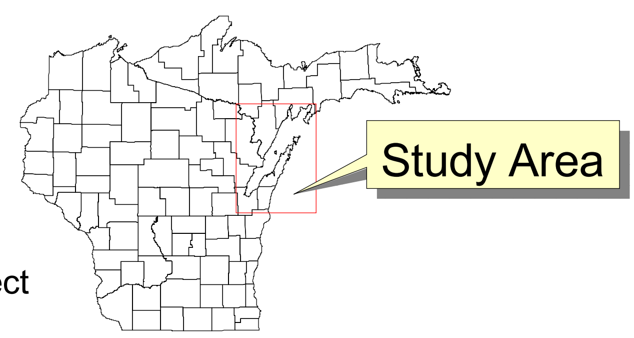

NOTES:
1. Basemap generated in ArcView GIS, version 3.2 , 1998, and TIGER census data, 1995.
2. Sediment sample point data obtained from Wisconsin Dept. of Natural Resources, 1999. and are included in the Fox River database.
3. Revised deposit outlines created by Nayak Polissar, Mountain-Whisper-Light Statistical Consulting, and Stephen Jesse, ThermoRetec Engineering Consultants, 2000.

ThermoRetec Smart Solutions. Positive Outcomes.	Natural Resource Technology	Risk Assessment	Sample Point Groups for Sediment Time Trend Analysis: De Pere to Green Bay	FIGURE NO: RA-14414-425-4
				PRINT DATE: 1/23/01
				CREATED BY: SCJ
			FIGURE 8	APPROVED: AGF

Figure 9 through Figure 12, show the location of each sample in a rectangular coordinate system devoid of map features. The "northing" and "easting" rectangular coordinates locate each sample along a north-south and east-west axis, respectively, based on a standard geographic coordinate system for Wisconsin State. Northing and easting are expressed in meters relative to an origin not shown on the plot.

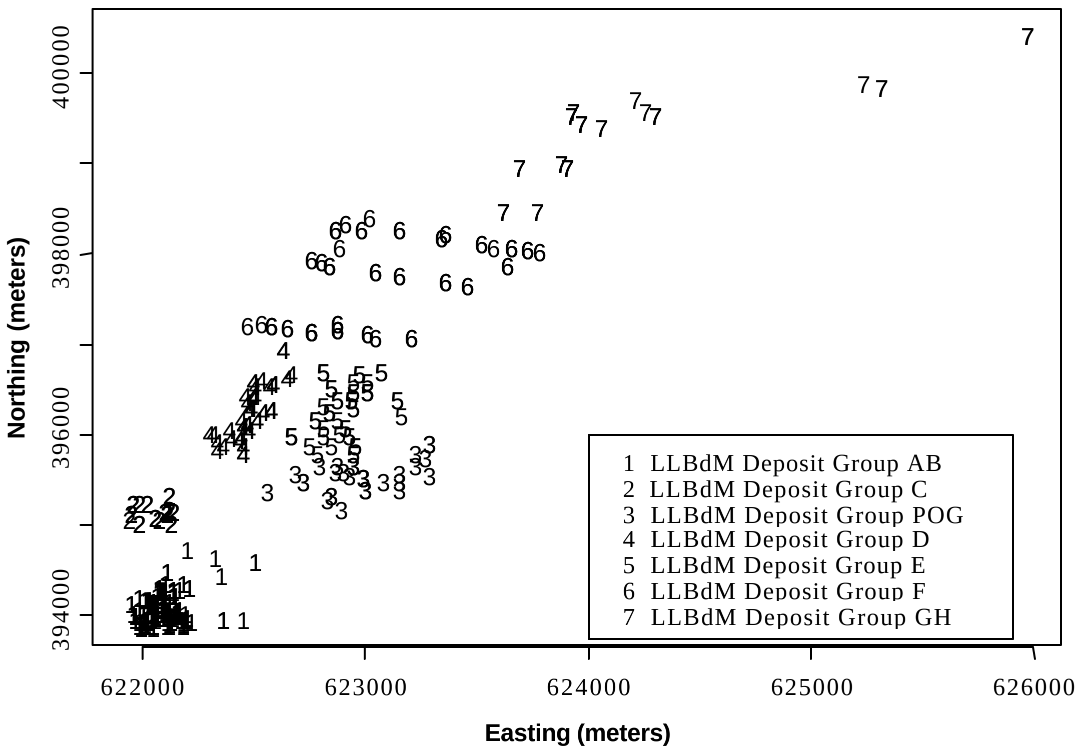

Figure 9 Locations of Deposit Groups in Little Lake Butte des Morts Reach

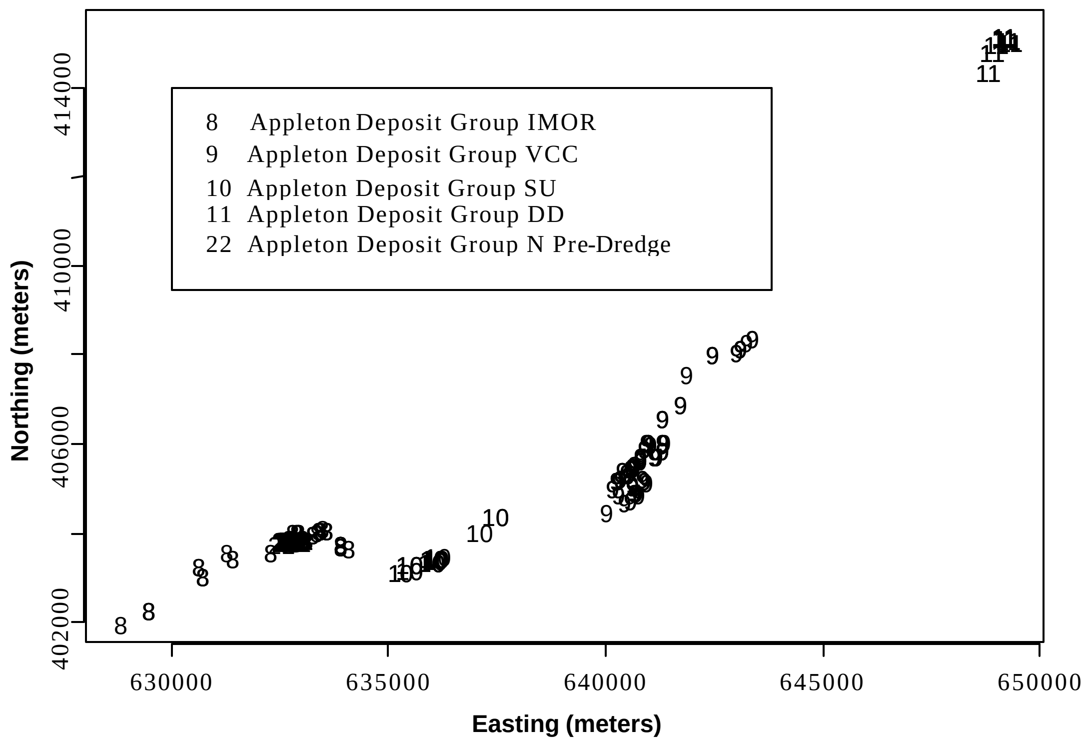

Figure 10 Locations of Deposit Groups in Appleton Reach

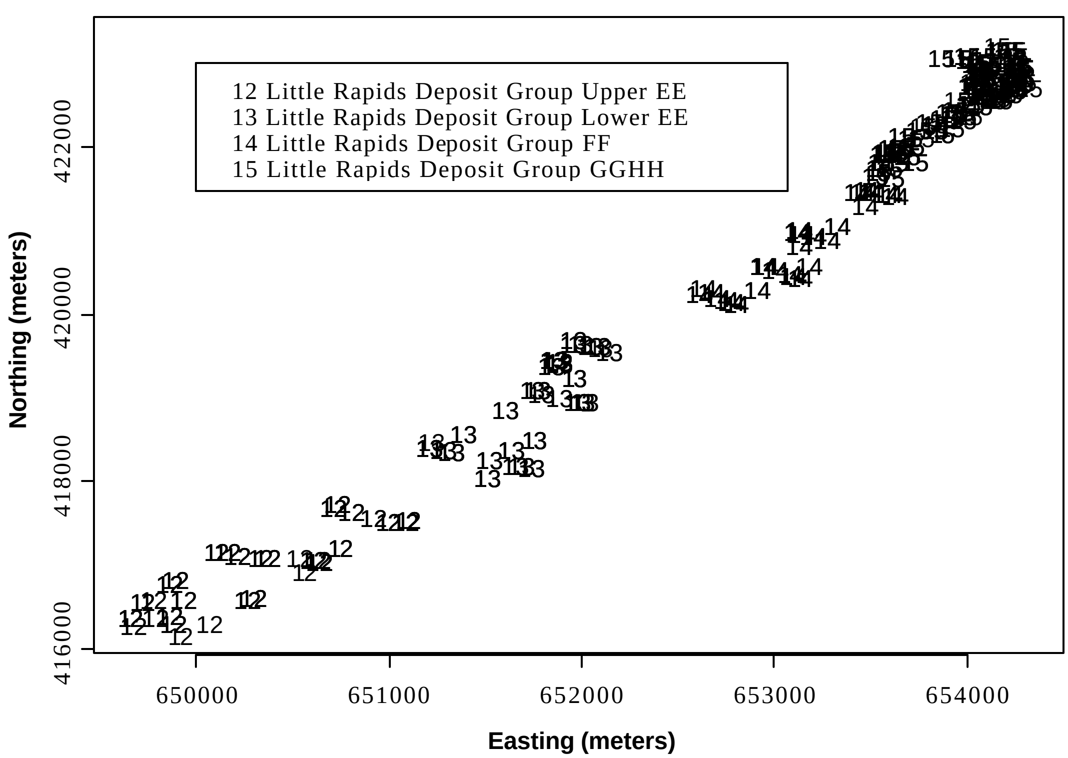

Figure 11 Locations of Deposit Groups in Little Rapids Reach

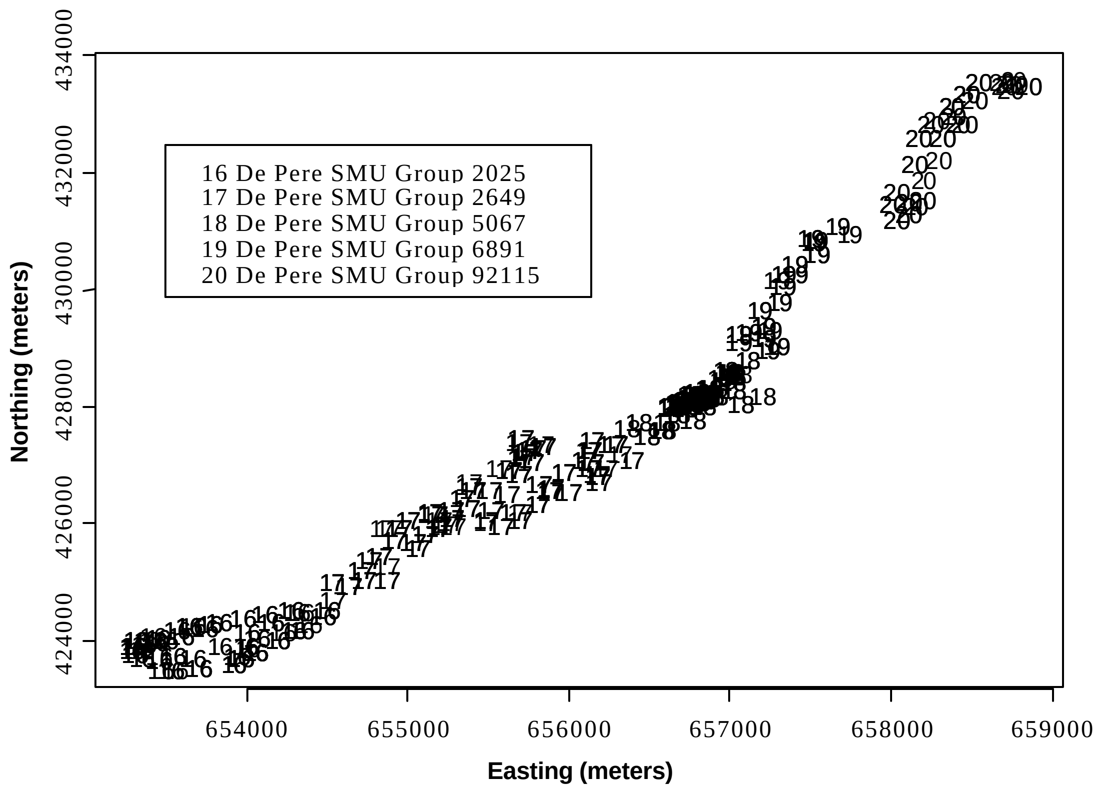

Figure 12 Locations of Deposit Groups in De Pere Reach

2.6 Models for Variation in PCB Concentration in Space and Time

Because PCB concentrations vary spatially as well as over time, we included spatial dimensions in our regression models. To characterize the spatial component in the models, we used linear and quadratic variables for "easting" and "northing" coordinates (east and north distances in meters) and a linear term for depth. For every stratum, depth was measured from a value of zero at the top of the 0- to 10-cm layer. Depth, thus, means simply distance from the surface of the river sediment at the time the sample was taken. We centered the northing and easting coordinates for each depth stratum in each deposit group. "Centering" involved finding the spatial centroid of the samples used in the regression analysis for the specific deposit group and depth stratum. Given a set of northing and easting coordinates, the sample centroid sits at the mean of the northing and easting coordinates. We produced the centered northing (N) and easting (E) coordinates by subtracting the centroid from the northing and easting coordinates of each sample.

Under this new coordinate system, the centroid of each deposit group at each depth stratum is the origin of a coordinate system with coordinates (0, 0). By centering, one avoids round-off problems when using the fitted regression models. Without centering, calculating a fitted concentration would involve subtracting a very large number from a second large number. The difference of interest (a log PCB concentration) is usually relatively close to zero. Thus, the later digits for the two large numbers must be tabulated accurately. A simple hypothetical example illustrates this point. Let us ignore time and consider only easting, where an equation

$$\log_{10} PCB = 2.24 + 0.016E_c$$

indicates that $\log_{10}$ PCB concentration increases by 0.016 for each meter to the east of the centroid of a deposit group. At the centroid, the $\log_{10}$ PCB concentration is 2.24 (the value of the intercept). *E* is the centered easting coordinate. If E^* is the original (uncentered) easting coordinate and the deposit group centroid E^* mean = 622,347 meters (a realistic value for this study), then the equation for $\log_{10}$ PCB concentration with the original easting coordinate would be

$$\log_{10} PCB = -9955.312 + 0.016E^*.$$

If this cumbersome second equation is used with E^* = 622,347 (the centroid), $\log_{10}$ PCB = 2.24 is calculated accurately for the centroid location. However, if –9955.312 is casually rounded to 9955, an estimate of 2.552 is obtained (instead of the correct 2.24), off by +0.312 units, which, on the natural scale (not log), corresponds to approximately a doubling of the concentration. Thus, centering helps computation and presentation. For the same reason, time was measured from January 1, 1989, taken as *time* = 0.

The specific regression model fitted to the PCB concentrations was:

Equation 2

$$\log_{10} PCB = b_0 + b_t \cdot t + b_D \cdot D + b_E \cdot E + b_N \cdot N + b_{E2} \cdot E^2 + b_{N2} \cdot N^2$$

where

$\log_{10}$ PCB	=	the logarithm (base 10) of the PCB concentration in µg/kg (ppb) by weight,
t	=	time in years since January 1, 1989,
D	=	depth in centimeters from the sediment-water interface,
E	=	the centered easting coordinate for the particular deposit group and depth stratum (meters), and
N	=	the centered northing coordinate (meters).

The intercept is b_0 and b_t, b_D, etc., are regression coefficients. E^2 and N^2 are the quadratic terms for centered easting and northing.

Based on scatter plots of PCB concentrations versus easting coordinate or northing coordinate, we included the quadratic terms (E^2 and N^2) for easting and northing in the regression models whenever we analyzed at least 20 samples. For sample sizes smaller than 20, we included the quadratic terms whenever we suspected a potential curvilinear trend of $\log_{10}$ PCB concentration versus northing or easting.

We note that we included up to five variables to describe spatial variation: D, E, N, E^2, and N^2. These five variables are sometimes needed to describe five unique kinds of spatial variation in concentrations of PCBs: linear trends in depth, easting and northing, and curvilinear trends in easting and northing. When there is a deposit group and stratum with little variation in one of these variables (e.g., little curvilinear trend in the easting direction), then the coefficient of that variable will be zero or close to zero, and it is virtually harmless to include it in a model. Because of widely varying sample sizes, we did not wish to tailor the spatial model to each deposit group and stratum; in some cases, the small sample sizes yield insufficient power to formally accept or reject a given type of spatial variation, such as curvilinearity. Due to low power to detect the need for variables for the spatial dimensions, one errs on the side of safety by including all, rather than erroneously excluding some. With fewer than 20 observations, however, we were concerned about over-fitting models to the data. (See discussion of over-fitting in the context of fish analysis, Section 5.2.1, subsection on Green Bay Zone 2.) Thus, we included the curvilinear terms (E^2 and N^2) only in the face of a visually apparent curvilinear trend in diagnostic plots (see below). We note that, regardless of their number, including appropriate spatial variables in a regression model increases the power to detect time trends notwithstanding a slight possibility that inappropriately including extra spatial terms could decrease power if there are correlations between space and time variables.

In addition to the spatial variables in the regression models, we introduced time as a simple linear term in all analyses. In each analysis, there was an insufficient number of distinct times of sampling to implement a curvilinear model for time. For this brief discussion, we considered a “distinct” time of sampling as a period of several months, or even a year, with at least two samples taken (see Figures A-44 through A-89, upper left panel). Of the 46 analyses ultimately carried out (specific combinations of deposit group and depth), 23 had observations at only two distinct points in time (e.g., 1989 and 1998), 20 had observations at three points in time, and 3 had observations at four points in time.

The dependent variable in all analyses was the $\log_{10}$ PCB concentration with a companion variable indicating whether the observation was below the detection limit or was a detected concentration. We examined residual plots for all regression analyses to detect outliers and assess the assumption of normality. Table 5 notes the removal of only one exceptional value from the formal sediment regression analysis. This sample is considered in the context of time trends in the results section.

Table 5 Sample Removed from Time Trends Analysis

Database ID	Reach	Original Deposit	Time Trends Deposit Group	Depth	Total PCBs (ppb)
A3_0-4	De Pere	SMU56/57	SMU Group 5067	0–10 cm	99,000

Note:
Other PCB values range from 400 to 7,800 in this depth stratum and SMU group.

Figure 13 through Figure 17 show examples of plots we used to determine choice of linear or quadratic terms for northing and easting in the regression models. The plots also show log PCB concentration versus time and log PCB concentration versus depth. We added a "smoother" line to the plots to depict the general trend for these variables taken one at a time. As can be noted in some of the plots, a common structure of the deposit groups shows PCB concentrations rising from minima at one or both sides of the deposit group to a maximum in the middle (e.g., see Figure 17). The quadratic terms (E^2 and N^2) for northing and easting in the regression models capture this curvilinear trend. Separate plots evaluate each variable (time, depth, easting, northing), though a single regression model uses them all.

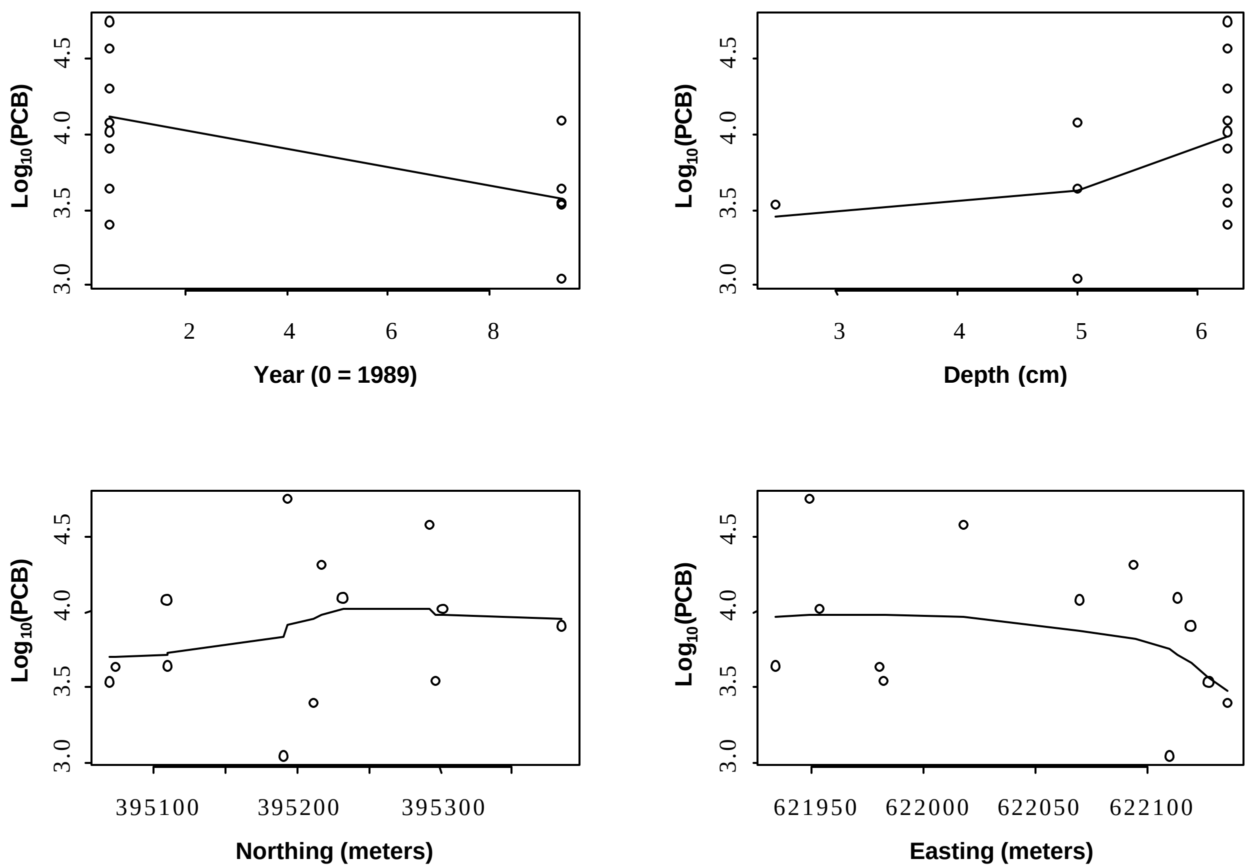

Figure 13 Log$_{10}$ PCB Concentration versus Time, Depth, Northing and Easting for Little Lake Butte des Morts Deposit Group C (0 to 10 cm) Including Fitted Smoothed Line

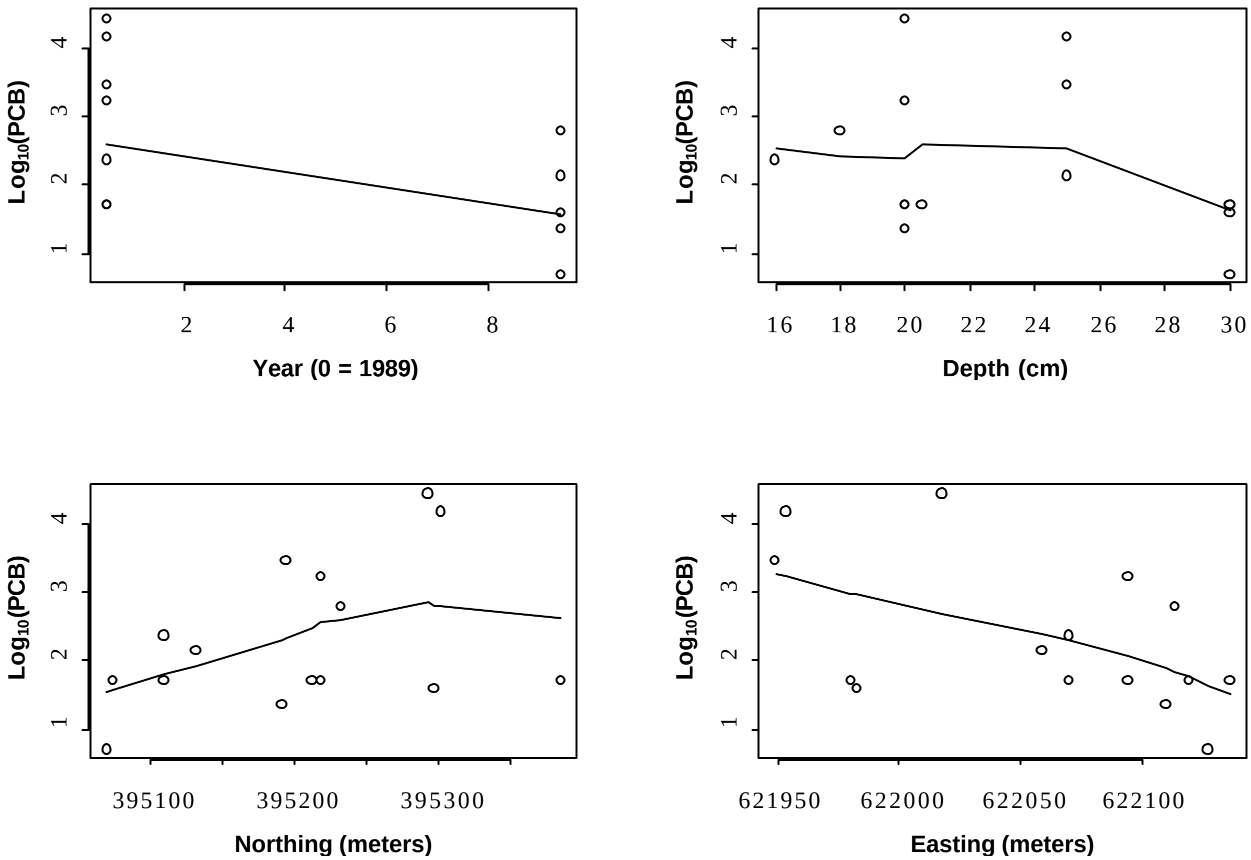

Figure 14 Log$_{10}$ PCB Concentration versus Time, Depth, Northing and Easting for Little Lake Butte des Morts Deposit Group C (10 to 30 cm) Including Fitted Smoothed Line

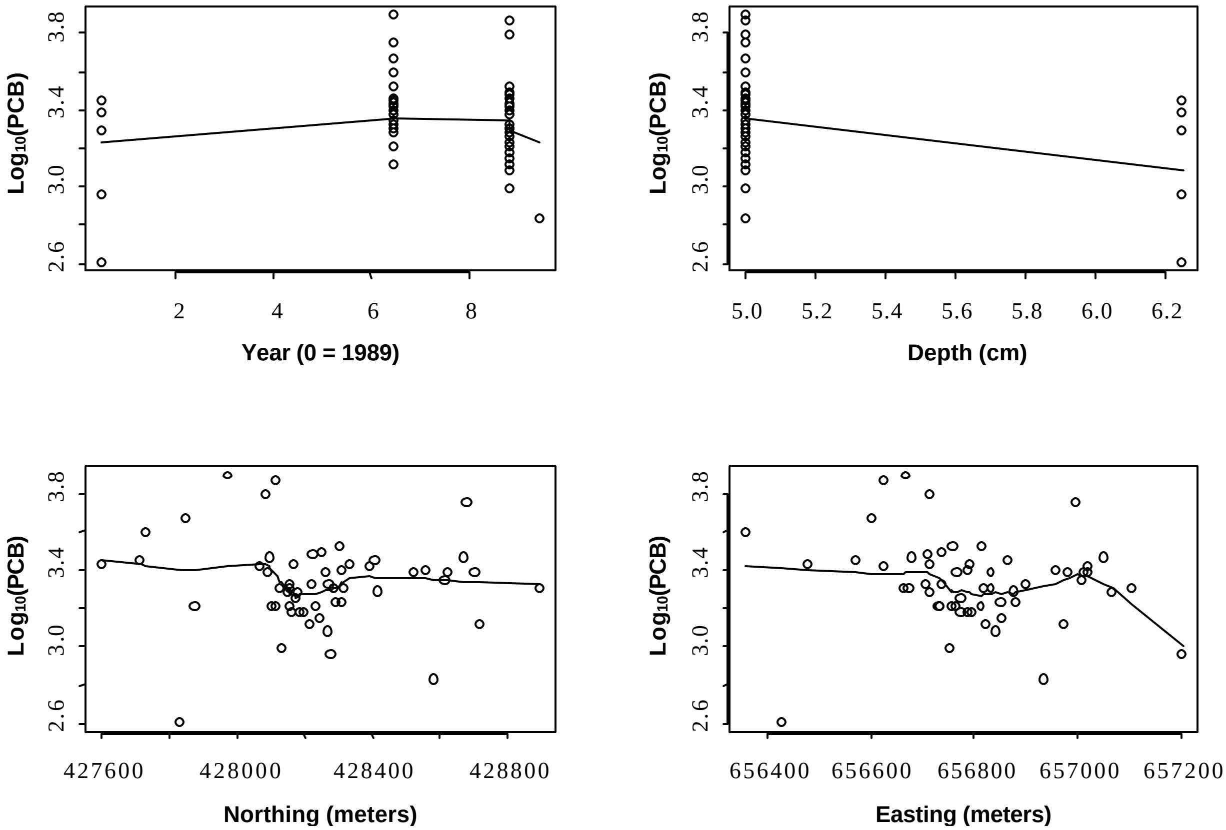

Figure 15 Log$_{10}$ PCB Concentration versus Time, Depth, Northing and Easting for De Pere SMU Group 5067 (0 to 10 cm) Including Fitted Smoothed Line

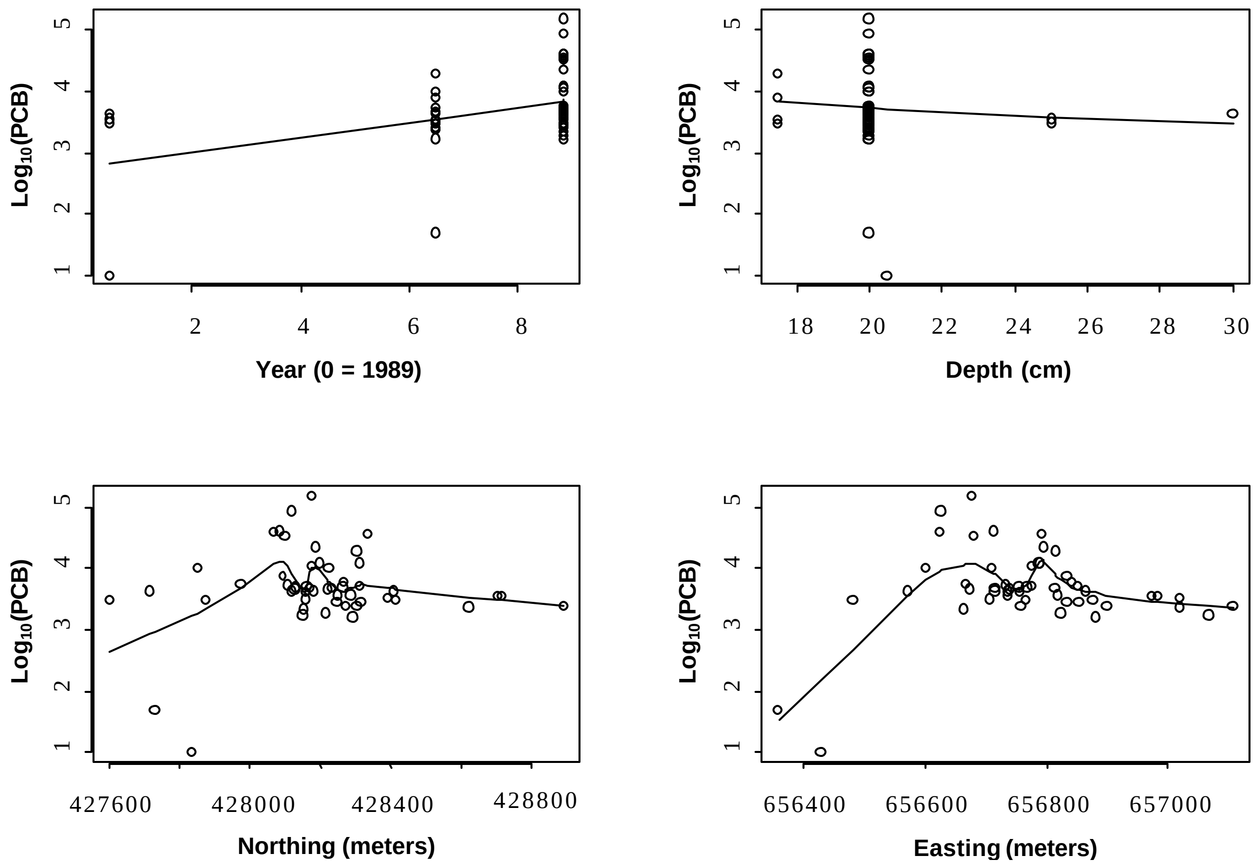

Figure 16 Log$_{10}$ PCB Concentration versus Time, Depth, Northing and Easting for De Pere SMU Group 5067 (10 to 30 cm) Including Fitted Smoothed Line

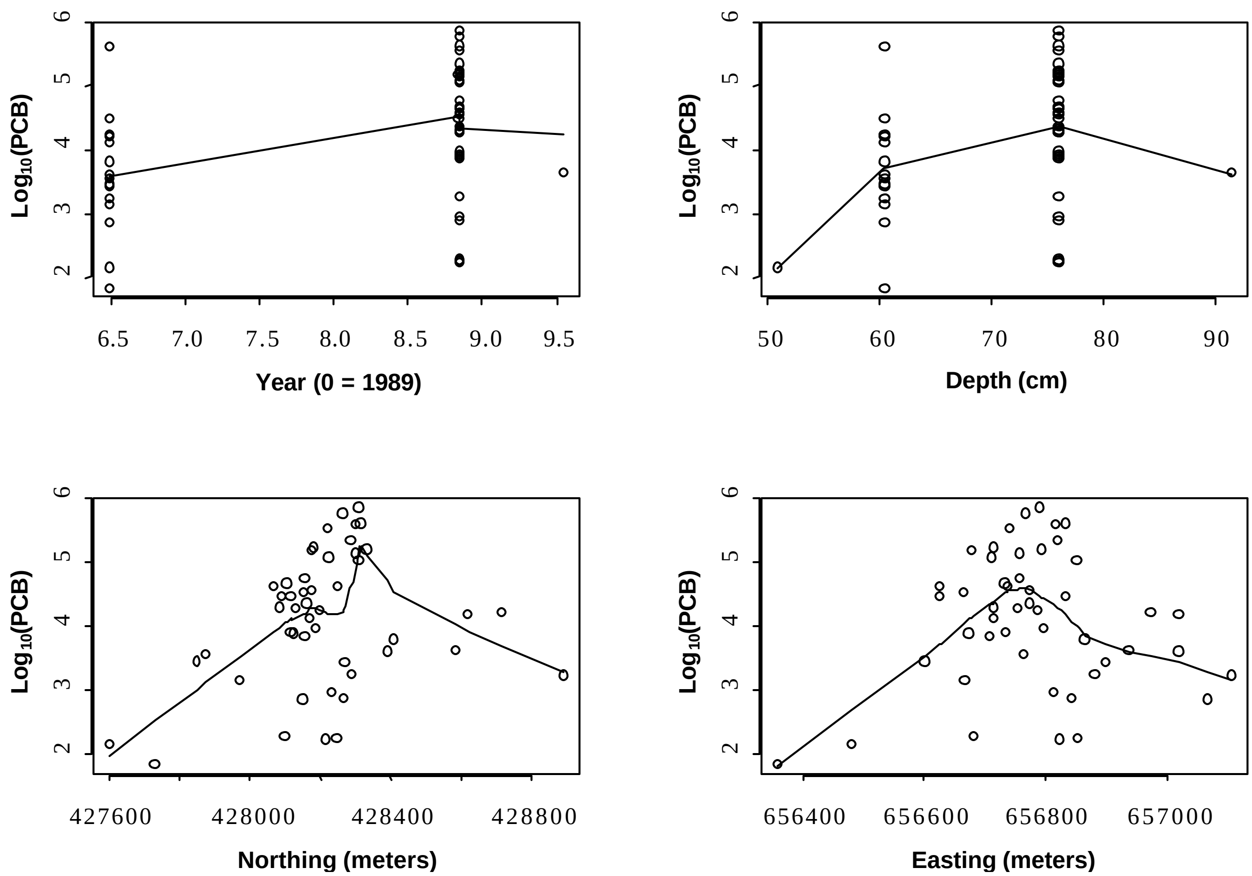

Figure 17 Log$_{10}$ PCB Concentration versus Time, Depth, Northing and Easting for De Pere SMU Group 5067 (50 to 100 cm) Including Fitted Smoothed Line

PCB concentration shows strong spatial variation, as shown on Figure 13 through Figure 17 and in the Appendix (i.e., space and PCBs are correlated). Controlling for spatial variation in the analysis allows for proper estimation of time trends in PCB concentrations. Similarly, the date and location of sampling may be correlated. These correlations can induce a spurious correlation between PCB concentration and time. This might happen, for example, if early samples were taken in the "hotter" location of a deposit (higher PCB concentrations) and later samples were drawn from a "cooler" location.

In order to determine the extent of the time-location correlation (which might create false time trends), we calculated the Pearson correlation coefficient between time and spatial variables. This correlation coefficient is +1.0 for perfect positive correlation, –1.0 for perfect negative correlation, and 0.0 (zero) if no correlation exists. We encountered a number of statistically significant correlations between the time that samples were drawn and either their depth within the stratum, their easting (centered) or easting-squared coordinates, or northing or northing-squared. Among the 46 combinations of deposit group and depth we analyzed, 22 had statistically significant correlation coefficients between time and depth, eight between time and easting or easting-squared, and nine between time and northing or northing-squared. Among all the correlations between time and spatial coordinates, one-quarter were of magnitude 0.3 or larger, and 10 percent of the correlations were of magnitude 0.5 or larger (corresponding to a moderate correlation or stronger), with a maximum observed correlation of 0.97. These numerous non-zero correlations between time and the spatial variables show the importance of controlling for spatial variables, lest spatial trends in the time of sampling combine with spatial trends in PCB concentrations to induce false time trends in PCB concentrations.

The values of $\log_{10}$ PCB also correlate with spatial coordinates. Again, among 46 analyzed combinations of deposit group and depth, six had statistically significant Pearson correlations between $\log_{10}$ PCB and depth within the stratum, 18 between $\log_{10}$ PCB and easting or easting-squared, and 10 between $\log_{10}$ PCB and northing or nothing-squared. The 75^{th} and 90^{th} percentile and maximum of all of the correlations of $\log_{10}$ PCB with spatial coordinates were of magnitude 0.3, 0.5 and 0.7, respectively. Peppered throughout these data are significant spatial trends either in time of sample acquisition or in PCB concentration. Thus, it behooves the analyst to include spatial variables in regression models for time trends of PCB concentrations in order to minimize the opportunity for a spatial trend in PCB concentration to masquerade as a time trend. (For purposes of exploring these correlations, concentrations below detection limits entered the analysis with the value of the detection limit. These limits and actual PCB concentrations were all log-transformed and used in the calculation of correlations.)

We also carried out an inspection of visual displays to detect glaring shifts over time in location of samples within a deposit group.

Figure 19 displays an example of these plots, showing northing and easting location of each sample, for each depth stratum, and for two time periods for Little Lake Butte des Morts Deposit Group AB. The key to interpretation of symbol size is included as Figure 18. Circles and squares indicate measured concentrations and concentrations below detection limits, respectively, and the size of the symbol indicates the magnitude of the PCB concentration. The upper row of the figure shows northing and easting location of each sample taken during 1989 through 1993 and the lower row corresponds to a later period, 1994 through 1999.

Working through the 0- to 10-cm plots (Figure 19, upper and lower left panels) as an example will help to clarify the role of space and its interaction with PCB concentrations and time. This is intended as a descriptive exploration. Note that in the 0- to 10-cm stratum, a larger fraction of early samples (upper panel, 1989–1993) occurs in the north of the deposit group than samples taken in the later period (lower panel, 1994–1999). Correlation coefficients can help to summarize such trends. The Pearson correlation coefficient ranges from $r = -1$ (perfect negative association) to $r = +1$ (perfect positive association). In a scatter plot, when $r = +1$, all points would fall on an upward sloping straight line. A correlation of $r = 0$ means no association between two variables. The correlation of the time of sampling and the northing coordinate is $r = -0.3$ ($p = 0.02$, statistically significant), indicating that sampling locations have a southward trend across the deposit over time. The correlation coefficient is negative because later ("larger") sampling times tend to occur with smaller northing coordinates. Smaller northing coordinates are farther south than larger ones. Also, earlier samples (upper plot) spread out more in the east and west directions than the samples from the later period (lower plot). The statistically significant correlation of –0.3 ($p = 0.03$) between time of sampling and the centered easting-squared term provides evidence for this. Over time, therefore, the sampling effort became more concentrated toward the south and west-center of this deposit group. This shift readily appears by comparing the upper and lower panels of Figure 19. In statistical parlance, time and spatial coordinates are confounded (and correlated). It is important to control for one when examining the role of the other.

We also found strong and highly significant spatial trends in $\log_{10}$ PCB concentrations. The correlation between $\log_{10}$ PCB concentration and easting is $r = -0.6$ ($p < 0.0001$). The negative correlation indicates that PCB concentration generally decreases from west to east. The correlation is $r = --0.5$ ($p < 0.0001$) for easting-squared, meaning that PCB concentrations decrease from the middle of the deposit to the east and west. The correlations of $r = -0.5$ ($p < 0.0001$) for northing, and $r = -0.6$ ($p < 0.0001$) for northing-squared, have similar interpretations to those just offered. The strong correlation of PCB concentration with linear and curvilinear (quadratic) spatial dimensions suggests a deposit group with a peak concentration near one edge of the area sampled. Concentrations taper off on all sides, but particularly to the east and north. In the upper plot for the 0- to 10-cm stratum (still Figure 19), the smaller circles toward the upper right corroborate this trend. Given that the PCB concentrations in the 0- to 10-cm stratum of Little Lake Butte des Morts Deposit Group AB have a distinct spatial structure, we have incorporated that structure in our model for a time trend in this deposit group. We also note that Figure 19 presents two time periods although time in the continuous form has been used in the analysis of time trends.

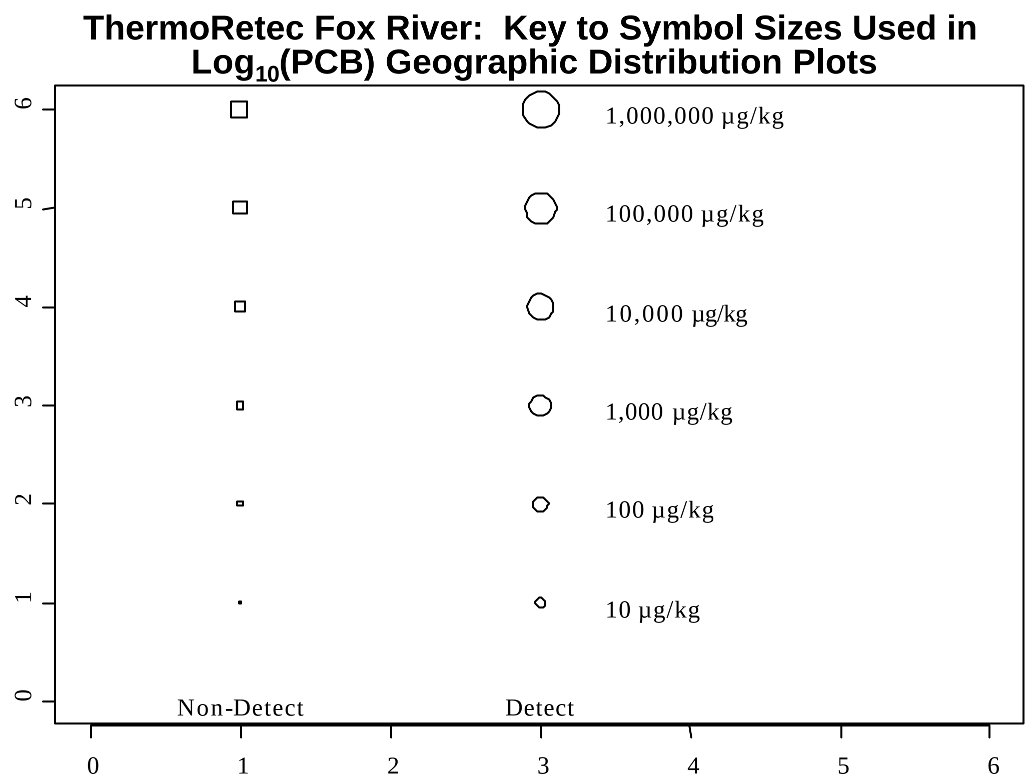

Figure 18 Northing/Easting Plot Key

Scale plot showing the size of circles (for samples with detected PCBs) and squares (for samples with PCBs below detection limit, the square conveys the level at which the PCBs would have been detected as reported by the various testing agencies) used to convey total PCB concentration in the northing/easting plots of sample locations.

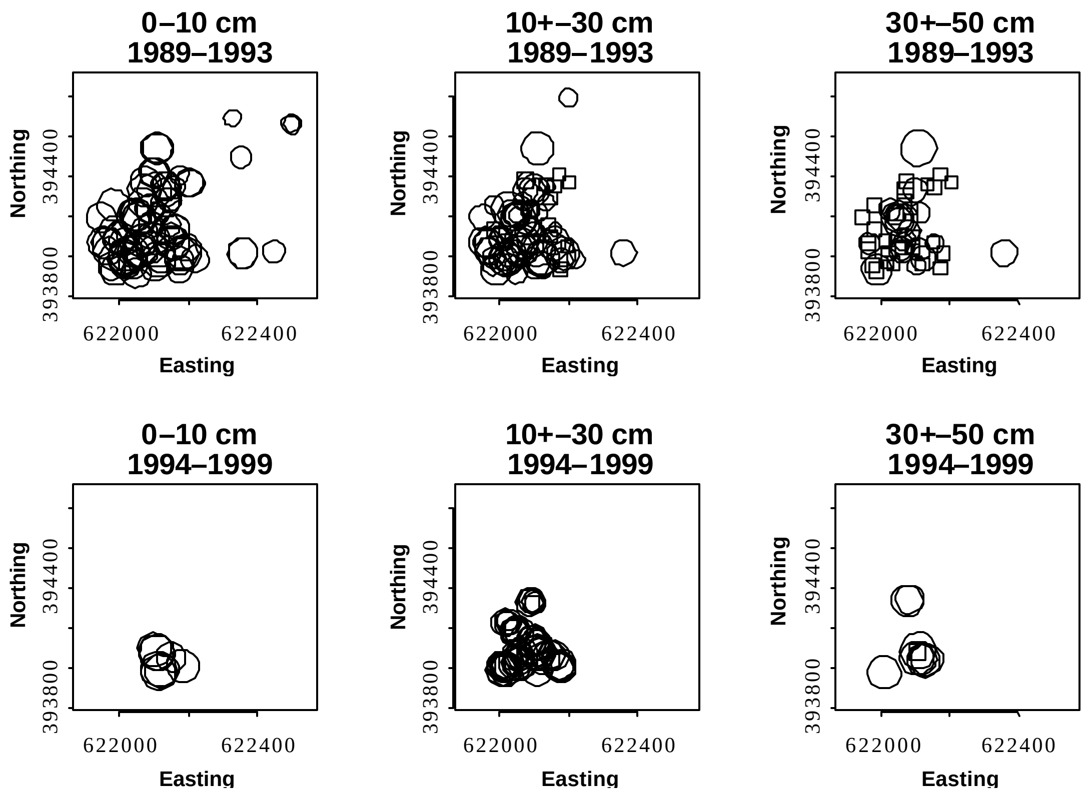

Figure 19 Sample Locations by Northing and Easting Coordinates During 1989–1993 and 1994–1999, Depth Strata of Little Lake Butte des Morts Deposit Group AB

Larger symbols indicate higher concentrations. Circles (○) indicate measured concentrations and squares (□) indicate the detection limit of concentrations below the detection limit. Coordinates are in meters.

3 Methods for Fish Analysis

For the reasons discussed earlier ("Logarithmic Transformation," Section 2.1.3), we used the log of PCB concentration as the outcome variable in all the regression models fitted. There are good reasons for using the log transformation. Expressing rate of change as percent change per year has more meaning than absolute change in concentration, which can lead to absurd negative concentration predictions. An analysis on the $\log_{10}$ scale corresponds to modeling percent change. The data have an approximately normal distribution on the log scale, but a strongly skewed distribution on the original scale.

We included two potential confounding factors in all regression models for $\log_{10}$ PCB concentration versus time: percent lipid in the sample by weight and seasonality. As described below in the results section, both of these factors added significantly to prediction of PCB concentrations in most analyses. The following paragraphs describe how we incorporated these two factors into the models. We could not introduce any procedures to handle spatial dependence of fish data due to the lack of easting and northing coordinates for the fish samples in each reach. Not being able to model or investigate spatial dependence of fish samples does not imply the absence of such dependence. We simply have no means to study or address it. Because fish move more than sediments do, we expect that fish samples are closer to independent than sediment samples.

3.1 Lipid Normalization

Analyses of PCB concentration in fish often utilize "lipid normalization" in order to account for the relationship between PCB concentration and percent lipid in fish tissue. PCBs tend to concentrate in fat tissue so that, in general, fatter fish have higher concentrations of PCBs per total weight than leaner fish. The direct lipid normalization commonly used consists of dividing the PCB concentration by the percent lipid content (by weight) of the sample. This results in a variable showing PCB concentration per unit weight of lipid. We have chosen a somewhat different approach, similar to that of Larsson *et al.* (1993) and Herbert *et al.* (1995). We regard the lipid variable as an independent variable rather than a direct divisor of the PCB concentration. This approach allows the data itself to specify the relationship of PCBs to lipids. The model we use is:

Equation 3

$$\log(PCB) = b_0 + b_1 \log_{10}(lipid) + \ldots + e$$

where

b_0 = the intercept term,
b_1 = the regression coefficient on log of percent lipid,
e = random error, and

additional variables such as time are included in the model as well (the time variable is considered below).

This model yields a predicted value for PCB concentration per unit tissue weight. Since the public consumes fish tissues (rather than just the lipid in the tissue), this offers a more useful prediction in many applications than the other normalization based on PCB per unit of lipid content.

An interesting fact should be noted about this model for PCB concentration (Equation 3). The model can be directly compared to the traditional "lipid normalization." Subtracting log(*lipid*) from both sides of Equation 3 gives the equivalent model:

Equation 4

$$\log_{10}\left(\frac{PCB}{lipid}\right) = b_0 + (b_1 - 1)\log_{10}(lipid) + \ldots + e$$

Comparing the two (Equation 3 and Equation 4), one clearly sees that as long as we treat log of percent lipid as a predictor, then it does not really matter whether we lipid-normalize the PCB concentration on the left-hand side of the equation or use PCB concentration without lipid normalization. Except for the coefficient for log of percent lipid differing by 1, all other coefficient and standard error estimates will remain unchanged. An analysis that has log of lipid-normalized PCB concentration on the left-hand side (such as in Equation 4), but does not include log of percent lipid on the right-hand side, amounts to forcing b_1 to be 1, so that $b_1 - 1$ will be zero. If direct lipid normalization represents the best model for the observed data, then we will estimate b_1 close to 1 in the regression approach. It is an advantage of the regression approach, model 3, that it will reduce to the direct lipid normalization if that is the correct model for the data considered in a given analysis. If PCB concentration and percent lipid do not have a directly proportional relationship, then we will estimate b_1 as something different than 1 (usually less than 1, as seen in the results below).

3.2 Seasonality

To account for the possibility that PCB concentration may vary by time of year, we incorporated into the model a sine curve as a function of the time of year.

Equation 5

$$\log_{10}(PCB) = b_0 + b_1 \log_{10}(lipid) + b_2 \sin(2p\ t^*) + b_3 \cos(2p\ t^*) + \ldots + e$$

where

t^* = time of year expressed as a fraction between 0 and 1.

Trigonometry shows that the weighted sum of the sine and cosine function in this equation gives a sine curve with a maximum at the time arctangent($-b_2/b_3$) and an amplitude equal to $(b_2^2 + b_3^2)^{0.5}$. We present these more meaningful quantities, time of maximum and amplitude, in our results tables rather than the more abstract b_1 and b_2. The time of maximum is coded to range from 1.0 (beginning of January) to 12.999... (end of December).

We note that the true seasonal cycle in PCB concentration may not be sinusoidal. Albeit likely, the presence of some average annual pattern of rise and fall of PCB concentration may not have the shape or smoothness of a sine curve. Nevertheless, the sine curve can serve as an approximation to seasonal variation. The statistical significance of the fitted sine curve (described later) strongly suggests that this simple function helps to capture and control seasonal variation in PCB concentration in fish.

Prior to model fitting, we centered the log of percent lipid variables. This step is analogous to the centering of northing and easting coordinates described earlier in the methodology section for sediment analysis. For each combination of reach, species, and sample type, we subtracted the mean $\log_{10}$ lipid percent within that reach/species/type from the $\log_{10}$ lipid value for each sample. Table 22 of the results displays these mean values. We also centered the sine and cosine terms by subtracting off the value of the sine and cosine variables at midyear (i.e., July 1). The advantage of the centering is that for forward projection we need only use the intercept and slope coefficient from the fitted models for PCB concentrations. Then, when using the intercept term and the coefficient on final slope to predict values of PCB at future time points, we are estimating the PCB concentration for a fish with average lipid content sampled on July 1. For numerical stability in estimating the slope coefficient for time, we centered time at the beginning of 1989 by subtracting January 1, 1989 from each sample date.

3.3 Time Trend Models

The simplest model for time trend in PCB concentration is a linear relationship between log of PCB concentration and time. A negative slope corresponds to an exponential decay in PCB concentration at a constant rate (for example, 5 percent per year). The first step in our analysis involved testing whether this simple model fit the data well, for each unique combination of reach, species and sample type (whole body, or fillet with skin). In statistical terms, this means testing the null hypothesis of a constant exponential rate of decay over all years versus the alternative of decay rate that is not constant over time. To perform such a hypothesis test, one must specify an alternative model, which we consider to be a competing model for the change in PCB concentration over time.

The simple linear model has the following equation:

Equation 6

$$\log_{10}(PCB) = b_0 + b_1 \log_{10}(lipid) + b_2 \sin(2p\ t^*) + b_3 \cos(2p\ t^*) + b_5\ time + e$$

We modeled the alternative nonlinear model as a two-slope model in the form of a linear spline, which appears as two straight lines joined at a kink, or breakpoint (Cressie, 1993). This is modeled in a linear regression equation as:

Equation 7

$$\log_{10}(PCB) = b_0 + b_1 \log_{10}(lipid) + b_2 \sin(2p\ t^*) + b_3 \cos(2p\ t^*) + b_4 early + b_5 time + e$$

The variable *early* equals (*time* – *breakpoint*) if time predates the breakpoint and 0 for time after the breakpoint. The coefficient of *time* (b_5) represents the slope of log PCB concentration versus time after the breakpoint, and the coefficient of *early* (b_4) measures how much the early slope differs from the late slope. That is, the early slope equals $b_4 + b_5$ and the late slope equals b_5.

This model offers simplicity and intuitive clarity: it means that PCBs were changing at two different constant rates of change—one before and one after the breakpoint. This model has been applied to PCB and DDT concentrations in fish in the Great Lakes (De Vault *et al.*, 1996). A visual inspection of scatter plots of log PCB versus time shows that, for many reach/species/type combinations, this model gives a good representation of the pattern apparent in the data. Since the model incorporates a constant rate of change after the breakpoint (coefficient b_5), it facilitates straightforward projections of concentrations into the future.

One could fit more complex models to the data. Given the fairly small number of distinct time points at which data were collected for each reach/species/type combination, however, one can not reliably fit models containing many parameters used to describe the time effect. The linear spline model, which includes a seasonal time effect, already uses five parameters explicitly modeling change with time: two seasonal terms (sine and cosine), early and late slope, and the location of the breakpoint.

3.4 Model Fitting and Hypothesis Testing

Fitting models and testing hypotheses involved several analyses. The first key steps were: 1) finding the best-fitting linear spline model, 2) determining if the spline model (Equation 7) offered a significant improvement over a simple linear model (Equation 6), and 3) choosing a spline or simple linear model accordingly.

If the breakpoint is specified, Equation 7 is a linear regression model that can be fitted using standard statistical software that accommodates concentrations below the detection limit. We used the S-PLUS procedure CensorReg for this analysis. As described earlier for sediment samples, CensorReg uses the maximum likelihood method to estimate parameters in the model while correctly accounting for the values below the detection limit. In order to find the optimal location of the breakpoint, we fit models using different possible breakpoint locations. To reduce the computation time required to a manageable level, we considered only one breakpoint per year, on January 1 for each year across the range of data. For all analyses, the 1-year span of uncertainty in the breakpoint is small compared to the total range of the observations over time. We considered only breakpoint locations that provided data extending at least 2 years on both sides of the breakpoint. This 2-year rule would provide at least a minimum of data needed to calculate slopes before and after the breakpoint. The best linear spline model, including the optimum breakpoint location was determined using the maximum likelihood method.

The best linear spline model (Equation 7) and the simple model (Equation 6) were compared and a choice between them was made, as follows:

In comparing the two models using the maximum likelihood method, a quantity called the "deviance" is calculated. The change in deviance relates to the change in probability (i.e., improvement in fit) when extra parameters are added to a model. For a given model, the deviance is $-2 * \log(L)$, where L is the likelihood of the model, given the data, as described in the sediment methods section.

The linear spline model (Equation 7) has two additional parameters compared to the simple linear model (Equation 6)—the location of the breakpoint and the early slope difference. Under the null hypothesis, the spline model would not be a true improvement over the simple linear model. The difference in deviance between the linear model and the best linear spline model should have a chi-square distribution with two degrees of freedom if the null hypothesis is true. If the chi-square test statistic is too large, we reject the null hypothesis and accept the spline model. The spline model, if selected, includes the parameter estimates in Equation 7 and their standard errors and *p*-values based on the likelihood method. A small chi-square value prompts selection of Equation 6.

If we know the true location of the breakpoint, the method behind the S-PLUS procedure CensorReg produces correct standard errors and *p*-values for slopes and other parameters in the spline model, which are reported in the tables. As the breakpoint is not known with absolute certainty, the data are used to estimate it. Thus, the reported standard errors and *p*-values for the intercept, time trend slopes, and other coefficients in a model based on Equation 7 do not account for the additional variance due to the estimated breakpoint location. Without compensating for the uncertainty in the breakpoint, the *p*-values and standard errors for other parameters are too small. Through bootstrapping, we could compute more accurate standard errors. We did not use the quite computer-intensive bootstrap given the resources available to the project. Instead, we used a more informal sensitivity analysis to determine the role of the breakpoint in slope estimates. This analysis tells us how sensitive the conclusions concerning time trend slopes are to shifts in the breakpoint.

As part of the breakpoint sensitivity analysis, we initially created a plausible range of breakpoints for those combinations of species, reach, and sample type where a spline model (Equation 7) fit significantly better than the simple linear model (Equation 6). We considered as plausible all breakpoints having a value of the likelihood that was close to the value of the likelihood at the best breakpoint, in that they fit the data almost as well as the best breakpoint. Formally, we settled on the plausible range of breakpoints as starting from the earliest and ending at the latest breakpoint year with a deviance within 3.84 of the best model. The value 3.84 corresponds to a *p*-value of 0.05 for a chi-square test with one degree of freedom and is analogous to testing whether the alternative breakpoint (and its associated early and late slopes and other parameters) fits the data significantly worse than the best breakpoint.

3.5 Testing for a Constant versus a Changing Final Slope

The fitted models assume that PCB decreases at a constant rate on the log scale (i.e., linear on the log scale) after the breakpoint, or for the entire range if there is no breakpoint. We tested the appropriateness of this assumption by fitting a model that includes a quadratic term in time for the interval after the breakpoint. This analysis simply adds a term to Equation 6 that is $b_6 \cdot (time^2)$ for time after breakpoint or $b_6 \cdot (0)$ for time before the breakpoint. This model allows for a curved rather than a linear relationship of log PCB concentration with time. A significant *p*-value for this quadratic term indicates that the curved model fits better than the model that assumes linearity after the breakpoint. Testing the quadratic model addresses the simple question: are the data consistent with a constant rate of change after the breakpoint (or entire range if there is no fitted breakpoint) or do the data imply a changing rate?

3.6 Meta Analyses—Combining Data on All Species Within a Reach

After completing all of the model fitting and hypothesis testing for each of the reach/species/type combinations, we performed analyses that combined results from all the species/type combinations within each reach. Three groups of hypothesis tests of interest emerged. The first group involved testing the null hypothesis that a simple linear model, without a breakpoint, for every species/type fits just as well as a spline model for all species/types within a reach. Formally, we accomplished this by summing up the chi-square statistics from the linear versus spline tests for each of the species/type combinations within the reach, and then comparing this sum to a chi-square distribution with degrees of freedom equal to twice the number of species/types combinations in the reach.

The second group of hypothesis tests is actually a single test. We tested the null hypothesis that the final slope is zero for all species/types in the reach versus the alternative that one or more species/types have a negative or positive slope. We accomplished this by first computing the directional or one-tailed *p*-value for each species/type. That is, *p* is close to 0 for large negative slopes and close to 1 for large positive slopes. Then, for each species/type within the reach we computed the statistic $X^2 = -2\log(p - value)$, where log is the natural log. Under the null hypothesis, X^2 has a chi-square distribution with two degrees of freedom.

Thus, summing up the X^2 values within a reach gives a quantity that should, under the null hypothesis that all final slopes are zero, have a chi-square distribution with degrees of freedom equal to twice the number of species/type combinations within the reach. We converted the statistic to a two-tailed *p*-value by counting either very large values or values very close to zero as rejecting the null hypothesis. These correspond to evidence for an overall negative or overall positive slope, respectively.

An average final slope estimate for the reach was defined as a weighted average of the final slope estimates for each species/type combination, where the weight was the inverse of the square of the standard error of the slope coefficient estimate. Thus, slope estimates with great precision (low standard error) have more weight than imprecise ones (high standard error). This weighting minimizes the variance of the resulting combined estimate and proves optimal if all of the true final slopes are in fact identical.

The third group of hypothesis tests examined the null hypothesis that the final slope is constant over time versus the curved alternative that the slope changes over time. We followed a similar procedure to that just described for testing for a zero final slope, since the null hypothesis corresponds to the coefficient on the quadratic term being zero. A positive coefficient on the quadratic term means the slope either curves upward or plateaus over time (on the log scale), while a negative coefficient means the slope curves downward or steepens over time.

3.7 Projecting into the Future

Predictions of concentration of PCBs in future years assumed that PCB concentration continues to decrease (or increase) at a constant rate, which is the final slope or the slope after the breakpoint. Based on this assumption, we can compute the estimate of the mean of log (PCB concentration) from the coefficients in Equation 6 or Equation 7as:

Equation 8

$$E\,[\log\,(PCB\;at\;time)] = b_0 + b_5\;time$$

where *E* indicates the expected value and time is years since 1989, the year at which time was centered prior to fitting the model. The formula predicts the mean of log (*PCB*) for a fish with average percent lipid content sampled on July 1 of the year, as long as the year follows the breakpoint. We obtain this formula from Equation 6 or Equation 7 by setting all other covariates in the model equal to zero. Since we centered log (*lipid*) at its mean, a zero value for the centered lipid variable is the same as setting log (*lipid*) equal to its mean. The seasonal variables and sine and cosine of time were centered at zero on July 1. The variable *early* in Equation 7 equals zero for all times after the breakpoint.

One computes the confidence interval for this predicted mean by first calculating the standard error:

Equation 9

$$SE\,(predicted\ \ mean\ at\ year\ t) = \sqrt{\left[SE\,(b_0)\right]^2 + t^2\left[SE\,(b_5)\right]^2 + 2t\,\mathrm{cov}(b_0, b_5)}$$

where cov(b_0, b_5) denotes the covariance between these two parameter estimates, b_0 and b_5 from Equation 6 or Equation 7. The predicted mean plus or minus twice the standard error gives the 95 percent confidence interval on the log scale.

One can convert the predicted mean on the log scale to an estimate of the mean on the original scale (i.e., ppb) by the formula:

Equation 10

$$E\,(PCB\,at\,time) = 10^{(E\,(\log(PCB\ at\ time)) + (MSE \div 2))}$$

where *MSE* is the mean squared error from the regression model on the natural log scale and is an estimate of the residual variance around the fitted regression model. This is just the formula for the mean of a lognormal distribution, based on the mean and variance on the log scale. We applied this formula to the predicted mean on the log scale and the lower and upper bounds of the confidence interval on the log scale in order to get the mean and confidence interval on the original (ppb) scale. This confidence interval does not consider the variance due to estimating the location of the breakpoint. A confidence interval that corrects for breakpoint estimation could be wider.

We also computed predicted time until mean PCB concentration reaches a specified concentration, *G*. The formula is:

Equation 11

$$time\,to\,specified\ \ concentration\,(G) = \frac{(\log_e(G) - b_0 - (MSE \div 2))}{b_5}$$

where

G	=	the specified level of PCB concentration in ppb,
time	=	time until that level is reached, in years since 1989,
MSE	=	mean squared error from a regression model fit to $\log_e$ of PCB concentration,
b_0	=	intercept from Equation 6 or Equation 7, and
b_5	=	coefficient of *time* from Equation 6 or Equation 7.

Computing confidence intervals for the predicted time to reach a specified level would seriously complicate our analysis, so we did not attempt to do so. A confidence interval based on the estimated standard errors would be wide and one that correctly accounted for the uncertainty due to estimating the breakpoint would be exceptionally wide. Therefore, we regard these “time to specified level” estimates as very uncertain.

In addition to the need to account for variance due to estimating the location of the breakpoint, the predictions are uncertain for yet another reason. Predictions of concentration of PCBs in future years assume that PCB concentration continues to decrease (or increase) at a constant rate. One cannot test this assumption except to continue collecting data in future years. Moreover, the assumption of a constant rate of change may not be very reasonable. A positive final slope, for example, implies that the PCB concentration continues to increase "forever" to higher and higher levels, an absurd conclusion. A negative final slope means that PCB concentration continues to decline to values near zero. But a scouring event that uncovered buried sediment more contaminated than surface sediment would likely lead to an increase in PCB concentration at the surface. Also, even a decreasing rate may level off well above a PCB concentration of zero. These future projections depend for their validity on an unverifiable future steady state.

4 Sediment Results

4.1 Number of Observations

A total of 1,980 observations (core-averaged) were initially available for analysis. Table 6 shows the distribution of these observations by our deposit group designation and depth. Due to the requirement of a sufficient number of observations and a sufficient time spread for an appropriate time trend analysis, only 1,618 samples qualified for the time trend analysis (Table 7). The reasons for dropping particular depth strata in specific deposit groups are explained in Table 8. Over one-third of the 1,618 usable observations occurred in the upper 10 cm of sediment, approximately one-third in the 10- to 30-cm stratum, about one-eighth in the 30- to 50-cm stratum, and the balance at greater depths. The greatest fraction of unusable data (due to lack of sufficient number of observations or lack of sufficient time spread) occurred at depths of 30 cm or lower, where approximately one-third of the core-averaged observations were unusable.

The fraction of observations below detection limit (BDL) varied widely by reach, deposit group, and depth, from a minimum of 0 percent (no BDL observations) to a maximum of 82 percent BDL observations. A majority of analyses included 20 percent or fewer BDL observations. The fraction of BDL observations, however, sufficiently requires the use of the maximum likelihood (ML) methods noted earlier. The number and percent of BDL observations by deposit group and depth is included in an appendix table. As noted in Section 2, all observations available for a given deposit group and depth stratum were included in the calculation of time trends. Due to the use of ML methods, BDL observations were neither modified nor excluded.

Table 6 Sample Size by Deposit Group and Depth after Core Averaging

TMWL Deposit Group	Sample Average Depth (cm)					Total
	0–10	10+–30	30+–50	50+–100	100+	
Little Lake Butte des Morts						
Deposit Group AB	67	105	54	12	2	240
Deposit Group C	13	15	8	2	0	38
Deposit Group POG	13	10	4	3	2	32
Deposit Group D	18	15	9	6	0	48
Deposit Group E	6	7	21	14	2	50
Deposit Group F	29	28	10	2	2	71
Deposit Group GH	15	12	3	0	0	30
Appleton						
Deposit Group IMOR	18	15	9	3	1	46
Deposit Group N Pre-dredge	51	40	18	4	0	113
Deposit Group VCC	41	34	17	9	3	104
Little Rapids						
Deposit Group Upper EE	31	25	13	3	1	73
Deposit Group Lower EE	30	33	13	5	3	84
Deposit Group FF	32	31	8	0	0	71
Deposit Group GGHH	49	45	75	54	36	259
De Pere						
SMU Group 2025	43	31	13	30	25	142
SMU Group 2649	66	48	10	46	45	215
SMU Group 5067	57*	51	34	48	50	240
SMU Group 6891	20	18	2	16	15	71
SMU Group 92115	27	15	3	7	1	53
Total:	**626**	**578**	**324**	**264**	**188**	**1,980**

Note:

* One additional sample, A3_0-4, not included in these sample sizes, had an exceptionally large PCB concentration and was considered separately.

Table 7 Sample Size by Deposit Group and Depth Included in Time Trends Analysis, after Core Averaging

TMWL Deposit Group	Sample Average Depth (cm)					Total
	0–10	10+–30	30+–50	50+–100	100+	
Little Lake Butte des Morts						
Deposit Group AB	67	105	54	—	—	226
Deposit Group C	13	15	—	—	—	28
Deposit Group POG	13	—	—	—	—	13
Deposit Group D	18	15	—	—	—	33
Deposit Group F	29	28	—	—	—	57
Deposit Group GH	15	—	—	—	—	15
Appleton						
Deposit Group IMOR	18	—	—	—	—	18
Deposit Group N Pre-dredge	32	27	17	—	—	76
Deposit Group VCC	41	34	17	—	—	92
Little Rapids						
Deposit Group Upper EE	31	25	13	—	—	69
Deposit Group Lower EE	30	33	13	—	—	76
Deposit Group FF	32	31	—	—	—	63
Deposit Group GGHH	49	45	75	54	36	259
De Pere						
SMU Group 2025	43	31	13	30	—	117
SMU Group 2649	66	48	—	46	45	205
SMU Group 5067	57*	51	—	48	50	206
SMU Group 6891	20	18	—	—	—	38
SMU Group 92115	27	—	—	—	—	27
Total:	**601**	**506**	**202**	**178**	**131**	**1,618**

Note:

* One additional sample, A3_0-4, not included in these sample sizes, had an exceptionally large PCB concentration and was considered separately.

A dash, "—," indicates that he particular cell could not be analyzed for time trends. An explanation is provided in Table 8.

Table 8 Deposit Groups Analyzed, Or Reasons for No Analysis

TMWL Deposit Group	Sample Average Depth (cm)					Total Yes
	0–10	10+–30	30+–50	50+–100	100+	
Little Lake Butte des Morts						
Deposit Group AB	Yes	Yes	Yes	I, T	I, T	3
Deposit Group C	Yes	Yes	I	I, T	N	2
Deposit Group POG	Yes	I, T	I, T	I, T	I, T	1
Deposit Group D	Yes	Yes	I, T	I, T	N	2
Deposit Group E	I, T	I	T	I, T	I, T	0
Deposit Group F	Yes	Yes	I, T	I, T	I, T	2
Deposit Group GH	Yes	I, T	I, T	N	N	1
Appleton						
Deposit Group IMOR	Yes	T	I, T	I, T	I, T	1
Deposit Group N Pre-dredge	Yes	Yes	Yes	I, T	N	3
Deposit Group SU	T	I, T	I, T	N	N	0
Deposit Group VCC	Yes	Yes	Yes	I, T	I, T	3
Deposit Sample POG	I, T	I, T	I, T	I, T	I, T	0
Deposit Group DD	I, T	I, T	I, T	N	N	0
Little Rapids						
Deposit Group Upper EE	Yes	Yes	Yes	I, T	I, T	3
Deposit Group Lower EE	Yes	Yes	Yes	I, T	I, T	3
Deposit Group FF	Yes	Yes	I	N	N	2
Deposit Group GGHH	Yes	Yes	Yes	Yes	Yes	5
De Pere						
SMU Group 2025	Yes	Yes	Yes	Yes	T	4
SMU Group 2649	Yes	Yes	T	Yes	Yes	4
SMU Group 5067	Yes	Yes	T	Yes	Yes	4
SMU Group 6891	Yes	Yes	I, T	I, T	I, T	2
SMU Group 92115	Yes	T	I, T	I, T	I, T	1
Total Yes:	**18**	**14**	**7**	**4**	**3**	**46**

Notes:

Yes - Deposit groups and depths with sufficient data to perform a time trend analysis.
I - Insufficient data (fewer than 10 observations).
N - No observations.
T - No time variation. Need at least two measured PCB concentrations (not below detection limits) at each of two distinct times.

4.2 Geographic Groups for Time Trend Analysis

As noted earlier, we regrouped the data into more compact geographic deposits (deposit groups, noted in Table 1 through Table 4). The majority of the original deposit designations transferred primarily, but not always wholly, into one of our time trend deposit groups. The exceptions, where a geographically extensive original deposit was broken into a number of separate groups for analysis, included Little Lake Butte des Morts Deposit E (which became our Little Lake Butte des Morts deposit groups E, F, and GH) and Little Rapids Deposit EE (which became our Little Rapids deposit groups Upper EE, Lower EE, FF and

GGHH). In addition, a number of observations in the database supplied to us had no deposit designation in the database supplied to us (e.g., noted as "No Designation," Table 1 through Table 4), and were allocated to one of our deposit groups based on location. As noted in Table 1 through Table 4, we were able to include a substantial number of observations in the time trends analysis by forming new deposit groups. For example, in the De Pere Reach, we analyzed 731 observations (Table 4) that had no deposit designation in the FRDB. The result of our grouping for time trend analysis is captured by Figure 5 through Figure 12. As can be seen from the plot, the deposit groups are fairly compact.

The data analyzed included diverse spatial configurations. An illustration of the variety of geographic configurations can be found on Figures A-1 through A-43 (see Appendix), an example of which can be found on Figure 19. The description and interpretation of the plot were presented earlier. The plot demonstrates how the geographic configuration is not necessarily the same for the two time periods, illustrating the importance of controlling for geography in analyzing time trends. By failing to control for sample geography, an apparent time trend could simply be due to sampling from, for example, a high concentration area in an earlier period and a lower concentration area in a later period without any real shift in concentration in either area over time. The figures show measured concentrations and concentrations below detection limits as circles and squares, respectively, with the magnitude of the PCB concentration indicated by the size of the square or circle.

4.3 Time Trends in Sediment Concentrations

Time trends in PCB concentrations differ both by depth and by deposit group. Appendix Table A-1 presents detailed numerical results, sections of which are reproduced here in Table 9 for 46 different analyses, representing different deposit groups and depths. The key results from the table are:

- Coefficient of the time term (this parameter represents the slope estimate on a $\log_{10}$ scale as rate of change in $\log_{10}$ PCB concentration per year),
- Standard error of the time coefficient based on the window subsampling empirical variance (WSEV) method,
- The annual percentage rate of change (compounded), and
- The *p*-value for the null hypothesis that the true slope is zero ($b_t = 0$ in Equation 2, Section 2.6). The "statistically significant" slopes are also designated by asterisk(s) in the table. The deposit group and depth combinations that are "statistically significant" will very likely have true non-zero rates of change over time.

Statistical significance plays an important role in interpreting Table 9 and other tables presenting rates of change. The *p*-value column in this and other tables shows the degree of statistical significance of the calculated rate of change of log PCB concentration versus time. The *p*-value, which constitutes the numeric statement of statistical significance, quantifies the strength of the evidence against the null hypothesis that the true rate of change is zero. The closer the *p*-value is to zero, the more confidence we have that the true rate of change is not zero. Formally, the *p*-value is defined of as the probability of observing a result as or more extreme than that actually observed if the null were, in fact, true. More explicitly, the *p*-value can be interpreted as the outcome of the following hypothetical experiment. We can imagine taking samples from a deposit group whose **true** rate of change is zero and repeating this operation many times. For example, Little Lake Butte des Morts Deposit Group AB has $n = 67$ samples at 0 to 10 cm depth. We would take many samples of size $n = 67$ from the deposit group and analyze them as we have here, yielding one slope for each set of 67 samples. Due to random variation in sampling, each calculated slope would differ to a greater or lesser extent from the true slope. If the true slope were really zero, then these random slopes would have some distribution around zero. For any slope value that we choose or observe, we can look at the distribution and determine what fraction of our random slopes are as large or larger than a given slope. Usually, we take the fraction of slopes that are larger in either the positive or negative direction from the value. For example, for the slope of –0.097, we would look at the fraction of random slopes smaller than –0.097 and larger than +0.097, because random variation can take us either in a positive or negative direction away from zero. The key concept is that if the true slope is really zero, the observed slope should not stray too far from zero. Traditionally (but with no other basis than that), $p < 0.05$ has been used to designate statistical significance. This *p*-value means that there are fewer than 5 chances in 100 that a slope as large or larger than that observed could have been generated by chance, if the **true** slope is zero. We adopt this definition and also designate $p < 0.05$ as "statistically significant." In the tables, we note this with one asterisk and also use the following conventions: ** $p < 0.01$, *** $p < 0.001$.

In reality, one need not compute the hypothetical experiment to get the *p*-value. In fact, the *p*-values computed in Table 9 use the very standard *t*-test. As a conservative measure, we have chosen the degrees of freedom for the *t*-test as the number of grid cells with at least one sample, determined in the WSEV method described earlier. The number of non-empty grid cells is included in an appendix table.

We have also included in Table 9 a 95 percent confidence interval for the percent rate of change of the PCB concentration over time (derived from the slope and its standard error using the *t*-distribution with the same degrees of freedom as in the calculation of the *p*-value). We can state with 95 percent confidence that the true rate of change lies in this interval. If this interval is especially narrow, we have a very precise idea of the true rate of change. A particularly wide interval casts much doubt on the true rate of change.

Appendix Table A-1 presents the form of the linear regression model—either linear or quadratic, fitted to the data. "Linear" indicates that depth, easting, and northing are used as linear terms in the regression model. "Quadratic" indicates that these terms plus squared terms for easting and northing are also used. Time is always introduced as a linear term, in years, and all models include an intercept.

Table 9 Sediment Time Trend Parameters by Depth and Deposit Group

Deposit Group	Depth Range (cm)	Log_{10}(PCB) Time Trend Slope Estimate	WSEV Standard Error	WSEV *p*-value	Statistically Significant Slopes	Est. Annual Compound Percent Increase in PCB Level	Estimated Annual Compound Percent Increase in PCB Level	
							95% Conf. Int. Lower-bound	95% Conf. Int. Upper-bound
Little Lake Butte des Morts								
AB	0–10	–0.0970	0.0348	0.0131	*	–20.0	–32.5	–5.2
	10–30	–0.0213	0.0647	0.7535		–4.8	–33.9	37.1
	30–50	–0.0144	0.1113	0.8995		–3.3	–45.0	70.0
C	0–10	–0.0612	0.0342	0.1481		–13.2	–30.2	8.1
	10–30	0.0317	0.0770	0.7018		7.6	–34.2	76.0
POG	0–10	–0.0893	0.0567	0.1900		–18.6	–43.3	16.9
D	0–10	–0.0755	0.0317	0.0307	*	–16.0	–28.1	–1.8
	10–30	0.3168	0.0454	0.0009	***	107.4	58.5	171.3
F	0–10	–0.0373	0.0136	0.0252	*	–8.2	–14.6	–1.4
	10–30	–0.0760	0.0749	0.3246		–16.1	–41.7	20.8
GH	0–10	–0.1244	0.0541	0.0443	*	–24.9	–43.1	–0.9
Appleton								
IMOR	0–10	0.0412	0.0255	0.1810		9.9	–6.6	29.4
N Pre-dredge	0–10	–0.0281	0.0065	0.0233	*	–6.3	–10.6	–1.7
	10–30	0.0572	0.0440	0.2061		14.1	–7.5	40.7
	30–50	0.0846	0.0932	0.3877		21.5	–25.2	97.4
VCC	0–10	–0.0582	0.0275	0.0878		–12.5	–25.7	2.9
	10–30	–0.1537	0.0164	0.0000	***	–29.8	–35.4	–23.7
	30–50	–0.0060	0.0151	0.6984		–1.4	–8.7	6.6
Little Rapids								
Upper EE	0–10	–0.0447	0.0435	0.3618		–9.8	–31.7	19.1
	10–30	–0.0944	0.0429	0.0554		–19.5	–35.6	0.6
	30–50	–0.0712	0.0536	0.2173		–15.1	–35.8	12.2
Lower EE	0–10	–0.0682	0.0193	0.0387	*	–14.5	–25.8	–1.5
	10–30	–0.0759	0.0390	0.0695		–16.0	–30.6	1.6
	30–50	0.0900	0.0330	0.0213	*	23.0	3.9	45.7
FF	0–10	–0.0549	0.0557	0.3400		–11.9	–32.9	15.8
	10–30	–0.0962	0.0390	0.0389	*	–19.9	–34.9	–1.4
GGHH	0–10	–0.0394	0.0231	0.1643		–8.7	–21.2	5.9
	10–30	–0.0182	0.0596	0.7631		–4.1	–27.7	27.3
	30–50	0.1762	0.1008	0.1188		50.0	–12.5	156.3
	50–100	0.1012	0.0700	0.1586		26.2	–9.2	75.4
	100+	0.0365	0.0249	0.1587		8.8	–3.5	22.6

Table 9 Sediment Time Trend Parameters by Depth and Deposit Group

Deposit Group	Depth Range (cm)	Log_{10}(PCB) Time Trend Slope Estimate	WSEV Standard Error	WSEV *p*-value	Statistically Significant Slopes	Est. Annual Compound Percent Increase in PCB Level	Estimated Annual Compound Percent Increase in PCB Level: 95% Conf. Int. Lower-bound	Estimated Annual Compound Percent Increase in PCB Level: 95% Conf. Int. Upper-bound
De Pere								
SMU Group 2025	0–10	–0.0528	0.0231	0.0838		–11.4	–23.6	2.6
	10–30	–0.0556	0.0750	0.4796		–12.0	–40.9	31.0
	30–50	–0.0580	0.0322	0.1016		–12.5	–25.8	3.2
	50–100	–0.0847	0.1058	0.4306		–17.7	–50.2	35.9
2649	0–10	–0.0608	0.0109	<0.0001	***	–13.1	–17.4	–8.5
	10–30	–0.2882	0.1440	0.0764		–48.5	–75.7	9.0
	50–100	0.1957	0.1419	0.2399		56.9	–36.6	288.7
	100+	0.0177	0.1548	0.9146		4.2	–61.3	180.3
5067	0–10	–0.0998	0.0345	0.0136	*	–20.5	–33.2	–5.5
	10–30	0.0912	0.0649	0.1800		23.4	–10.3	69.6
	50–100	0.3677	0.0684	0.0030	**	133.2	55.5	249.5
	100+	–0.1963	0.2223	0.4112		–36.4	–81.8	122.6
6891	0–10	–0.2208	0.0944	0.1013		–39.9	–69.9	20.1
	10–30	–0.1685	0.0765	0.0550		–32.2	–54.4	1.0
92115	0–10	0.0413	0.0426	0.3493		10.0	–10.9	35.8

Notes:
* $p < 0.05$
** $p < 0.01$
*** $p < 0.001$

The annual percentage rate of change corresponding to a given slope, b_t, is calculated as

Equation 12

$$Percentage = 100\% * (10^{b_t} - 1).$$

The halving time is $\frac{\log_{10}(0.5)}{b_t}$ if b_t is negative (decrease over time). If b_t is positive, the doubling time is $\frac{-\log_{10}(0.5)}{b_t}$. The 95 percent confidence interval for the slope, b_t, is given by:

Equation 13

$$[b_t - t_{0.025,df} * SE(b_t), b_t + t_{0.025,df} * SE(b_t)]$$

where

$SE(b_t)$ = the WSEV standard error of b_t, and

$t_{0.025, df}$	=	from the *t*-distribution, 0.025 tail area, with degrees of freedom = *df* = number of non-empty grid cells, noted in Table A-1.

The 95 percent confidence interval for the percent rate of change is calculated by first deriving the confidence interval for the slope and then using Equation 12 to convert the upper and lower bounds for the slope to upper and lower bounds for the percentage.

The percent increase and the 95 percent confidence interval for the percent increase/decrease (along with the scale for the doubling time or halving time) are presented on Figure 20 through Figure 28. The figures show a number of statistically significant trends. Apparent from Table 9 and the figures is a tendency for more negative slopes to occur at shallower depths and more positive slopes to occur at greater depths. For example, in our Little Lake Butte des Morts Deposit Group D, the slope in the upper 10 cm of sediment is –0.0755 per year, implying a rate of decrease of 16 percent compounded per year; and in the 10- to 30-cm stratum, the slope is 0.317 per year, indicating a rate of increase of 107 percent, compounded annually with trends in both depths being statistically significant ($p = 0.03$ for 0 to 10 cm, $p = 0.0009$ for 10 to 30 cm).

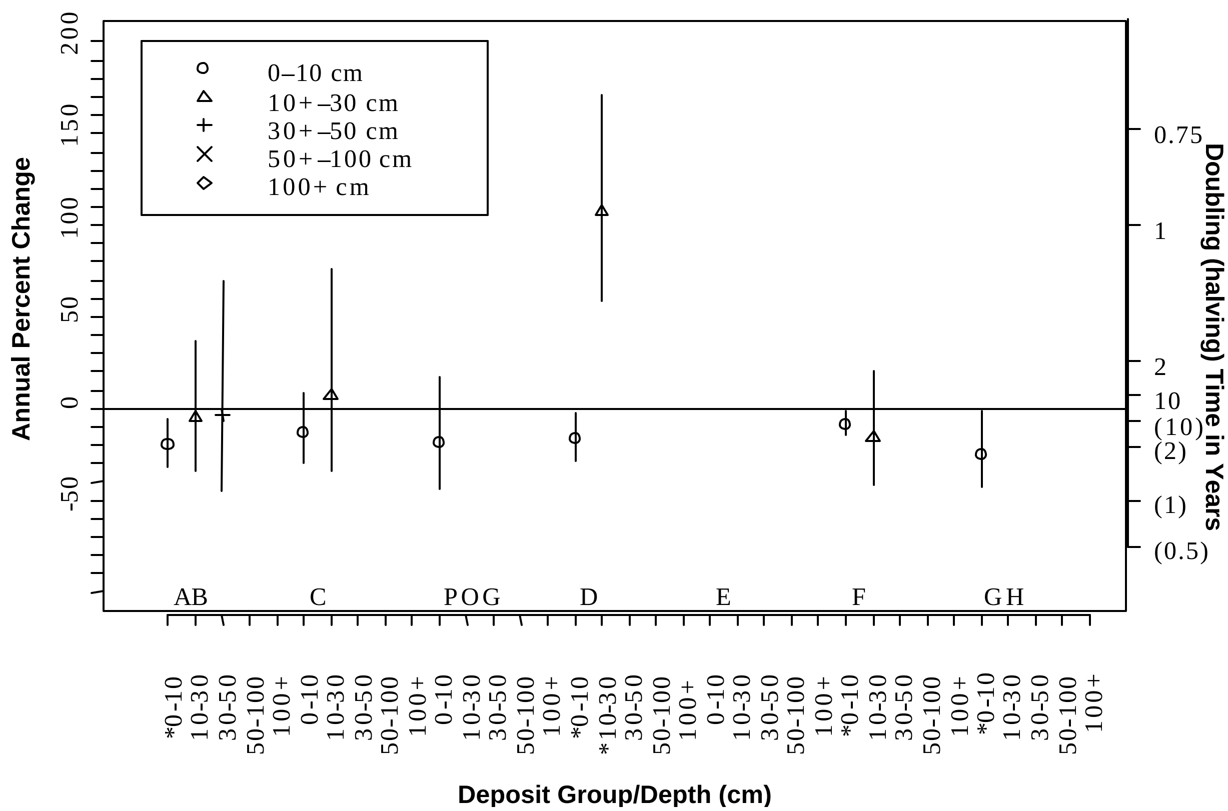

Figure 20 95 Percent Confidence Intervals Showing Annual Percent Rate of Change (Left Vertical Axis) in PCB Concentration

for Little Lake Butte des Morts Deposit Group and Depth Strata

An asterisk (*) below the depth label indicates that a rate of change differs significantly from zero. Right vertical axis expresses time trend change in terms of doubling and halving times. Confidence intervals are shown for all deposit groups and depths with sufficient data to perform an analysis of time trend.

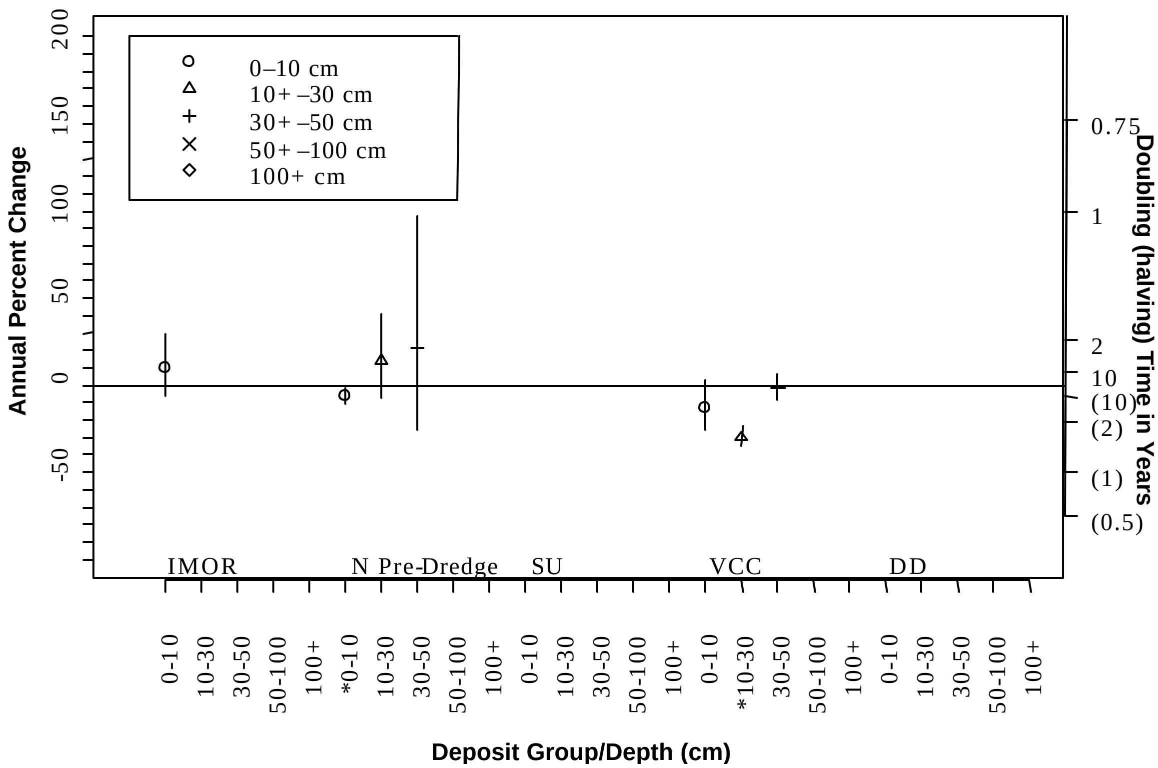

Figure 21 95 Percent Confidence Intervals Showing Annual Percent Rate of Change (Left Vertical Axis) in PCB Concentration for Appleton Deposit Group and Depth Strata

An asterisk (*) below the depth label indicates that a rate of change differs significantly from zero. Right vertical axis expresses time trend change in terms of doubling and halving times.

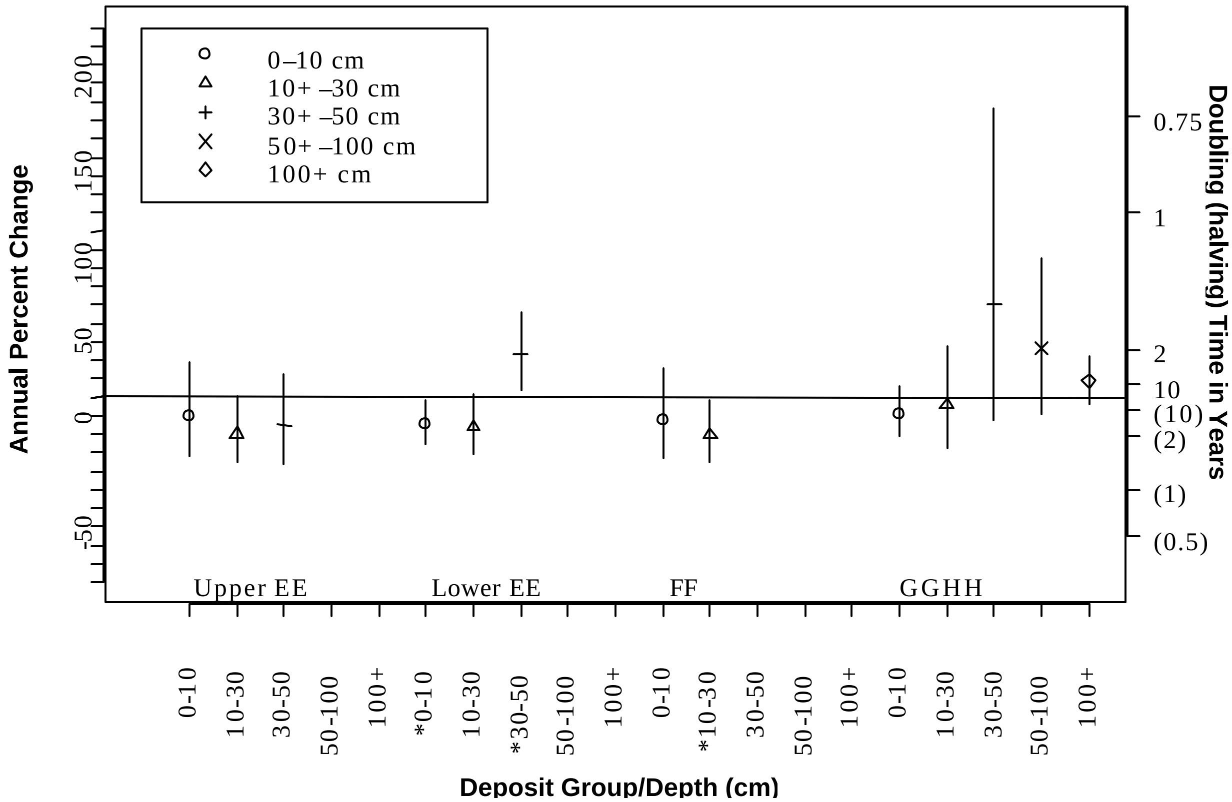

Figure 22 95 Percent Confidence Intervals Showing Annual Percent Rate of Change (Left Vertical Axis) in PCB Concentration for Little Rapids Deposit Groups and Depth Strata

An asterisk (*) below the depth label indicates that a rate of change differs significantly from zero. Right vertical axis expresses time trend change in terms of doubling and halving times.

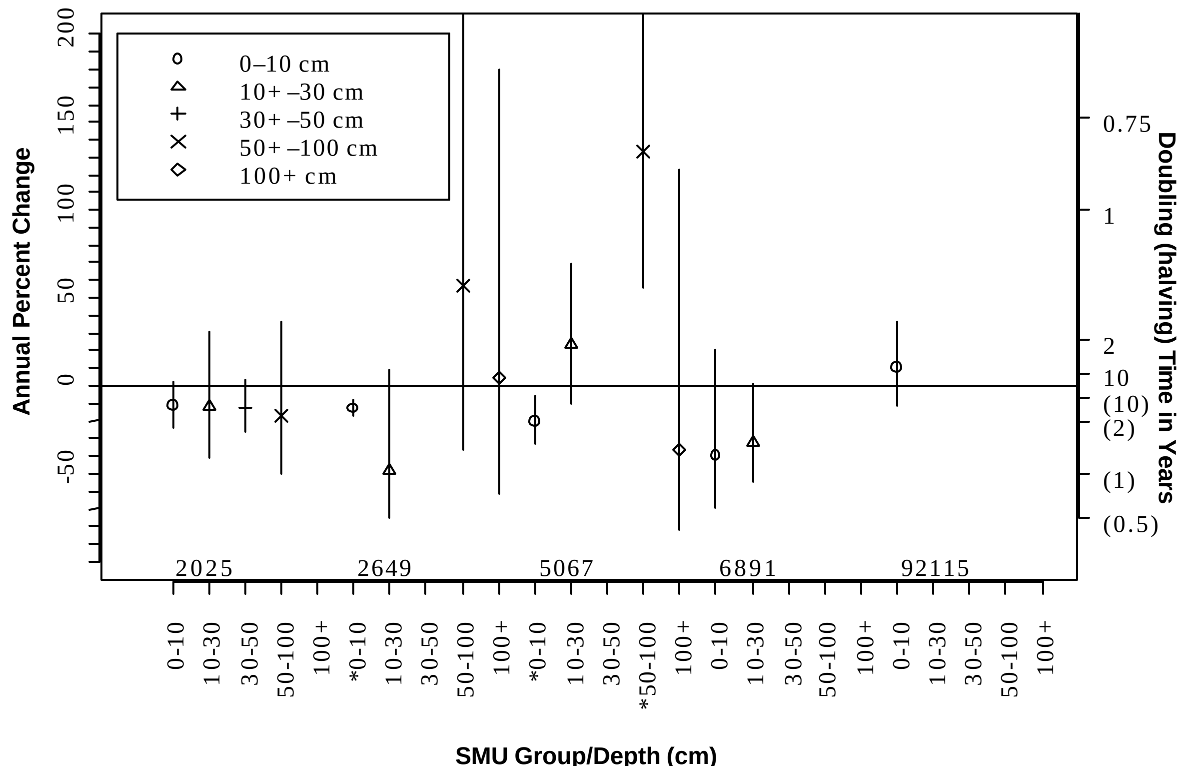

Figure 23 95 Percent Confidence Intervals Showing Annual Percent Rate of Change (Left Vertical Axis) in PCB Concentration for De Pere SMU Groups and Depth Strata

An asterisk (*) below the depth label indicates that a rate of change differs significantly from zero. Right vertical axis expresses time trend change in terms of doubling and halving times.

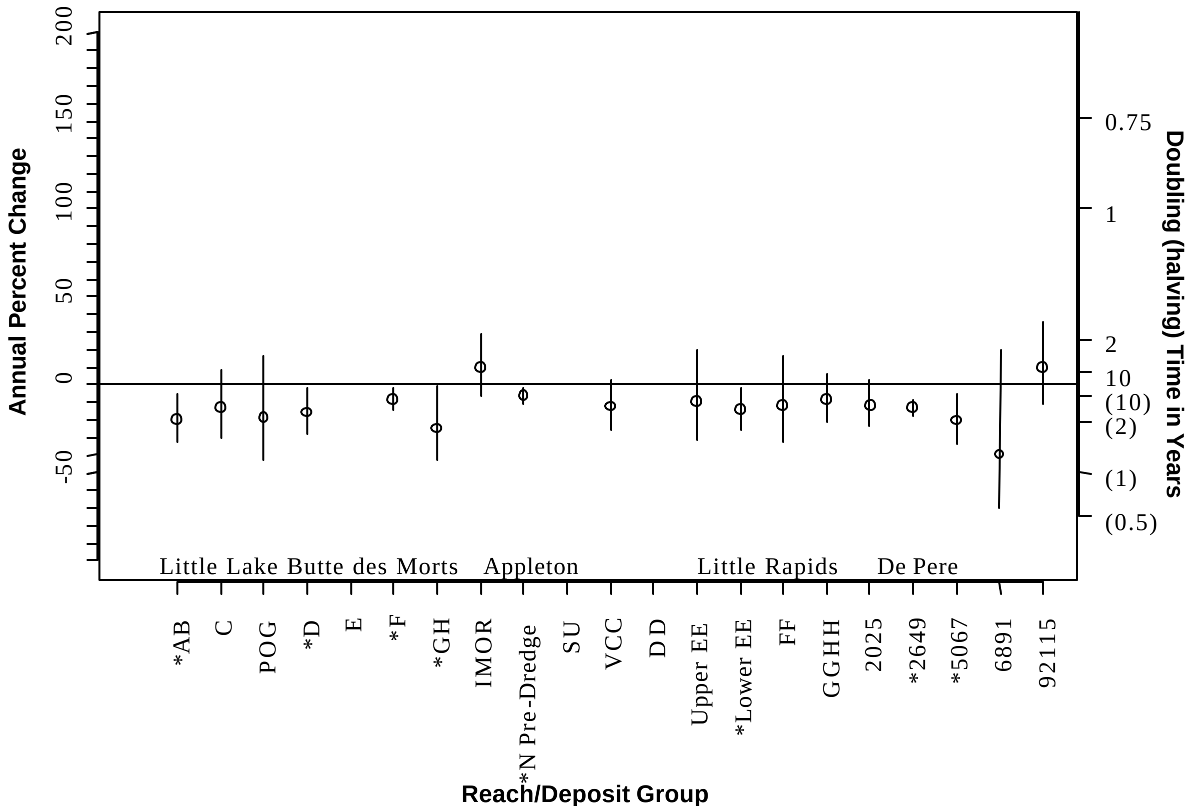

Figure 24 95 Percent Confidence Intervals for Annual Percent Rate of Change at Depth 0 to 10 cm

An asterisk (*) below the depth label indicates that a rate of change differs significantly from zero. Right vertical axis expresses time trend change in terms of doubling and halving times.

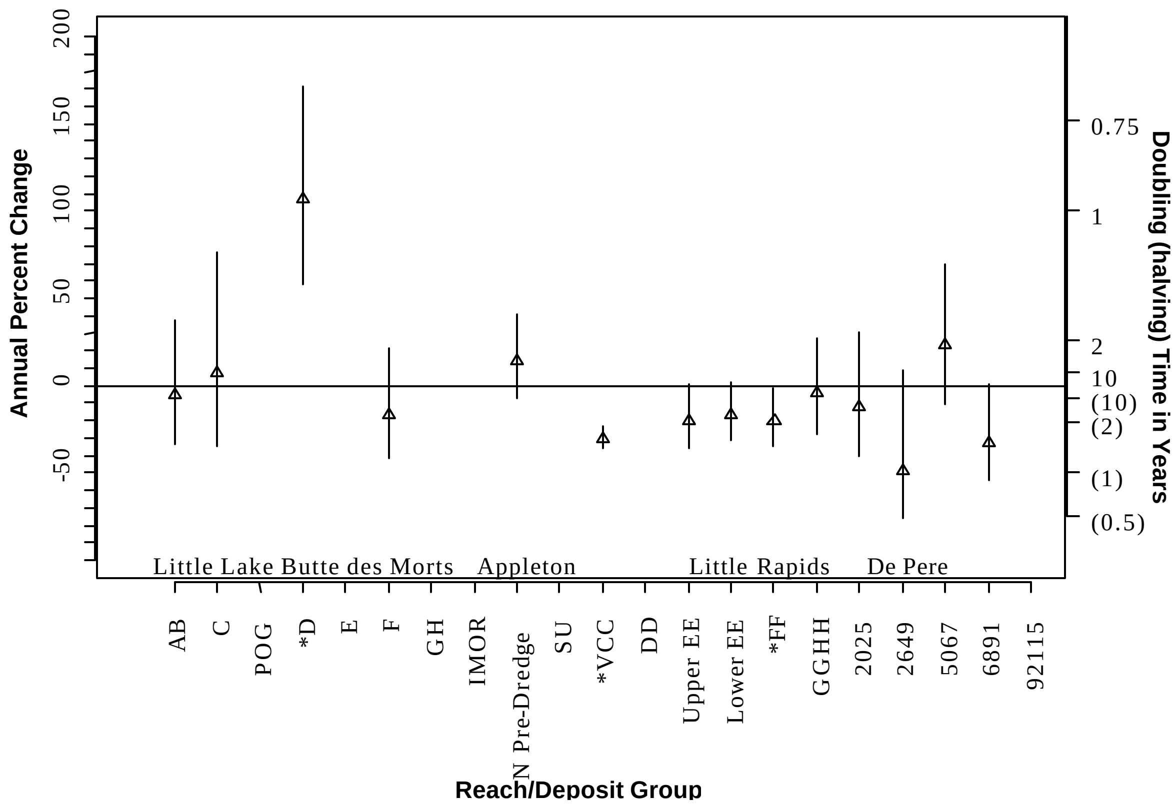

Figure 25 95 Percent Confidence Intervals for Annual Percent Rate of Change at Depth 10+ to 30 cm

An asterisk (*) below the depth label indicates that a rate of change differs significantly from zero. Right vertical axis expresses time trend change in term s of doubling and halving times.

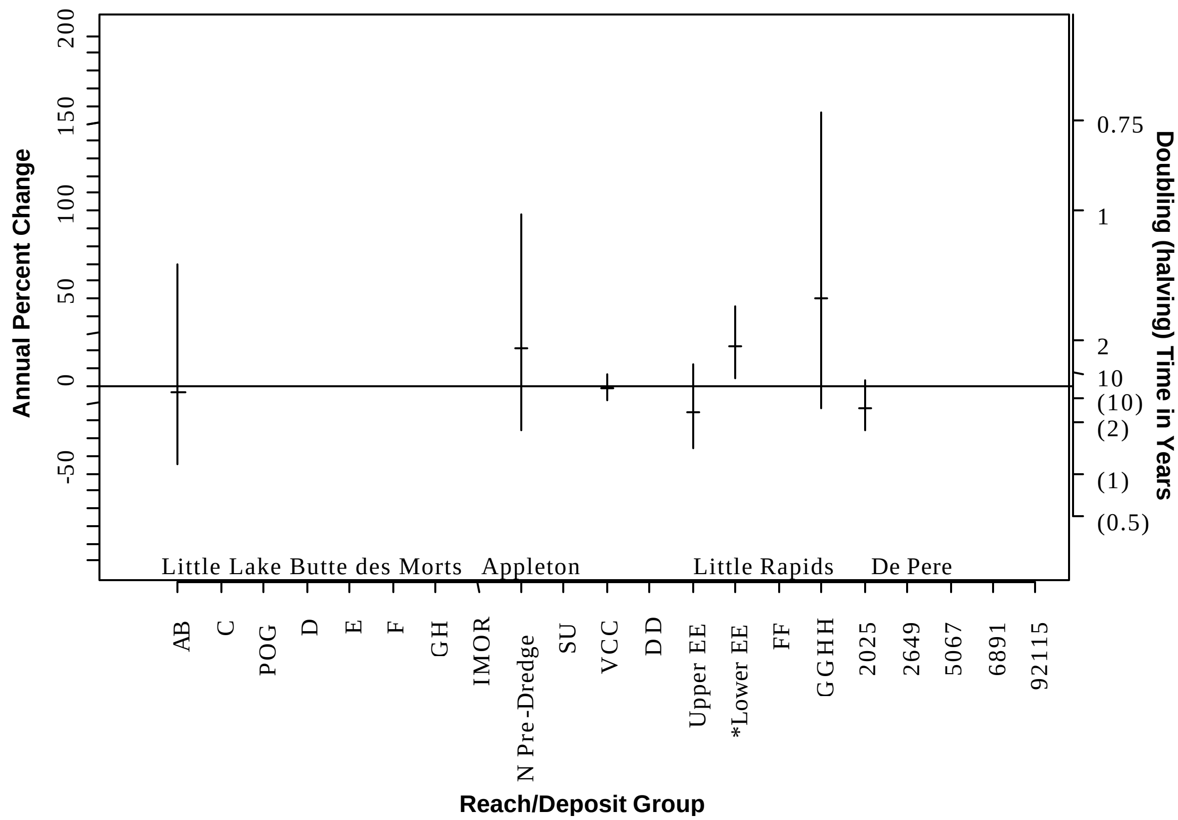

Figure 26 95 Percent Confidence Intervals for Annual Percent Rate of Change at Depth 30+ to 50 cm

An asterisk (*) below the depth label indicates that a rate of change differs significantly from zero. Right vertical axis expresses time trend change in terms of doubling and halving times.

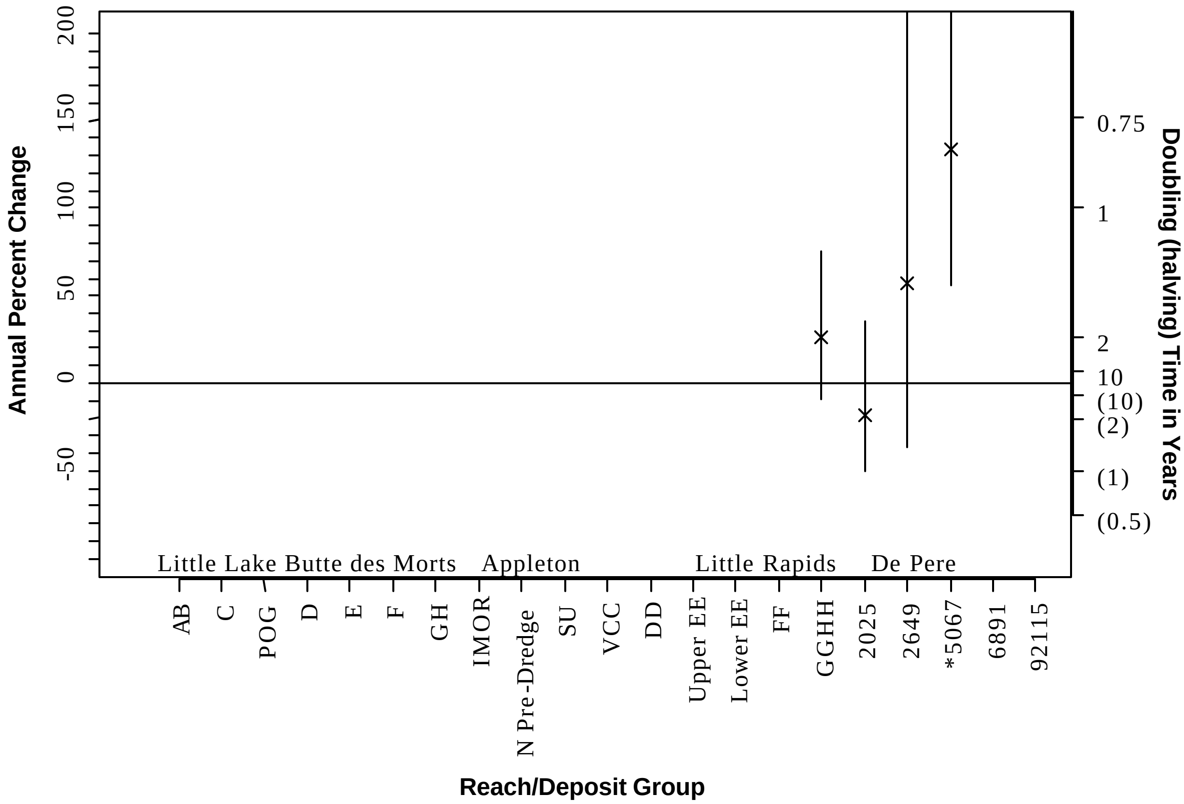

Figure 27 95 Percent Confidence Intervals for Annual Percent Rate of Change at Depth 50+ to 100 cm

An asterisk (*) below the depth label indicates that a rate of change differs significantly from zero. Right vertical axis expresses time trend change in terms of doubling and halving times.

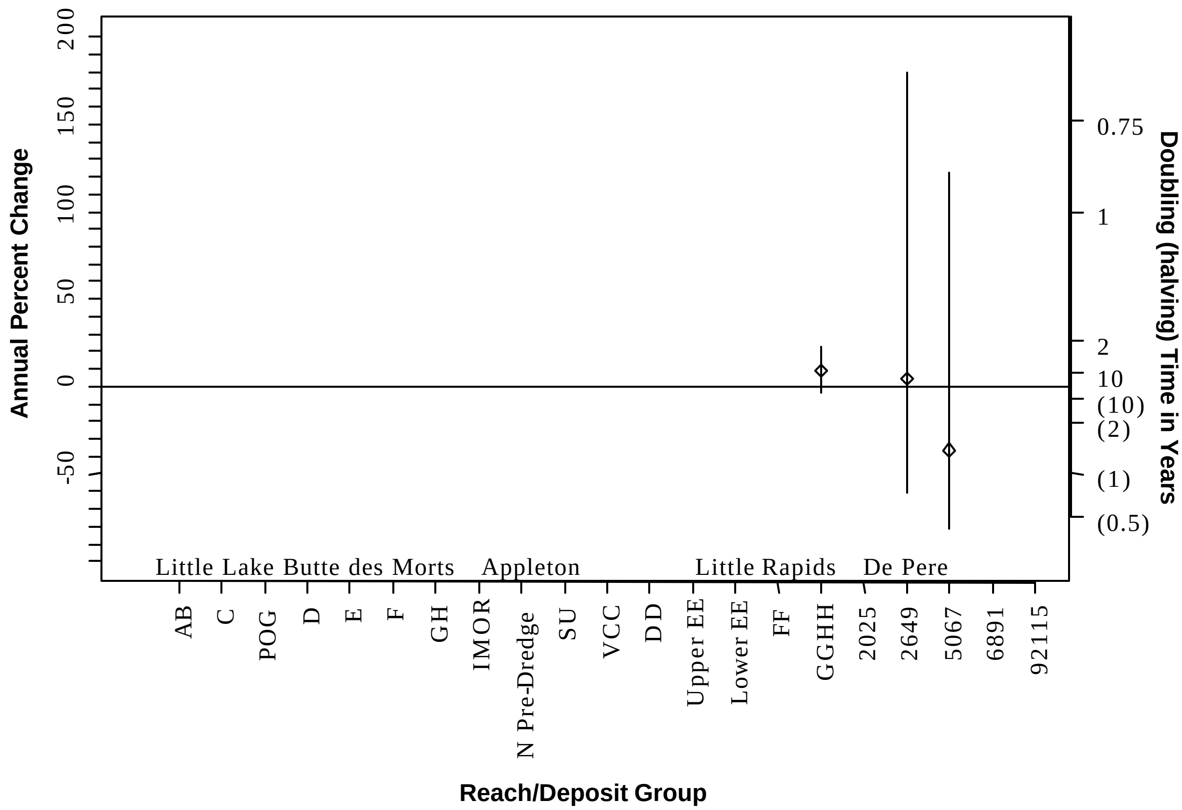

Figure 28 95 Percent Confidence Intervals for Annual Percent Rate of Change at Depth 100+ cm

Right vertical axis expresses time trend change in terms of doubling and halv ing times.

We note that negative slopes are 89 percent of the calculated slopes from 0 to 10 cm, 71 percent (10/14) of the slopes (16/18) at 10 to 30 cm, 57 percent (4/7) at 30 to 50 cm, 25 percent (1/4) at 50 to 100 cm, and 33 percent (l/3) at 100 cm and over. This indicates a powerful trend toward fewer or weaker negative slopes and more or stronger positive slopes at greater depths. This suggests either that some of the PCBs may transfer out of the river and into Green Bay, instead moving to greater depths, or that attrition of PCBs slows at greater depths, or even that both mechanisms are occurring. These findings can be compared with mass balance studies discussed in the Remedial Investigation for the Lower Fox River and Green Bay.

4.4 Time Trends by Reach

4.4.1 Little Lake Butte des Morts

With the exception of two strata at 10 to 30 cm in two separate deposit groups, slopes are negative (9 out of 11 analyses). Statistically significant negative slopes (decreasing PCB concentration over time) occur in surface sediments (0 to 10 cm) of four deposit groups (AB, D, F, GH) with estimated rates of decrease ranging from 8 to 24 percent per year (Table 9 and Figure 24). The only statistically significant increasing trend of PCB concentrations occurs at 10 to 30 cm in Deposit Group D, where the rate of increase is 108 percent per year. The confidence intervals for these rates of change are quite wide. For the significantly decreasing slopes in the surface 0- to 10-cm stratum, the confidence intervals indicate a rate of decrease of as little as 1 to 5 percent and as much as 15 to 43 percent per year. The confidence interval for the significantly increasing slope at 10 to 30 cm in Deposit Group D indicates a rate as low as 59 percent and as high as 171 percent per year. This must represent a temporary positive trend because a projection of the PCB concentration even at the minimum of 59 percent per year yields an absurd 10,000-fold increase in PCB concentration after 20 years. Again, the negative slopes also refer to the period of data collection, and one cannot guarantee that such negative slopes would continue indefinitely into the future.

An additional calculation for the surface strata of this reach yields an average slope. This average slope is a weighted mean, where the weights are estimated PCB masses for our deposit groups using mass estimation methods developed in other Fox River studies (WDNR, 1999b). The mass estimates for surface deposits (0 to 10 cm) refer to the boundaries noted on Figure 5 through Figure 8. Because new boundaries have been drawn for these deposit groups, the masses here differ from the masses quoted in other documents for the original deposit designations. Using the estimated PCB mass in the surface sediments (0 to 10 cm) as a relative weight, the weighted mean slope is -0.071 ± 0.018 $\log_{10}$ PCB concentration per year (*mean* ± *SE*, Table 11) with $p = 0.0001$ for the null hypothesis of zero slope (i.e., the weighted mean slope is significantly negative and corresponds to an 18 percent rate of decrease of PCB concentration per year). The weighted mean slope is calculated as:

Equation 14

$$b_{wt} = \frac{\left(\sum_{i=1}^{K} b_i \cdot w_i\right)}{\left(\sum_{i=1}^{K} w_i\right)}$$

where the b_i are the slopes of the individual deposit groups, $i = 1, \ldots, K$, from Table 9 and the w_i are the PCB masses in the strata (see Table 10). The standard error of b_{wt} is calculated as:

Equation 15

$$SE\,(b_{wt}) = \left[\sum_{i=1}^{K} (SE \cdot (b_i))^2\,(w_i^*)^2\right]^{0.5}$$

where the $SE(b_i)$ are the standard errors of the individual b values and $w_i^* = \frac{w_i}{\left(\sum_{i=1}^{K} w_i\right)}$. The statistical significance of the weighted slope is based on a two-sided, single-sample Z-test (twice the tail area of the normal distribution lying beyond $Z = \frac{b_{wt}}{SE(b_{wt})}$).

Table 10 Mass-weighted Combined Time Trend for 0 to 10 cm Depth by Reach

Deposit Group	Log_{10}(PCB) Time Trend Slope Est.	WSEV Standard Error	PCB Mass (kg)	*p*-value	Annual Percent Change in PCB Conc.	Percent Change 95% Lower-bound	Percent Change 95% Upper-bound
Little Lake Butte des Morts							
AB	−0.09705	0.034798	71.7				
C	−0.06124	0.03423	25.4				
POG	−0.08935	0.056669	113.5				
D	−0.07554	0.031669	32.1				
F	−0.0373	0.013582	142.5				
GH	−0.12443	0.054119	15.7				
Reach, Combined	**−0.07071**	**0.01831**	**400.9**	**0.0001*****	**−15.0**	**−21.8**	**−7.7**
Appleton							
IMOR	0.041186	0.025457	13.7				
N Pre-dredge	−0.02805	0.006544	6.9				
VCC	−0.05816	0.02746	5.2				
Reach, Combined	**0.0025**	**0.01469**	**25.9**	**0.9**	**0.6**	**−5.9**	**7.5**
Little Rapids							
Upper EE	−0.04473	0.043487	85.0				
Lower EE	−0.06819	0.019322	25.4				
FF	−0.05486	0.055669	36.7				
GGHH	−0.03936	0.023149	131.6				
Reach, Combined	**−0.04567**	**0.018764**	**278.7**	**0.01***	**−10.0**	**−17.3**	**−2.0**
De Pere							
SMU Group 2025	−0.05279	0.02305	225.6				
2649	−0.06078	0.010894	356.8				
5067	−0.09978	0.034549	92.4				
6891	−0.22081	0.094396	72.1				
92115	0.041293	0.042639	37.1				
Reach, Combined	**−0.07296**	**0.012829**	**784.0**	**<0.0001*****	**−15.5**	**−20.2**	**−10.4**

Notes:

* $p < 0.05$
** $p < 0.01$
*** $p < 0.001$

Table 10 provides the weighted slope of surface sediment for each reach. One should interpret the weighted mean slope carefully. This descriptive statistic shows how rapidly the PCB mass is changing at the particular reference date for the mass estimations (1989–1990), assuming that the rates of change in Table 9 correctly reflect the rates of change at the reference date. The weighted mean slope itself has a straightforward interpretation: it is the rate at which mass is decreasing from the 0- to 10-cm stratum of the collection of deposit groups in the reach. We caution readers when comparing the statistical significance of trends in individual deposit groups (Table 9) to the significance of the weighted mean pooled across all deposit groups in the reach (Table 10). One can calculate a non-significant weighted mean slope although one of the slopes shows, for example, a significant or even highly significant decrease in PCBs over time in the specific deposit group. This can arise where considerable uncertainty exists in some of the slopes being weighted, and when combined, overwhelms the relative certainty of one or two highly significant individual slopes. Thus, one can clearly interpret the value of the slope as representing the rate of decline of the PCB mass at the reference date used for total PCB mass evaluation. One must interpret statistical significance, however, as the likelihood that the observed weighted mean slope could arise, differing from zero, given *within-deposit* sampling variation. It could happen that one sees a significantly negative slope for an individual deposit group with a non-significant overall weighted mean slope. This could occur if, among other deposit groups, the slopes have values close to zero and large enough standard errors such that the mass could conceivably be increasing in these deposit groups. Hence, individual deposit groups with statistically significant slopes alongside a non-significant overall weighted slope should not alarm the reader. In fact, we face just such a contradiction in Appleton, the next reach considered.

The weighted mean slope should not be used for projection of PCB concentrations for the entire reach, because deposit groups with the lowest rate of decrease will in the future dominate the decay of PCB mass over time. The weighted mean slope serves as a summary descriptive value representing average change during the period of data collection and, also, as a statistic used to derive a significance level (*p*-value) for the hypothesis of no change. The PCB mass remaining in the future, w, can be estimated as:

Equation 16

$$w = \sum_{i=1}^{K} w_i * 10^{b_i t}$$

where time, t, is measured in decimal years since January 1, 1989, w_i are the PCB masses in the K strata, and b_i is the coefficient of time term in the model for the i^{th} stratum. The equation works for any collection of K strata.

4.4.2 Appleton Reach

Two strata have statistically significant slopes. The, 0 to 10 cm in the Deposit Group N (pre-dredge) has a statistically significant negative slope of b = --0.028 ($\log_{10}$ PCB concentration per year). This slope translates into a rate of decrease of 6 percent per year with a 95 percent confidence interval of 2 percent to 11 percent decrease per year (Table 9). The 10- to 30-cm stratum of Deposit Group VCC has a statistically significant decrease of –0.154 (log_{10} PCB concentration per year), implying a 30 percent rate of decrease per year with a 95 percent confidence interval of –35 to –24 percent (Table 9).

The weighted slope for surface strata is 0.003 per year, implying a rate of increase of 0.6 percent per year with a 95 percent confidence interval of –6 to +7 percent per year. This mass-weighted mean slope of –0.011 per year is not statistically significant (p = 0.4). Even though the N Pre-dredge Deposit Group has a significantly decreasing slope in the 0- to 10-cm stratum (equivalent to a 2.6% decrease per year), the total PCB mass in surface sediments in the entire Appleton Reach may be either increasing, decreasing, or remaining constant over time. The reach includes the one statistically significant negative slope for surface sediments, as well as an additional positive and negative slope. Thus, while it is likely that one surface deposit is, indeed, decreasing in PCB concentration, the combination of positive and negative slopes convey a state of uncertainty as to the trends in total PCB mass in the combined surface deposits in the reach.

4.4.3 Little Rapids to De Pere Reach

This reach has a majority of negative slopes (change in log_{10}[PCB concentration] per year). Two of the three significant slopes are negative and occur in the 0- to 10-cm and 10- to 30-cm depth strata. One large positive statistically significant slope occurs at the 30- to 50-cm depth (Table 9).

The surface sediment (0 to 10 cm) in the Lower EE Deposit Group has a significantly negative slope (–0.068 per year), implying a rate of decrease of 15 percent per year with a 95 percent confidence interval of 2 to 26 percent rate of decrease per year. In the same deposit group, the deeper 30- to 50-cm stratum shows a significantly positive slope, indicating a rate of increase of 23 percent per year and a 95 percent confidence interval of 4 to 46 percent per year. In Deposit Group FF, the 10 to 30 cm layer has a significantly negative slope with a rate of PCB concentration decrease of 20 percent per year with a 95 percent confidence interval of 1 to 35 percent. Again, while the estimates speak to significant decreasing or increasing PCB concentrations over time in these strata and deposit group combinations, we still encounter notably wide confidence intervals.

Although only one surface sediment has a statistically significant decline, we nonetheless find an overall statistically significant combination of declining PCB concentrations in the reach, with a slope of –0.046 per year (p = 0.01), implying a 10 percent per year rate of decrease (95 percent confidence interval: –17 to –2 percent). While some uncertainty may persist in the individual surface deposits, the PCB mass in the surface of this reach appears to be generally declining as of the mass estimation date, 1989 through 1990.

4.4.4 De Pere to Green Bay Reach

This reach, again, has primarily negative slopes (Table 9). Statistically significant negative slopes occur in three combinations of deposit group and depth. Our SMU Group 2649 has a significantly negative slope in the surface deposit (0 to 10 cm), with a rate of decrease of 13 percent per year (95 percent confidence interval of 8 to 17 percent per year) and $p < 0.0001$. SMU Group 5067, 0 to 10 cm, also has a significantly negative slope implying an annual rate of decrease of 21 percent (95 percent confidence interval of 5 to 33 percent) and $p = 0.01$. In the same SMU group (5067), at a greater depth of 50 to 100 cm, we observe a statistically significant and large positive slope with a rate of increase of 133 percent per year (95 percent confidence interval of 56 to 250 percent) and $p = 0.003$.

We noted earlier (Section 2.6 and Table 5) an exceptional value of PCB concentration in SMU Group 5067. Sample A3_0-4 had a concentration of 99,000 ppb, whereas all other samples in the 0- to 10-cm stratum in this deposit ranged from 400 to 7,800 ppb. In a statistical sense, the sample is an “outlier,” but that does not imply error in the value of 99,000. We have no reason to suspect invalidity of the concentration of 99,000 ppb for sample A3_0-4, especially given internal evidence in the deposit corroborating it (see below). However, the sample is a statistical outlier to the spatial relationships of PCB concentrations in the deposit, as we shall show. The spatial layout of the samples in the 0- to 10-cm stratum of SMU Group 5067 is shown on Figure 29. The samples occur in an intensively sampled area (see Figure 8). Sample A3_0-4 lies close to the shore of the river, and we have been informed that this sample was located in the vicinity of direct deposition of PCBs. The more immediate vicinity of the sample is shown on Figure 30, which includes 34 out of the 58 samples in the 0- to 10-cm layer of the deposit. Figure 30 also designates the exceptional sample A3_0-4 (#1 in the plot) and the six samples closest to it.

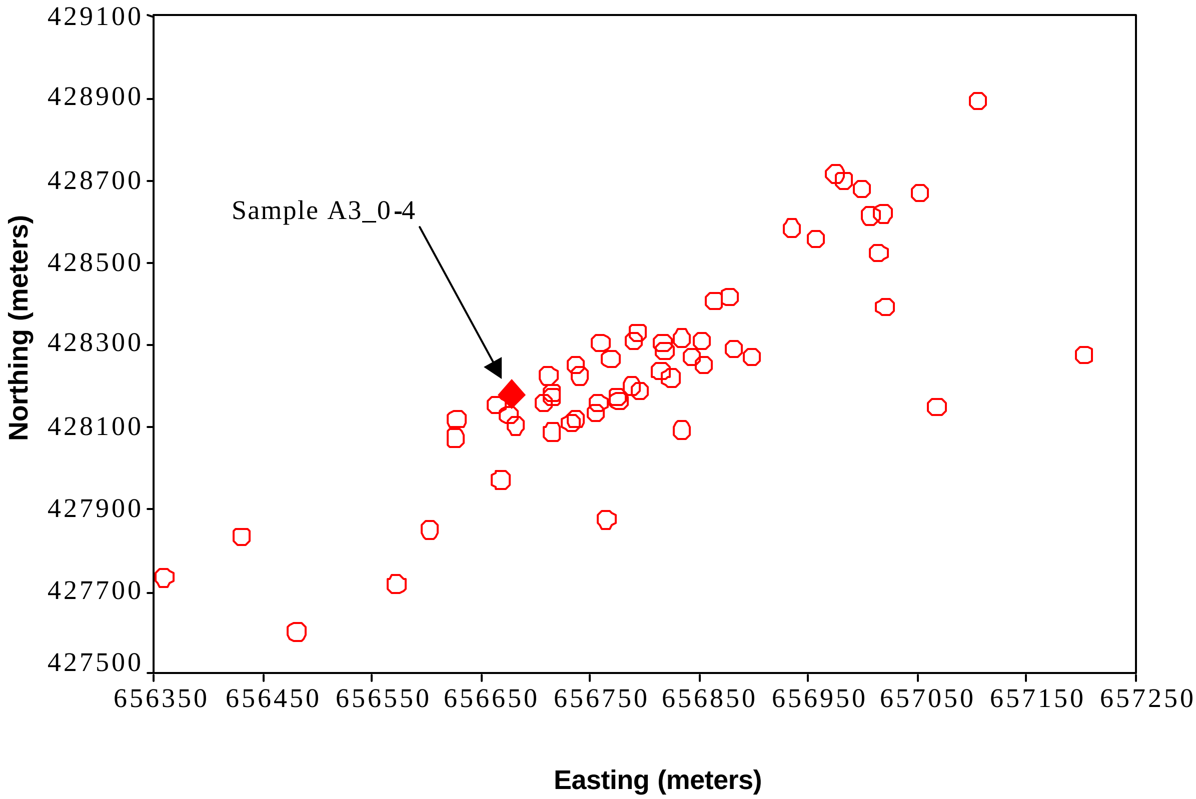

Figure 29 De Pere SMU Group 5067: Location of 0 to 10 cm Core-averaged Samples with Sample A3_0-4 Identified

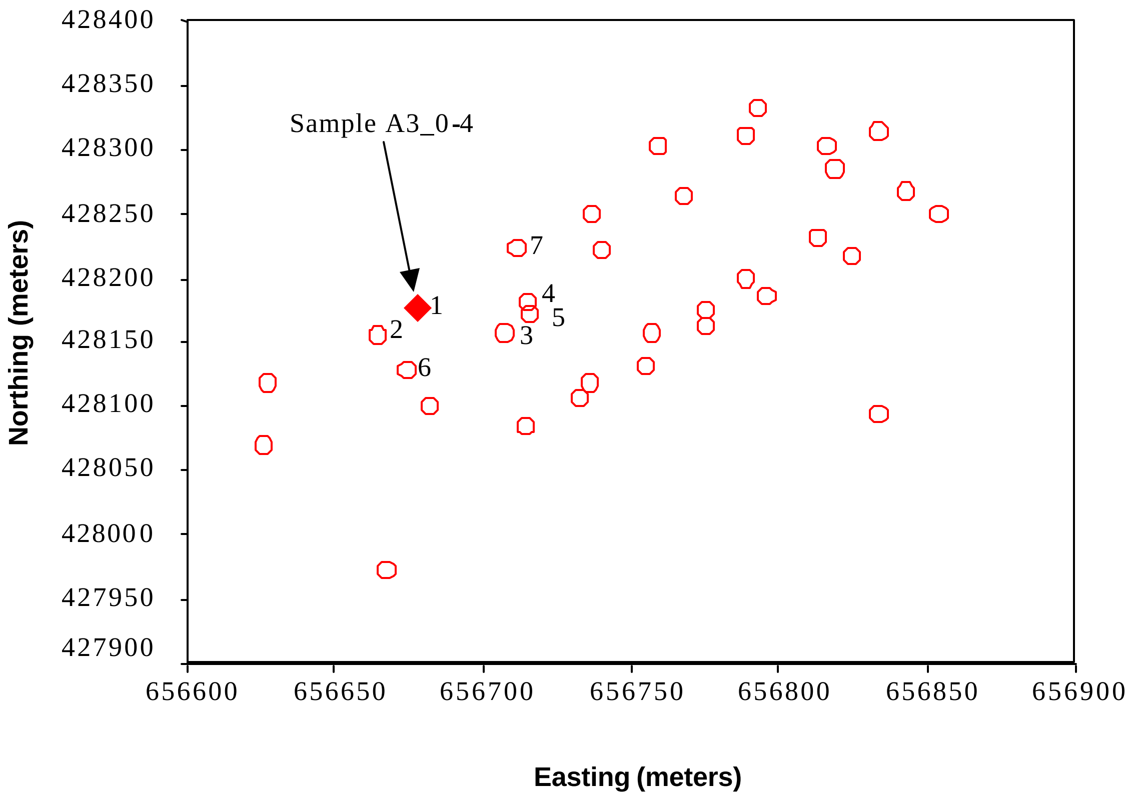

Figure 30 Sample Locations for SMU Group 5067, 0 to 10 cm Depth, Samples Closest to Sample A3_0-4 (Less than 208 meters Distance)

A3_0-4 and the six samples closest to it are labeled.

The specific concentrations of the samples near sample A3_0-4 are shown in Table 11, which includes not only concentrations for the 0- to 10-cm layer, but concentrations in lower sediment layers in precisely the same locations. (The samples have the same northing and easting coordinates down through the layers, presumably because multilayer samples were collected in a single coring operation.) These seven samples all occur within a radius of less than 60 meters from the location of A3_0-4. We note that in the 0- to 10-cm layer, all of these nearby samples are in the 2,000 to 3,000 ppb range, less than one-twentieth of the concentration of sample A3_0-4. In the next layer down, 10 to 30 cm, the highest concentration by a wide margin occurs at the same location as sample A3_0-4, suggesting that this sample location does, indeed, have a high concentration of PCBs and that the location differs from immediately neighboring sediment. We excluded the layer 30 to 50 cm from our time trends analysis (due to lack of time variation of samples) and, therefore, it does not appear in the table. The 50- to 100-cm layer shows a high concentration at the location of sample A3_0-4, but the other samples near it also show high concentrations. At 100+ cm, the PCB concentration no longer stands out at the location of sample A3_0-4.

Table 11 PCB Concentrations at Various Depths and Distances from Sample A3_0-4

Sample	0–10 cm	10–30 cm	50–100 cm	100+ cm	Year	Easting (meters)	Northing (meters)	Distance (meters)
1	99,000	150,000	150,000	53,122	1997	656678	428177	0
2	2,000	2,200	34,000	18,128	1997	656664	428155	26
3	2,100	3,100	7,000	61,094	1997	656707	428158	35
4	1,900	4,300	170,000	66,106	1997	656715	428182	37
5	2,700	4,800	13,000	30,948	1995	656716	428172	38
6	2,000	4,500	7,800	41,729	1997	656675	428128	49
7	3,000	9,900	120,000	6,665	1997	656711	428224	58

The value of 99,000 ppb stands out as considerably larger than nearby samples, which have quite uniform concentrations of PCBs and thereby heighten the contrast. We do not imply that the value of 99,000 is artificial, but it cannot readily be included in a regression analysis for the deposit. A valid regression analysis depends upon the included concentrations approximately following a normal (bell-shaped) distribution around the fitted regression model. A model fitted to the log concentrations in the 0- to 10-cm layer with sample A3_0-4 included shows that the sample is 5.5 standard deviations away from the model-fitted value, whereas all other samples are at most 2.6 standard deviations from their model-fitted values. With a sample of this size (n = 58, including A3_0-4), the occurrence of observations lying three or more standard deviations from the model questions the accuracy of the model. The deviation of 5.5 is exceptionally large. Even ignoring the modeling process, the log concentration of A3_0-4 is 7.4 standard deviations above the mean of the balance of observations, and the next largest observation is only 2.5 standard deviations above the same mean.

Thus, sample A3_0-4 appears to represent a real but exceptional concentration in the 0- to 10-cm layer. The regression model excluding it thus covers all of the 0- to 10-cm layer in the deposit except the immediate vicinity of this sample. The statistically significant decline in PCBs noted for this layer in Table 9 does not, then, necessarily apply to this small area. It is impossible to develop an estimate of the time trend for this "hotspot" alone. Of the nearby samples (Table 11), all except one occur at the same time as sample A3_0-4—1997. The lack of time variation of samples in the vicinity of A3_0-4 precludes a separate regression analysis for this sub-area.

The large concentration at the same location as A3_0-4, but one layer down—the 150,000 ppb concentration at 10 to 30 cm, is not an outlier to its layer. Its nearby samples vary considerably more among themselves relative to the variability observed in the corresponding samples from the 0- to 10-cm layer. Thus, the 150,000 value does not stand out with nearly as much contrast relative to the 99,000 value among its neighbors. The residuals from the regression analysis of the PCB concentrations in the 10- to 30-cm layer also show no statistical outliers. One reason that the concentration at this location in the 10- to 30-cm layer is so large may be that a hotspot extends from the 0- to 10-cm layer into at least part of the 10- to 30-cm layer.

In summary, the 0- to 10-cm layer of the deposit, outside of the vicinity of A3_0-4, shows a statistically significant decline in PCB concentration over time. The vicinity of A3_0-4 encompassed an area of exceptionally high concentrations with an unknown time trend. The exceptional vicinity of A3_0-4 is a small fraction of the total deposit area. A circle centered on A3_0-4 and bounded by the nearest sample (which has a typical concentration), 26 meters away, would have an area of 2,100 square meters, or approximately 0.3 percent of the 840,000-square meter total area covered by all samples of SMU Group 5067 in the 0- to 10-cm layer.

The mean slope for surface sediments in this reach, weighted by PCB mass, is --0.073 ± 0.013 and highly significant ($p < 0.0001$, Table 10). The negative slope implies a rate of decrease of 15 percent per year (95 percent confidence interval: –20 to –10 percent per year).

4.5 Comments on Combined Reaches

There may be some concern about the many analyses carried out and the possibility that some of the trends, both positive and negative, are statistically significantly different from zero by chance alone. We carried out a formal test for the hypothesis that the slopes, positive and negative, are simply randomly distributed around zero (i.e., the statistically significant differences from zero result from the large number of analyses carried out). Under the null hypothesis that the true slopes are all 0, the *p*-values should be uniformly distributed between 0 and 1.0, and minus twice the sum of the natural log of the *p*-values will yield a chi-squared variable with degrees of freedom equal to twice the total number of analyses (*p*-values) included. Carrying out this operation and obtaining a *p*-value for this null hypothesis of all zero true slopes yields $p < 0.0001$ for depth 0 to 10 cm, $p < 0.0001$ for depth 10 to 30 cm, $p = 0.07$ for 30 to 50 cm, $p = 0.01$ for 50 to 100 cm, and $p = 0.46$ for 100+ cm. Thus, it appears clear that there exist non-random changes in slope, both positive and negative, for all depths, except, possibly, 30 to 50 cm and 100+ cm. We conclude that real changes in concentrations are taking place over time in the Lower Fox River.

5 Fish Results

5.1 Number of Observations

A total of 1,742 fish samples were available for analysis, including sample types of fillet without skin, fillet with skin, and whole body. We excluded samples of eggs, stomach, carcass, and other miscellaneous sample types, as well as those for which percent lipid was unknown. As a criterion for analysis, we included only unique combinations of species and sample type for a given reach with at least 14 observations. In general, our largest model included seven parameters to be estimated. Thus, the minimum of 14 observations ensures at least twice as many observations as parameters. As some statistical "rules of thumb" require at least four or five times as many observations as parameters, our rule might strike many as rather generous. Nevertheless, we decided to err on the side of inclusiveness and to interpret with some caution analyses with a small number of observations. As an important additional condition, we required sufficient variation in time to provide a meaningful estimate of a time trend. The data provided 108 combinations of reach, species, and sample type with at least one observation, but only 19 of these had sufficient numbers of samples and an adequate time spread for analysis (see Table 12). In Little Lake Butte des Morts, 6 out of 23 combinations could be analyzed. For the other reaches, corresponding numbers are 1 of 20 for Appleton Reach, 0 of 16 for Little Rapids Reach, 7 of 24 for De Pere Reach, and 5 of 25 for Green Bay Zone 2. The 19 combinations that could be analyzed for time trends represent 868 samples—over half of all samples of whole body, fillet with skin, and fillet without skin. Carp and walleye provided the largest number of observations. None of the observations of fillet without skin would be analyzed due to either inadequate sample size or inadequate time variation. One outlier was detected and removed (see Appendix Table A-2).

Table 12 Sample Sizes for Total PCB Time Trend Analyses by Reach, Species, and Sample Type

	Fillet/Fillet No Skin	Skin-on Fillet	Whole Fish, Whole Body, Whole Body Composite	Eggs, Stomach, Carcass, Other	Total Sample Size: Fillet, Fillet No Skin, Skin-on Fillet, Whole Fish, Whole Body, Whole Body Composite
Little Lake Butte des Morts					
Brown Bullhead	4	8	6		18
Carp	20	55*	40*		115
Gizzard Shad			4		4
Northern Pike		19*	5		24
Smallmouth Bass		7	2		9
Walleye	7	63*	18*		88
White Bass		26		2	26
White Sucker	10	19	8		37
Yellow Perch		34*	7	1	41
Other	2	10	5	1	17
Appleton to Little Rapids					
Brown Bullhead	1	2			3
Carp		24	13		37
Channel Catfish	6				6
Northern Pike		7	4		11
Smallmouth Bass		5	4		9
Walleye		30*	4		34
White Bass		8	2		10
White Sucker		17	6		23
Yellow Perch		2	7		9
Other	1	10	3		14
Little Rapids to De Pere					
Carp		2	22		24
Channel Catfish	3				3
Gizzard Shad			3		3
Northern Pike		3	1		4
Smallmouth Bass		16	2		18
Walleye		48	4		52
White Bass		14			14
Yellow Perch		3	2		5
Other	4	6	8		18

Table 12 Sample Sizes for Total PCB Time Trend Analyses by Reach, Species, and Sample Type

	Fillet/Fillet No Skin	Skin-on Fillet	Whole Fish, Whole Body, Whole Body Composite	Eggs, Stomach, Carcass, Other	Total Sample Size: Fillet, Fillet No Skin, Skin-on Fillet, Whole Fish, Whole Body, Whole Body Composite
De Pere to Green Bay					
Alewife			15		15
Brown Bullhead			2		2
Carp		12	90*	13	102
Channel Catfish	17				17
Gizzard Shad		2	19*		21
Northern Pike		40*	6		46
Smallmouth Bass		15	4		19
Walleye	14	120*	58*	8	192
White Bass	3	58*	9	8	70
White Sucker		44*	22	2	66
Yellow Perch		11	9		20
Other	6	36	42	1	84
Green Bay Zone 2 (2A and 2B)					
Alewife		3	44*		47
Brown Bullhead	6	2	1		9
Carp		28*	57*	28	85
Channel Catfish	5				5
Gizzard Shad		1	32*		33
Northern Pike		7	1		8
Rainbow Smelt		2	33		35
Smallmouth Bass			2		2
Walleye		17	34		51
White Bass		3			3
White Sucker		7	1		8
Yellow Perch		19*	5		24
Other	3	33	2		38
Total (all reaches):					**1,678**

Note:
* Included in time trends analysis. Total *n* = 868.

While inadequate sample size for some species from some reaches presented the greatest obstacle to analysis, several cases with substantial numbers of observations suffered from inadequate spread over time, such as whole body white sucker in the De Pere to Green Bay Reach, with 22 observations. Notably, Little Rapids to De Pere Reach had no groups with both sufficient sample size and time spread.

Overall, only a small fraction of the observations had values below detection limit (BDL). Among the 19 combinations with a total of 868 samples, only *n* = 28 (3%)

were BDL. Several combinations had no BDL concentrations (0%), and BDL observations occurred mainly in four combinations, which had 13 to 29 percent BDL values. All observations, both above and below detection limits, in the selected combinations of reach, species, and sample type were used in the time trends analysis. Appendix Table A-3 indicates the number of observations below detection limits.

5.2 Time Trends in PCB Concentrations in Fish

We organize results in three major sections:

First, we introduce some ancillary results relevant to the process of model fitting, such as identifying the optimal location of the breakpoint and coefficients on percent lipids and seasonality (Section 5.2.1).

Then we turn to the main results, concerning rates of decline of PCB concentrations. The time trends for each species and sample type, within each reach, can be found in this section (Section 5.2.2).

Finally, we consider alternative models, such as those with a common breakpoint at 1985 for all fish categories and curvilinear (quadratic) models to test whether trends are constant or changing over time (Section 5.2.3).

5.2.1 Testing Spline Model versus Simple Linear Model

Table 13 shows results of testing the null hypothesis of a linear relationship between log of PCB concentration and time over the entire time period of the data versus the alternative hypothesis of a spline: two linear segments joined at a breakpoint. The year of the best-fitting spline model is shown in Table 13, and the *p*-value indicates whether the spline model significantly improves the fit to the data. With one exception (yellow perch, skin-on fillet in Green Bay Zone 2), the spline model has been used if $p < 0.05$ in Table 13; this means that a spline model fits significantly better than a simple, single-slope linear model.

Table 14 through Table 16 provide a description, reach by reach, of the final slopes from the fitted models (or the only slope, if there is no breakpoint) and Table 18 provides other model parameters discussed in this section. One can find the complete model in Appendix Table A-3 or A-6.

Table 13 Testing the Null Hypothesis that a Straight Line Fits As Well As a Spline Model with a Breakpoint

Reach and Species	Sample Type	Year of Best-fitting Breakpoint	Sample Size (*n*)	Breakpoint	
				p-value	Statistically Significant
Little Lake Butte des Morts					
Carp	skin-on fillet	1979	55	0.0347	*
Carp	whole fish+	1987	40	0.0263	*
Northern Pike	skin-on fillet	1996	19	0.2723	
Walleye	skin-on fillet	1990	63	0.0423	*
Walleye	whole fish+	1987	18	0.0088	**
Yellow Perch	skin-on fillet	1981	34	0.0062	**
Combined++			**229**	**<0.0001**	***
Appleton					
Walleye	skin-on fillet	1983	30	0.4526	
De Pere					
Carp	whole fish+	1995	90	0.0087	**
Gizzard Shad	whole fish+	1990	19	0.4672	
Northern Pike	skin-on fillet	1996	40	0.1421	
Walleye	skin-on fillet	1993	120	0.5680	
Walleye	whole fish+	1996	58	0.5550	
White Bass	skin-on fillet	1996	58	0.6059	
White Sucker	skin-on fillet	1990	44	0.1986	
Combined++			**429**	**0.0906**	
Green Bay Zone 2 (2A and 2B)					
Alewife	whole fish+	1986	44	0.0863	
Carp	skin-on fillet	1985	28	0.1811	
Carp	whole fish+	1983	57	0.0001	***
Gizzard Shad	whole fish+	1996	32	0.6655	
Yellow Perch	skin-on fillet+++	1986	19	0.0008	***
Combined++			**180**	**<0.0001**	***

Notes:

- * $p < 0.05$
- ** $p < 0.01$
- *** $p < 0.001$
- \+ Whole fish, or whole body, or whole body composite.
- ++ Indicates *p*-value for testing the null hypothesis that all fish categories in a reach do not have a breakpoint.
- +++ A model with a breakpoint was rejected. See text.

Reach 1 — Little Lake Butte des Morts

In the first reach, for five of the six fish categories, the spline model fit significantly better than the linear model. In all cases, the initial slope decreased more steeply than the final slope, as seen by the negative coefficient for the slope difference. Figure 31 for carp fillet with skin in Little Lake Butte des Morts shows an example of an initial steep slope until 1979, followed by a continuing decline, but at a slower rate. Similar plots for all analyses are found in the Appendix. Figure 32 shows an example of initial decline until 1990, followed by a virtually flat line implying no further decline in PCBs. Figure 33 shows an example in which PCB concentration actually increases after the breakpoint in 1987. With only 18 data points and 9 distinct time points, one should interpret this result cautiously. Of note, the fitted line appears to fit poorly prior to 1987 because all of the observations lie above the fitted line. The fitted line, however, represents the prediction for fish with percent lipid equal to the mean, sampled on July 1. For this fish category, samples were taken prior to 1987 in late August and early September, and after 1987 mainly in July and some as early as April. This discrepancy, plus evidence for a significant seasonal effect for this fish category, explains the poor visual fit on the plot. The row at the bottom of the panel for Little Lake Butte des Morts in Table 14 reports the *p*-value from a meta-analysis for this reach. This meta-analysis combines the results from all species within this reach to test the global null hypothesis that a linear model fits well for **all** species/types versus the alternative that a spline model with a breakpoint gives a better fit for at least one species. The highly significant *p*-value provides strong evidence to reject the null hypothesis that every species has a constant rate of decline over the entire time frame in Little Lake Butte des Morts.

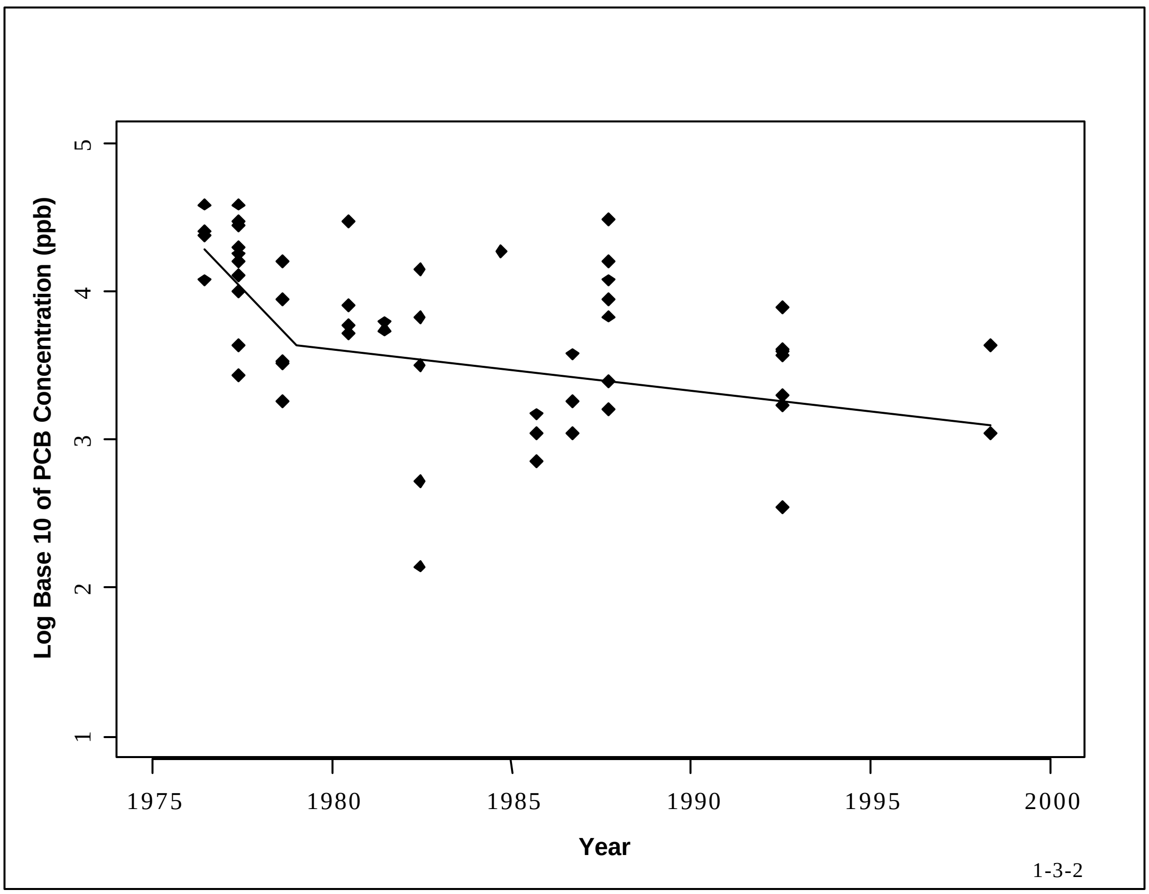

Figure 31 Log$_{10}$ PCB Concentration (ppb) in Little Lake Butte des Morts Carp, Skin-on Fillet, versus Time

Breakpoint = 1979 (p = 0.03), Final Slope (log$_{10}$ PCB versus time) = –0.028 (p = 0.02), Rate of Change of PCB Concentration During Period of Final Slope = --6.1% (95% confidence interval: –10.9% to –1.1%).

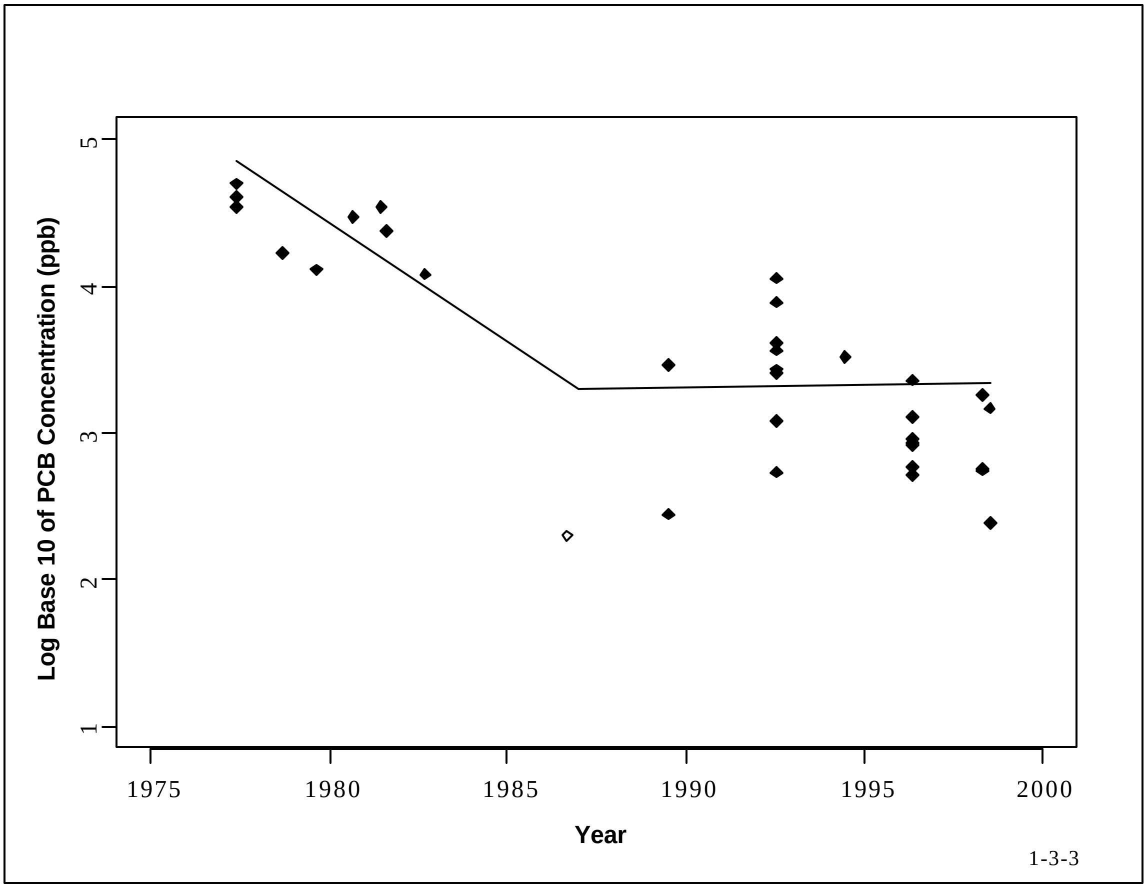

Figure 32 Log$_{10}$ PCB Concentration (ppb) in Little Lake Butte des Morts Carp, Whole Body, versus Time

Breakpoint = 1987 (p = 0.03), Final Slope (log$_{10}$ PCB versus time) = 0.003 (p = 0.9), Rate of Change of PCB Concentration During Period of Final Slope = 0.7% (95% confidence interval: –12.3% to 15.6%). Any values below detection limit are depicted as ◇.

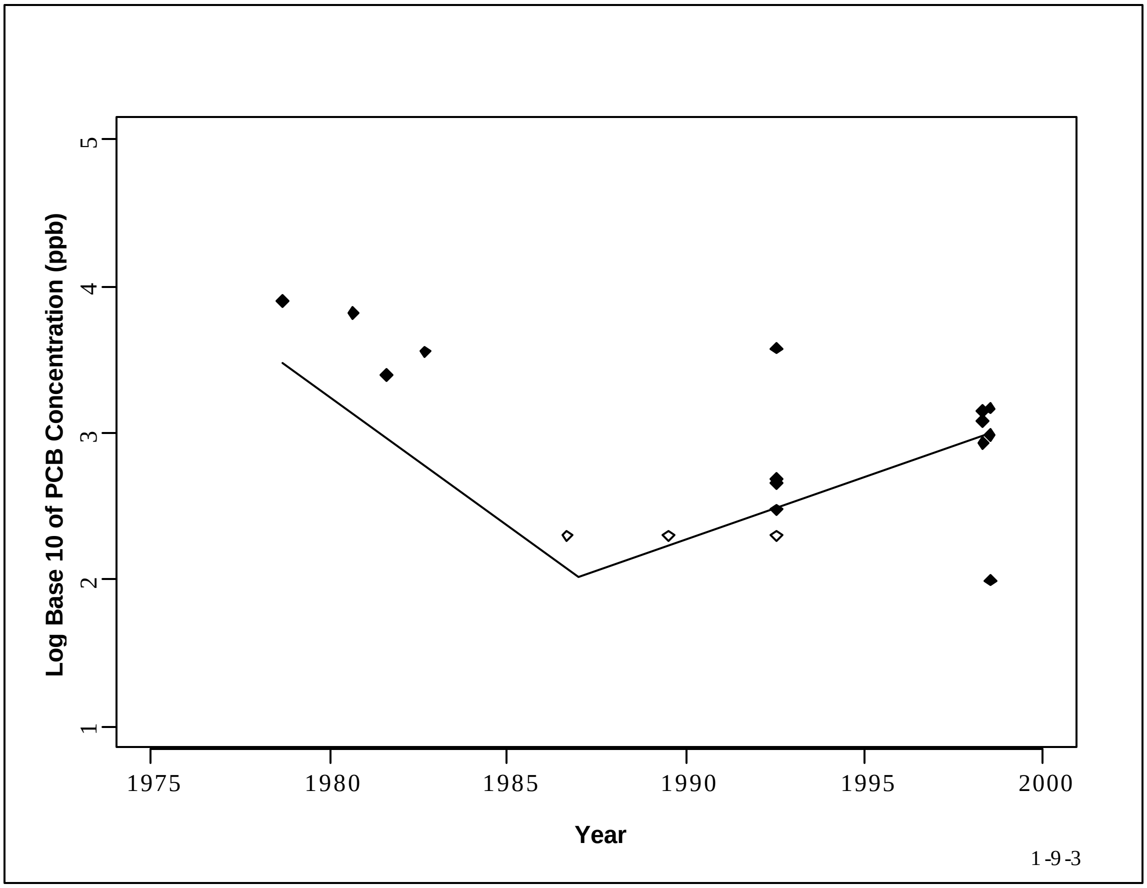

Figure 33 Log$_{10}$ PCB Concentration (ppb) in Little Lake Butte des Morts Walleye, Whole Body, versus Time

Breakpoint = 1987 (p = 0.009), Final Slope ($\log_{10}$ PCB versus time) = 0.084 (p = 0.09), Rate of Change of PCB Concentration During Period of Final Slope = 21.5% (95% confidence interval: –3.5% to 52.9%). Any values below detection limit are depicted as ◇.

Table 14 PCB Time Trend Results for Fish Samples in Little Lake Butte des Morts Reach

Species	Sample Type	Year of Break-point	*n*	Final (post-break) Slope				95% Confidence Interval	
				Final Slope	SE	*p*-value	% per Year	LCL	UCL
Carp	skin-on fillet	1979	55	–0.028	0.011	0.0177*	–6.1	–10.9	–1.1
	whole body	1987	40	0.003	0.030	0.9172	0.7	–12.3	15.6
Northern Pike	skin-on fillet	N/A	19	–0.055	0.011	0.0003***	–11.8	–16.7	–6.7
Walleye	skin-on fillet	1990	63	0.015	0.025	0.5576	3.4	–7.8	16.0
	whole body	1987	18	0.084	0.045	0.0874	21.5	–3.5	52.9
Yellow Perch	skin-on fillet	1981	34	0.003	0.012	0.8025	0.7	–5.0	6.8

Notes:

N/A – Not applicable; no breakpoint.
* $p < 0.05$
** $p < 0.01$
*** $p < 0.001$

Reach 2 — Appleton to Little Rapids

Only data for walleye can be analyzed for this reach. The data provide no evidence to reject the null hypothesis of a constant rate of decline over the time span of observation. $P = 0.5$ for the spline model versus the simple linear model (Table 13).

Table 15 PCB Time Trend Results for Fish Samples in Appleton to Little Rapids Reach

Species	Sample Type	Year of Break-point	*n*	Final (post-break) Slope				95% Confidence Interval	
				Final Slope	SE	*p*-value	% per Year	LCL	UCL
Walleye	skin-on fillet	N/A	30	–0.046	0.014	0.0028**	–10.0	–15.7	–3.9

Notes:

N/A – Not applicable; no breakpoint.
* $p < 0.05$
** $p < 0.01$
*** $p < 0.001$

Reach 3 — Little Rapids to De Pere

No fish species with both an adequate sample size and sufficient spread of samples over time for analysis occurred in this reach.

Reach 4 — De Pere to Green Bay

In this reach, six of the seven fish categories show no significant improvement in fit of the spline model over the linear model. Figure 34 shows an example where the linear model fits quite well. For one species, though, a model with a change point in 1995 fits significantly better than the linear model (De Pere to Green Bay, carp, whole body). As seen in Figure 35, this model shows a large increase in log PCB concentration between 1997 and 1999. The substantial number of samples at these two time points may in fact represent a real increase in PCB concentration.

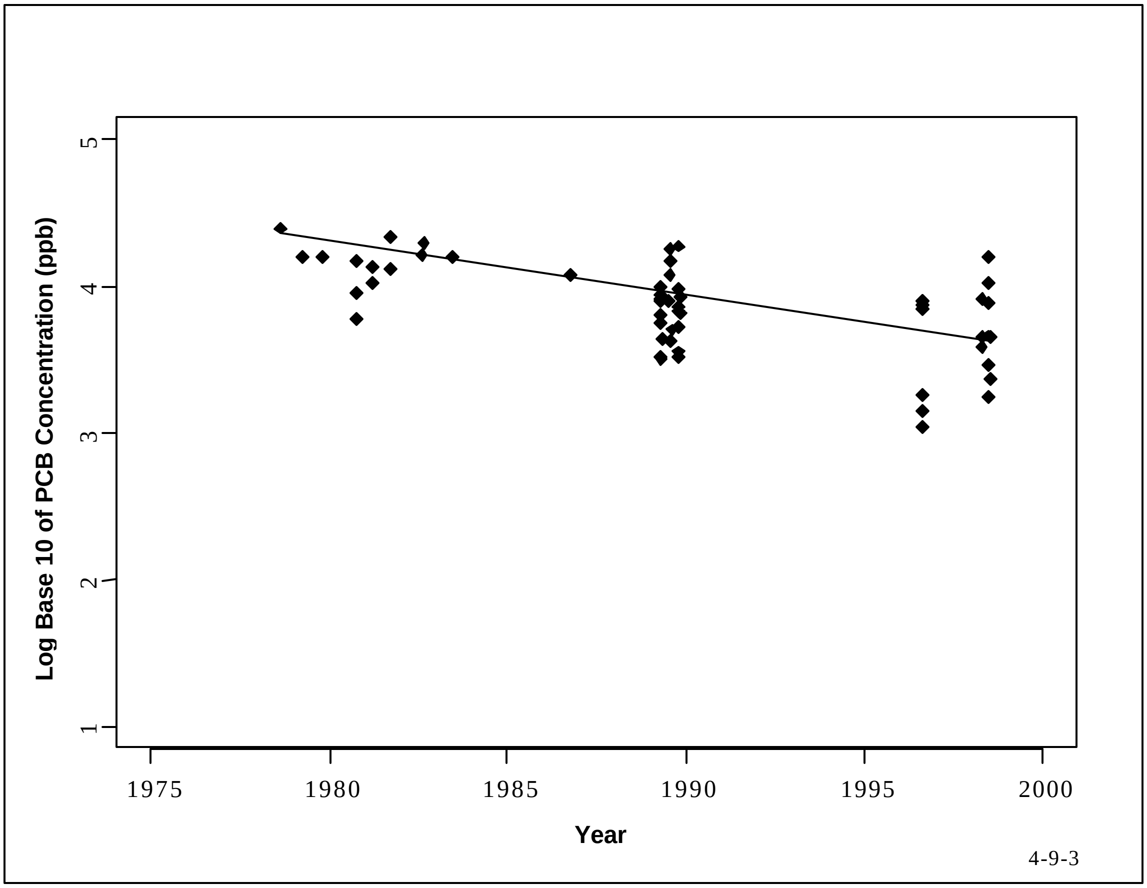

Figure 34 Log_{10} PCB Concentration (ppb) in De Pere to Green Bay Walleye, Whole Body, versus Time

No Breakpoint, Final Slope (log_{10} PCB versus time) = –0.037 ($p < 0.0001$), Rate of Change of PCB Concentration During Period of Final Slope = –8.1% (95% confidence interval: –10.4% to –5.8%).

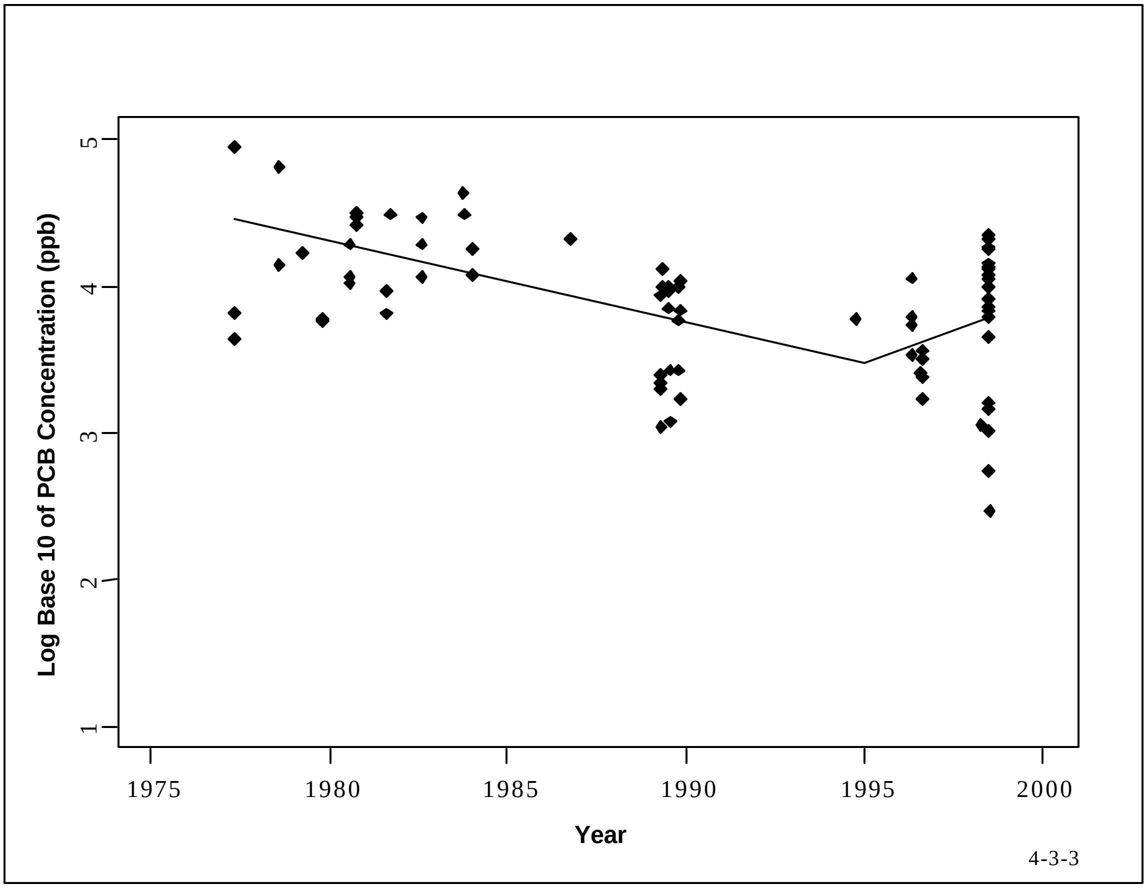

Figure 35 Log_{10} PCB Concentration (ppb) in De Pere to Green Bay Carp, Whole Body, versus Time

Breakpoint = 1995 (p = 0.009), Final Slope (log_{10} PCB versus time) = 0.086 (p = 0.03), Rate of Change of PCB Concentration During Period of Final Slope = 21.8% (95% confidence interval: 2.2% to 45.0%).

The non-significant (p = 0.09) meta-analysis for this reach indicates only weak evidence to reject the overall null hypothesis of a constant rate of change for all species within this reach over the time span of observation (Table 13). The meta-analysis partially remedies the problem of multiple comparisons. That is, if one conducts seven independent hypothesis tests and uses the standard criterion $p < 0.05$ to designate statistical significance, the probability of finding at least one significant p-value out of these seven tests, when the null hypothesis is really true, approaches 30 percent. This considerably exceeds the 5 percent false positives behind "$p < 0.05$." Thus, the single significant breakpoint for this reach in Table 16 with p = 0.009 may have occurred by chance.

Table 16 PCB Time Trend Results for Fish Samples in De Pere to Green Bay Reach

Species	Sample Type	Year of Break-point	*n*	Final (post-break) Slope				95% Confidence Interval	
				Final Slope	SE	*p*-value	% per Year	LCL	UCL
Carp	whole body	1995	90	0.086	0.038	0.0277*	21.8	2.2	45.0
Gizzard Shad	whole body	N/A	19	–0.023	0.005	0.0002***	–5.1	–7.2	–2.9
Northern Pike	skin-on fillet	N/A	40	–0.046	0.007	<0.0001***	–10.0	–13.0	–6.8
Walleye	skin-on fillet	N/A	120	–0.032	0.004	<0.0001***	–7.2	–8.7	–5.6
	whole body	N/A	58	–0.037	0.005	<0.0001***	–8.1	–10.4	–5.8
White Bass	skin-on fillet	N/A	58	–0.021	0.006	0.0020**	–4.7	–7.5	–1.8
White Sucker	skin-on fillet	N/A	44	–0.036	0.006	<0.0001***	–7.9	–10.3	–5.5

Notes:

N/A – Not applicable; no breakpoint.
* $p < 0.05$
** $p < 0.01$
*** $p < 0.001$

Reach 5 — Green Bay Zone 2

In the final reach considered, two of the fish categories show a highly significant improvement of the change point model over the linear model. For carp whole body samples, PCB concentration rises sharply until 1983 and then drops. Prior to 1983, there were samples for only five fish at two distinct time points. A similar pattern holds for carp fillet with skin samples, though the spline is statistically non-significant compared to the linear model.

For yellow perch skin-on fillet, we rejected the spline model, even though it formally provided a "better" fit, which can be seen in Figure 36. In this model, one finds a very steep fitted decrease until 1986, followed by a fitted steep increase. The huge amplitude of the estimated seasonal effect, however, exceeds by five- or ten-fold that for other fish categories. These strange results raised the concern that we may have over-fit the model for this species. The spline model for Figure 36 relied on 19 samples collected at seven distinct time points. There are six parameters in time (intercept, final slope, initial slope difference, location of breakpoint, sine and cosine of time of year) and only seven distinct time points. Introducing as many parameters in time as time points risks over-fitting and uncertain or erroneous estimates.

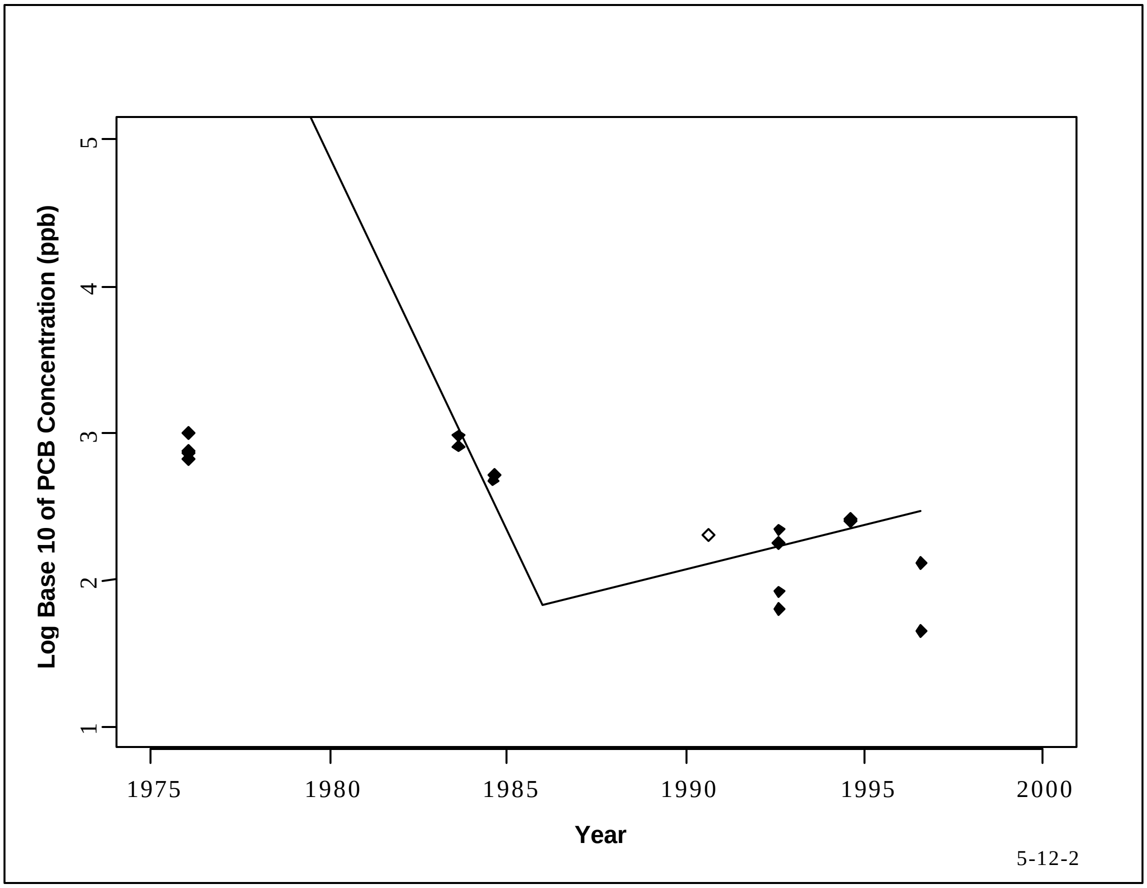

Figure 36 Rejected Spline Model for Green Bay Zone 2 Yellow Perch, Skin-on Fillet

Let us explain over-fitting by analogy. Suppose we choose six distinct time points. At each time point we randomly generate 10 values for log(*PCB*) as if 10 fish were sampled at that time point, for a total of 60 values. Then we fit a polynomial with six parameters (powers of time = X, from constant—X^0—through X^5) and plot the raw data and fitted line on a scatter plot. This polynomial will fit perfectly in time—it will go exactly through the mean value at each time point. Of course, it will probably generate an implausible curve that varies drastically, perhaps with extremely large peaks or valleys between time points. This hypothetical example speaks to our situation. Fitting our model with six parameters in time mirrors fitting a polynomial with six parameters and, therefore, may give ridiculous results. In the example of yellow perch fillet with skin, we encounter only one additional, distinct time point (seven time points instead of six), which reduces but does not eliminate the risk of over-fitting. We recommend discarding the fitted model with a breakpoint at 1986 for yellow perch fillet with skin in this reach, as it exemplifies over-fitting. Therefore, we will use the simple linear model as the best-fitting model for these data (Figure 37). The model provides not only a more plausible fit, but a visually acceptable fit as well.

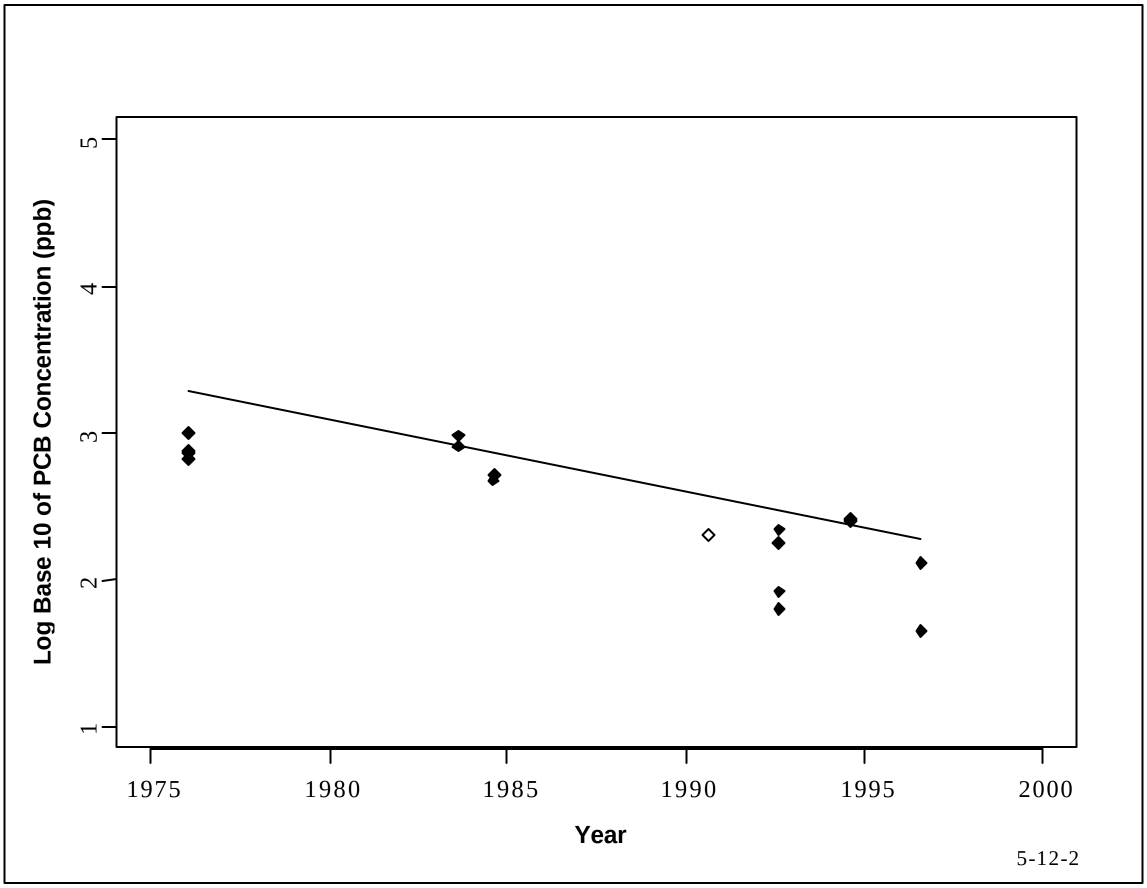

Figure 37 Log$_{10}$ PCB Concentration in Green Bay Zone 2 Yellow Perch, Skin-on Fillet, versus Time

No Breakpoint, Final Slope ($\log_{10}$ PCB versus time) = –0.049 (p = 0.004), Rate of Change of PCB Concentration During Period of Final Slope = –10.7% (95% confidence interval: –16.8% to –4.2%). Any values below detection limit are depicted as ◊.

Table 17 PCB Time Trend Results for Fish Samples in Green Bay Zone 2

Species	Sample Type	Year of Break-point	*n*	Final (post-break) Slope				95% Confidence Interval	
				Final Slope	SE	*p*-value	% per Year	LCL	UCL
Alewife	whole body	N/A	44	−0.018	0.009	0.0497*	−4.0	−7.8	0.0
Carp	skin-on fillet	N/A	28	−0.023	0.015	0.1557	−5.1	−11.8	2.2
	whole body	1983	57	−0.073	0.010	<0.0001***	−15.5	−19.5	−11.4
Gizzard Shad	whole body	N/A	32	0.025	0.010	0.0144*	5.9	1.2	10.8
Yellow Perch	skin-on fillet	N/A	19	−0.049	0.014	0.0038**	−10.7	−16.8	−4.2

Notes:

N/A – Not applicable; no breakpoint.
* $p < 0.05$
** $p < 0.01$
*** $p < 0.001$

Impact of Seasonality and Lipid Content on Best-fitting Model

For each fish category (reach/species/type combination), we determined the best-fitting model, either the linear model or the spline model with one breakpoint, if that showed a significantly better fit than the linear model. Table 18 shows details of the fitted models.

From left to right, Table 18 shows the year of the breakpoint or "N/A" for no breakpoint) in units of $\log_{10}$ (PCB concentration as ppb) per year and the standard error and *p*-value of the slope; the rate of change per year as a percentage along with a 95 percent confidence interval for the percentage; the difference between early and late slope, if applicable, in units of $\log_{10}$ (PCB concentration as ppb) per year, along with the standard error and *p*-value for the difference between early and late slope; the coefficient of $\log_{10}$ (lipid percent) and its standard error and *p*-value; and the month of the maximum amplitude of the seasonal effect and the amplitude (A) and the *p*-value for the seasonal effect. The quantities 10^{A} and 10^{-A} are multipliers that show the relative increase or decrease, respectively, of the seasonal maximum or minimum compared to the annual mean.

We note some interesting features about the covariates in Table 18. The coefficient of log of percent lipid departs significantly from zero for almost all fish categories. This coefficient approaches one for many fish categories, meaning that an analysis using the log of lipid-normalized PCB concentration as the outcome variable, without including percent lipids as a covariate, would be approximately correct. (As noted earlier, lipid normalization is usually calculated as PCB concentration divided by the percent lipid in the tissue.) Yet for several species the coefficient fails to reach 1. This suggests that traditional lipid normalization alone does not control the lipid contribution adequately. The amplitude of the seasonal effect is significantly non-zero for the majority of fish categories, falling mainly in the 0.2 to 0.6 range. We define the amplitude as the height of the seasonal sine curve from zero to the maximum on the log scale, so the range from minimum to maximum is twice this value. On the log scale, the majority of species would fall between 0.4 and 1.2. Calculating the antilog of 0.4 and 1.2 (i.e., 10 raised to that power) tells us that the ratio of maximum to minimum over a year ranges from 2.5 to 16 for the majority of species. This represents substantial seasonal variation. The month in which the peak PCB concentration occurs varies quite a bit across fish categories. A footnote to Appendix Table A-3 explains how to calculate estimated PCB concentration for any time of year, taking account of seasonal variation.

As seen in the plots, we observe quite a bit of variation in log of PCB concentration around the fitted line. Even fish samples taken at the same time vary greatly in PCB concentration. The residual standard deviation (SD), after fitting the model, measures the magnitude of this variation. Using the approximation of plus or minus two SDs allows us to estimate the range, which covers most of the data (from low to high end), at about four SDs. From an appendix table, most of the standard deviation values (calculated as the square root of the mean squared error) fall between 0.15 and 0.35. Four SDs is thus between 0.60 and 1.40 for most species. Taking the antilog of 0.60 and 1.40 gives 4.0 and 25, respectively. This implies very high variation in PCB concentration for a particular reach/species/type: for species with the least variation, the values differ from the low end to the high end by roughly a factor of four, corresponding to an SD of 0.15. That is, for the species with an SD of 0.15, it would not be uncommon to find different samples with a fourfold difference in PCB concentration when sampled at the same time of year and with the same lipid content (e.g., whole body alewife, in Green Bay Zone 2 has an SD = 0.17, similar to 0.15). For species with an SD of 0.35 (such as carp fillet with skin, Little Lake Butte des Morts), it would not be uncommon to find samples differing by a factor of 25 in PCB concentration. Figure 31 shows just such variation and supports the notion of highly variable PCB concentrations within species.

Table 18 Model Parameters and Other Statistics for the Best-fitting Model

Species	Sample Type	Year of Break-point	*n*	Final (post-break) Slope				95% Confidence Interval		Pre-break Slope Minus Final Slope	SE	*p*-value Slope Change	Coef-ficient of Log (% lipid)	SE	*p*-value for Log (% lipid)	Seasonal Peak		*p*-value for Seasonal Effect
				Final Slope	SE	*p*-value	% per Year	LCL	UCL							Mo.	Ampli-tude	
Little Lake Butte des Morts																		
Carp	skin-on fillet	1979	55	−0.028	0.011	0.0177*	−6.1	−10.9	−1.1	−0.228	0.085	0.0102	0.87	0.15	0.0000	12.9	0.39	0.0078
	whole body	1987	40	0.003	0.30	0.9172	0.7	−12.3	15.6	−0.165	0.059	0.0084	0.86	0.33	0.0131	7.0	0.83	0.0025
Northern Pike	skin-on fillet	N/A	19	−0.055	0.011	0.0003***	−11.8	−16.7	−6.7				0.45	0.30	0.1554	1.3	0.67	0.1594
Walleye	skin-on fillet	1990	63	0.015	0.025	0.5576	3.4	−7.8	16.0	−0.095	0.037	0.0140	0.50	0.15	0.0011	11.6	0.20	0.0273
	whole body	1987	18	0.084	0.045	0.0874	21.5	−3.5	52.9	−0.261	0.080	0.0069	0.99	0.36	0.0185	11.6	0.46	0.0040
Yellow Perch	skin-on fillet	1981	34	0.003	0.012	0.8025	0.7	−5.0	6.8	−0.247	0.077	0.0034	0.49	0.21	0.0236	7.0	0.22	0.0007
Appleton																		
Walleye	skin-on fillet	N/A	30	−0.046	0.014	0.0028**	−10.0	−15.7	−3.9				1.08	0.16	0.0000	8.1	0.43	0.0010
De Pere																		
Carp	whole body	1995	90	0.086	0.038	0.0277*	21.8	2.2	45.0	−0.141	0.044	0.0022	0.79	0.11	0.0000	6.7	0.06	0.0004
Gizzard Shad	whole body	N/A	19	−0.023	0.005	0.0002***	−5.1	−7.2	−2.9				0.51	0.09	0.001	8.6	0.58	0.0000
Northern Pike	skin-on fillet	N/A	40	−0.046	0.007	<0.0001***	−10.0	−13.0	−6.8				0.72	0.17	0.0001	10.1	0.17	0.3531
Walleye	skin-on fillet	N/A	120	−0.032	0.004	<0.0001***	−7.2	−8.7	−5.6				0.85	0.07	0.0000	9.5	0.02	0.7566
	whole body	N/A	58	−0.037	0.005	<0.0001***	−8.1	−10.4	−5.8				0.44	0.12	0.0007	7.0	0.12	0.2038
White Bass	skin-on fillet	N/A	58	−0.021	0.006	0.0020**	−4.7	−7.5	−1.8				0.82	0.11	0.0000	6.7	0.33	0.1043
White Sucker	skin-on fillet	N/A	44	−0.036	0.006	<0.0001***	−7.9	−10.3	−5.5				0.43	0.15	0.0071	6.9	0.08	0.5528
Green Bay Zone 2																		
Alewife	whole body	N/A	44	−0.018	0.009	0.0497*	−4.0	−7.8	0.0				0.91	0.14	0.0000	6.1	0.17	0.0335
Carp	skin-on fillet	N/A	28	−0.023	0.015	0.1557	−5.1	−11.8	2.2				0.76	0.15	0.0000	3.9	0.24	0.0288
	whole body	1983	57	−0.073	0.010	<0.0001***	−15.5	−19.5	−11.4	0.266	0.059	0.0000	0.90	0.10	0.0000	6.9	0.24	0.0000
Gizzard Shad	whole body	N/A	32	0.025	0.010	0.0144*	5.9	1.2	10.8				−0.13	0.12	0.2811	2.6	0.34	0.0300

Table 18 Model Parameters and Other Statistics for the Best-fitting Model

Species	Sample Type	Year of Break-point	*n*	Final (post-break) Slope				95% Confidence Interval		Pre-break Slope Minus Final Slope	SE	*p*-value Slope Change	Coef-ficient of Log (% lipid)	SE	*p*-value for Log (% lipid)	Seasonal Peak		*p*-value for Seasonal Effect
				Final Slope	SE	*p*-value	% per Year	LCL	UCL							Mo.	Ampli-tude	
Yellow Perch	skin-on fillet	N/A	19	−0.049	0.014	0.0038**	−10.7	−16.8	−4.2				1.09	0.47	0.353	4.7	0.45	0.5489

Notes:

N/A – Not applicable; no breakpoint.
* $p < 0.05$
** $p < 0.01$
*** $p < 0.001$

5.2.2 Best-fitting Model, Meta-analysis, Sensitivity Analysis, and Future Projections

In the preceding section, Table 13 and the related discussion presented decisions for each reach, species, and sample type on the choice between a model including a breakpoint in the time trend and a model without a time trend. Accepting that decision, Table 14 through Table 17 presented the final slopes for the best-fitted models. Table 18 presented additional parameters for each best-fitted model. The Appendix includes the full set of parameters for each model.

Table 19 shows the results of meta-analyses for each reach. The final row in each reach gives a combined species analysis. The combined post-breakpoint slope is a weighted average of all the slopes within this reach, weighted by the inverse of the standard error squared. The inverse standard error squared provides weights leading to a minimum variance of the weighted mean estimate in many common sampling situations. Unlike the meta-analysis of surface sediments introduced in Section 4.4.1 (Table 10), where PCB mass provided a natural set of weights, there is no *a priori* set of weights available to use with fish. Thus, weights with good statistical properties have been chosen for the fish meta-analysis. This weighting gives high weights to more precise estimates, usually based on a large sample size, and low weights to imprecise estimates, usually derived from small sample sizes. The *p*-value (based on the normal distribution) tests whether this summary slope differs significantly from zero.

The fish species included in the meta-analysis have diverse habitats, lifecycles, and feeding patterns. Nevertheless, the PCB concentration in each species serves as a sentinel of PCBs in their environment. Just as the economic growth rate of each unique industrial sector of a nation can combine into a single growth rate for a national economy, the time trends of diverse species can combine into a meaningful descriptive statistical time trend for fish species in a reach. This summary rate of change cannot replace the individual species' rates of change. It means only what its definition implies: weighting more heavily on species with more precise slope estimates and less heavily on species with less precise slope estimates provides a reach mean slope which can be compared to zero. An individual species may possibly have a real slope that differs substantially from the combined reach slope. While the combined slope is a summary, the individual slopes cannot be ignored. Also, as noted in Section 4.4.1 in reference to sediment, the combined slope should not be used to project PCB concentrations for all species in the reach.

In addition to the combined reach slope in Table 19, the percent rate of change of PCB concentration implied by the combined slope, *b*, is also presented, using the following equation:

Equation 17

$$percent\ change = 100 * \left(10^{b} - 1\right)$$

The 95 percent confidence interval for the percent change is also shown in the table (calculated by deriving the 95 percent confidence interval for the slope of log PCB concentration versus time—using the normal distribution and converting the upper and lower confidence bounds to percentages by Equation 17).

In this section, we also address an issue of uncertainty associated with the breakpoint. As mentioned in the methods section, the standard errors for time trend slopes and *p*-values for the best-fitting model do not incorporate the variation due to estimating the location of the breakpoint. They therefore underestimate the uncertainty in the time trend slope. The standard errors shown in the table are too small for those species where the model has a breakpoint. We addressed this problem by performing a sensitivity analysis for each of the seven reach/species/type combinations with a breakpoint model. We identified the earliest and the latest breakpoints that were "plausible," as described in the methods section. Table 20 shows results for these "earliest" and "latest" models, when there is a breakpoint.

Table 19 Meta-analysis of Fish Time Trends

Species	Sample Type	Log_{10} (PCB) Time Trend Final Slope Estimate	Standard Error	Statistical Weight[+]	*p*-value	Annual % Change in PCB Concentration	% Change 95% Lower Bound	% Change 95% Upper Bound
Little Lake Butte des Morts								
Carp	skin-on fillet	–0.028	0.011	0.31				
	whole body	0.003	0.30	0.05				
Northern Pike	skin-on fillet	–0.055	0.011	0.30				
Walleye	skin-on fillet	0.015	0.025	0.06				
	whole body	0.084	0.045	0.02				
Yellow Perch	skin-on fillet	0.003	0.012	0.26				
Combined		**–0.022**	**0.006**	**1.00**	**0.0006**	**–4.9**	**–7.5**	**–2.1**
Appleton								
Walleye	skin-on fillet	–0.056	0.016		0.003	–10.0	–17.9	–5.6
De Pere								
Carp	whole body	0.086	0.038	0.00				
Gizzard Shad	whole body	–0.023	0.005	0.21				
Northern Pike	skin-on fillet	–0.046	0.007	0.08				
Walleye	skin-on fillet	–0.032	0.004	0.32				
	whole body	–0.037	0.005	0.15				
White Bass	skin-on fillet	–0.021	0.006	0.10				
White Sucker	skin-on fillet	–0.036	0.006	0.14				
Combined		**–0.031**	**0.002**	**1.00**	**<0.0001**	**–6.9**	**–7.8**	**–6.0**

Table 19 Meta-analysis of Fish Time Trends

Species	Sample Type	Log_{10} (PCB) Time Trend Final Slope Estimate	Standard Error	Statistical Weight⁺	*p*-value	Annual % Change in PCB Concen-tration	% Change 95% Lower Bound	% Change 95% Upper Bound
Green Bay Zone 2								
Alewife	whole body	−0.018	0.009	0.31				
Carp	skin-on fillet	−0.023	0.015	0.10				
	whole body	−0.073	0.010	0.22				
Gizzard Shad	whole body	0.025	0.010	0.26				
Yellow Perch	skin-on fillet	−0.049	0.014	0.12				
Combined		**−0.033**	**0.007**	**1.00**	**<0.0001**	**−5.1**	**−7.2**	**−3.0**

Note:

⁺ Statistical weight is proportional to the inverse of the squared standard error. Weights sum to 1.0 within each reach.

Figure 38 captures the estimated percent change per year for the best-fitting model for each fish category. The confidence intervals shown in these plots obtain from the results of the best-fitting model and do not incorporate the extra uncertainty due to estimating the location of the breakpoint. Therefore, the reader must remember that the plotted confidence intervals are too narrow for the seven analyses with a breakpoint.

Table 20 Final Slope and Percent Change per Year for Best-fitting Model and Sensitivity Analysis

Species	Sample		Best-fitting Model			Earliest Breakpoint			Latest Breakpoint		
	Type	*n*	Break point Year	% Change per Year	*p*-value (% = 0)	Year	Final Slope: % Change per Year	*p*-value (% = 0)	Year	Final Slope: % Change per Year	*p*-value (% = 0)
Little Lake Butte des Morts											
Carp	skin-on fillet	55	1979	−6.15	0.0177	1979	−6.15	0.0177	1985	−1.56	0.7419
	whole body	40	1987	0.71	0.9172	1985	−4.04	0.5264	1990	−0.25	0.9765
Northern Pike	skin-on fillet	19	N/A	−11.83	0.0003						
Walleye	skin-on fillet	63	1990	3.44	0.5576	1979	−8.37	0.0000	1994	8.82	0.4482
	whole body	18	1987	21.47	0.0874	1984	15.10	0.2024	1990	21.11	0.1324
Yellow Perch	skin-on fillet	34	1981	0.73	0.8025	1979	0.27	0.9252	1996	333.61	0.0122
Appleton											
Walleye	skin-on fillet	30	N/A	−9.97	0.0028						
De Pere											
Carp	whole body	90	1995	21.76	0.0277	1990	−0.69	0.8232	1996	29.80	0.0191
Gizzard Shad	whole body	19	N/A	−5.07	0.0002						
Northern Pike	skin-on fillet	40	N/A	−9.95	0.0000						
Walleye	skin-on fillet	120	N/A	−7.19	0.0000						
	whole body	58	N/A	−8.11	0.0000						
White Bass	skin-on fillet	58	N/A	−4.72	0.0020						
White Sucker	skin-on fillet	44	N/A	−7.90	0.0000						
Green Bay Zone 2											
Alewife	whole body	44	N/A	−3.96	0.0497						
Carp	skin-on fillet	28	N/A	−5.06	0.1557						
	whole body	57	1983	−15.54	0.0000	1983	−15.54	0.0000	1984	−16.15	0.0000
Gizzard Shad	whole body	32	N/A	5.91	0.0144						
Yellow Perch	skin-on fillet	19	N/A	−10.75	0.0038						

Note:

N/A – Not applicable; no breakpoint.

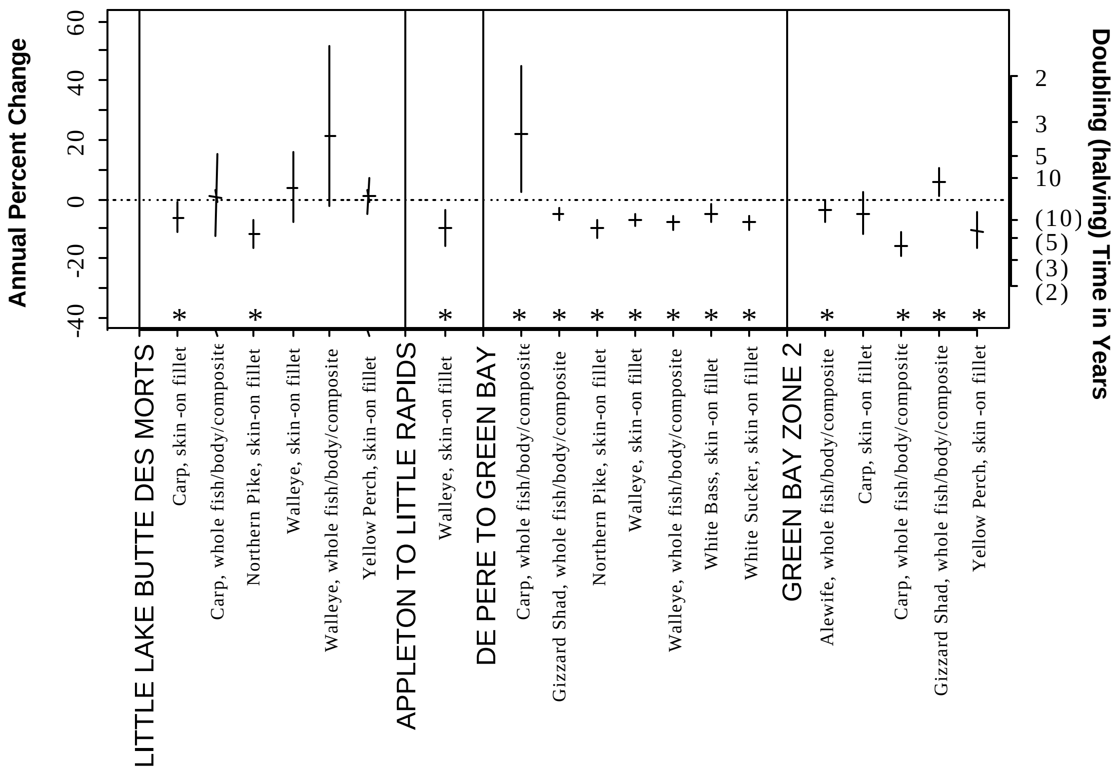

Figure 38 95 Percent Confidence Intervals Showing Annual Percent Rate of Change (Left Vertical Axis) in PCB Concentrations by Reach, Species, and Sample Type

An asterisk (*) indicates a rate of change that differs significantly from zero. Right vertical axis expresses time trend change in terms of doubling and halving times.

Table 21 shows projections into the future based on the best-fitting model, spline, or simple linear trend. We present the estimated mean PCB concentration in the years 1999 and 2020, with 95 percent confidence intervals for the concentration at each year. For fish categories with a negative final slope (the post-breakpoint slope for the spline models), the table also shows estimated times until PCB concentration drops below specified concentrations. The methods section provided the formulae for computing these quantities.

Table 21 Projecting into the Future—Predicted Mean PCB Concentration (ppb) in 1999 and 2020 and Time When Specified PCB Concentrations Will Be Reached

Species	Sample Type	Year of Break point	Estimate of Mean PCB Concentration in 1999			Estimate of Mean PCB Concentration in 2020			Year in Which Specified PCB Concentration (ppb) Is Reached								
			Mean PCB (ppb)	Lower 95% CI	Upper 95% CI	Mean PCB (ppb)	Lower 95% CI	Upper 95% CI	1,400	240	220	140	63	38	20	5	0.5
Little Lake Butte des Morts																	
Carp	skin-on fillet	1979	1,399	589	3,319	369	56	2,429	1999	2027	2028	2035	2048	2056	2066	2088	2124
	whole body	1987	2,506	1,055	5,954	2,910	78	109,080									
Northern Pike	skin-on fillet	N/A	149	59	375	11	2	73	1981	1995	1996	1999	2006	2010	2015	2026	2044
Walleye	skin-on fillet	1990	251	131	483	511	27	9,824									
	whole body	1987	1,266	515	3,113	75,208	534	10,591,388									
Yellow Perch	skin-on fillet	1981	255	110	590	296	40	2,173									
Appleton																	
Walleye	skin-on fillet	N/A	376	117	1,212	41	3	496	1986	2003	2004	2008	2016	2021	2027	2040	2062
De Pere																	
Carp	whole body	1995	7,526	5,439	10,414	470,285	9,207	24,021,513									
Gizzard Shad	whole body	N/A	1,709	1,463	1,995	573	329	1,000	2003	2037	2038	2047	2062	2072	2085	2111	2156
Northern Pike	skin-on fillet	N/A	542	364	807	60	25	145	1990	2007	2008	2012	2020	2024	2030	2044	2066
Walleye	skin-on fillet	N/A	781	647	941	163	103	257	1991	2015	2016	2022	2033	2039	2048	2067	2098
	whole body	N/A	4,343	3,384	5,575	736	374	1,449	2012	2033	2034	2040	2049	2055	2063	2079	2106
White Bass	skin-on fillet	N/A	2,693	1,659	4,370	975	342	2,781	2013	2049	2051	2060	2077	2087	2100	2129	2177
White Sucker	skin-on fillet	N/A	637	414	981	113	48	268	1989	2011	2012	2017	2027	2033	2041	2058	2086
Green Bay Zone 2																	
Alewife	whole body	N/A	2,106	1,378	3,219	901	269	3,022	2009	2053	2055	2066	2086	2098	2114	2148	2205

Table 21 Projecting into the Future—Predicted Mean PCB Concentration (ppb) in 1999 and 2020 and Time When Specified PCB Concentrations Will Be Reached

Species	Sample Type	Year of Break point	Estimate of Mean PCB Concentration in 1999			Estimate of Mean PCB Concentration in 2020			Year in Which Specified PCB Concentration (ppb) Is Reached								
			Mean PCB (ppb)	Lower 95% CI	Upper 95% CI	Mean PCB (ppb)	Lower 95% CI	Upper 95% CI	1,400	240	220	140	63	38	20	5	0.5
Carp	skin-on fillet	N/A	4,852	2,224	10,587	1,630	180	14,784	2023	2057	2059	2067	2083	2092	2105	2131	2176
	whole body	1983	1,468	935	2,305	42	10	175	1999	2010	2010	2013	2018	2021	2024	2033	2046
Gizzard Shad	whole body	N/A	3,159	2,129	4,687	10,549	2,965	37,524									
Yellow Perch	skin-on fillet	N/A	150	23	997	14	1	143	1979	1995	1996	2000	2007	2011	2017	2029	2049

Note:

N/A – Not applicable; no breakpoint.

All of the estimated times to reach specified concentrations in Table 21, as well as the estimated concentrations for 1999 and 2020, require extremely careful interpretation. We have based all of these estimates on the untestable assumption that the PCB concentration will continue to change in the future at the same rate as during the post-breakpoint period. In addition, as noted repeatedly, the confidence intervals for models that include a breakpoint do not incorporate the extra uncertainty related to breakpoint estimation and are too narrow.

A striking feature of the table is that most of the confidence intervals are very wide. For instance, for carp whole body in Little Lake Butte des Morts, the expected mean concentration in the year 2020 is 2,910 ppb, but the range is huge: 78 to 109,080 ppb. For those cases with a wide confidence interval in 2020 (or 1999), the time to reach specified concentrations (in the right half of the table) can also be expected to have a wide confidence interval.

We now discuss these tables for each reach. The appendix contains plots of observed values and fitted time trends for every fish category referred to below. Remember that the fitted values represent fish sampled on July 1 of the given year and with mean log lipid content as observed in the samples used to build the model. The values of mean log percent lipid are shown in Table 22. Thus, the fitted trend lines may differ from a best visual fit that does not account for lipids or season. This apparent lack of correspondence occurs in several plots.

Table 22 Mean Log_{10} Percent Lipid in Fish Tissue

Reach	Species	Type	Mean Log Percent Lipid
Little Lake Butte des Morts	Carp	skin-on fillet	0.68
		whole body	0.90
	Northern Pike	skin-on fillet	0.00
	Walleye	skin-on fillet	0.11
		whole body	0.73
	Yellow Perch	skin-on fillet	–0.01
Appleton	Walleye	skin-on fillet	–0.03
De Pere	Carp	whole body	0.88
	Gizzard Shad	whole body	0.82
	Northern Pike	skin-on fillet	0.07
	Walleye	skin-on fillet	0.31
		whole body	0.97
	White Bass	skin-on fillet	0.60
	White Sucker	skin-on fillet	0.23
Green Bay Zone 2	Alewife	whole body	0.97
	Carp	skin-on fillet	0.82
		whole body	0.98
	Gizzard Shad	whole body	0.77
	Yellow Perch	skin-on fillet	–0.29

Reach 1 — Little Lake Butte des Morts

Carp, Skin-on Fillet

After the breakpoint in 1979, PCP concentration declines at a rate of 6 percent per year (p = 0.02, Table 14) down to about 1,400 ppb by 1999. Projecting the same rate of decline out to the year 2020 gives an estimated mean PCB concentration of 370 ppb (Table 21), but with a very wide 95 percent confidence interval. Note in particular that the 2,400 ppb upper-bound on the confidence interval for the concentration in 2020 is higher than the estimated concentration 21 years earlier in 1999. Sensitivity analysis (Table 20) shows that a later breakpoint, at 1985, agrees with the data and gives a lower estimate of the post-breakpoint rate of decline, namely, 1.6 percent per year.

The significant negative slope from the best model (Table 14) and the negative slopes from both the earliest and latest breakpoints in the sensitivity analysis (Table 20) consistently suggest that PCBs are decreasing in this species/type in Little Lake Butte des Morts.

Carp, Whole Body

After the breakpoint at 1987, PCB concentration stays almost constant at a level of about 2,500 ppb (0.7% per year, p = 0.9). Figure 39 identifies two rather low values in 1987 and 1990. These values do not warrant rejection from the analysis, and the slope calculated with them is appropriate. As a learning exercise, on the other hand, one can illustrate the strong influence of individual observations by omitting these values. A calculation of slope without these two samples would show a continuing decline in PCB concentration to less than 1,000 ppb by 1999.

The barely positive and non-significant slope from the best model versus the negative and barely negative slopes from the earliest and latest breakpoint models, respectively, show no clear evidence of a slope differing from zero for carp whole body samples in Little Lake Butte des Morts.

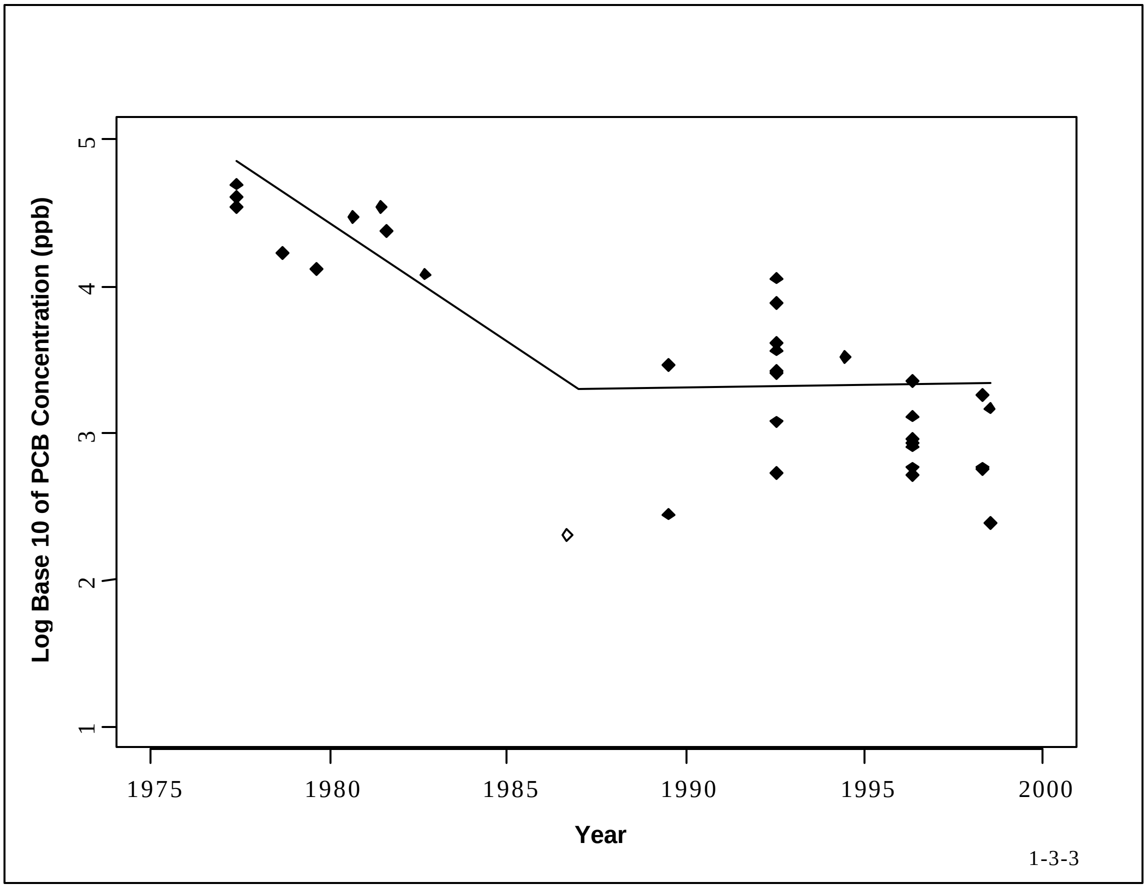

Figure 39 Log_{10} PCB Concentration (ppb) in Little Lake Butte des Morts Carp, Whole Body, versus Time

Breakpoint = 1987 (p = 0.03), Final Slope (log_{10} PCB versus time) = 0.003 (p = 0.09), Rate of Change of PCB Concentration During Period of Final Slope = 0.7% (95% confidence interval: –12.3% to 15.6%). Any values below detection limit are depicted by ◇.

Northern Pike, Skin-on Fillet

The best-fitting model has no breakpoint, but rather a constant rate of decline of 12 percent per year (p = 0.0003) yielding a concentration of about 150 ppb by 1999, with a projected mean in the year 2020 of 10 ppb. This is a case of a clear decline during the observation period.

Walleye, Skin-on Fillet

After the breakpoint in 1990, we view a barely increasing PCB concentration hovering around 250 ppb (3.4% per year, p = 0.6). The sensitivity analysis (Table 20) shows that a model with an earlier breakpoint, in 1979, also suits the data, producing a post-breakpoint decline of 8 percent per year, and the late 1994 breakpoint produces an increase of 9 percent per year. There is no strong evidence of a slope differing from zero.

Walleye, Whole Fish

The best-fitting model shows a decline in PCB concentration to about 100 ppb in 1987, then a sharp increase at 21 percent per year up to a level of 1,300 ppb by 1999. These parameter estimates are rather imprecise since this model relied upon only 18 samples. The estimated final slope of a 21 percent increase per year is not significantly different from zero, and its confidence interval is very wide: –4 to 53 percent.

Yellow Perch, Skin-on Fillet

PCB concentration declines sharply until 1981 at 43 percent per year and stays fairly constant thereafter at a level of about 250 ppb (+0.7% per year, $p = 0.8$). There is no evidence of a decreasing late trend.

Summary of Results for Reach 1 — Little Lake Butte des Morts

For most of the fish categories in this reach, we observe an early rapid decline followed by either a slower decline or a flattening without further decline. We find strong evidence against the rate of decline being constant over the whole time range.

On Figure 38, we notice narrow confidence intervals for three fish categories (carp, skin-on fillet; northern pike, skin-on fillet; yellow perch, skin-on fillet). The confidence intervals are much wider for the other three categories, which indicates that the data from these categories do not provide sufficient information to accurately estimate the final slope. The meta-analysis that combines all six results assigns almost all the weight to the three with narrow confidence intervals. Two of these show a negative final slope while one shows a final slope of virtually zero. The combined analysis gives an estimated post-breakpoint rate of decline of 4.9 percent per year—significantly different from zero ($p = 0.0006$). This combined analysis leads us to conclude that PCB concentrations were declining, on the average, at a slow rate during the data collection period. During future periods, species with lower rates of decline would gradually dominate the average rate of decline across species. As noted earlier, the combined rate of change cannot be used for forward projection.

Reach 2 — Appleton to Little Rapids

Walleye, Skin-on Fillet

PCB concentration declines at a constant rate of 10 percent per year over the whole time period ($p = 0.003$), down to an estimated mean of 380 ppb in 1999 and a projected mean of 40 ppb by the year 2020. The sensitivity analysis also shows a negative slope for both the earliest (1982) and latest (1994) breakpoints.

Reach 4 — De Pere to Green Bay

Carp, Whole Fish

This model shows decline in PCB concentration to a minimum of about 3,200 ppb in 1995 (the breakpoint), followed by a sharp increase of 22 percent per year ($p = 0.03$) up to a mean of 7,500 ppb by 1999. We find a rather wide confidence interval for this rate of increase, but it does not quite include zero. The sensitivity analysis, on the other hand, shows that the data are also consistent with an earlier breakpoint in 1990, followed by a slightly negative slope, close to zero. Thus, despite the *p*-value of 0.03 for the post-breakpoint negative slope, when we add in the uncertainty due to the breakpoint, the final slope is not convincingly different than zero.

Gizzard Shad, Whole Fish

PCB concentration declines at a constant rate of 5 percent per year ($p = 0.0002$) to a mean of 1,700 ppb in 1999 and a projected mean of 570 ppb in 2020.

Northern Pike, Skin-on Fillet

PCB concentration declines at a constant rate of 10 percent per year ($p < 0.0001$) to a mean of 540 ppb in 1999 and projected mean of 60 ppb in 2020.

Walleye, Skin-on Fillet

PCB concentration declines at a constant rate of 7 percent per year ($p < 0.0001$) to a mean of 780 ppb in 1999 and projected mean of 160 ppb in 2020. The spread of observations (more than 20 years) in this analysis, and in the preceding analysis for northern pike, helps to considerably improve the precision of the combined slope estimates for this reach (see below).

Walleye, Whole Fish

PCB concentration declines at a constant rate of 8 percent per year ($p < 0.0001$) to a mean of 4,300 ppb in 1999 and projected mean of 740 ppb in 2020.

White Bass, Skin-on Fillet

PCB concentration declines at a constant rate of 5 percent per year ($p = 0.002$), to a mean of 2,700 ppb in 1999 and projected mean of 980 ppb in 2020. Sensitivity analysis shows the data are consistent with a late breakpoint at 1996 followed by a slope that slightly increases.

White Sucker, Skin-on Fillet

PCB concentration declines at a constant rate of 8 percent per year ($p < 0.0001$), to a mean of 640 ppb in 1999 and projected mean of 110 ppb in 2020.

Summary of Results for Reach 4 — De Pere to Green Bay

All but one of the fish categories show a decline in PCB concentration at a constant rate. The meta-analysis results reflect this, with an estimated rate of decline of 7 percent per year, highly significantly different from zero

($p < 0.0001$). Whole body carp, with a breakpoint in 1995, emerges as the only exception to this pattern of monotonically decreasing PCB concentration, occurring in six out of seven of the analyses. These slopes have relatively tight confidence intervals. One can explain the large increase after 1995 in carp due to high PCB concentrations observed in a large number of fish sampled on July 2 and July 6, 1998. Such a phenomenon might reflect a scouring event that exposed buried sediment with a high PCB concentration. Or the large positive slope for the carp may be random, given that the sensitivity analysis accords with a slightly negative to a large positive slope for this reach/species/type combination, as discussed earlier.

Reach 5 — Green Bay Zone 2

Alewife, Whole Body

PCB concentration declined at a constant rate of 4 percent per year ($p = 0.05$) to a mean of 2,100 ppb in 1999 and a projected mean of 900 ppb in 2020.

Carp, Skin-on Fillet

PCB concentration declines at a constant rate of 5 percent per year ($p = 0.16$, not significantly different from zero) to a mean of 4,900 ppb in 1999 and projected mean of 1,630 ppb in 2020.

Carp, Whole Fish

PCB concentration increases to a maximum of about 25,000 ppb in 1983, and then declines at a rate of 16 percent per year ($p < 0.0001$) down to a mean of 1,500 ppb in 1999 and projected mean of 40 ppb in 2020. An informal sensitivity analysis does not alter the combination of an initially positive and final negative slope. However, we are concerned about having potentially over-fit the model. We have only 5 years during which data were collected over a period covering about 20 years. Given that five parameters in the model relate to time (breakpoint, final slope, slope difference [early minus late], and two season parameters), it is possible to fit a spline model "too well" to the limited number of years with observations. In any case, the final slope does appear firmly negative, though it may be less negative than the 16 percent. A model fitted without a breakpoint yields a single negative slope with a rate of decline of 9 percent per year.

Gizzard Shad, Whole Fish

Samples were only taken over a relatively short time period from 1989 to 1999. PCB concentration appears to increase over this time period at a rate of 6 percent per year ($p = 0.01$) to a mean of 3,200 in 1999.

Yellow Perch, Skin-on Fillet

PCB concentration declines at a constant rate of 11 percent per year ($p = 0.004$) to a mean of 150 ppb in 1999 and projected mean of 14 ppb in 2020.

We have rejected a model with a breakpoint at 1986, even though the breakpoint is, formally, highly significant ($p = 0.0008$). The breakpoint model yields a final rate of change of plus 15 percent per year and a pre-break rate of minus 69 percent per year. We regard this implausible combination as due to over-fitting (mentioned earlier) and accept, instead, the single-slope model noted in the figure and table.

Summary of Results for Reach 5 — Green Bay Zone 2

Four out of the five fish categories for this reach show a continuing decline in PCB concentration. The meta-analysis results reflect this, yielding a combined estimate of final rate of decline of 5 percent per year ($p < 0.0001$).

5.2.3 Additional Analysis of Alternative Models

Results for Fitting Models with Breakpoint at 1985

In addition to showing results for the best-fitting model, we fit models to the 19 fish categories using a single common breakpoint. The best year for this breakpoint is 1985. A breakpoint at 1985 fits nearly as well as the optimal breakpoint for almost all fish categories. Table 23 shows results of fitting this model to every fish category.

Testing for a Non-constant Final Slope

Projection of PCB concentrations presumes some kind of steady or predictable state. In this section, we consider the “steadiness” of time trends. In order to test the assumption of a constant linear slope in the time period after the breakpoint, we fit models including a quadratic term for that time period. Table 24 shows the results of these analyses for the best-fitting model.

Table 23 Details of Fitting Models with a Breakpoint at 1985 for Every Fish Category

Species	Type	Model	Break-point Year	*n*	Inter-cept	SE Int	Estimate of Final (post-1985) Slope			Early Slope Difference			Coefficient of Log of Percent Lipids			Peak of Seasonal Variation		
							Slope	SE	*p*-value	Dif-ference	SE	*p*-value	Log_{10}	SE	*p*-value	Mo.	Amp.	*p*-value
Little Lake Butte des Morts																		
Carp	skin-on fillet	2	1985	55	3.23	0.12	−0.007	0.021	0.7419	−0.090	0.043	0.0403	0.86	0.16	0.0000	12.9	0.59	0.0268
	whole body	2	1985	40	3.41	0.16	−0.018	0.028	0.5264	−0.158	0.072	0.0360	0.87	0.34	0.0148	7.0	0.69	0.0099
Northern Pike	skin-on fillet	2	1985	19	2.84	0.19	−0.079	0.024	0.0053	0.071	0.061	0.2663	0.57	0.31	0.0854	1.8	0.56	0.0829
Walleye	skin-on fillet	2	1985	63	2.46	0.09	−0.026	0.012	0.0379	−0.061	0.032	0.0570	0.43	0.14	0.0038	12.7	0.25	0.1026
	whole body	2	1985	18	2.22	0.39	0.074	0.045	0.1285	−0.310	0.103	0.0106	0.97	0.36	0.0206	11.9	0.66	0.0077
Yellow Perch	skin-on fillet	2	1985	34	2.10	0.10	0.018	0.019	0.3297	−0.133	0.049	0.0110	0.34	0.21	0.1144	10.7	0.11	0.0025
Appleton																		
Walleye	skin-on fillet	2	1985	30	3.20	0.20	−0.065	0.022	0.0059	0.103	0.089	0.2574	1.23	0.20	0.0000	7.4	0.56	0.0005
De Pere																		
Carp	whole body	2	1985	90	3.94	0.09	−0.025	0.011	0.0238	−0.031	0.033	0.3508	0.82	0.12	0.0000	6.9	0.15	0.0304
Northern Pike	skin-on fillet	2	1985	40	3.13	0.11	−0.039	0.010	0.0005	−0.020	0.024	0.4111	0.71	0.17	0.0002	9.0	0.13	0.2505
Walleye	skin-on fillet	2	1985	120	3.21	0.05	−0.035	0.005	0.0000	0.011	0.018	0.5282	0.86	0.07	0.0000	8.7	0.02	0.6196
	whole body	2	1985	58	4.00	0.07	−0.039	0.009	0.0000	0.009	0.028	0.7440	0.45	0.12	0.0007	7.0	0.12	0.1931
White Bass	skin-on fillet	2	1985	58	3.61	0.07	−0.019	0.007	0.0065	−0.117	0.109	0.2897	0.83	0.11	0.0000	6.8	0.32	0.0592
White Sucker	skin-on fillet	2	1985	44	3.12	0.08	−0.032	0.010	0.0020	−0.013	0.025	0.6010	0.43	0.15	0.0065	7.3	0.08	0.4813
Green Bay Zone 2																		
Alewife	whole body	2	1985	44	3.42	0.06	−0.002	0.011	0.8200	−0.087	0.040	0.0341	0.90	0.13	0.0000	5.4	0.09	0.0034
Carp	skin-on fillet	2	1985	28	3.84	0.08	−0.063	0.026	0.0226	0.105	0.055	0.0698	0.74	0.14	0.0000	3.0	0.41	0.0052
	whole body	2	1985	57	3.89	0.06	−0.075	0.013	0.0000	0.135	0.040	0.0013	0.87	0.10	0.0000	6.6	0.23	0.0013
Yellow Perch	skin-on fillet	2	1985	19	2.60	0.35	0.015	0.018	0.4061	−0.745	0.170	0.0007	1.54	0.35	0.0008	7.2	2.99	0.0008

Table 24 Test for Curvature in Final Slopes

Species	Type	Coefficient of *t*-squared	SE of *t*-squared Coefficient	Tests for Curvature		
				p-value⁺ (2-sided)	*p*-value⁺ (1-sided, plus)	*p*-value⁺ (1-sided, minus)
Little Lake Butte des Morts						
Carp	skin-on fillet	−0.0014	0.0024	0.56	0.718	0.564
	whole body	−0.0144	0.0067	0.04*	0.981	0.039*
Northern Pike	skin-on fillet	−0.0033	0.0024	0.19	0.905	0.190
Walleye	skin-on fillet	−0.0095	0.0094	0.32	0.842	0.317
	whole body	−0.0202	0.0101	0.07	0.965	0.070
Yellow Perch	skin-on fillet	−0.0021	0.0059	0.72	0.639	0.722
Appleton to Little Rapids						
Walleye	skin-on fillet	−0.0047	0.0041	0.26	0.872	0.255
De Pere to Green Bay						
Carp	whole body	0.0168	0.0362	0.64	0.644	0.678
Gizzard Shad	whole body	0.0032	0.0029	0.29	0.290	0.855
Northern Pike	skin-on fillet	0.0009	0.0008	0.25	0.249	0.876
Walleye	skin-on fillet	−0.0005	0.0006	0.42	0.791	0.418
	whole body	0.0000	0.0008	0.97	0.514	0.971
White Bass	skin-on fillet	0.0015	0.0018	0.41	0.410	0.795
White Sucker	skin-on fillet	0.0011	0.0010	0.30	0.300	0.850
Green Bay Zone 2						
Alewife	whole body	0.0019	0.0011	0.10	0.099	0.950
Carp	skin-on fillet	−0.0061	0.0035	0.10	0.952	0.096
	whole body	0.0034	0.0018	0.06	0.062	0.969
Gizzard Shad	whole body	−0.0007	0.0032	0.82	0.591	0.818
Yellow Perch	skin-on fillet	0.0126	0.0034	0.003**	0.003**	0.999
All				**0.008****	**0.4**	**0.2**

Notes:

⁺ The three *p*-values indicate the statistical significance of the *t*-squared (curvature) term in the regression model for time trends. In all three columns, the null hypothesis is no curvature (i.e., there is a straight-line constant slope after the breakpoint—or the whole period, if there is no breakpoint). In the first *p*-value column, the alternative hypothesis is that the final time period has some curvature (i.e., the slope is shifting **either** toward more positive **or** more negative values). In the second *p*-value column, the alternative hypothesis is that the slope is shifting toward more positive values (less decline in PCB concentrations). In the third column, the alternative hypothesis is that the slope is shifting toward more negative values (greater decline in PCB concentrations).

* $p < 0.05$

** $p < 0.01$

*** $p < 0.001$

This model introduces a time-squared term for the final period. It is an implausible model for projection of PCB concentration, but readily works to detect a non-constant rate of decline of PCBs during the final period. We refer to this as "curvature." A positive sign for the time-squared term indicates a shifting slope over time toward either less reduction in PCBs or more accrual of PCBs. A negative sign indicates a shift toward more reduction or less accrual.

The results (Table 24) show two categories with significant curvature, discussed below. Overall, curvature may be a general phenomenon. A meta-analysis using chi-squared calculated from the 19 *p*-values for curvature yields $X^2 = 61.3$, with 38 degrees of freedom and $p = 0.008$. Thus, we reject the null hypothesis that **all** of the final periods, after the breakpoints (including the entire period, if there is no breakpoint), have a simple linear trend (on the log scale). We note, also, that 6 out of the 19 *p*-values for curvature are less than 0.10, whereas only 2 would be expected by chance. This excess of small *p*-values suggests that "curvature," or changing slopes over time, is common and not a feature confined to one or two of the categories analyzed here. Further, it appears that the curvature is a mixture of positive and negative changes (i.e., there are slopes that may shift toward either more negative or more positive rates of change as time passes). The evidence for a mixture of positive and negative changes is two-fold. First, there is both a positive and a negative curvature result among the two fish categories with $p < 0.05$ on the curvature test. In Green Bay Zone 2, yellow perch samples of skin-on fillet evidence that their rate of decline is decreasing (toward less reduction of PCBs) with $p = 0.002$, and in Little Lake Butte des Morts carp whole body samples evidence that their recent barely positive slope is changing toward an either flat or negative trend with more reduction of PCBs ($p = 0.04$). Among the six fish categories with $p < 0.10$ for curvature (marginally significant results) we again find quite an even mixture of positive and negative curvature—three of each. Overall, 9 categories with fitted curvature with a positive coefficient (rates of decline shifting toward slower reduction of PCBs over time) and 10 have negative curvature (rates of decline shifting toward faster reduction of PCBs over time).

There is a second reason we feel that slopes are shifting both positively and negatively. A meta-analysis using a one-sided test to detect an excess of fish categories with positive curvature (toward less reduction of PCBs) yields $p = 0.4$, and the *p*-value for an excess of negative curvature (toward more reduction of PCBs) yields $p = 0.2$. These two *p*-values indicate no significant excess of either only positively or only negatively curving slopes, but there is a significant excess of curving slopes in general (either positive or negative). Thus, we find evidence for changing slopes ($p = 0.008$, noted above), but of mixed direction among the fish categories. We can only be confident that there is change.

The generally non-significant *p*-values in the two-sided *p*-value column of Table 24, and in other *p*-value columns inspire confidence of curvature in very few cases. Except for the four *p*-values noted with asterisks (not including "All"), it is difficult to ascribe curvature to the specific combinations of species, reach, and sample type. However, the excess of relatively small two-sided *p*-values overall (even if individual *p*-values are not significant) does allow us to conclude with some confidence that there is changeability in the final slopes ($p = 0.008$). That is, we reject the notion that, during the period of final slopes, rates of changes were utterly constant for every combination of reach, species, and sample type. We accept the alternative that rates of change were shifting over time, both in a negative and positive direction for at least some combinations.

5.3 Conclusions about Trends over Time in PCB Concentration in Fish

The meta-analyses within three reaches with more than one fish category available for analysis show that PCB concentration was declining at a rate of 5 to 7 percent per year (Table 19, Little Lake Butte des Morts, De Pere, Green Bay Zone 2). The single fish category that could be analyzed for the Appleton Reach also shows a decline of 10 percent per year. Reach 1, Little Lake Butte des Morts, calls attention to a steeper decline in earlier years. All analyses with a breakpoint in this reach show a steeper decline before than after the breakpoint. But in the other reaches, except for 2 out of 13 categories, the data for each fish category considered individually are consistent with a constant rate of decline over the whole time period.

The majority of fish categories have data consistent with only a simple linear trend, and the balance of categories (with breakpoints) have post-break data fit well by a linear trend. Nevertheless, the collective evidence is that slopes (on the log scale) tend to be non-constant, as evidenced by the rejection of the hypothesis of no curvature in the final slopes based on the meta-analysis (Table 24).

We cannot project into the future with precision for several reasons. Many species suffer from rather sparse data with observations occurring at only a few time points. Models based on these data do not provide highly precise estimates. Incorporating the extra uncertainty due to estimating the breakpoint presents a challenge. We have done so in an informal fashion using a sensitivity analysis. The uncertainty in future projections would be greater if the uncertainty in the breakpoint were formally incorporated into calculations. Finally, some of the unusual changes in slope from before to after a breakpoint may be genuine, due to unpredictable events such as floods accompanied by scouring and deposition. If so, such events will continue adding variability to PCB concentration over time, making predictions based on the assumption of a future decline at a constant rate questionable. The presence of curvature (non-constant slopes) is consistent with the more dramatic changes represented by breakpoints and suggests a dynamic process, liable to change, rather than a steady state with constant rates of change.

5.4 Comparison of De Pere Reach to Green Bay Zone 2

We compared species and sample types between the De Pere to Green Bay Reach (equivalent to “Green Bay Zone 1” and so labeled in some reports) and Green Bay Zone 2. The two sets of observations from the two bodies of water are usually significantly different; either in the mean PCB concentration, the time trend of PCB concentration, or in the relationship of PCB concentration to lipid content of tissue.

We were able to carry out these analyses for some additional species and sample type combinations for which time trends could not be calculated by using a snapshot during a single year or short span of years. Table 25 shows which comparisons could be made. We carried out five analyses comparing De Pere Reach and Green Bay Zone 2 during a short "snapshot" cross-sectional period of years, and there were three analyses where time trends could be compared between reaches. In order to have a consistent period of years for the time trend comparison and to avoid differences between reaches arising from different sampling patterns over time, we limited the time trend analyses to a common period of years, 1989 through 1998.

We note that we limited our analysis and discussion to the data provided to us. A discussion of the biological and physical comparisons between the two bodies of water can be found in Technical Memorandum 7c (WDNR, 2001), the Remedial Investigation, and the Baseline Risk Assessment for the Lower Fox River and Green Bay (ThermoRetec, 2001a; ThermoRetec, 2001b).

Table 25 De Pere Reach and Green Bay Zone 2: Fish Types and Sample Types with Sufficient Data for PCB Comparisons

Sample Type	Species	Type of Analysis	
		Single Time Snapshot PCB Comparison - Years	Time Trend Analysis Across Years
Whole Fish/Whole Body/Composite	alewife	1989	1989–1998
Whole Fish/Whole Body/Composite	carp	1989	1989–1998
Whole Fish/Whole Body/Composite	gizzard shad	1989	1989–1998
Skin On Fillet	walleye	1989–1991	
Whole Fish/Whole Body/Composite	walleye	1989	

The equation used to analyze the De Pere and Zone 2 reaches based on the snapshot data is:

Equation 18

$$\log_{10}(PCB) = b_0 + b_1 L + b_2 R + b_3 L \cdot R + e$$

where

PCB = PCB concentration in units of ppb,
L = $\log_{10}$(percent lipid content),
R = dichotomous indicator of Zone 2 versus De Pere Reach, and
e = random error.

For the comparison of time trends in the De Pere and Zone 2 reaches, the equation is extended to:

Equation 19

$$\log_{10}(PCB) = b_0 + b_1 L + b_2 R + b_3 L \cdot R + b_4 t + b_5 t \cdot R + e$$

where
t = time in years since January 1, 1989.

In both the snapshot and time trends equations, all coefficients of terms involving R (reach) should be zero or close to zero if a given fish species takes in PCBs at a similar level and processes PCBs in a similar way in the two reaches. For example, in the snapshot equation if b_3 (the coefficient of $L \cdot R$) is zero, the increase in PCB concentration for a specified increase in fat content is the same in the two reaches. In addition, if b_2 (the coefficient of R) is also zero, then the mean PCB concentration is the same in the two reaches, given equal lipid content. As another example, if b_5 (coefficient of $t \cdot R$) is zero in the time trends model, then the rate of change of $\log_{10}$ (PCB) is the same in the two reaches. Thus, comparing the two reaches involves testing whether certain coefficients in regression models are significantly different from zero.

We detected one outlier, which was removed from the De Pere Reach versus Green Bay Zone 2 analysis. The outlier is noted in Table 27.

Table 26 Outlier from Analysis of De Pere Reach versus Green Bay Zone 2

Database ID	Reach	Fish Type	Sample Type	Total PCBs
WDF209006BC1	Green Bay Zone 2	alewife	whole body	19,000

Reason:
Large outlier. Other PCB values range from 990 to 4,500.

5.4.1 De Pere Reach versus Green Bay Zone 2: "Snapshot" Analysis

Four out of five snapshot analyses (Figure 40 through Figure 44) showed statistically significant differences between the two reaches (Table 27). In two of the analyses, PCB concentrations varied with percent lipid in a different way in the two reaches, and in two analyses the mean log PCB concentration differed between the two reaches, controlling for lipid content.

The two species with different PCB-lipid relationships were carp and gizzard shad, both whole body samples. For carp (whole body) the coefficient of the log lipid term L, in the snapshot equation above, when, combined with the coefficient of $L \cdot R$, yields different rates of change of log PCB with changes in log lipid content (p = 0.02). The slope of log PCB versus log lipid is 0.68 and 1.01 in De Pere and Green Bay Zone 2 reaches, respectively. (In all De Pere versus Zone 2 analyses, reach was coded as "1" for De Pere to Green Bay and "2" for Green Bay Zone 2. Thus, based on the snapshot equation, the slope of log PCB versus log lipid in the De Pere Reach, coded as "1," is 0.3426 + 0.3346 × 1 = 0.6772, and, in Green Bay Zone 2, coded as "2," the slope is 0.3426 + 0.3346 × 2 = 1.0118.)

Table 27 Fitted Models for Log_{10} (PCB Concentration) versus Log_{10} (Percent Lipid) in De Pere Reach and Green Bay Zone 2 for Species with Sufficient Data During 1989

Sample Type	Species	Single Time Snapshot PCB Comp: Years	De Pere Reach		Green Bay Zone 2		Equal Slopes Likelihood Ratio *p*-value	Equal Intercepts Likelihood Ratio *p*-value
			Intercept	Slope	Intercept	Slope		
Whole Fish/ Whole Body/ Composite	alewife+	1989	2.943	0.663	2.668	0.663	0.32	0.00006***
Whole Fish/ Whole Body/ Composite	carp+	1989	3.092	0.677	2.675	1.012	0.016*	
Whole Fish/ Whole Body/ Composite	gizzard shad+	1989	3.559	–0.204	2.846	0.496	0.0009***	
Skin On Fillet	walleye	1989–1991	3.040	0.348	3.040	0.348	0.69	0.66
Whole Fish/ Whole Body/ Composite	walleye+	1989	3.390	0.501	3.269	0.501	0.17	0.0058**

Notes:

\+ Fish types significantly different between reaches at 5 percent significance level or better.
* $p < 0.05$
** $p < 0.01$
*** $p < 0.001$

To illustrate the implication of these coefficients, consider a doubling of lipid content (e.g., from 5 to 10 percent). It can be derived from Equation 18 that an increase in lipid content by any multiplicative factor F, such as $F = 2$, leads to an increase in PCB concentration by a multiplicative factor of $F^{b_1 + R \cdot b_3}$. Thus, a doubling of lipid content leads to an increase in PCB concentration (ppb, not log) by a factor of $2^{0.6772} = 1.60$ in the De Pere Reach, and in Green Bay Zone 2, by a factor of $2^{1.0118} = 2.02$. The increase in Green Bay Zone 2 is larger by 26 percent.

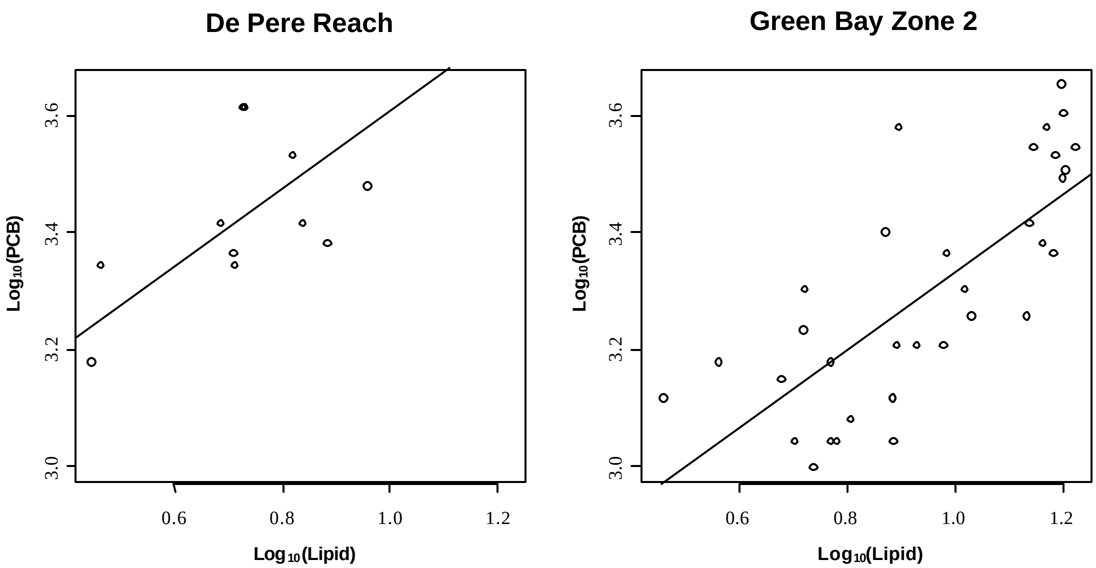

Figure 40 Log PCB Concentration versus Log Percent Lipid for De Pere Reach and Green Bay Zone 2 for Alewife, Whole Body, 1989

For the alewife species, there was no apparent difference in the slope of the relationship between $\log_{10}$ (PCB) and $\log_{10}$ (percent lipid) (p = 0.3, likelihood ratio test for slope differences). The intercepts were significantly different (p = 0.00006, likelihood ratio test). Thus, the mean PCB concentrations for alewife fish in the two zones are significantly different. Figure 40 shows that alewife in the De Pere Reach tend to have a higher PCB content at all lipid levels.

The carp whole body samples (Table 27, Figure 42) in Green Bay Zone 2 showed a greater rate of increase of PCBs with increasing lipid content than samples from the De Pere Reach. (See the steeper slope in Figure 42, right, than in the left panel.) The difference is statistically significant (p = 0.02).

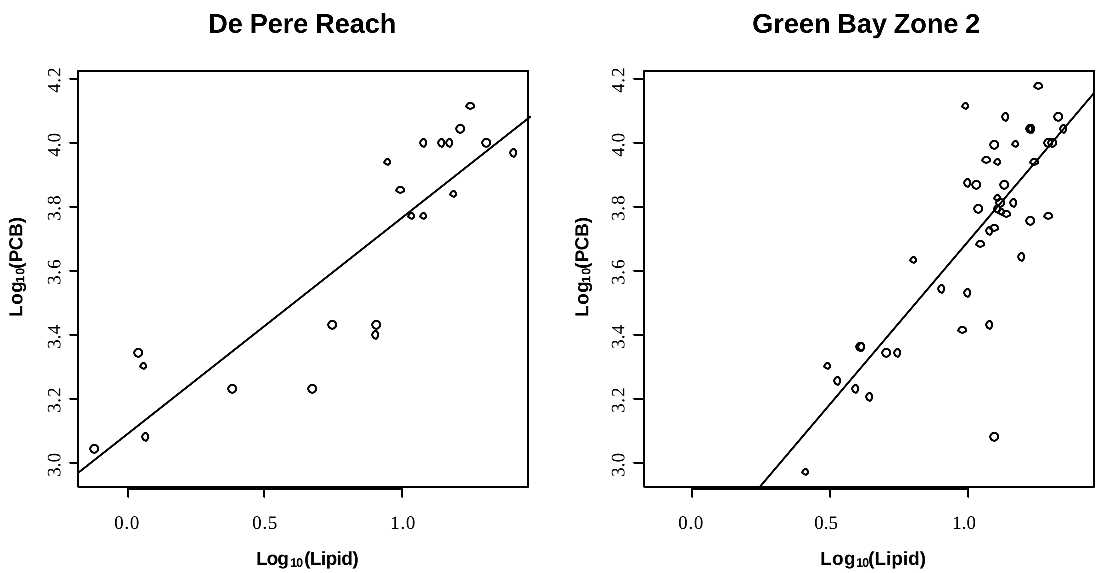

Figure 41 Log PCB Concentration versus Log Percent Lipid for De Pere Reach and Green Bay Zone 2 for Carp, Whole Body, 1989

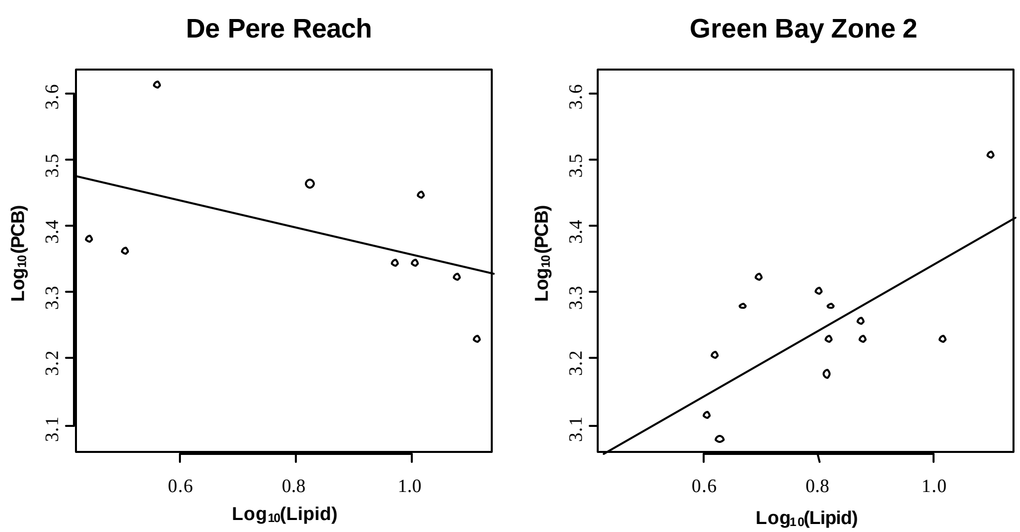

Figure 42 Log PCB Concentration versus Log Percent Lipid for De Pere Reach and Green Bay Zone 2 for Gizzard Shad, Whole Body, 1989

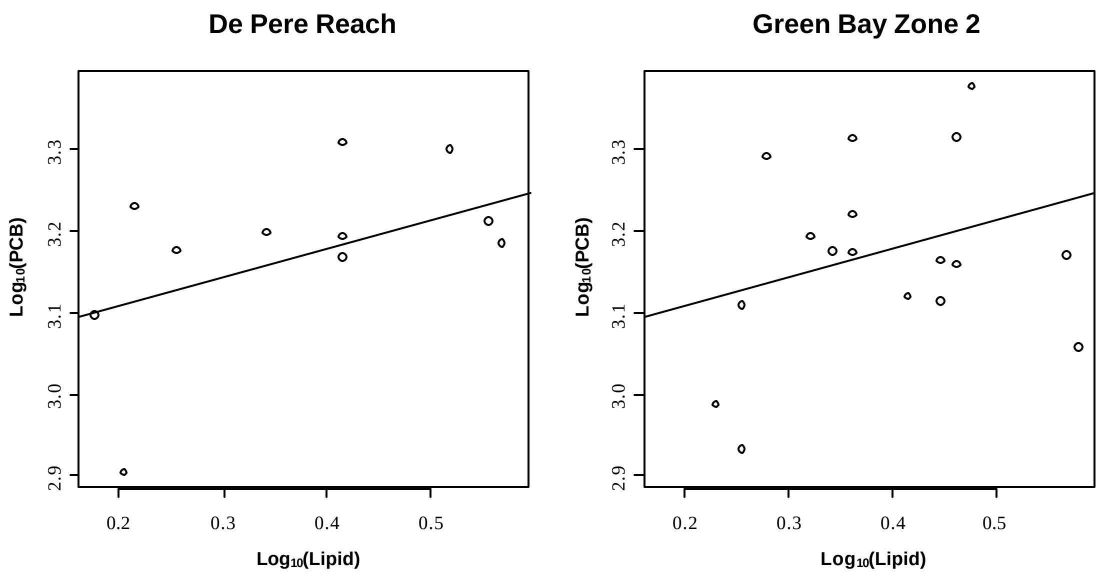

Figure 43 Log PCB Concentration versus Log Percent Lipid for De Pere Reach and Green Bay Zone 2 for Walleye, Skin-on Fillet, 1989–1991

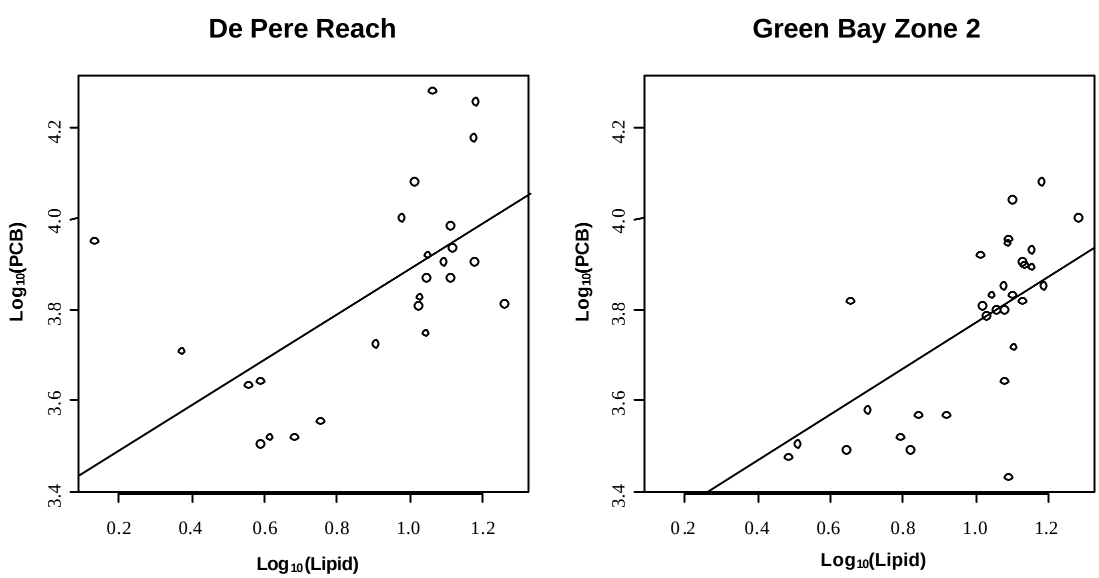

Figure 44 Log PCB Concentration versus Log Percent Lipid for De Pere Reach and Green Bay Zone 2 for Walleye, Whole Body, 1989

In the gizzard shad samples, the slope of log PCB versus log lipid in the De Pere Reach is –0.20 (Table 27, Figure 42). That slope is negative in the De Pere Reach is biologically implausible and probably randomly different from zero or a slightly positive value. The negative slope is significantly different ($p = 0.0009$) from the positive coefficient of 0.50 in Green Bay Zone 2. In Green Bay Zone 2, a doubling of percent lipid in the gizzard shad species would yield an expected 41 percent increase in PCB concentration, while in the De Pere Reach, if one takes the fitted model at face value, the PCB concentration would decrease. If zero or a small positive value is the true slope for log PCB concentration versus log percent lipid in the De Pere Reach, a doubling of lipid content in this reach would cause only a slight change in PCB concentration.

For these two species, carp and gizzard shad, the plots (Figure 41 and Figure 42) indicate that the PCB concentrations differ most at low lipid levels and tend to converge at higher lipid levels. Thus, for each of the two species, the fish samples in the two reaches will have similar PCB concentrations at higher lipid levels and dissimilar PCB concentrations at lower lipid levels.

In two of the three other snapshot analyses (alewife and walleye, both "whole body"), slopes of log PCB versus log lipid were not significantly different between the reaches ($p = 0.3$ and 0.2, respectively), but the mean PCB concentration differed, controlling for lipid level ($p = 0.0001$ and 0.006, respectively). The plots (Figure 40 and Figure 44) clearly convey this offset between the PCB-lipid relationship.

The difference between reaches in mean log PCB concentration for a specified lipid content is the coefficient b_2 in the snapshot equation with, in these two analyses, b_3 set equal to zero and the $L \cdot R$ term excluded from the model. The De Pere Reach minus Green Bay Zone 2 difference in expected log PCB is 2.943 – 2.668 = 0.275 for alewife and 0.121 for walleye. These differences correspond to a geometric mean PCB concentration that is $10^{0.275} = 1.9$ times higher (90 percent higher) for alewife in De Pere Reach than in Green Bay Zone 2, and $10^{0.121} = 1.3$ times higher (30 percent higher), correspondingly, for walleye.

5.4.2 De Pere Reach versus Green Bay Zone 2: Time Trends Analysis

All three analyses comparing alewife, carp, and gizzard shad between De Pere Reach and Green Bay Zone 2 yield statistically significant differences in time trends between the reaches, as shown in Table 28. The trends are also plotted on Figure 45 through Figure 47. All results here are based on analyses of whole body samples. The slopes for alewife (log PCB versus time in years) are –0.023 for the De Pere Reach and 0.004 for Green Bay Zone 2. They imply that the PCB concentration in De Pere Reach alewife has been decreasing by 5 percent per year and increasing by 1 percent per year in Green Bay Zone 2, a difference in rates of 6 percent per year. Similar comparisons for the other species, based on the slopes in the table, yield, for carp, a 14 percent per year greater rate of decrease in

Green Bay Zone 2 than in the De Pere Reach. For gizzard shad, De Pere Reach concentrations have been decreasing 10 percent per year faster than the Green Bay Zone 2 concentrations.

Table 28 Log_{10} (PCB Concentration) versus Time in De Pere Reach and Green Bay Zone 2 for Species with Sufficient Data During 1989–1998

Sample Type	Species	Time Trend PCB Comp: Years	De Pere Reach		Green Bay Zone 2		Equal Slopes Likelihood Ratio *p*-value
			Intercept	Slope	Intercept	Slope	
Whole Fish/Whole Body/Composite	alewife	1989–1998	49.743	−0.0232	−4.336	0.00382	0.045*
Whole Fish/Whole Body/Composite	carp	1989–1998	−6.218	0.005	105.89	−0.05131	0.0099**
Whole Fish/Whole Body/Composite	gizzard shad	1989–1998	55.954	−0.0264	−24.037	0.01368	0.0031**

Notes:
* $p < 0.05$
** $p < 0.01$
*** $p < 0.001$

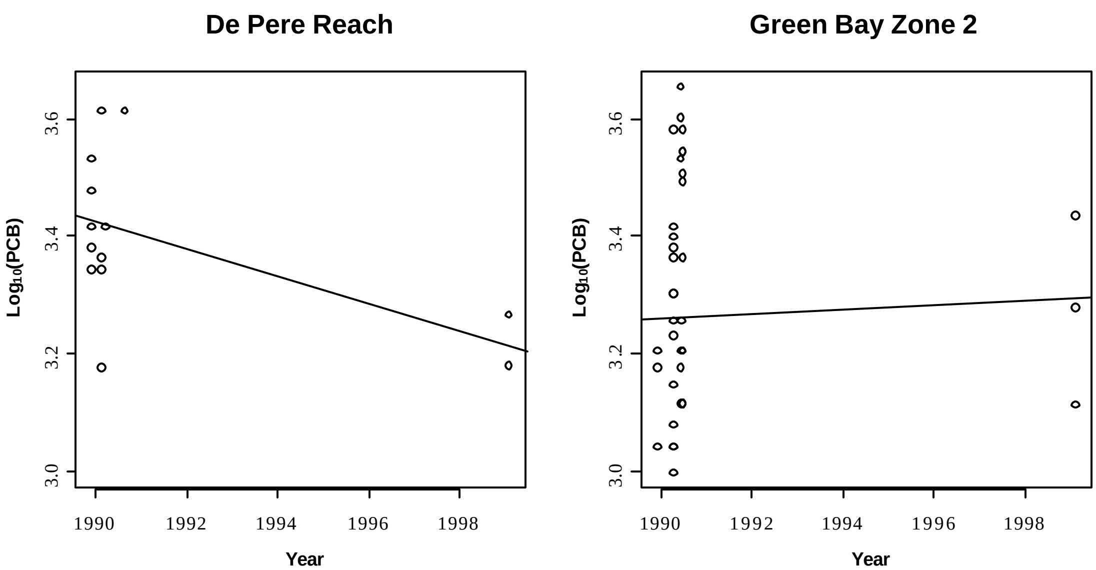

Figure 45 1989–1998 Time Profile Comparison of PCBs Between De Pere Reach and Green Bay Zone 2 for Alewife, Whole Body

Alewife whole body samples from the De Pere Reach show higher levels of PCBs around 1989–1990 than alewife in Green Bay Zone 2. By 1998, the PCB levels in the De Pere Reach appear to have dropped to levels comparable to those of Green Bay Zone 2.

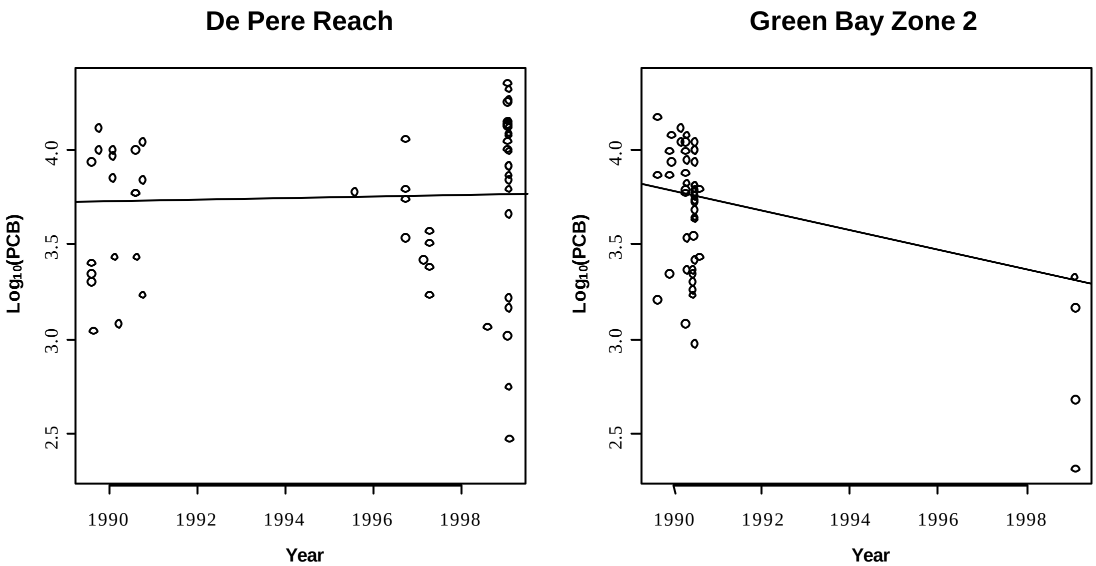

Figure 46 1989–1998 Time Profile Comparison of PCBs Between De Pere Reach and Green Bay Zone 2 for Carp, Whole Body Samples

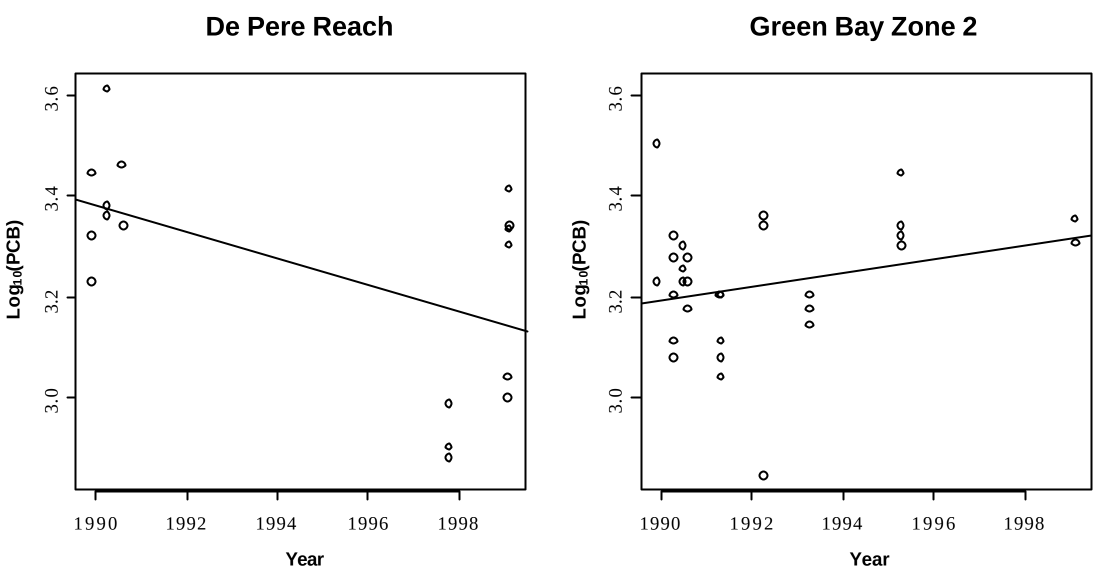

Figure 47 1989–1998 Time Profile Comparison of PCBs Between De Pere Reach and Green Bay Zone 2 for Gizzard Shad, Whole Body Samples

The majority of the analyses of species comparing De Pere Reach and Green Bay Zone 2 show statistically significant differences. Although no solid barriers separate the two zones, the fishes sampled exhibit enough differences to suggest that the fish in the two zones are heterogeneous in either exposure to PCBs or processing of PCBs or both.

5.4.3 De Pere Reach versus Green Bay Zone 2: Without Adjustment for Lipid Concentrations

We carried out a second comparison of De Pere Reach and Green Bay Zone 2 in terms of PCB concentrations in fish. In this second analysis, the lipid weight as a percentage of tissue weight was excluded from the analysis. Analyses of PCB concentrations in fish often proceed without lipid normalization. Results presented here can then be compared to such “lipid-less” analyses. Lipid-based analyses are preferred when available, however, due to the occurrence of many highly significant associations of PCB concentration and lipid content.

The statistical model used for comparing the PCB concentration between De Pere Reach and Green Bay Zone 2 for samples collected during a short time period (snapshot analysis) is:

Equation 20

$$\log_{10}(PCB) = b_0 + b_2 R + e$$

where log PCB parameters and variables have the same definition as for the lipid-based analysis. We defined R = 1 for De Pere Reach and R = 2 for Green Bay Zone 2.

Fish sampled from De Pere Reach have an expected log concentration $b_0 + b_2$; those sampled from Green Bay Zone 2 have an expected log concentration is $b_0 + 2b_2$. Thus, if the coefficient b_2 is zero or if its difference from zero is small and not statistically significant, we would accept the hypothesis that the mean PCB concentrations in the given species and sample type are equal in the two reaches.

The model for comparing De Pere Reach and Green Bay Zone 2 when data on PCB concentrations have been collected over a longer period expands on the previous model by inserting terms involving time. The model is:

Equation 21

$$\log_{10}(PCB) = b_0 + b_2 R + b_4 t + b_5 t \cdot R + e$$

where the parameters and variables are as defined earlier (with R = 1 or 2). The time trend slope for De Pere Reach in this model is ($b_4 + b_5$) and ($b_4 + 2b_5$) for Green Bay Zone 2.

For the comparison of fish PCB concentrations in the De Pere Reach versus those in Green Bay Zone 2, we would accept the hypothesis that a given fish species and sample type has an equal mean PCB concentration in the two reaches at any specified time if the coefficients b_2 and b_5 are small and not significantly different from zero. When these two coefficients are zero, then the rate of change (slope) of log PCB concentrations versus time in the two reaches is the same (b_5 = 0), and there is no difference in the expected mean log concentration (b_2 = 0) at any given time.

The results of the lipid-less snapshot analysis can be presented readily as a comparison of geometric means of PCB concentrations (see Table 29). For reference, we include the corresponding results for a lipid-based analysis, using 6 percent lipid content as a "plug-in" for the lipid-based snapshot equation (3 percent for walleye). We note, in general, the weaker contrast in geometric mean PCB concentration between the two reaches without the lipid variable (compare "percent increase" columns of the table). Also, only two, rather than four, of the differences are statistically significant.

The time trend lipid-less analysis is presented in Table 30. There, three out of the four analyses show statistically significant differences between the reaches with, in each case, quite striking disparities in the annual percent change in PCB concentration. (See the top row for each species/type to find the difference in rates of change in the two reaches—parameter b_5—and the row with "+" to view the final model after all non-significant terms have been dropped.) As noted earlier, we prefer models based on lipid content, a key variable, the absence of which may mislead.

5.4.4 De Pere Reach versus Green Bay Zone 2: Summary

The De Pere and Green Bay Zone 2 reaches do not have an equivalent relationship to PCBs based on the comparisons presented here. The same species and sample types generally differ between reaches either in the slope of time trends, the relationship of PCBs to lipid content, or in the mean PCB concentration, controlling for lipid content. As can be seen from the plots associated with this analysis, the De Pere Reach generally has higher PCB concentrations than Green Bay Zone 2.

5.4.5 Lipid Normalization

The lipid content of samples strongly predicts PCB concentrations in most of our analyses, and, therefore, is an important variable to include in the time trends models. Its association with PCB concentrations is statistically significant—and often highly significant—in 17 out of the 19 analyses of individual sample types (see Table 18). Also, 7 out of the 19 analyses have coefficients of the log lipid variable that differ significantly from 1.0, the value that yields results equivalent to the traditional lipid normalization calculated as (*PCB concentration*)/(*percent lipid content*). Only one such significant difference—rather than seven—would be expected by chance if 1.0 were the true value for all species and sample types. Thus, the traditional lipid normalization does not always control for the lipid effect.

Table 29 Comparison of Geometric Mean Concentrations of PCB Concentrations in De Pere Reach and Green Bay Zone 2, With and Without an Adjustment for Lipid Content, Samples from 1989–1991 ("snapshot" analysis)

Species	Sample Type	Lipids				No Lipids				Years	Sample Size: Total (DP/Z2)
		De Pere Geometric Mean Conc. (mg/kg)*	Zone 2 Geometric Mean Conc. (mg/kg)*	Zone 2 GM Percent Increase over De Pere	Reaches differ? *p*-value	Zone 2 Geometric Mean Conc.	Zone 2 Geometric Mean Conc.	Zone 2 Percent Increase over De Pere*	Reaches differ? *p*-value		
Alewife	Whole Fish/ Whole Body/ Composite	2,799	1,504	86	**0.00006**	2,654	1,963	35	**0.04**	1989	45 (11/34)
Carp	Whole Fish/ Whole Body/ Composite	4,158	2,896	44	**0.02**	4,528	5,116	–11	0.5	1989	66 (21/45)
Gizzard Shad	Whole Fish/ Whole Body/ Composite	2,514	1,706	47	**0.0009**	2,450	1,717	43	**0.002**	1989	23 (9/14)
Walleye	Skin-on Fillet	1,672	1,562	7	0.7	1,511	1,476	2	0.8	1989–1991	28 (11/17)
Walleye	Whole Fish/ Whole Body/ Composite	6,201	4,242	46	**0.006**	6,995	5,835	20	0.1	1989	56 (25/31)

Note:

* Based on a fitted model and a lipid percentage of 6 percent of weight except for walleye fillet with skin, where 3 percent was used.

Table 30 Models Comparing Log (PCB Concentration) versus Time in De Pere Reach and Green Bay Zone 2, Without Adjustment for Lipid Content

			Regression Model Parameter Statistics								Likelihood Ratio Tests			Sample Size		
Sample Type	Species	Model	Constant Parameter (b_0)	Std. Err. (b_0)	Time Parameter (b_4)	Std. Err. (b_4)	Reach Parameter (b_2)	Std. Err. (b_2)	Time × Reach Interaction Parameter (b_5)	Std. Err. (b_5)	III vs. II Equal Slopes: Time × Reach Effect *p*-value	II vs. I Equal Intercepts: Reach Effect *p*-value	III vs. I Equal Slopes and Intercepts: Full Reach Effect *p*-value	De Pere Reach	Green Bay Zone 2	Total
Whole Fish/Whole Body / Composite	alewife	III	89.7407	63.163	−0.0433	0.0317	−42.95	37.59	0.0215	0.0189	0.26		0.10	13	37	50
		II	20.8587	18.597	−0.0087	0.0093	−0.105	0.057	0	0		0.068				
		I(+)	18.2357	19.169	−0.0075	0.0096	0	0	0	0						
Whole Fish/Whole Body/ Composite	carp	III(+)	−242.08	64.123	0.1230	0.0322	219.60	49.47	−0.1100	0.0248	0.00002***		0.00005***	64	49	113
		II	27.37	22.514	−0.0118	0.0113	−0.1161	0.0926	0	0		NA				
		I	11.30	18.635	−0.0038	0.0094	0	0	0	0						
Whole Fish/Whole Body/ Composite	gizzard shad	III(+)	143.151	37.016	−0.0701	0.0186	−85.6	25.41	0.0429	0.013	0.0014**		0.0028**	18	32	50
		II	25.6608	13.639	−0.0112	0.0068	−0.06	0.048	0	0		NA				
		I	20.0254	13.061	−0.0084	0.0066	0	0	0	0						
Whole Fish/Whole Body/ Composite	walleye	III(+)	−24.0765	49.96	0.0141	0.0251	70.136	38.47	−0.0353	0.019	0.0707		0.0319*	44	34	78
		II	62.2372	16.529	−0.0293	0.0083	−0.119	0.062	0	0		0.0569				
		I	51.1061	15.85	−0.0238	0.008	0	0	0	0						

Notes:

(+) Model indicated by likelihood ratio test. Coefficients appear in Equation 21.
* $p < 0.05$
** $p < 0.01$
*** $p < 0.001$

The statistically significant coefficients of the log percent lipid term in the models range from 0.43 up to 1.09. We noted earlier that a change in the lipid content by a multiplicative factor of F (e.g., $F = 2$, doubling the percent) leads to a change in PCB concentration by a multiplicative factor of F^{b_1}, where b_1 is the coefficient of $\log_{10}$ lipid percentage in a regression model. The percentage change corresponding to F is $100\% * (F^{b_1} - 1)$. The observed range of significant lipid coefficients of 0.43 to 1.09 in the 19 analyses implies that a doubling of lipid percentage, for example, leads to a range of 34 to 113 percent increase in PCB concentration. The strong association between lipids and PCB concentration is illustrated by an example, Figure 48, where the positive association between log (PCB concentration) and log (percent lipid) is evident from the sparseness of points in the upper left and lower right of the plot.

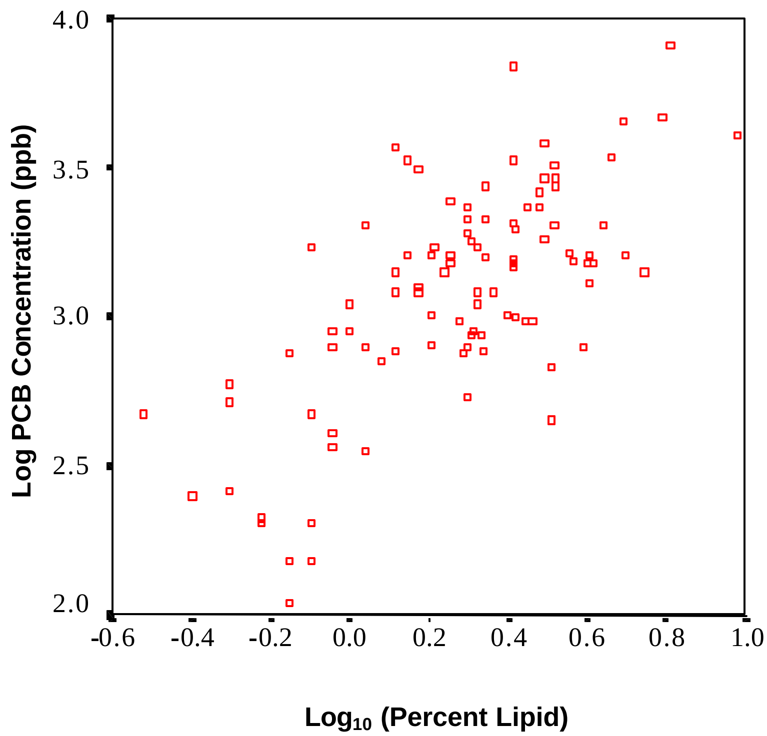

Figure 48 Log_{10} PCB Concentration (ppb) versus Log_{10} Percent Lipid Content for Walleye, Skin-on Fillet, De Pere to Green Bay Reach

The relationship between total PCBs and percent lipids (a measure of body fat) is strong. To adjust for this relationship, $\log_{10}$ (percent lipids) must be included as an independent covariate in regression analyses.

6 Conclusions and Discussion

The analysis of trends in fish tissue and sediment over time in the Lower Fox River has led us to several significant conclusions. These conclusions, supporting statements, and discussion are included in Section 6.1. In addition, Section 6.3 identifies uncertainties associated with this trends analysis.

6.1 Conclusions

Data collected in the Lower Fox River and Green Bay show that concentrations of PCBs in fish tissue and surface sediments declined following the elimination of PCB point source discharges. However, further analysis of that data has identified statistically significant breakpoints in the decline for most of the fish species examined, suggesting that the decline has slowed down or, in some cases, that tissue concentrations of PCBs have increased. Furthermore, the analysis shows that it is not possible to project PCB concentrations into the future for fish or sediment with confidence because time trends appear to be quite changeable and confidence intervals for rates are quite wide.

Data on PCBs in sediment samples taken from surface sediments suggest that PCB concentrations have generally declined over time. Trends in concentrations of PCBs in subsurface sediments are less clear—some deposits show declining trends, while others show trends either close to zero or not significantly different from zero and yet others show increasing trends.

Specific conclusions of the time trends analysis include:

- **Fish tissue concentrations have generally declined over the period of time for which there are data in the Lower Fox River and Green Bay Zone 2.** Fish tissue PCB concentrations generally showed a slow rate of decline throughout the Lower Fox River and Green Bay Zone 2. Most time trend slopes were negative, and all statistically significant slopes were negative except one.

- **Significant "breakpoints" in the decline were identified for most of the fish species examined, suggesting that rates of decline in PCB tissue concentrations are changeable and slowing and, in some cases, tissue concentrations may be increasing.** Fish tissue concentrations have not declined at a constant rate since the 1970s. Among fish time trends analyzed, 7 out of 19 combinations of reach, species, and sample type showed a statistically significant change in slope (log scale) between earlier and later periods. In Little Lake Butte des Morts, De Pere Reach, and in Green Bay Zone 2, there were steep declines in fish tissue PCB concentrations from the 1970s, but with significant breakpoints in declines for some species beginning around

1980. A meta-analysis of time trends showed that the most recent slopes averaged across species showed a 5 to 7 percent decline per year for three of the reaches. Six species showed an increasing rate in their final slope, but only two of these rates were statistically significant (carp, whole body, in De Pere Reach and in Green Bay Zone 2). The existence of breakpoints plus a meta-analysis to detect non-constant trends suggest that rates of change are changeable and not constant.

- **PCBs in surface sediment samples have generally declined over the period of time for which there are data for the Lower Fox River.** Surface sediment PCB concentrations combined within each reach showed statistically significant decreasing trends in all reaches except Appleton to Little Rapids. There were wide confidence intervals for rates of change, both for individual deposits and combined deposits, indicating that rate estimates are not precise. This imprecision and other uncertainties associated with the data do not support accurate future projections. Surface sediments of individual deposits within the reaches included a mixture of positive and negative slopes. Among the 16 negative slopes, 6 were statistically significant; neither of the 2 positive slopes were statistically significant.

- **Time trends in PCB concentrations in sediments below the surface sediment are less clear—some indicate a decline, others indicate no change or increases, others are unchanging or even increasing.** There is a strong trend toward fewer and weaker negative slopes at increasing depths. For Little Lake Butte des Morts, subsurface trends are mixed. The only statistically significant subsurface trend shows an increase and the other trends are a mixture of positive and negative trends. In the Appleton and De Pere reaches, there is a mixture of positive and negative trends that is not clearly distinguishable from a zero overall trend. For Little Rapids to De Pere, there are consistently negative trends in the 10- to 30-cm strata, but in the lower strata, the data are consistent with either a zero trend (30 to 50 cm), or an increasing trend (50 to 100 cm and 100+ cm).

- **Projection of PCB concentrations into the future for fish or sediments is questionable because of imprecision and other uncertainties identified in the analysis.** The analyses carried out cannot assure a continued decline in PCB concentrations over time. Even though there are a number of negative time trends that suggest PCB declines, future projection is questionable. Increases in PCB concentrations in some deeper sediments and breakpoints, and other non-linear phenomena in fish PCB time trends (on the log scale) suggest that the river, its sediment, and its fish species could experience an arrest or reversal of such a decline.

- **PCB concentrations may increase or decrease in the future.** Some, perhaps all, of the changes in slope from before to after a breakpoint in the fish analysis may be genuine, due to unpredictable events, such as floods accompanied by scouring and deposition. As discussed in the Remedial Investigation, sediment bed elevations have been altered historically and may also undergo changes in the future due to scouring and redistribution of sediments. The occurrence of these breakpoints in the past suggests that the river may change again in the future. The presence of non-constant slopes (which we refer to as "curvature") in the post-breakpoint period also suggests change. If so, such events will continue adding variability to PCB concentration over time, making predictions based on the assumption of a future decline at a constant rate questionable. The presence of curvature is consistent with the more dramatic changes represented by breakpoints and supports the notion of a dynamic process, liable to change, rather than a steady state with future constant linear rates of change.

The last two bullets are especially germane to use of the time trends analysis in other elements of the Lower Fox River Risk Assessment and Feasibility Study. The time trends were estimated only for the period of time for which data exist. These analyses are not suitable for accurately projecting trends into the future. Of particular importance, the data do not provide assurance of a continuing future decline in PCB concentrations.

The time trends analysis has dealt strictly with the testing of changes in PCB concentrations over time in the Lower Fox River, and not with the mechanisms that could control changes in sediment and tissue loads. The apparent decline of PCBs observed in surface sediments and fish from the Lower Fox River are consistent with the continued observed transport of PCBs from the river to Green Bay, as discussed in detail in the Remedial Investigation. Changes in sediment bed elevations have been documented and are discussed in Technical Memorandum 2g (WDNR, 1999a) and in the Remedial Investigation. Some of the variability observed in the data may be accounted for by changes in river profile, burial, scour by flood or ice, and propeller wash in the lower reaches of the river. As the analysis focused solely on the existing data in the Lower Fox River and Zone 2 of Green Bay, these potential mechanisms were not introduced into the analysis and thus could not be controlled. What is important to note, however, is that the trends analysis is dependent upon the existing hydraulic conditions in the Lower Fox River. Any changes in those conditions might result in exposure of underlying PCB-laden sediments or burying of sediments, and lead to new trends that may not be similar to the trends from this analysis.

The conclusions of a general historical decrease in PCB burdens in sediments and fish of the Lower Fox River and in Zone 2 of Green Bay are similar to those reported by other Great Lakes researchers. Decreases in PCB concentrations have been observed in Lake Michigan (Offenberg and Baker, 2000; DeVault *et al.*, 1996; Lamon *et al.*, 1998), Lake Ontario (DeVault *et al.*, 1996; Gobas *et al.*, 1995), Lake Superior (Smith, 2000; DeVault *et al.*, 1996) and lakes Huron and Erie (DeVault *et al.*, 1996). The yearly rate of decline for PCBs in biota and sediment of Lake Superior has been estimated at 3 to 8 percent per year and is expected to continue at 5 to 10 percent per year (Smith, 2000), which is generally consistent with the trends observed in the Lower Fox River. However, several other researchers have also noted breakpoints, or constant levels of PCBs beginning in the mid- to late 1980s. PCB concentrations in lake trout and smelt are reported to have been relatively constant in Lake Ontario since 1985 (Gobas *et al.*, 1995) while concentrations in other fish and in sediments show a decline during the period of observed data (to about 1990) and a projected continuing decline (see Gobas *et al.*, 1995, Figures 2 and 3). PCB body burdens in Lake Erie walleye were shown to be declining during the period of 1977 through 1982, but after that period remained constant through 1990 (DeVault *et al.*, 1996). Time tends analysis for salmonids and trout in Lake Michigan showed generally decreasing tissue concentrations (Lamon *et al.*, 1998). The uncertainty in rates is often large, and some trends are not significantly different from a zero rate or have confidence intervals that include positive rates of increase (e.g., lake trout, see DeVault *et al.*, 1996, Figure 3). These findings are consistent with the time trends analysis for the Lower Fox River and suggest that there may continue to be slow, gradual declines, or a steady state in PCB concentrations in fish and sediment in the future. The possibility of some increases cannot be ruled out.

6.2 Time Trends Discussion

6.2.1 General Issues

The time trends analysis has shown that PCB concentrations in surface sediments (0 to 10 cm) and fish are generally decreasing over time. In both sediment and fish analyses, the magnitude and level of statistical significance of time trends varies widely. All except one statistically significant fish time trend indicated decreasing concentrations. The time trends in subsurface (10+ cm) sediments contain a mixture of positive and negative rates of change, and it is difficult to reach a firm conclusion about the subsurface PCB time trends. The time trends in sediment generally exceed in magnitude (positive or negative) those in fish. Most significant and non-significant sediment trends were negative, but there were some statistically significant positive trends for deeper strata. More is known about the trends in surface deposits because a larger fraction of the surface deposit groups than subsurface deposits were analyzed.

Sediment samples taken from the surface sediments have more negative than positive slopes. However, there was a trend toward fewer negative and more positive slopes as depth increased. In sediments sampled from the surface, 89 percent of slopes were negative. Below 50 cm, 71 percent of slopes were positive. The time trend analysis has shown that rates of change of PCB concentrations in fish are themselves liable to change, calling into question the value of projecting concentrations under an assumed but unverifiable steady-state model. By implication, sediment—particularly surface sediment—as the primary source of PCBs in fish, is also likely to be changeable in its time trends of PCB concentrations.

The meta-analysis (pooled results from all surface sediment deposits) for trends in surface sediments showed an average rate of decrease in PCB concentrations of 18 percent per year in Little Lake Butte des Morts, 0.6 percent per year increase in the Appleton Reach, 10 percent per year decrease in the Little Rapids Reach, and 15 percent per year decrease in the De Pere Reach. These meta-analysis trends were statistically significant except for the small trend in the Appleton Reach. Thus, surface sediments show decreasing PCB concentrations over time, and at a fairly rapid average rate during the period covered by the data, except for the Appleton Reach.

It is important to emphasize that it is the average rate of change over a period of time that is strikingly negative in three out of the four reaches, and not necessarily the individual deposit rates or even the rates at each point in time covered by the data. Given the findings of fish time trends that seem to vary over time, as evidenced by both breakpoints and curvature, it is likely that the sediment time trends may also be volatile over time, perhaps due to scouring and deposition, which are described in a companion document (WDNR, 1999a). There are simply too few distinct time points of measurement of sediment concentrations to support a breakpoint and curvature analysis such as that carried out for fish. Since the ultimate source of PCBs in fish is sediment, however, it is difficult to imagine that fish have volatile time trends with sediment volatility.

The fish meta-analyses within the three out of four reaches with more than one fish category available for analysis show that PCB concentration was most recently declining at a rate of 5 to 7 percent per year (Little Lake Butte des Morts, De Pere, Green Bay Zone 2). The single fish category that could be analyzed for the Appleton Reach also shows a decline of 10 percent per year.

However, the fish time trends are changeable. Little Lake Butte des Morts had a steeper decline in PCB concentrations in earlier years. All analyses with a breakpoint in this reach show a steeper decline before the breakpoint. In the other reaches, the data for each fish category considered individually are consistent with a constant rate of decline over the whole time period, except for 2 out of 12 combinations of species and sample type. Nevertheless, the collective evidence demonstrates that slopes (on the log scale) tend to be non-constant. Based on a meta-analysis, the hypothesis of constant final slopes for all species was rejected and we must accept the concept of non-constant time trends for the post-breakpoint period for at least some species. In this regard, we note that it is possible to not detect curvature for analysis of individual species and yet to detect the presence of curvature from a global meta-analysis (and accept changing slopes for some individual species), because the meta-analysis has more power.

A practical dilemma in estimating future concentrations of PCBs is the choice of a statistical model to use in projecting concentrations forward in time, both for sediment and fish. For sediment, there are insufficient data to test for "curvature" (a non-constant slope over time), though the fish analysis implies curvature and changeability of slopes. Using the fitted time trends as presented in this report for projection and ignoring the possibility of non-constant sediment time trend slopes assumes a steady state in the river and, consequently, could lead to erroneous future projections. Such error in the projection is likely to be smaller, when one aggregates the results of projections of individual deposits into larger geographic units, such as a reach or the entire river. There is disagreement between fish and sediment time trends. The average rates of decrease of PCB concentration in the meta-analysis of surface sediments generally exceed those observed in the meta-analysis of fish PCB trends. Biologically, fish rates should have to be linked with and similar to those for sediment. One possible explanation for the mismatch is that the sediment rate of decrease may have slowed down recently. There are too few time points with sediment data, per deposit group and depth, to detect such a slowing, and the calculated rate of change for sediment PCB concentration may be an average of a faster earlier rate and a slower recent rate.

6.2.2 Fish Lipids

Lipid content of samples distinctly assisted in reducing unexplained variance for most analyses of fish PCB time trends. Since it is so helpful, efforts should be taken in the future to explore ways to more powerfully incorporate lipids into the analysis. The time trend analysis used lipid content as a linear independent variable. We prefer this approach to the alternative of dividing PCB concentration by the percent lipid content, which is equivalent to using lipids as an independent variable but forcing its coefficient to be unity.

Only two analyses of time trends in gizzard shad (for two different reaches) showed no significant relationship between lipids and PCBs, suggesting that some species may handle PCBs in a different fashion. The variety of coefficients relating PCBs to lipid content among the various species and sample types suggests that species are not identical in their PCB-lipid relationships.

6.2.3 Strengths of the Study

There are a number of strengths of the study. The maximum likelihood method used to handle data below a detection limit allowed these values to contribute to the analysis without having to impute a proxy value. The methods used to detect and handle spatial correlation of sediment samples have allowed us to avoid overstating statistical significance of time trends. In fact, statements of statistical significance should be quite conservative. Our approaches to quantifying and testing for non-constant rates of change in fish time trends (breakpoints and curvature) have allowed us to assess the changeability of time trends. Our use of regression analysis of lipid content as a factor in PCB concentrations makes good use of the lipid data and does not impose a pre-specified coefficient relating PCBs to lipid content. The use of meta-analysis of rates has increased precision and power in time trend estimates. The remarkable agreement of the data with the lognormal distribution and the need to address only two outliers in over 2,000 observations, support the overall validity of the PCB concentrations used in the time trends analysis. The inherent very great variability of the PCB concentrations has been thoroughly described quantitatively, through confidence intervals of slopes, and graphically, by scatter plots of concentrations versus time. Finally, clear statements about confidence in and statistical significance of the various quantitative trends have been provided to guide the reader in the use of the trends.

6.3 Sources of Uncertainty in the Time Trends Analysis

The conclusions and discussion presented above are based upon the statistical analyses of the data as received by us. However, there are areas of uncertainty that may have played a role in this analysis. By “uncertainty,” we mean either random variation (such as fish-to-fish variation in PCB concentration) or systematic variation due to unmeasured factors, such as age and gender of fish or changes in the absolute elevation of the sediment-water interface. While statisticians use terms such as “variation” and “sources of unexplained variation” for these two effects, we will use the term “uncertainty,” a term more familiar to readers, to specifically designate the combination of these two effects. While there is no uncertainty about the methodology, the results should be considered as possibly influenced by unmeasured factors, hence uncertain to that extent.

In addition to the uncertainty arising from sheer randomness, there are sources of uncertainty associated with laboratory and analytical variation and other factors that could not be included in the analysis. The various sources of uncertainty are discussed below.

6.3.1 Statistical Uncertainty — Statistical Significance and Confidence Intervals

The data used for both sediment and fish time trends analyses are inherently quite variable. A wide scatter of points typically surrounds the regression lines for fitted models. This variability has led to some wide confidence intervals around estimated values. The lack of statistical significance of a time trend does not imply the absence of a real trend, even a strong one. Some attention to confidence intervals shows the possibility of strong trends that may not have been detected due to the large random component in the data.

We suggest that the reader take note of the statistically significant trends and use the confidence intervals for these and other trends as statements ruling out (with high confidence) certain slopes outside the confidence intervals. Slopes within the confidence intervals (usually quite wide) are all quite plausible and consistent with the data. These confidence intervals are usually quite wide. Because the confidence intervals are generally wide, they cannot usually be used to state that a trend is close to zero. Within the intervals, there are differing rates of change.

By examining the standard errors of slope estimates of $\log_{10}$ PCB concentration versus time, a quantitative notion of the statistical uncertainty in the time trend estimates can be expressed. A standard error (SE) of 0.0054 for a slope estimate on the $\log_{10}$ scale would indicate "excellent" precision because, for example, a slope of zero (zero percent change per year) with an SE of 0.0054 would lead to a 95 percent confidence interval (CI) for the rate of change of --2.5 to +2.5 percent, a tight range of 5 percentage points. None of the 46 sediment trends and only 3 out of the 19 fish trends have this precision (Table 9 and Table 18).

"Good" or "fair" precision would be an SE of 0.01 or less, which, for a zero slope, would have a 95 percent CI of ±5 percent, a range of 10 percentage points. Two sediment and nine fish time trends have this precision. Among the meta-analyses, all of the fish combined time trend slopes have good-to-excellent precision (Table 19), but none of the combined surface sediment time trends has this precision (Table 10). Even "good" or "fair" precision of ±5 percent provides room for very different future scenarios. A rate of 5 percent decrease per year for 10 years leads to a 40 percent loss in PCB concentration, while a 5 percent increase per year for 10 years leads to a 63 percent increase in PCB concentration. The range –40 to +63 percent is a wide zone of uncertainty.

Indeed, one of the firm conclusions of this study must be that, in some cases, a firm conclusion cannot be reached. An increasing or decreasing time trend that is statistically significant, or a trend that is not significantly different from zero but with a tight confidence interval around zero, provides a clear outcome. Non-significant trends with wide confidence intervals impart little information and do not provide a clear outcome. Thus, Table 31 and Table 32 show which calculated time trends provide a "clear outcome" and which trends have "good" or "fair" precision.

Table 31 Sediment Time Trends: Analyses with Clear Outcomes and Good Precision

Type of Analysis			Clear Outcome: Significant Increase or Decrease, or Confidently Close to Zero?[+]	Is Precision Good or Fair?[++]
Sediment				
Little Lake Butte des Morts				
Deposit Group	AB	0–10 cm	Decrease	—
		10–30 cm	—	—
		30–50 cm	—	—
	C	0–10 cm	—	—
		10–30 cm	—	—
	POG	0–10 cm	—	—

Table 31 Sediment Time Trends: Analyses with Clear Outcomes and Good Precision

Type of Analysis			Clear Outcome: Significant Increase or Decrease, or Confidently Close to Zero?+	Is Precision Good or Fair?++
	D	0–10 cm	Decrease	—
		10–30 cm	Increase	—
	F	0–10 cm	Decrease	—
		10–30 cm	—	—
	GH	0–10 cm	Decrease	—
Little Lake Butte des Morts Surface Meta-analysis			**Decrease**	**—**
Appleton Reach				
Deposit Group	IMOR	0–10 cm	—	—
	N Pre-dredge	0–10 cm	Decrease	Yes
		10–30 cm	—	—
		30–50 cm	—	—
	VCC	0–10 cm	—	—
		10–30 cm	Decrease	—
		30–50 cm	—	—
Appleton Reach Surface Meta-analysis			**—**	**—**
Little Rapids Reach				
Deposit Group	Upper EE	0–10 cm	—	—
		10–30 cm	—	—
		30–50 cm	—	—
	Lower EE	0–10 cm	Decrease	—
		10–30 cm	—	—
		30–50 cm	Increase	—
	FF	0–10 cm	—	—
		10–30 cm	Decrease	—
	GGHH	0–10 cm	—	—
		10–30 cm	—	—
		30–50 cm	—	—
		50–100 cm	—	—
		100+ cm	—	—
Little Rapids Reach Surface Meta-analysis			**Decrease**	**—**

Table 31 Sediment Time Trends: Analyses with Clear Outcomes and Good Precision

Type of Analysis			Clear Outcome: Significant Increase or Decrease, or Confidently Close to Zero?+	Is Precision Good or Fair?++
De Pere Reach				
SMU Group	2025	0–10 cm	—	—
		10–30 cm	—	—
		30–50 cm	—	—
		50–100 cm	—	—
	2649	0–10 cm	Decrease	Yes
		10–30 cm	—	—
		50–100 cm	—	—
		100+ cm	—	—
	5067	0–10 cm	Decrease	—
		10–30 cm	—	—
		50–100 cm	Increase	—
		100+ cm	—	—
	6891	0–10 cm	—	—
		10–30 cm	—	—
	92115	0–10 cm	—	—
De Pere Reach Surface Meta-analysis			**Decrease**	**—**

Notes:

\+ 1. "Yes" indicates increase or decrease is statistically significant compared to zero rate of change ($p < 0.05$), **or** 95 percent confidence interval for percent change is within ±5 percent of zero.

\+ 2. Uncertain outcome noted by "—" (not "Yes" to above).

++ Standard error of slope ≤ 0.1.

Of the 46 deposit group analyses in Table 31 and 4 surface sediment analyses, only 16 cases can offer us a reasonably firm conclusion on time trends. Two indicate increasing, and 14 indicate decreasing, trends. The remaining 34 analyses have uncertain trends. All cases noted with a dash ("—") in the "Clear Outcome" column may have trends that deviate more than ±5 percent per year from a constant, 0 percent rate of change, and the rate may plausibly be either positive or negative. In these cases, a zero rate is just one among a wide range of possible rates bracketing zero. As noted in the "Precision" column of Table 31, only two analyses provide good or fair precision for their time trends.

The fish analyses provide a firmer set of conclusions (Table 32). Among the 19 primary analyses and 3 meta-analyses, 17 clearly demonstrate an "increase" or "decrease." The other five analyses do not support a solid "no change," zero-slope conclusion, but instead leave us with a fairly wide range of plausible increasing or decreasing slopes. As far as precision goes, 14 out of the 22 analyses provide "good" or "fair" precision for fish trend estimates.

Table 32 Fish Time Trends: Analyses with Clear Outcomes and Good Precision

Type of Analysis	Clear Outcome: Significant Increase or Decrease, or Confidently Close to Zero?+	Is Precision Good or Fair?++
Fish		
Little Lake Butte des Morts		
Carp, skin-on fillet	Decrease	Yes
Carp, whole body	—	—
Northern Pike, skin-on fillet	Decrease	Yes
Walleye, skin-on fillet	—	—
Walleye, whole body	—	—
Yellow Perch, skin-on fillet	—	—
Little Lake Butte des Morts Meta-analysis	**Decrease**	**Yes**
Appleton Reach		
Walleye, skin-on fillet	Decrease	—
De Pere Reach		
Carp, whole body	Increase	—
Gizzard Shad, whole body	Decrease	Yes
Northern Pike, skin-on fillet	Decrease	Yes
Walleye, skin-on fillet	Decrease	Yes
Walleye, whole body	Decrease	Yes
White Bass, skin-on fillet	Decrease	Yes
White Sucker, skin-on fillet	Decrease	Yes
De Pere Reach Meta-analysis	**Decrease**	**Yes**
Green Bay Zone 2		
Alewife, whole body	Decrease	Yes
Carp, skin-on fillet	—	—
Carp, whole body	Decrease	Yes
Gizzard Shad, whole body	Increase	Yes
Yellow Perch, skin-on fillet	Decrease	Yes
Green Bay Zone 2 Meta-analysis	**Decrease**	**Yes**

Notes:

\+ 1. "Yes" indicates increase or decrease is statistically significant compared to zero rate of change ($p < 0.05$), **or** 95 percent confidence interval for percent change is within ±5 percent of zero.
2. Uncertain outcome noted by "—" (not "Yes" to above).

++ Standard error of slope ≤ 0.1.

6.3.2 Physical Sources of Uncertainty

Depth of Sediments

The time trend analysis has shown that shallower sediment layers tend to have greater rates of decrease than deeper layers, where PCB concentrations may even be increasing. In Little Lake Butte des Morts, for example, Deposit Group D bears a strong and statistically significant decreasing trend at 0 to 10 cm and a strong and highly significant increasing tend at 10 to 30 cm. Deposits with these trend patterns may be experiencing either burying of more contaminated surface sediments over time into deeper strata, or some mechanism whereby PCBs migrate downward.

Depth of sediment is closely related to PCB concentration. We used depth defined as the distance to the sediment-water interface. The Fox River database (the source of our data) does not include the absolute depth of deposits (in relation to fixed points and elevations on land). Such data would undoubtedly help in the analysis. The data available now do not allow us to track a given parcel of sediment over time. The interface may change over time due to scouring or deposition. Some of the time trends noted here may be due to a change in the depth from the sediment-water interface, where that boundary has shifted up or down due to deposition or scouring over time, so that different parcels of sediment are identified with the same depth label at different times. Time trends based on an absolute definition of depth would more accurately track what happens to PCBs in a specific volume of sediment over time.

Hydraulic Conditions

As noted above, there was no way to control in the time trends analysis for changes that may have occurred in sediment or fish tissue concentrations that could be attributed to flooding, ice scouring, propeller wash, or other mechanisms that would have caused changes to the hydraulic conditions in the river. Changes in bed elevations have been previously documented (WDNR, 1999a). While in one sense, the analysis of trends over time is concerned only with change, and not necessarily the underlying mechanism(s), an understanding of episodic events that may have influenced observed upward or downward trends would have facilitated the overall understanding of those results.

The trends reported here pertain to hydraulic conditions in the river at the time the data were collected. The system of locks and dams on the Lower Fox River currently control to a large degree where deposition and scouring occur. In the future, should those conditions change, any comparison of rates of change of PCB concentrations to the rates presented in this report, for the purpose of determining slowing or quickening of rates over time, would have to be done very cautiously.

6.3.3 Sources of Biological Uncertainty

Age and Gender of Fish

Age of fish may relate to PCB concentrations, due to different feeding habits and locations during the lifecycle. Incorporating age proxy variables (either length or mass) might reduce unexplained variance and increase power to detect trends. The relation of age to PCB concentration could be explored as either linear, curvilinear, or some type of step function (e.g., representing juveniles versus adults). (Length data have recently become available for some samples as this analysis was completed.) Similarly, the gender of the fish and whether or not it recently spawned may be factors in PCB uptake and retention, and these factors can easily be incorporated into the analysis when data become available.

Spatial Dependence

The time trend analysis was not adjusted for and cannot, with present data, adjust for potential spatial dependence of data from fish samples. While individual fish do not have specific geographic coordinates, fish caught at about the same time and location may exhibit some dependence due to similar feeding sources.

6.3.4 Uncertainty Due to Laboratory and Analytical Factors

Our time trends analysis did not incorporate potential laboratory variation into the study. Multiple laboratories engaged in the analysis of sediments and fish tissues for the Lower Fox River and Green Bay, which is not uncommon for large environmental projects. Analytical variability amongst those laboratories is discussed in the Data Management Report (EcoChem, 2000). A "laboratory effect," whereby different laboratories would produce a different mean PCB concentration on split samples, is possible. In addition, analytical techniques may have changed over the 1989-through-1998 period of sediment sample collection. Similarly, the 1976-through-1998 period of the fish samples included in the analysis may well have seen changes and refinements in laboratory equipment and techniques. Both the "laboratory effect" and changes in technique may have influenced the time trends.

7 References

Cressie, N. A., 1993. *Statistics for Spatial Data*. John Wiley and Sons, New York.

DeVault, D. S., R. Hesselberg, P. W. Rodgers, and T. J. Feist, 1996. Contaminant trends in lake trout and walleye from the Laurentian Great Lakes. *Journal of Great Lakes Research*. 22:884–895.

EcoChem, 2000. *Data Management Summary Report: Fox River Remedial Investigation and Feasibility Study*. Prepared for Wisconsin Department of Natural Resources. October 3.

Gobas, F. A. P. C., M. N. Z'Graggen and X. Zhang, 1995. Time response of the Lake Ontario Ecosystem to virtual elimination of PCBs. *Environmental Science and Technology*. 29(8):2038–2046.

Heagerty, P., and T. Lumley, 2000. Window subsampling of estimating functions with application to regression models. *Journal of the American Statistical Association*. 95:197–211.

Herbert, C., and K. Keenleyside, 1995. To normalize or not to normalize? Fat is the question. *Environment Toxicology and Chemistry*. 14:801–807.

Lamon III, E. C. and S. R. Carpenter *et al*., 1998. Forecasting PCB concentrations in Lake Michigan salmonids: A dynamic linear model approach. *Ecological Applications*. 8(3):659–668.

Larsson, P., L. Lennart Okla, and L. Collvin, 1993. Reproductive status and lipid content as factors in PCB, DDT and HCH contamination of a population of pike (*Esox lucius* l.). *Environment Toxicology and Chemistry*. 12:855–861.

Lawless, J., 1982. *Statistical Models and Methods for Lifetime Data*. John Wiley and Sons, New York.

Lumley, T., and P. Heagerty, 1999. Weighted empirical adaptive variance estimators for correlated data regression. *Journal of the Royal Statistical Society B*. 61(2)459–477.

Offenberg, J. H. and J. E. Baker, 2000. PCBs and PAHs in southern Lake Michigan in 1994 and 1995: Urban atmospheric influences and long-term declines. *Journal of Great Lakes Research*. 26(2):196–208.

Smith, D. W., 2000. Analysis of rates of decline of PCBs in different Lake Superior media. *Journal of Great Lakes Research*. 26(2):152–163.

ThermoRetec, 2001a. *Remedial Investigation: Lower Fox River, Wisconsin.* Prepared by ThermoRetec Consulting Corporation, St. Paul, Minnesota. Prepared for Wisconsin Department of Natural Resources, Madison, Wisconsin.

ThermoRetec, 2001b. *Draft Baseline Human Health and Ecological Risk Assessment: Lower Fox River, Wisconsin Remedial Investigation and Feasibility Study*. Prepared by ThermoRetec Consulting Corporation, Seattle, Washington and Pittsburgh, Pennsylvania. Prepared for Wisconsin Department of Natural Resources, Madison, Wisconsin.

WDNR, 1999a. *Model Evaluation Workgroup Technical Memorandum 2g: Quantification of Lower Fox River Sediment Bed Elevation Dynamics through Direct Observations*. Prepared by Wisconsin Department of Natural Resources. July 23.

WDNR, 1999b. *Model Evaluation Workgroup Technical Memorandum 2e: Estimation of Lower Fox River Sediment Bed Properties*. Prepared by Wisconsin Department of Natural Resources. March 31.

WDNR, 2001. *Technical Memorandum 7c: Recommended Approach for a Food Web/Bioaccumulation Assessment of the Lower Fox River/Green Bay Ecosystem*. Prepared by Wisconsin Department of Natural Resources. January.

Appendix

Additional Data and Plots

APPENDIX B-1
TIME TRENDS IN PCB CONCENTRATIONS IN SEDIMENT AND FISH

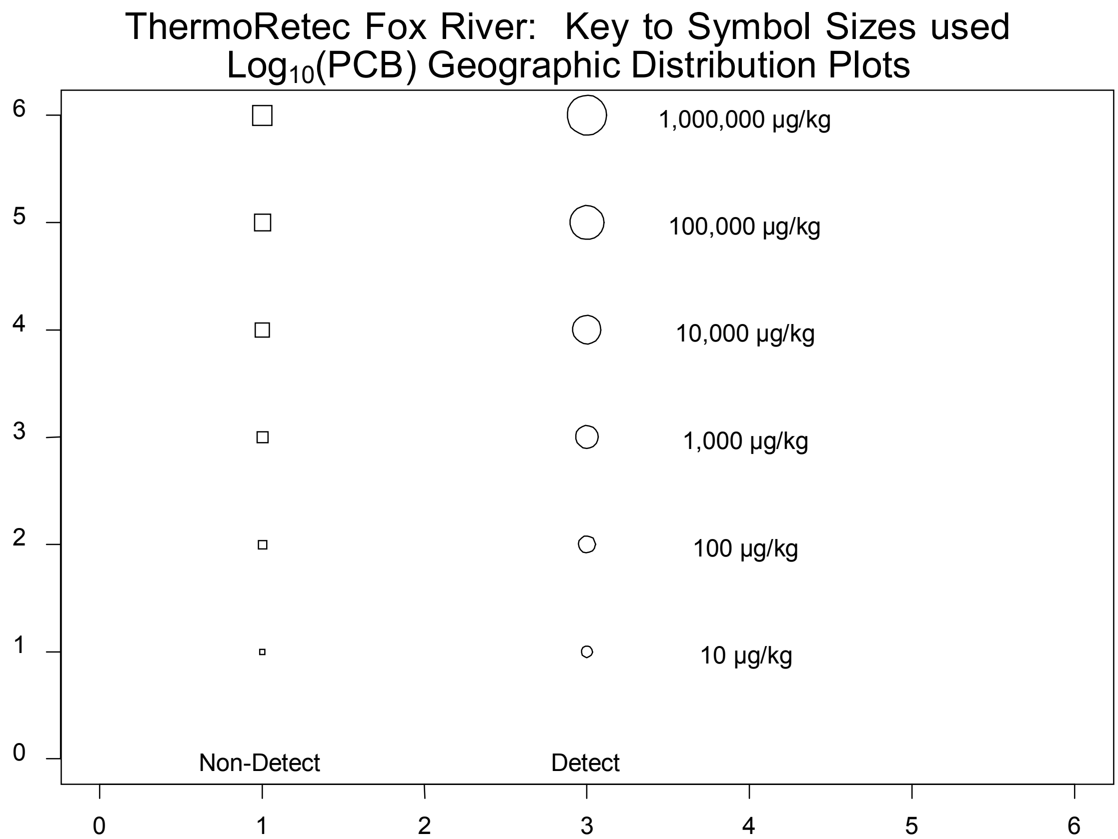

Figure A-1 Northing/Easting Plot Key

Scale plot showing the size of circles (for samples with detected PCBS) and squares (for samples with PCBs below detection limit, the square conveys the level at which the PCBs would have been detected as reported by the various testing agencies) used to convey total PCB level in the northing/easting plots of sample locations.

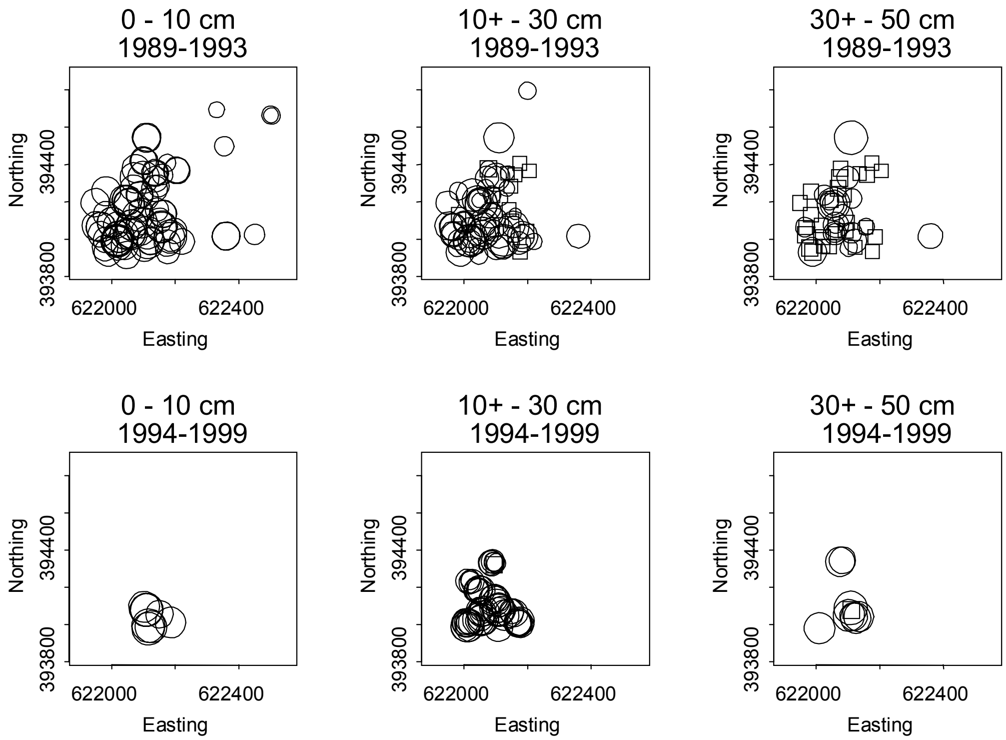

Figure A-2 Sample Locations by Northing and Easting Coordinates During 1989–1993 and 1994–1999, Depth Strata of Little Lake Butte des Morts Deposit Group AB (0 to 50 cm)

Larger symbols indicate higher concentrations. Circles (○) indicate measured concentrations and squares (□) indicate the detection limit of concentrations below the detection limit. Coordinates are in meters.

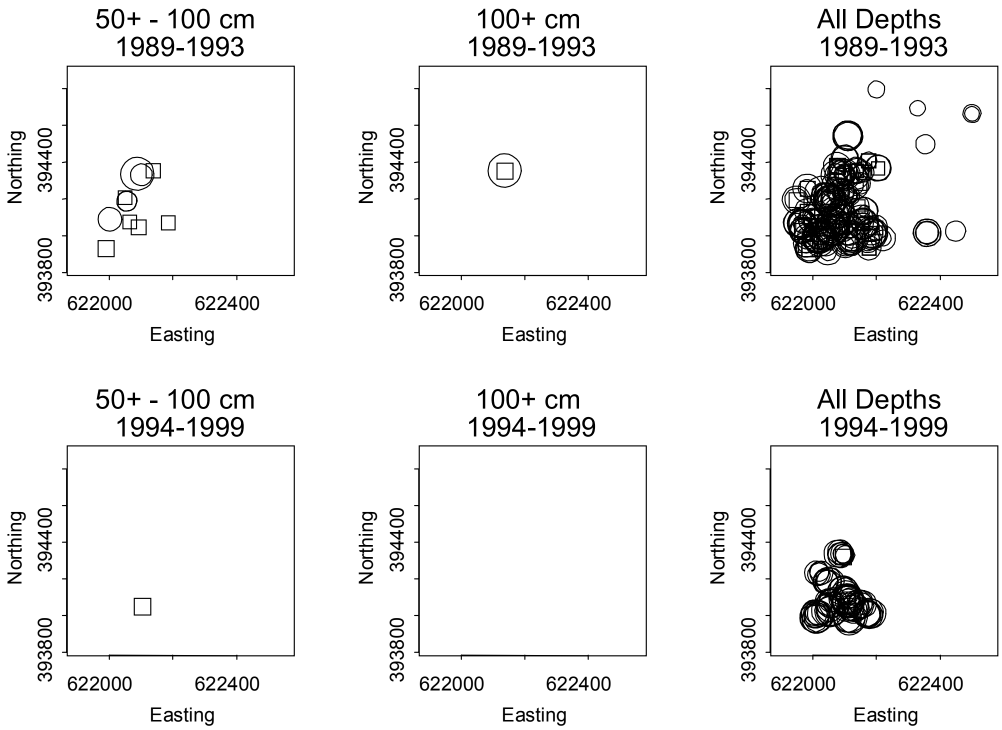

Figure A-3 Sample Locations by Northing and Easting Coordinates During 1989–1993 and 1994–1999, Depth Strata of Little Lake Butte des Morts Deposit Group AB (50 to 100+ cm)

Larger symbols indicate higher concentrations. Circles (○) indicate measured concentrations and squares (□) indicate the detection limit of concentrations below the detection limit. Coordinates are in meters.

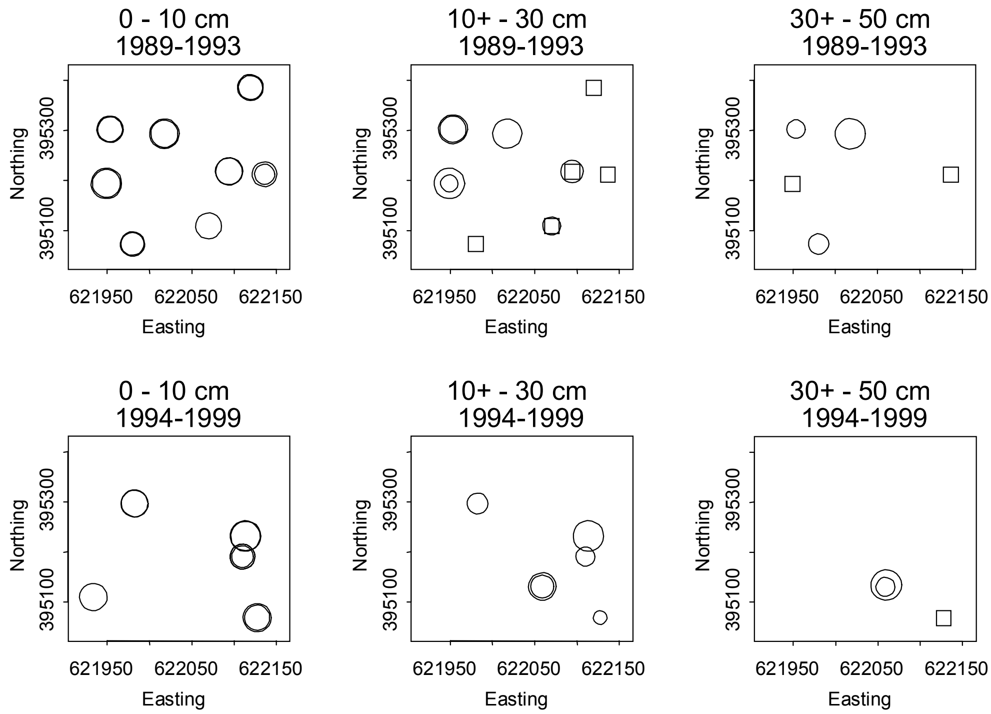

Figure A-4 Sample Locations by Northing and Easting Coordinates During 1989–1993 and 1994–1999, Depth Strata of Little Lake Butte des Morts Deposit Group C (0 to 50 cm)

Larger symbols indicate higher concentrations. Circles (○) indicate measured concentrations and squares (□) indicate the detection limit of concentrations below the detection limit. Coordinates are in meters.

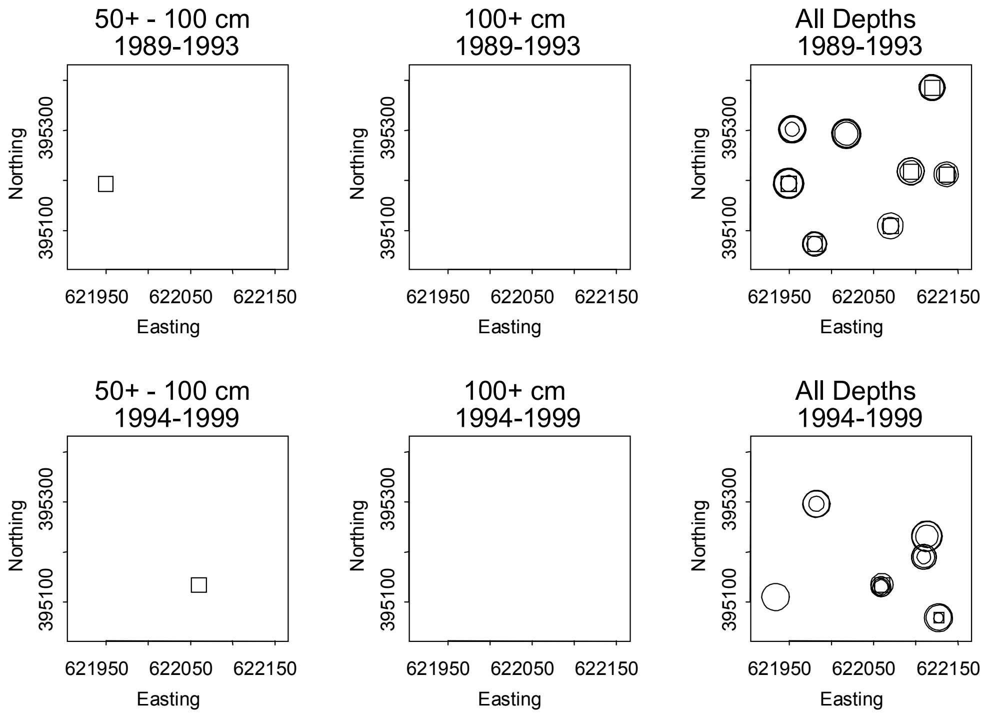

Figure A-5 Sample Locations by Northing and Easting Coordinates During 1989–1993 and 1994–1999, Depth Strata of Little Lake Butte des Morts Deposit Group C (50 to 100+ cm)

Larger symbols indicate higher concentrations. Circles (○) indicate measured concentrations and squares (□) indicate the detection limit of concentrations below the detection limit. Coordinates are in meters.

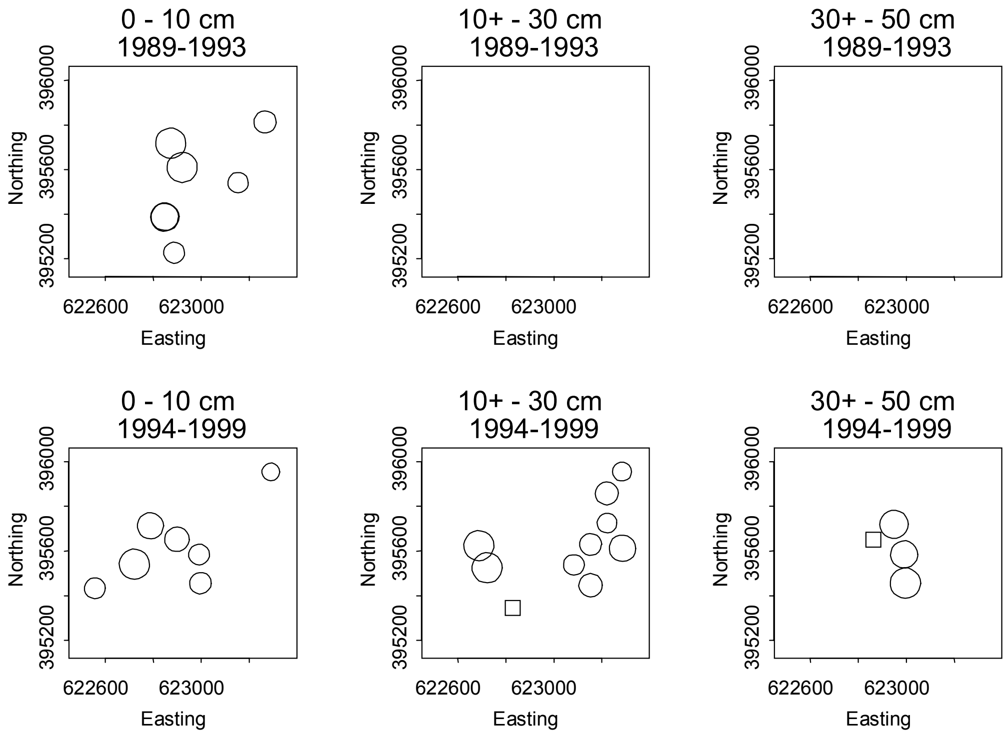

Figure A-6 Sample Locations by Northing and Easting Coordinates During 1989–1993 and 1994–1999, Depth Strata of Little Lake Butte des Morts Deposit Group POG (0 to 50 cm)

Larger symbols indicate higher concentrations. Circles (○) indicate measured concentrations and squares (□) indicate the detection limit of concentrations below the detection limit. Coordinates are in meters.

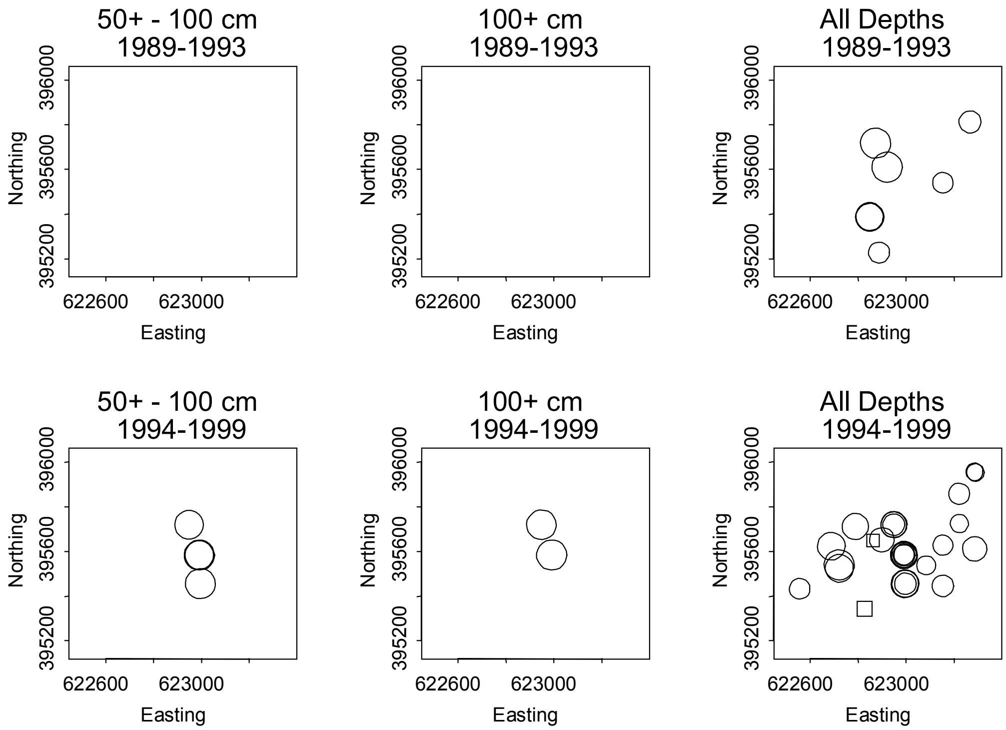

Figure A-7 Sample Locations by Northing and Easting Coordinates During 1989–1993 and 1994–1999, Depth Strata of Little Lake Butte des Morts Deposit Group POG (50 to 100+ cm)

Larger symbols indicate higher concentrations. Circles (○) indicate measured concentrations and squares (□) indicate the detection limit of concentrations below the detection limit. Coordinates are in meters.

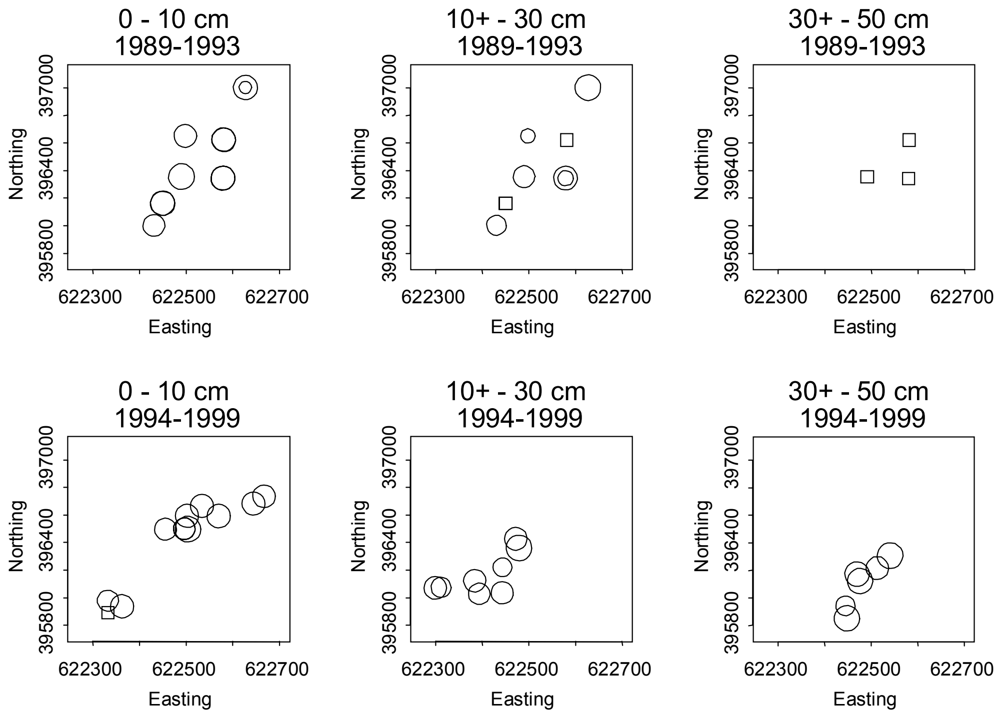

Figure A-8 Sample Locations by Northing and Easting Coordinates During 1989–1993 and 1994–1999, Depth Strata of Little Lake Butte des Morts Deposit Group D (0 to 50 cm)

Larger symbols indicate higher concentrations. Circles (O) indicate measured concentrations and squares (□) indicate the detection limit of concentrations below the detection limit. Coordinates are in meters.

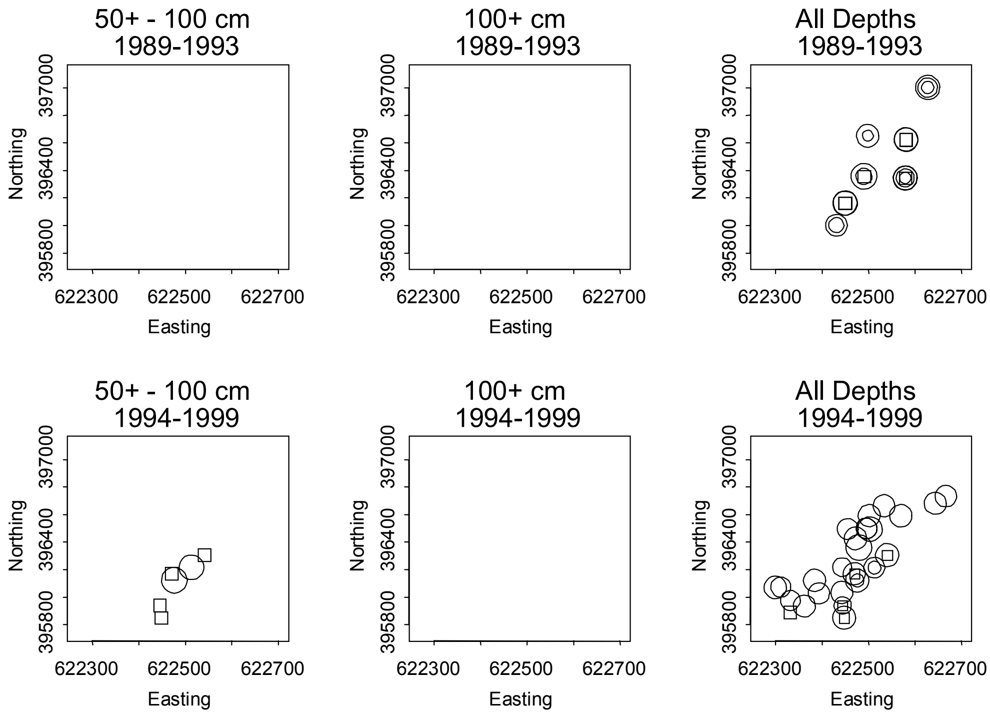

Figure A-9 Sample Locations by Northing and Easting Coordinates During 1989–1993 and 1994–1999, Depth Strata of Little Lake Butte des Morts Deposit Group D (50 to 100+ cm)

Larger symbols indicate higher concentrations. Circles (○) indicate measured concentrations and squares (□) indicate the detection limit of concentrations below the detection limit. Coordinates are in meters.

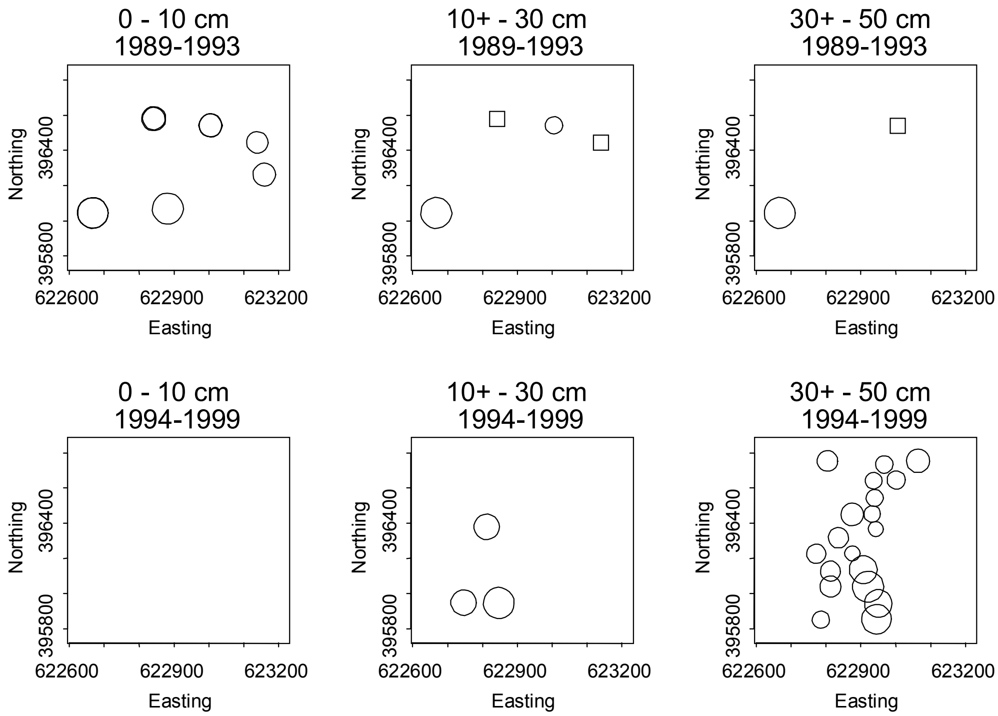

Figure A-10 Sample Locations by Northing and Easting Coordinates During 1989–1993 and 1994–1999, Depth Strata of Little Lake Butte des Morts Deposit Group E (0 to 50 cm)

Larger symbols indicate higher concentrations. Circles (○) indicate measured concentrations and squares (□) indicate the detection limit of concentrations below the detection limit. Coordinates are in meters.

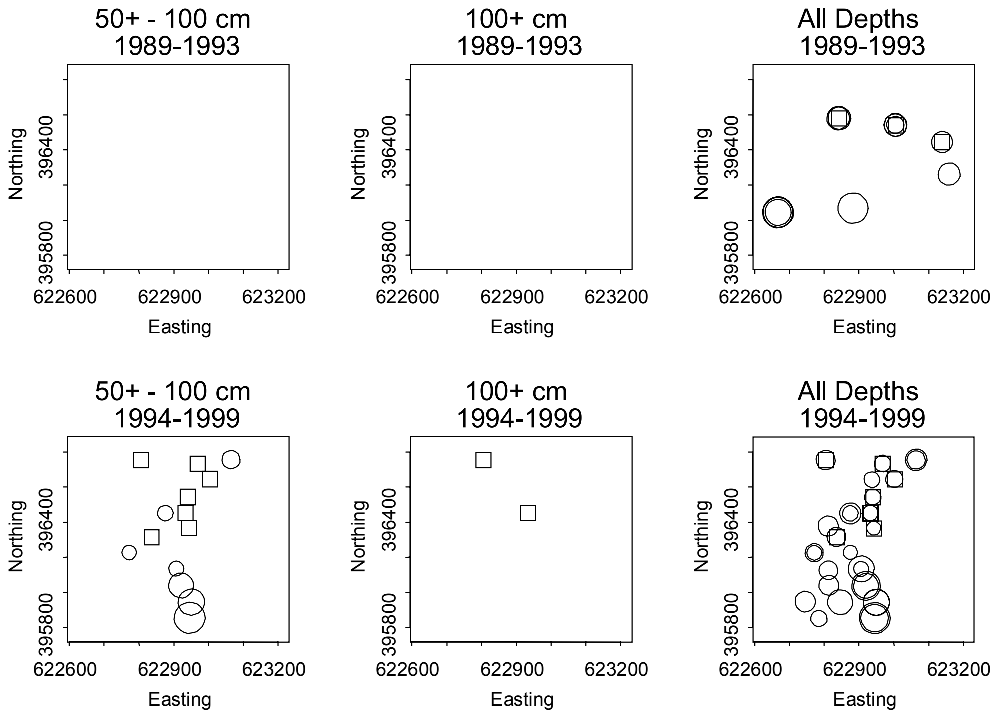

Figure A-11 Sample Locations by Northing and Easting Coordinates During 1989–1993 and 1994–1999, Depth Strata of Little Lake Butte des Morts Deposit Group E (50 to 100+ cm)

Larger symbols indicate higher concentrations. Circles (○) indicate measured concentrations and squares (□) indicate the detection limit of concentrations below the detection limit. Coordinates are in meters.

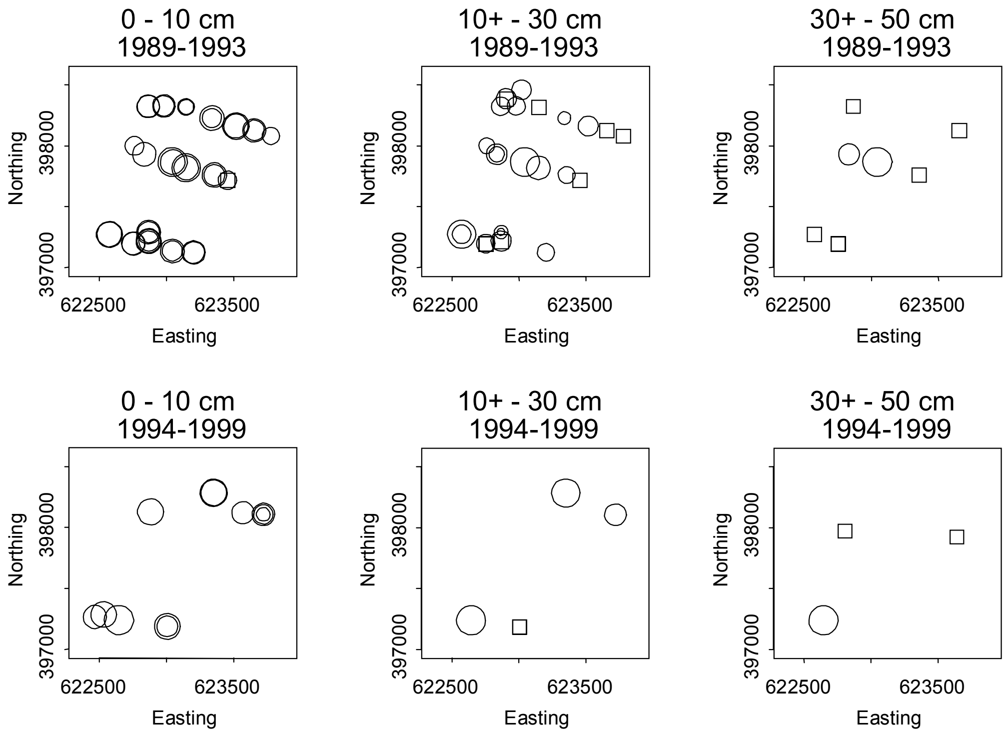

Figure A-12 Sample Locations by Northing and Easting Coordinates During 1989–1993 and 1994–1999, Depth Strata of Little Lake Butte des Morts Deposit Group F (0 to 50 cm)

Larger symbols indicate higher concentrations. Circles (○) indicate measured concentrations and squares (□) indicate the detection limit of concentrations below the detection limit. Coordinates are in meters.

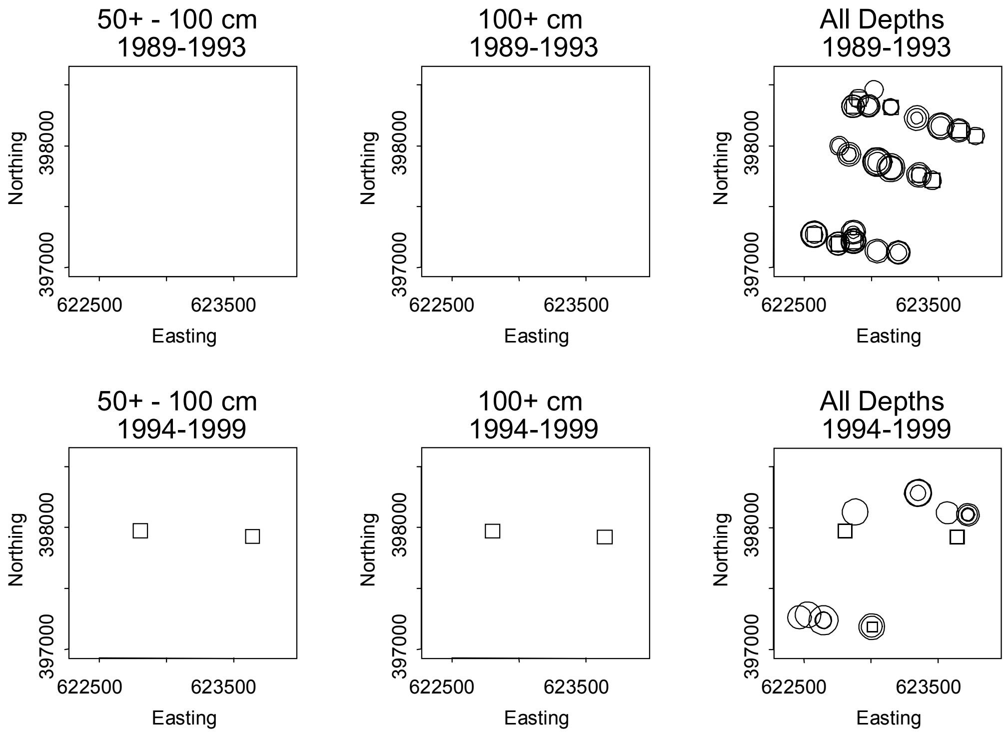

Figure A-13 Sample Locations by Northing and Easting Coordinates During 1989–1993 and 1994–1999, Depth Strata of Little Lake Butte des Morts Deposit Group F (50 to 100+ cm)

Larger symbols indicate higher concentrations. Circles (○) indicate measured concentrations and squares (□) indicate the detection limit of concentrations below the detection limit. Coordinates are in meters.

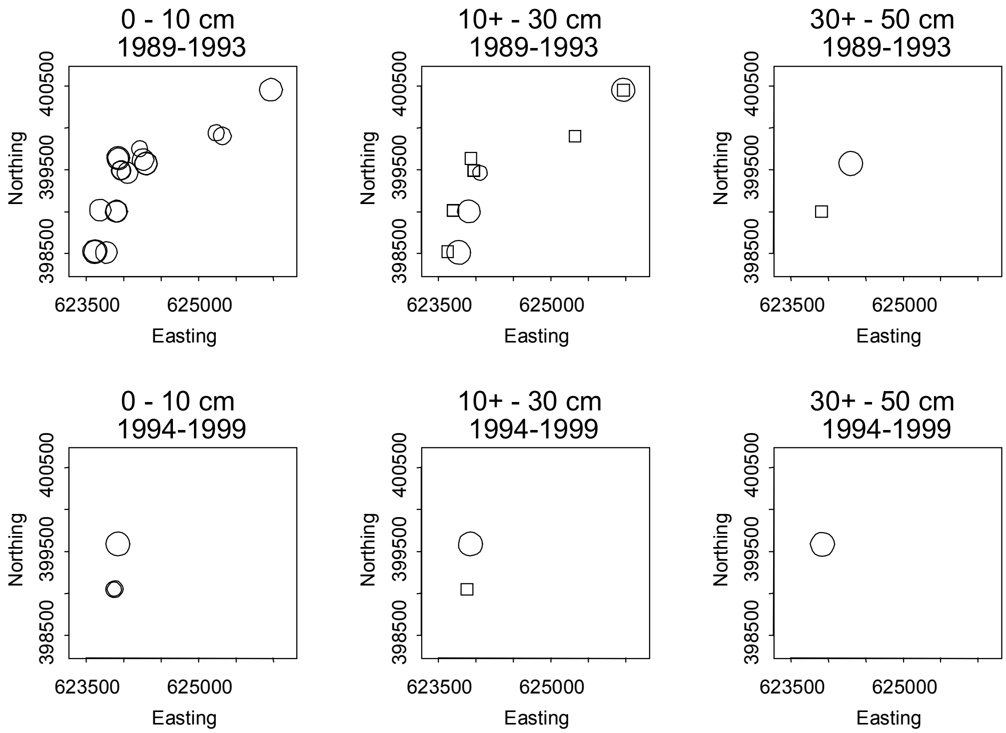

Figure A-14 Sample Locations by Northing and Easting Coordinates During 1989–1993 and 1994–1999, Depth Strata of Little Lake Butte des Morts Deposit Group GH (0 to 50 cm)

Larger symbols indicate higher concentrations. Circles (○) indicate measured concentrations and squares (□) indicate the detection limit of concentrations below the detection limit. Coordinates are in meters.

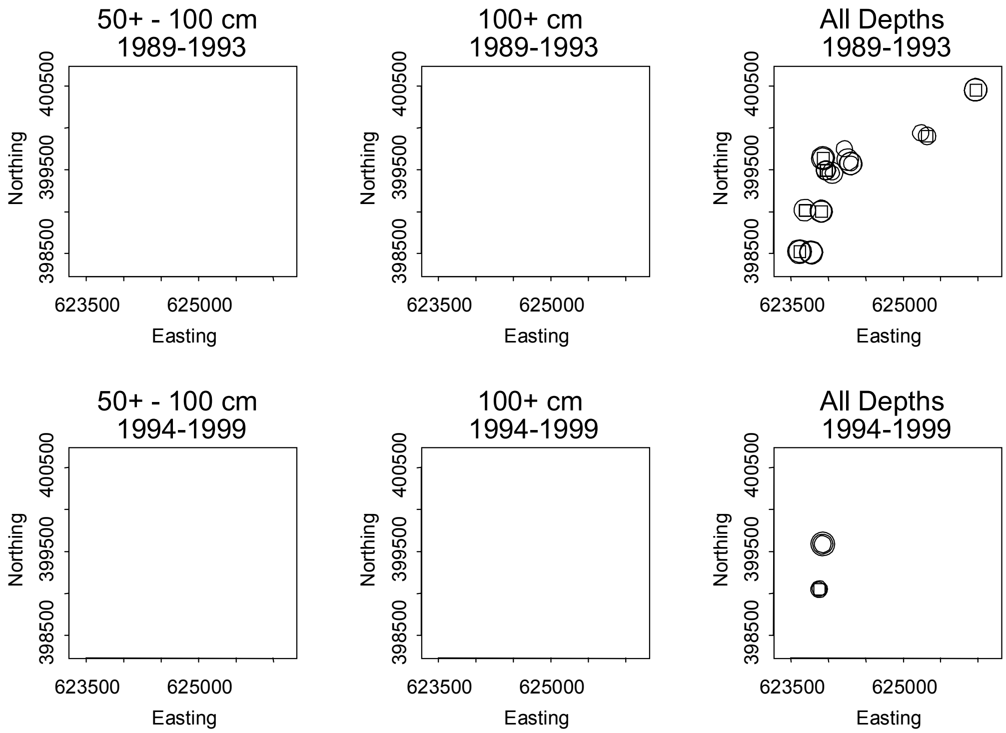

Figure A-15 Sample Locations by Northing and Easting Coordinates During 1989–1993 and 1994–1999, Depth Strata of Little Lake Butte des Morts Deposit GH (50 to 100+ cm)

Larger symbols indicate higher concentrations. Circles (○) indicate measured concentrations and squares (□) indicate the detection limit of concentrations below the detection limit. Coordinates are in meters.

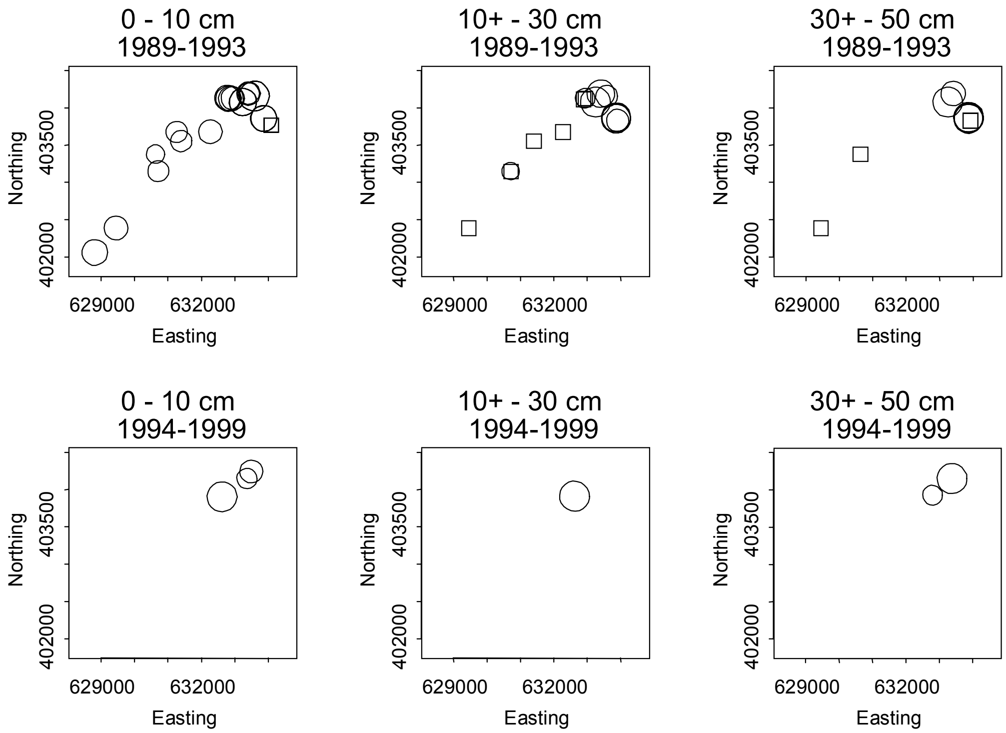

Figure A-16 Sample Locations by Northing and Easting Coordinates During 1989–1993 and 1994–1999, Depth Strata of Appleton Deposit Group IMOR (0 to 50 cm)

Larger symbols indicate higher concentrations. Circles (○) indicate measured concentrations and squares (□) indicate the detection limit of concentrations below the detection limit. Coordinates are in meters.

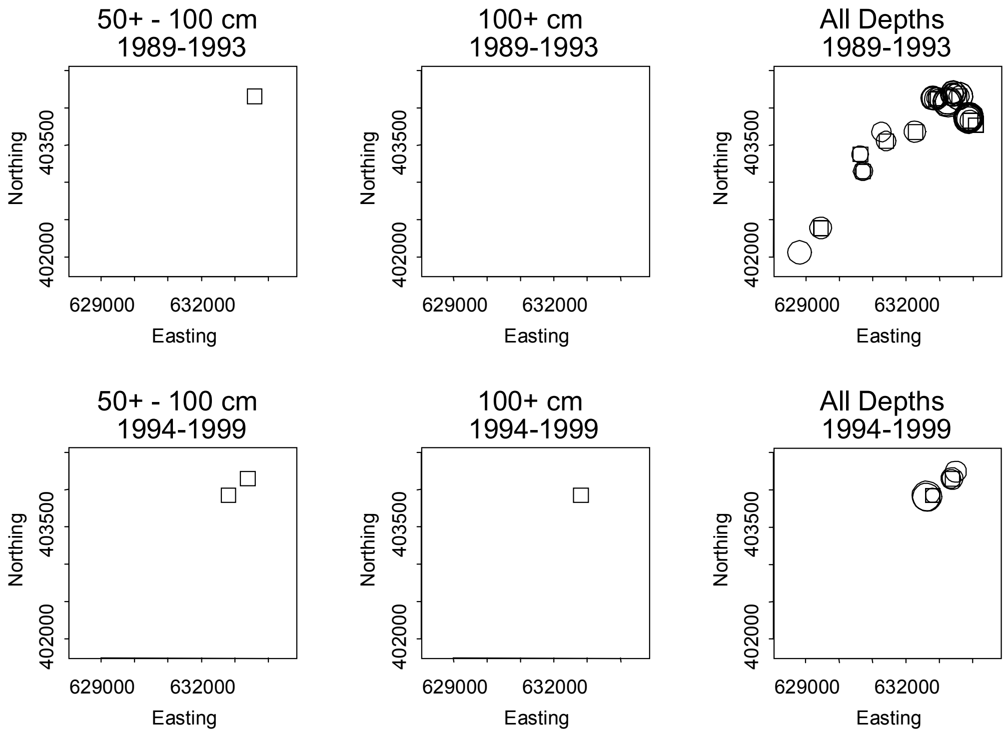

Figure A-17 Sample Locations by Northing and Easting Coordinates During 1989–1993 and 1994–1999, Depth Strata of Appleton Deposit Group IMOR (50 to 100+ cm)

Larger symbols indicate higher concentrations. Circles (○) indicate measured concentrations and squares (□) indicate the detection limit of concentrations below the detection limit. Coordinates are in meters.

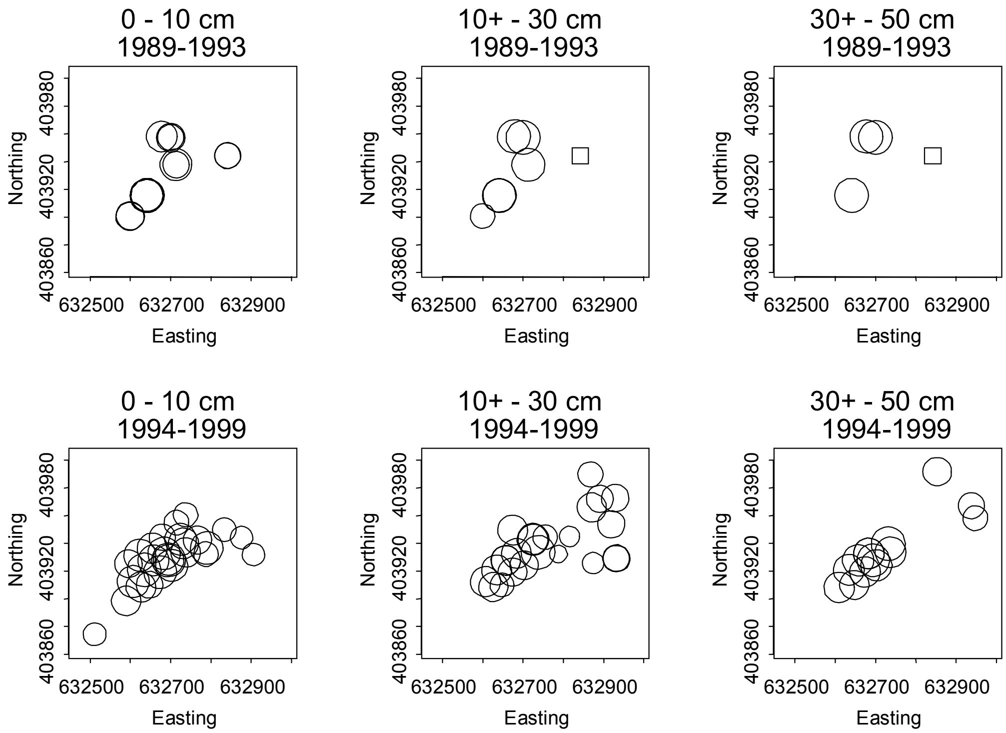

Figure A-18 Sample Locations by Northing and Easting Coordinates During 1989–1993 and 1994–1999, Depth Strata of Appleton Deposit Group N Before Demonstration Project (0 to 50 cm)

Larger symbols indicate higher concentrations. Circles (○) indicate measured concentrations and squares (□) indicate the detection limit of concentrations below the detection limit. Coordinates are in meters.

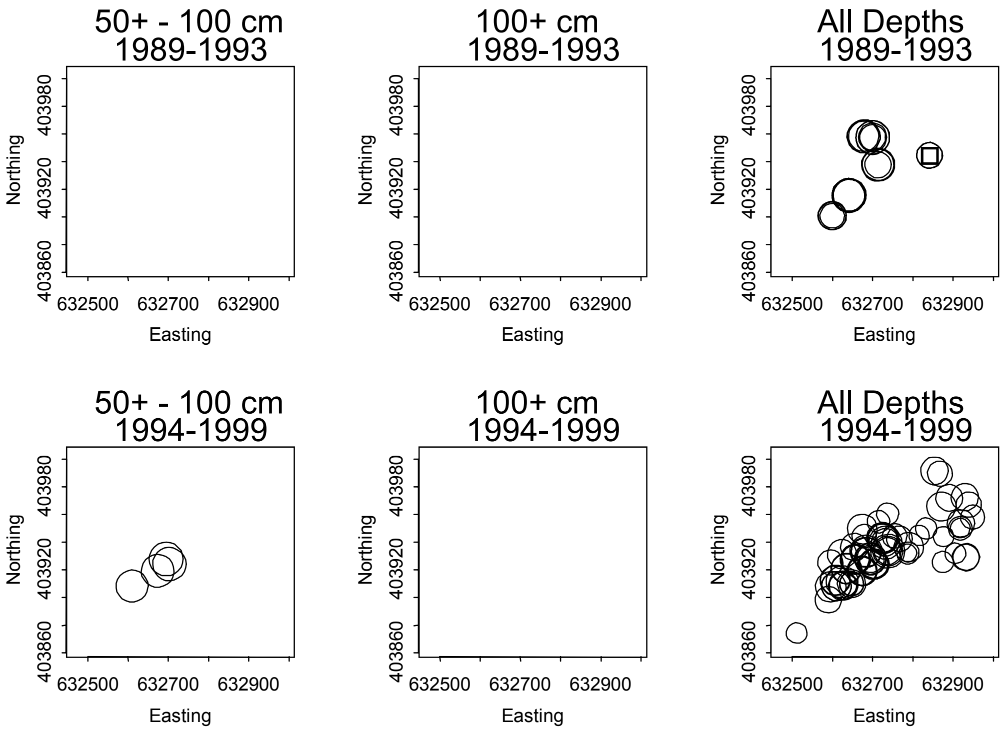

Figure A-19 Sample Locations by Northing and Easting Coordinates During 1989–1993 and 1994–1999, Depth Strata of Appleton Deposit Group N Before Demonstration Project (50 to 100+ cm)

Larger symbols indicate higher concentrations. Circles (○) indicate measured concentrations and squares (□) indicate the detection limit of concentrations below the detection limit. Coordinates are in meters.

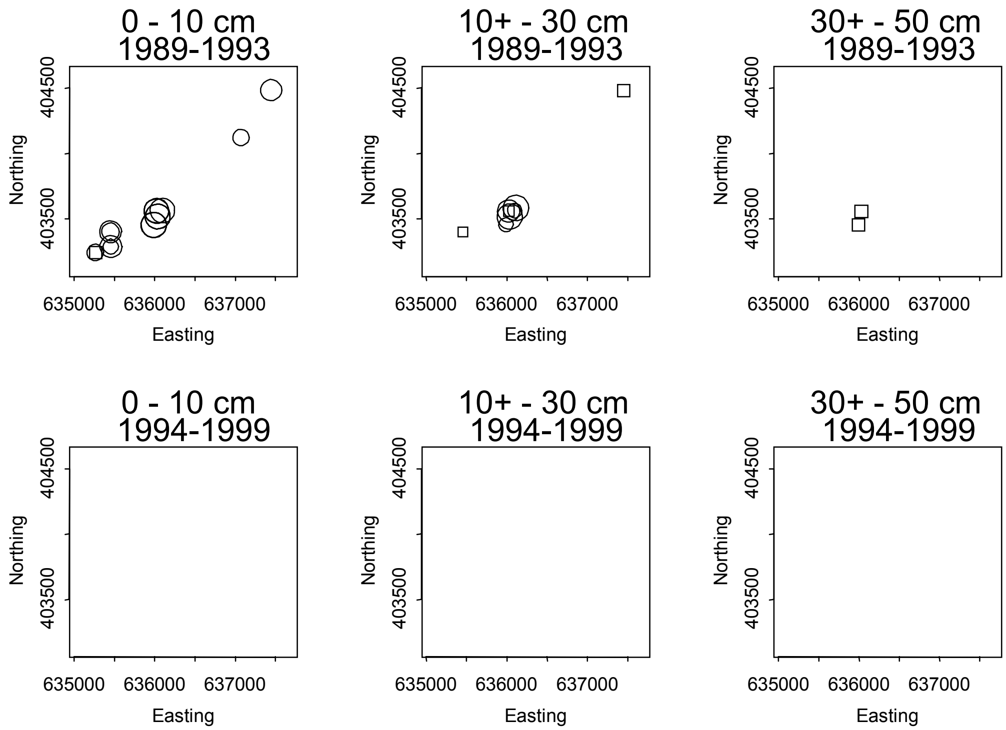

Figure A-20 Sample Locations by Northing and Easting Coordinates During 1989–1993 and 1994–1999, Depth Strata of Appleton Deposit Group SU (0 to 50 cm)

Larger symbols indicate higher concentrations. Circles (○) indicate measured concentrations and squares (□) indicate the detection limit of concentrations below the detection limit. Coordinates are in meters.

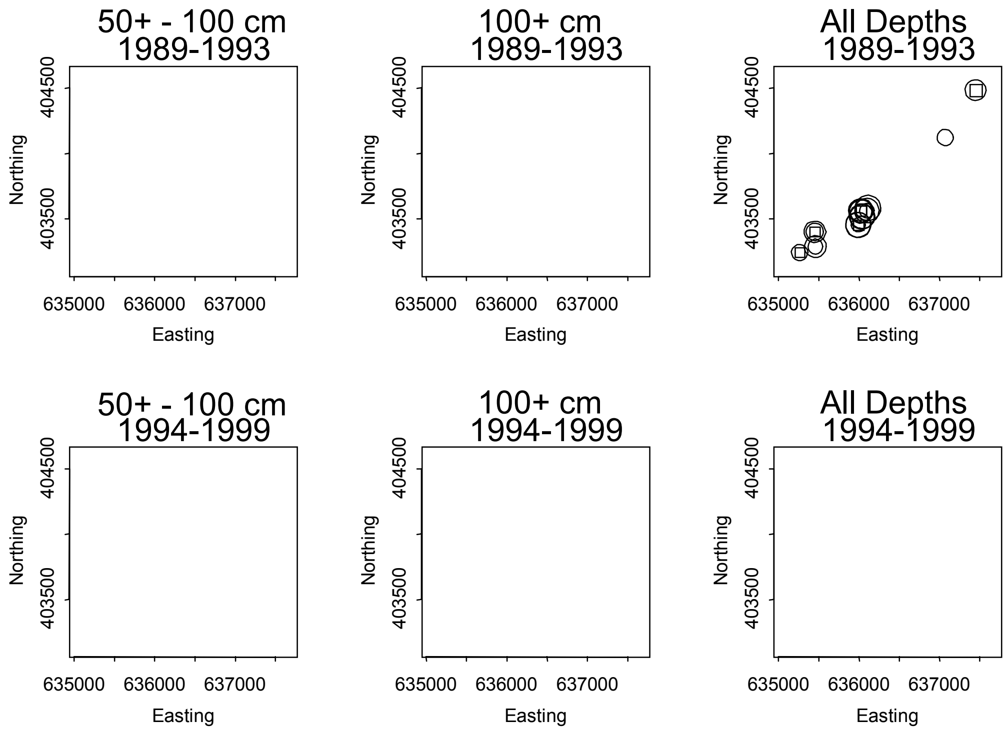

Figure A-21 Sample Locations by Northing and Easting Coordinates During 1989–1993 and 1994–1999, Depth Strata of Appleton Deposit Group SU (50 to 100+ cm)

Larger symbols indicate higher concentrations. Circles (○) indicate measured concentrations and squares (□) indicate the detection limit of concentrations below the detection limit. Coordinates are in meters.

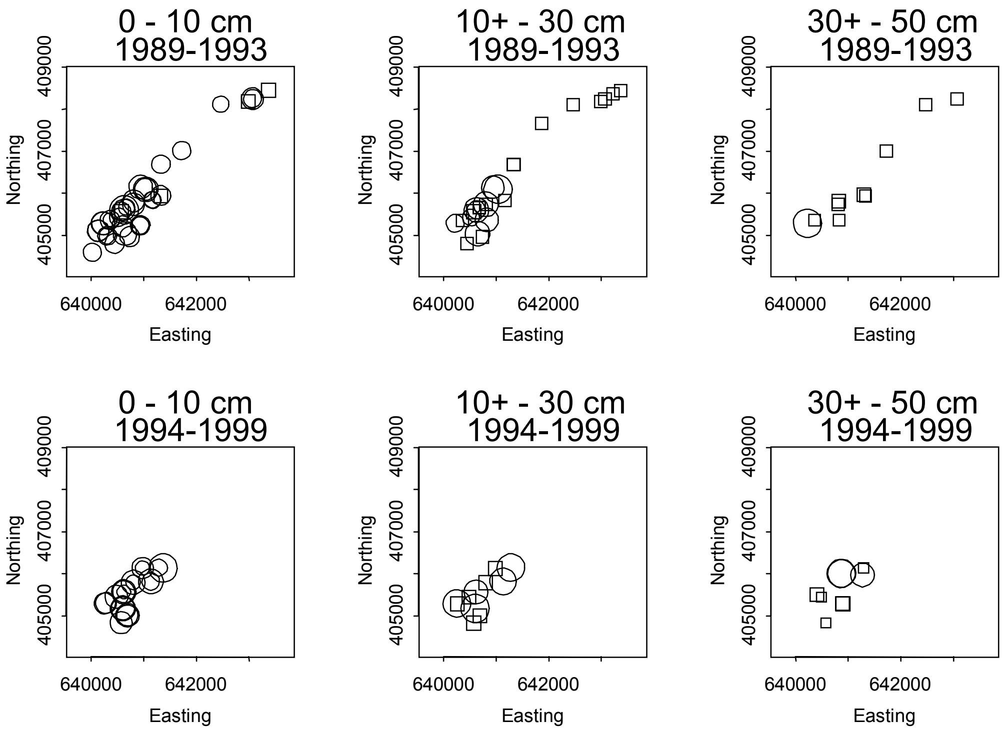

Figure A-22 Sample Locations by Northing and Easting Coordinates During 1989–1993 and 1994–1999, Depth Strata of Appleton Deposit Group VCC (0 to 50 cm)

Larger symbols indicate higher concentrations. Circles (○) indicate measured concentrations and squares (□) indicate the detection limit of concentrations below the detection limit. Coordinates are in meters.

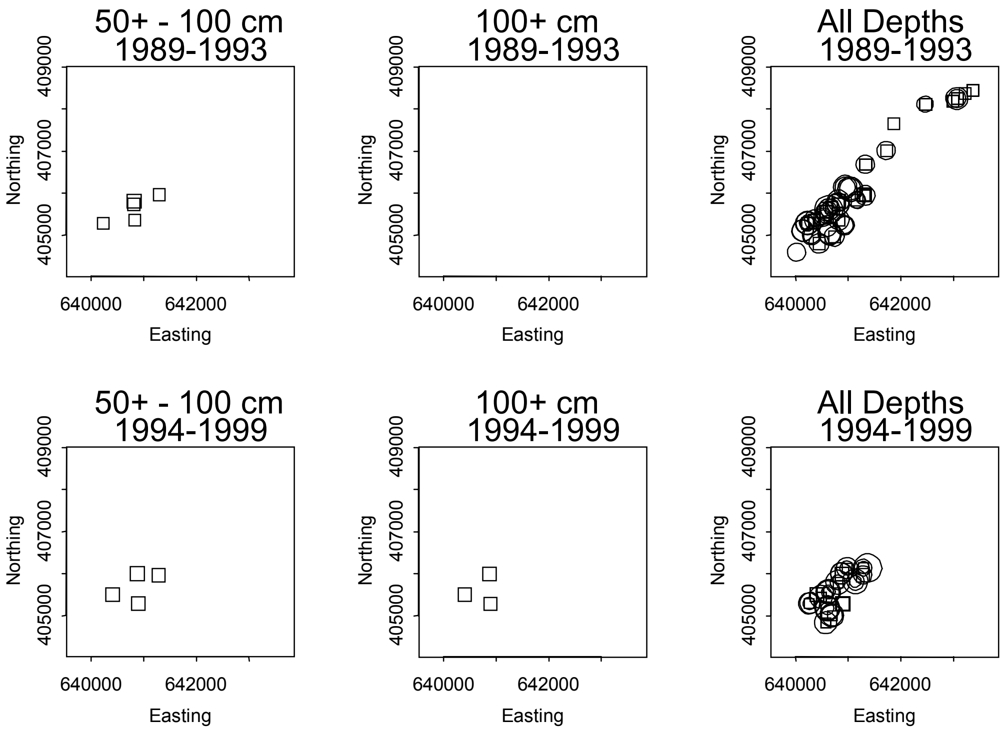

Figure A-23 Sample Locations by Northing and Easting Coordinates During 1989–1993 and 1994–1999, Depth Strata of Appleton Deposit Group VCC (50 to 100+ cm)

Larger symbols indicate higher concentrations. Circles (○) indicate measured concentrations and squares (□) indicate the detection limit of concentrations below the detection limit. Coordinates are in meters.

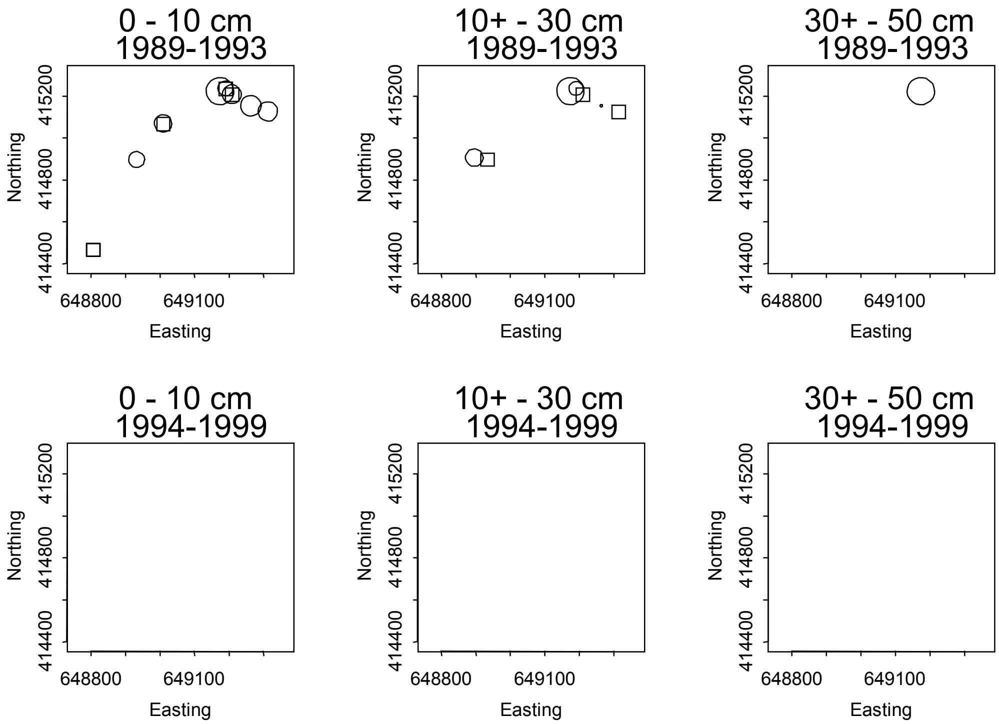

Figure A-24 Sample Locations by Northing and Easting Coordinates During 1989–1993 and 1994–1999, Depth Strata of Appleton Deposit Group DD (0 to 50 cm)

Larger symbols indicate higher concentrations. Circles (○) indicate measured concentrations and squares (□) indicate the detection limit of concentrations below the detection limit. Coordinates are in meters.

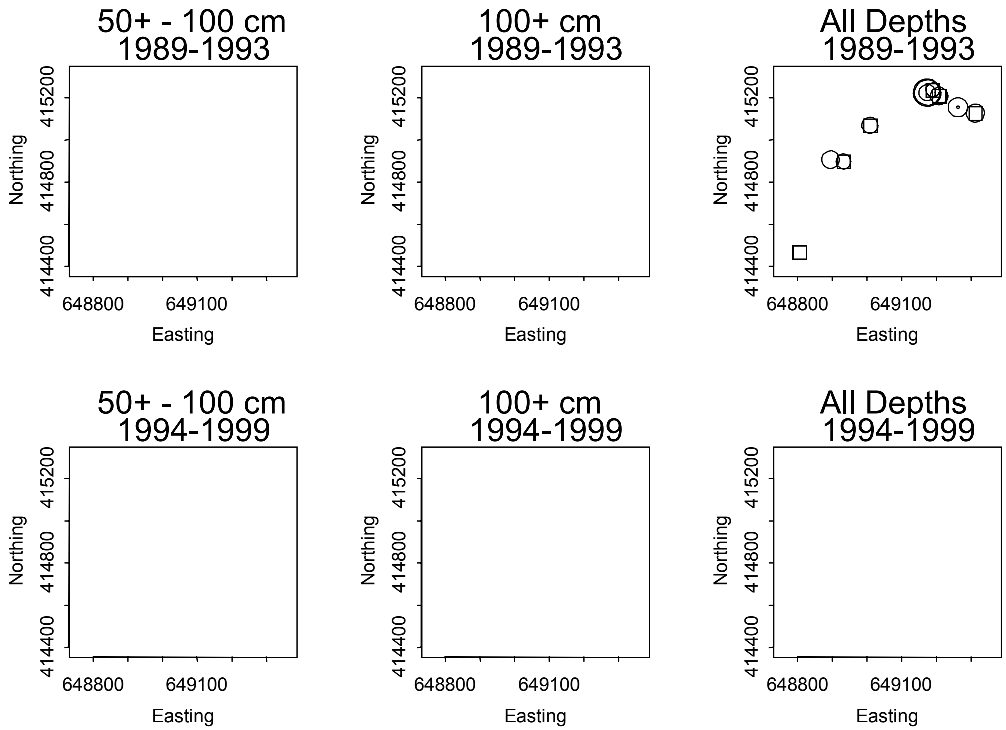

Figure A-25 Sample Locations by Northing and Easting Coordinates During 1989–1993 and 1994–1999, Depth Strata of Appleton Deposit Group DD (50 to 100+ cm)

Larger symbols indicate higher concentrations. Circles (○) indicate measured concentrations and squares (□) indicate the detection limit of concentrations below the detection limit. Coordinates are in meters.

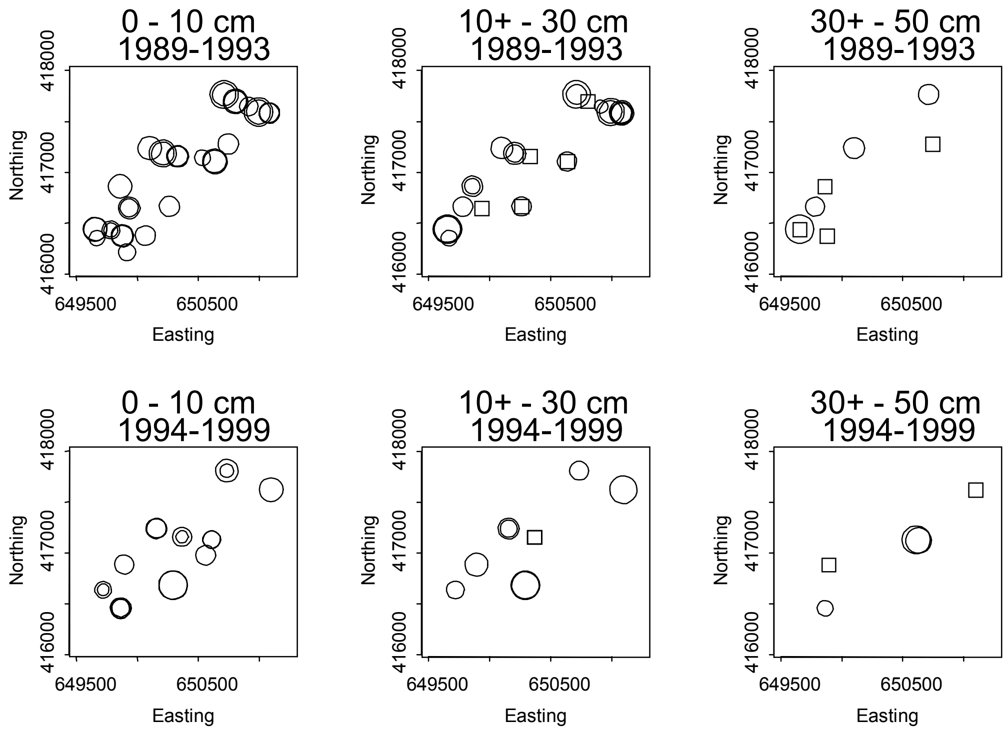

Figure A-26 Sample Locations by Northing and Easting Coordinates During 1989–1993 and 1994–1999, Depth Strata of Little Rapids Deposit Group Upper EE (0 to 50 cm)

Larger symbols indicate higher concentrations. Circles (○) indicate measured concentrations and squares (□) indicate the detection limit of concentrations below the detection limit. Coordinates are in meters.

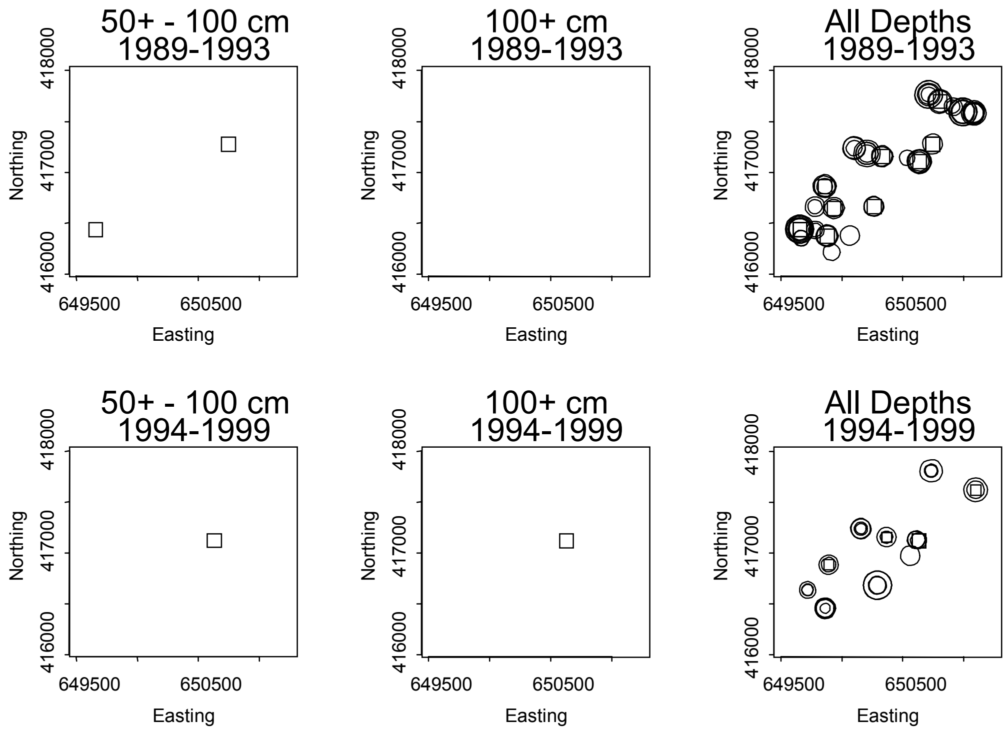

Figure A-27 Sample Locations by Northing and Easting Coordinates During 1989–1993 and 1994–1999, Depth Strata of Little Rapids Deposit Group Upper EE (50 to 100+ cm)

Larger symbols indicate higher concentrations. Circles (○) indicate measured concentrations and squares (□) indicate the detection limit of concentrations below the detection limit. Coordinates are in meters.

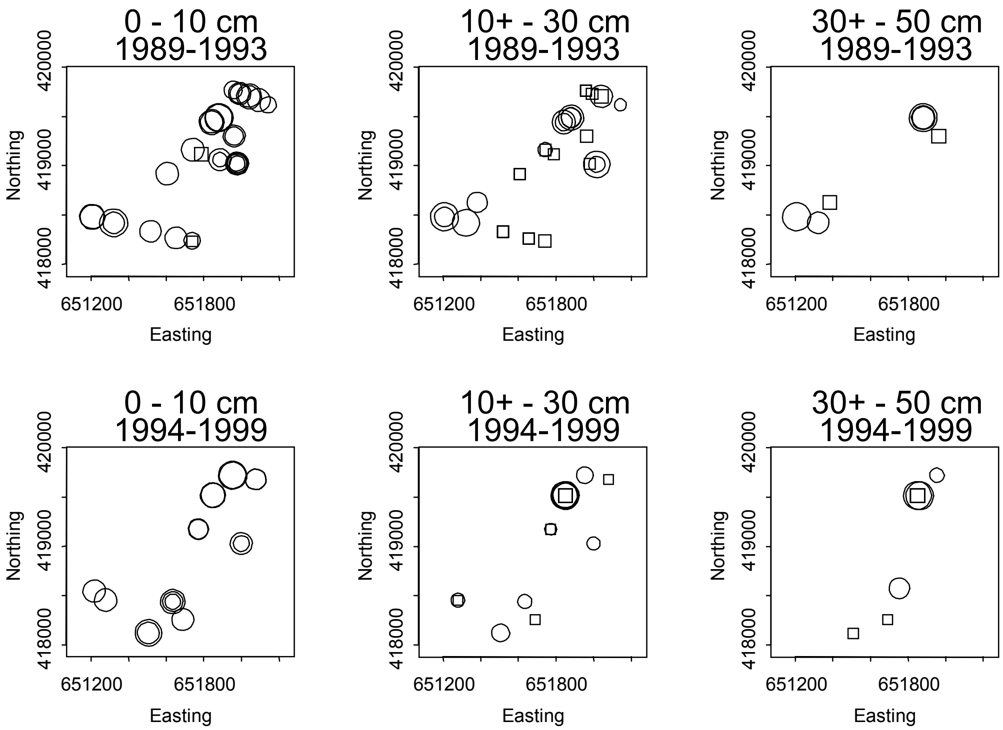

Figure A-28 Sample Locations by Northing and Easting Coordinates During 1989–1993 and 1994–1999, Depth Strata of Little Rapids Deposit Group Lower EE (0 to 50 cm)

Larger symbols indicate higher concentrations. Circles (○) indicate measured concentrations and squares (□) indicate the detection limit of concentrations below the detection limit. Coordinates are in meters.

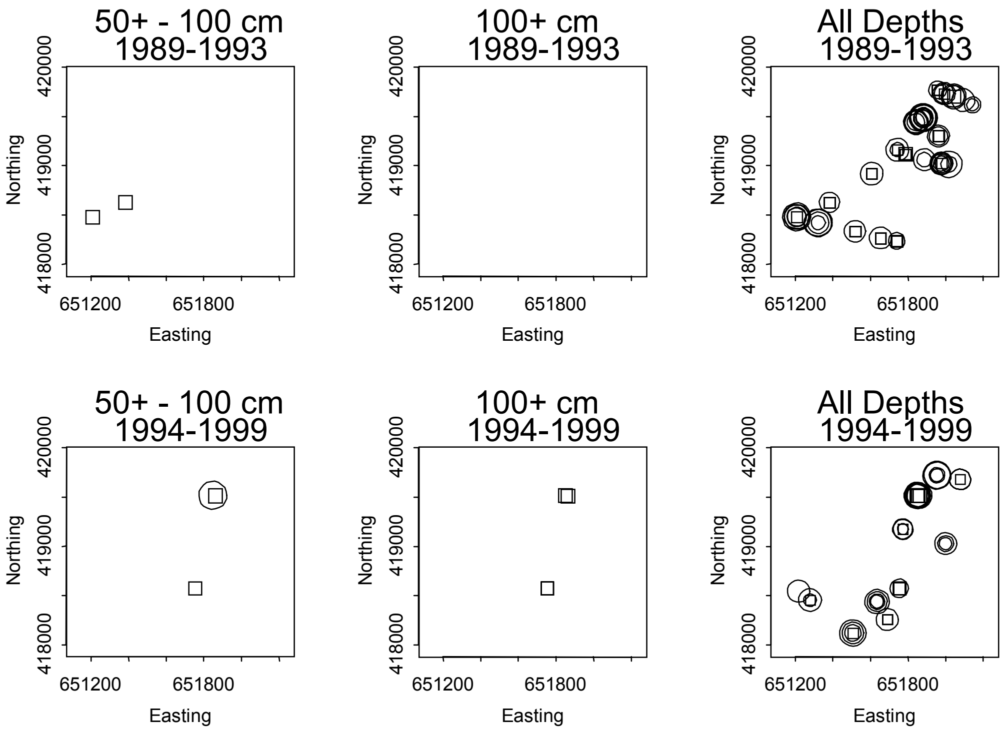

Figure A-29 Sample Locations by Northing and Easting Coordinates During 1989–1993 and 1994–1999, Depth Strata of Little Rapids Deposit Group Lower EE (50 to 100+ cm)

Larger symbols indicate higher concentrations. Circles (○) indicate measured concentrations and squares (□) indicate the detection limit of concentrations below the detection limit. Coordinates are in meters.

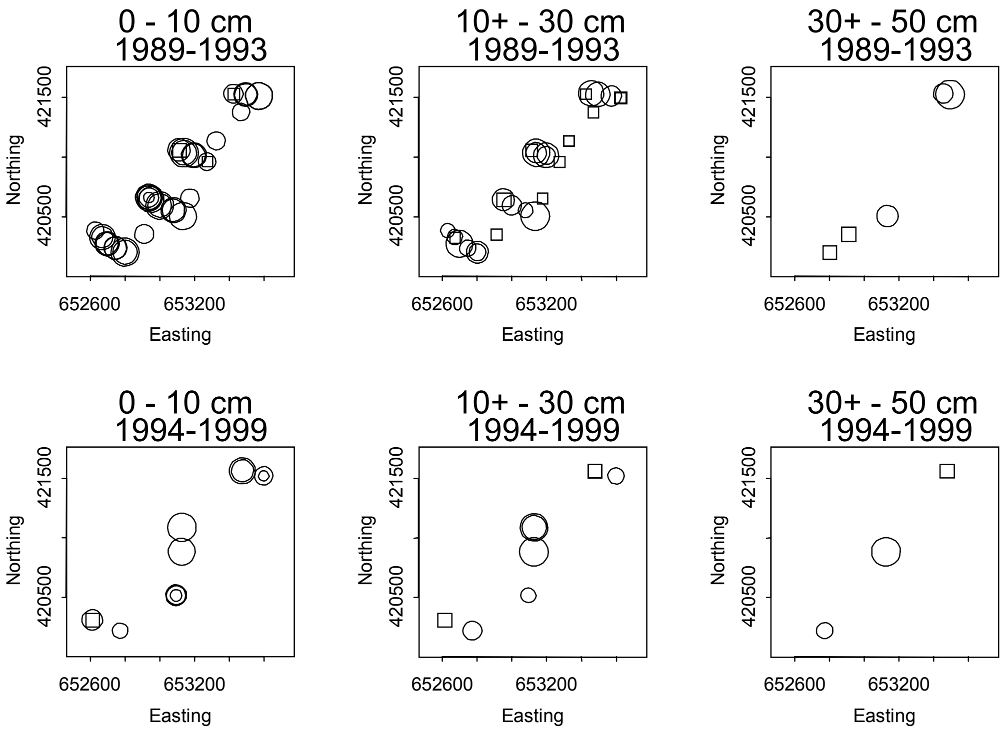

Figure A-30 Sample Locations by Northing and Easting Coordinates During 1989–1993 and 1994–1999, Depth Strata of Little Rapids Deposit Group FF (0 to 50 cm)

Larger symbols indicate higher concentrations. Circles (○) indicate measured concentrations and squares (□) indicate the detection limit of concentrations below the detection limit. Coordinates are in meters.

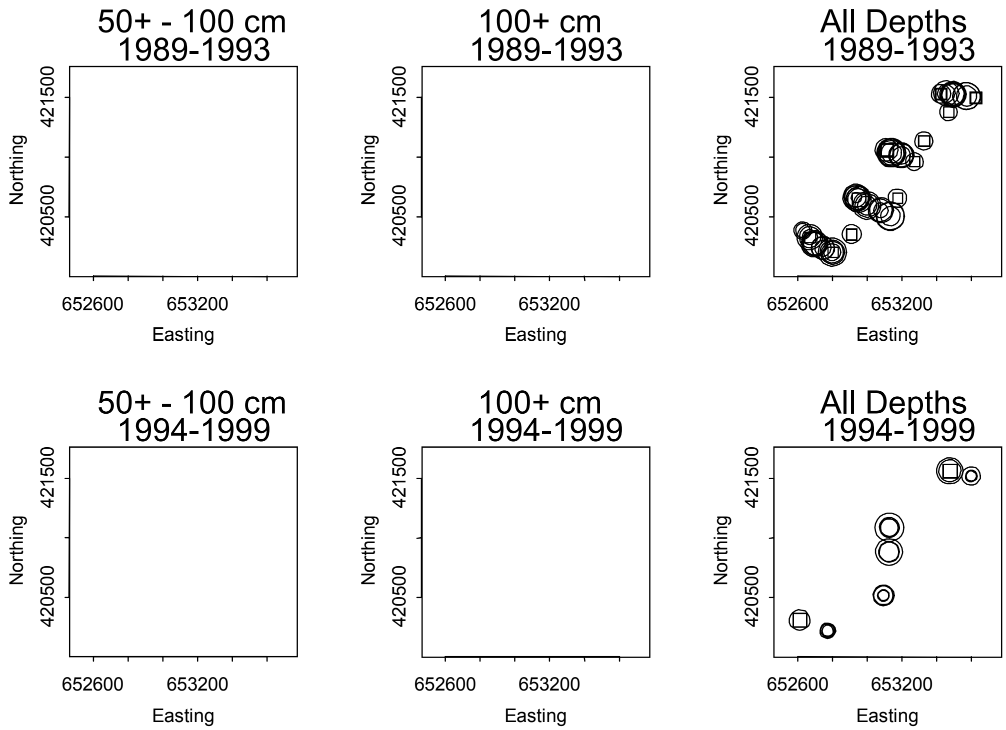

Figure A-31 Sample Locations by Northing and Easting Coordinates During 1989–1993 and 1994–1999, Depth Strata of Little Rapids Deposit Group FF (50 to 100+ cm)

Larger symbols indicate higher concentrations. Circles (○) indicate measured concentrations and squares (□) indicate the detection limit of concentrations below the detection limit. Coordinates are in meters.

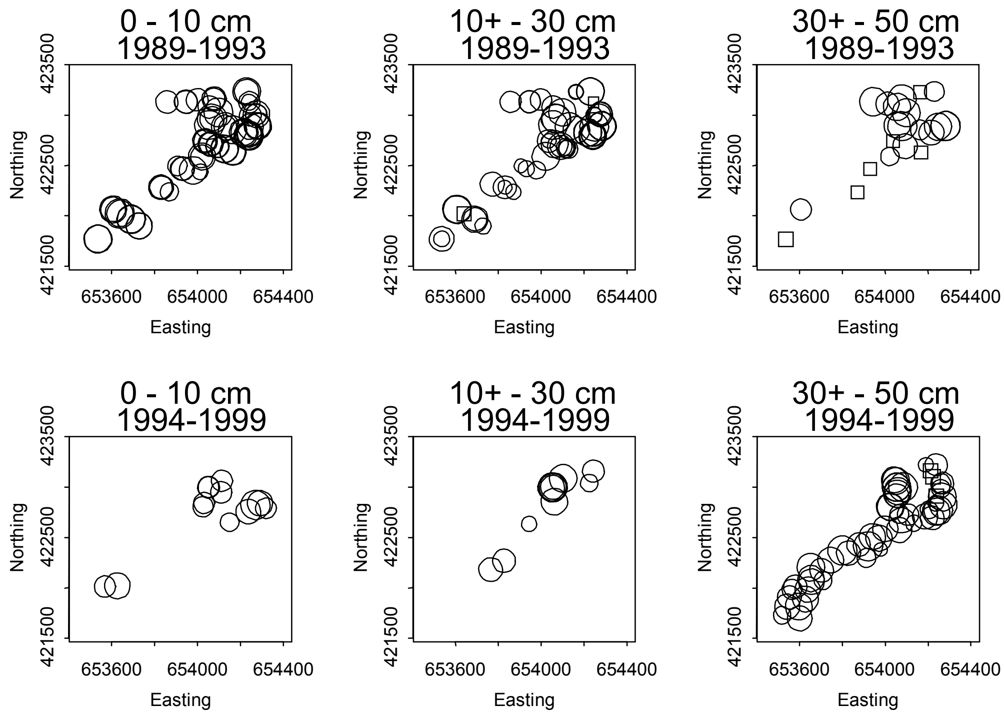

Figure A-32 Sample Locations by Northing and Easting Coordinates During 1989–1993 and 1994–1999, Depth Strata of Little Rapids Deposit Group GGHH (0 to 50 cm)

Larger symbols indicate higher concentrations. Circles (○) indicate measured concentrations and squares (□) indicate the detection limit of concentrations below the detection limit. Coordinates are in meters.

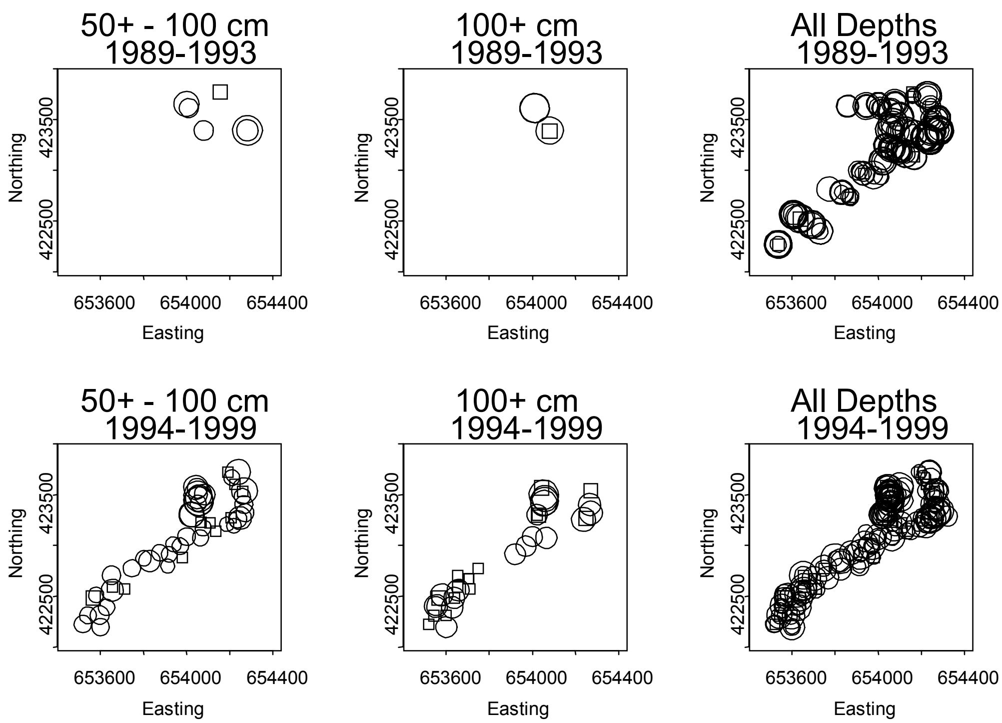

Figure A-33 Sample Locations by Northing and Easting Coordinates During 1989–1993 and 1994–1999, Depth Strata of Little Rapids Deposit Group GGHH (50 to 100+ cm)

Larger symbols indicate higher concentrations. Circles (○) indicate measured concentrations and squares (□) indicate the detection limit of concentrations below the detection limit. Coordinates are in meters.

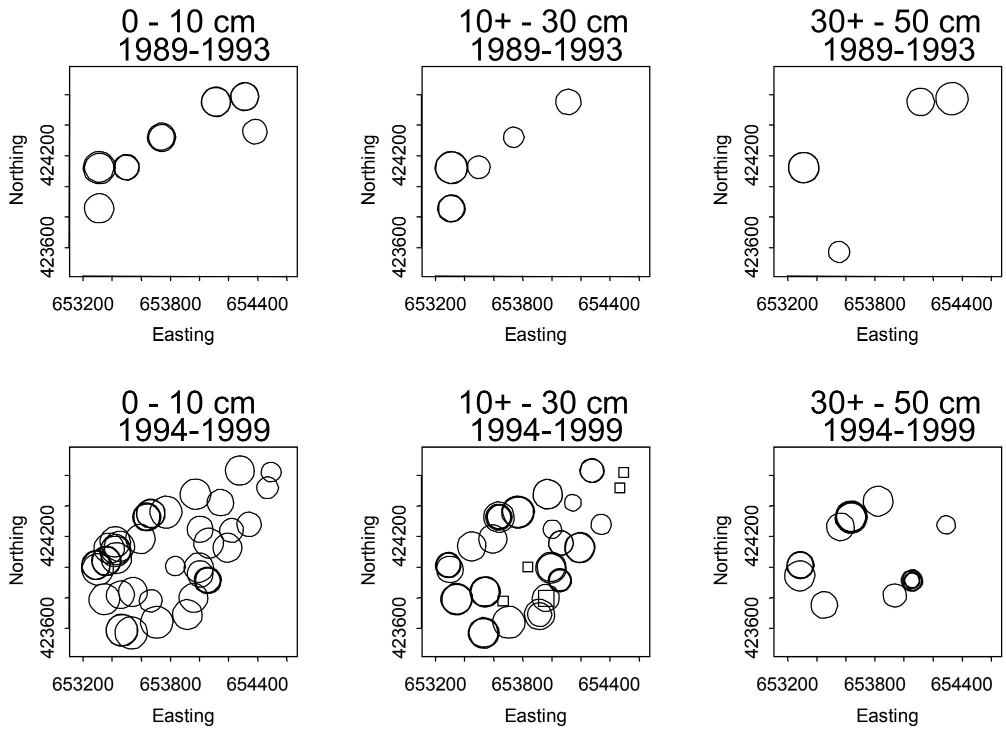

Figure A-34 Sample Locations by Northing and Easting Coordinates During 1989–1993 and 1994–1999, Depth Strata of De Pere SMU Group 2025 (0 to 50 cm)

Larger symbols indicate higher concentrations. Circles (○) indicate measured concentrations and squares (□) indicate the detection limit of concentrations below the detection limit. Coordinates are in meters.

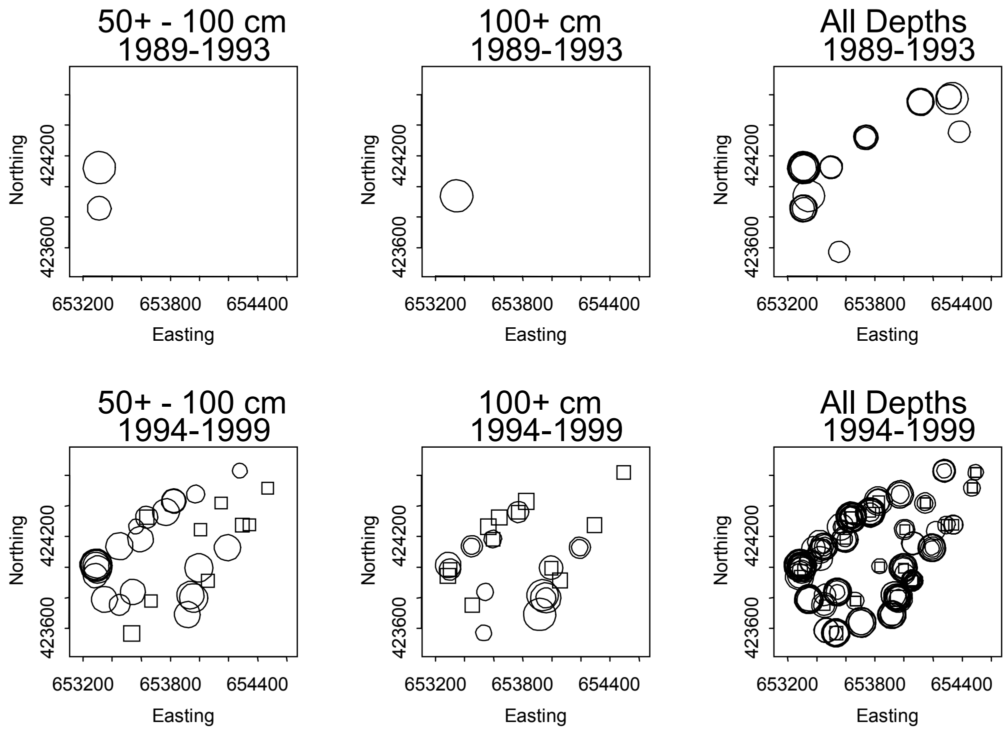

Figure A-35 Sample Locations by Northing and Easting Coordinates During 1989–1993 and 1994–1999, Depth Strata of De Pere SMU Group 2025 (50 to 100+ cm)

Larger symbols indicate higher concentrations. Circles (○) indicate measured concentrations and squares (□) indicate the detection limit of concentrations below the detection limit. Coordinates are in meters.

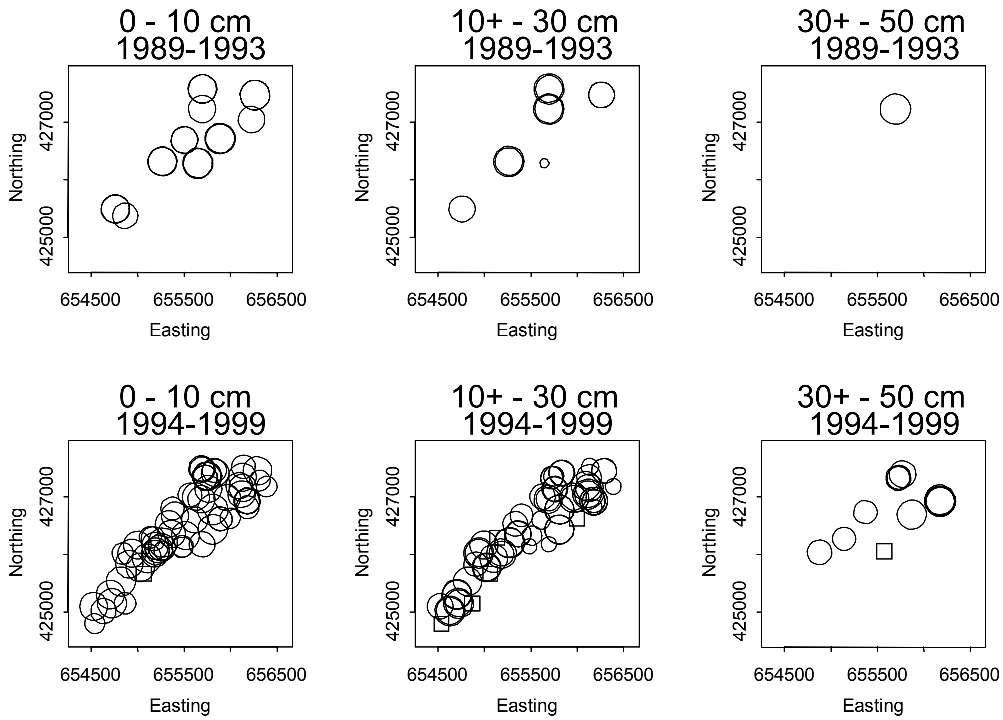

Figure A-36 Sample Locations by Northing and Easting Coordinates During 1989–1993 and 1994–1999, Depth Strata of De Pere SMU Group 2649 (0 to 50 cm)

Larger symbols indicate higher concentrations. Circles (○) indicate measured concentrations and squares (□) indicate the detection limit of concentrations below the detection limit. Coordinates are in meters.

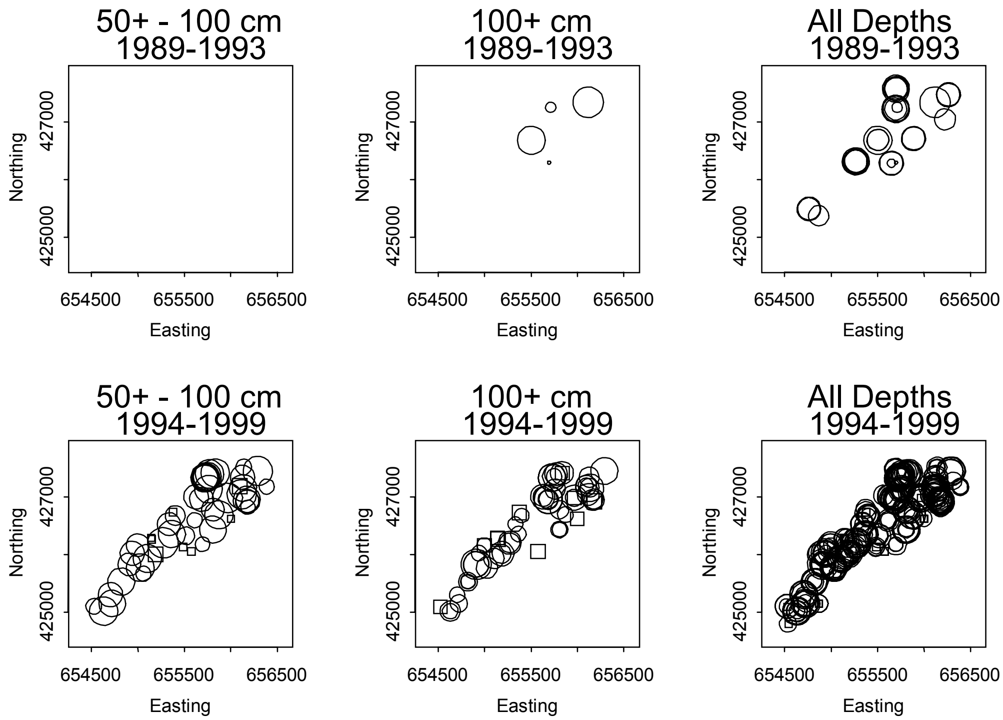

Figure A-37 Sample Locations by Northing and Easting Coordinates During 1989–1993 and 1994–1999, Depth Strata of De Pere SMU Group 2649 (50 to 100+ cm)

Larger symbols indicate higher concentrations. Circles (○) indicate measured concentrations and squares (□) indicate the detection limit of concentrations below the detection limit. Coordinates are in meters.

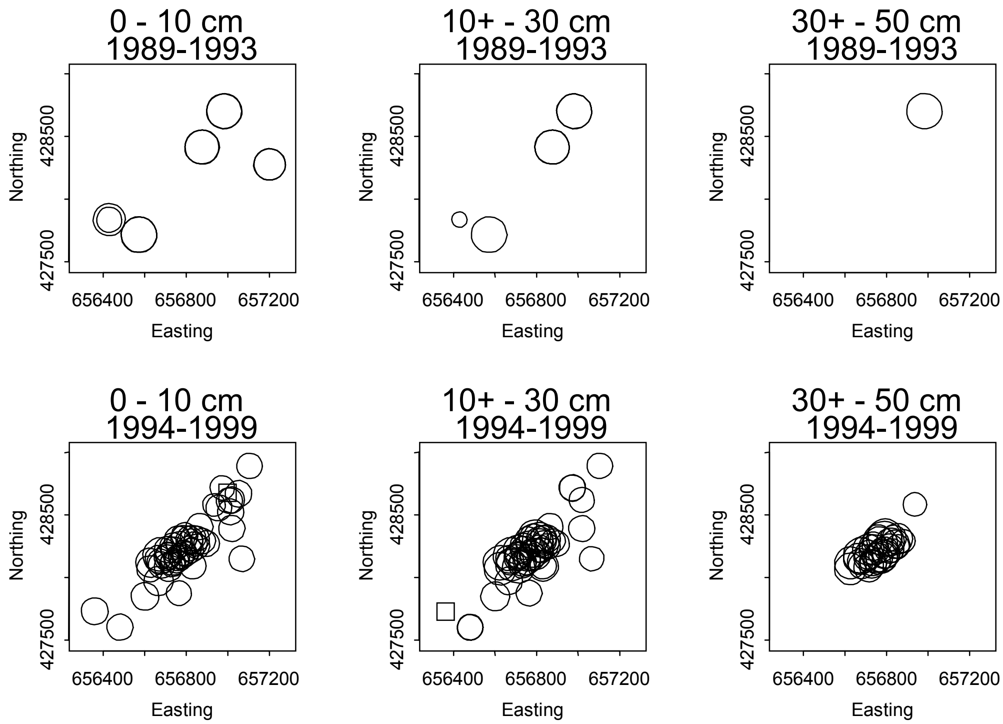

Figure A-38 Sample Locations by Northing and Easting Coordinates During 1989–1993 and 1994–1999, Depth Strata of De Pere SMU Group 5067 (0 to 50 cm)

Larger symbols indicate higher concentrations. Circles (○) indicate measured concentrations and squares (□) indicate the detection limit of concentrations below the detection limit. Coordinates are in meters.

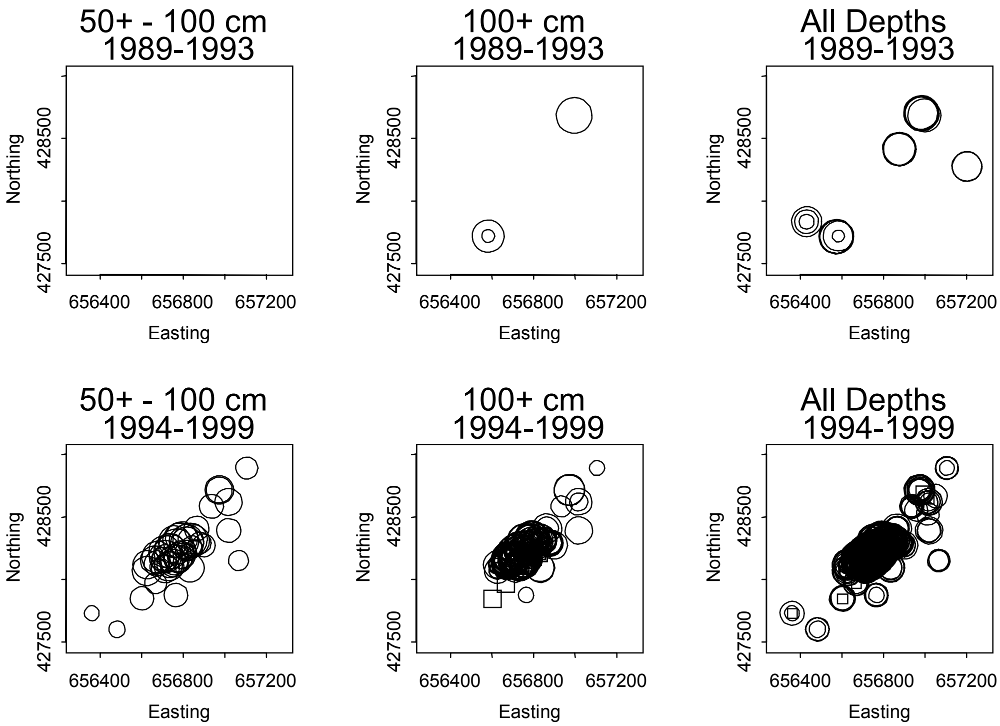

Figure A-39 Sample Locations by Northing and Easting Coordinates During 1989–1993 and 1994–1999, Depth Strata of De Pere SMU Group 5067 (50 to 100+ cm)

Larger symbols indicate higher concentrations. Circles (○) indicate measured concentrations and squares (□) indicate the detection limit of concentrations below the detection limit. Coordinates are in meters.

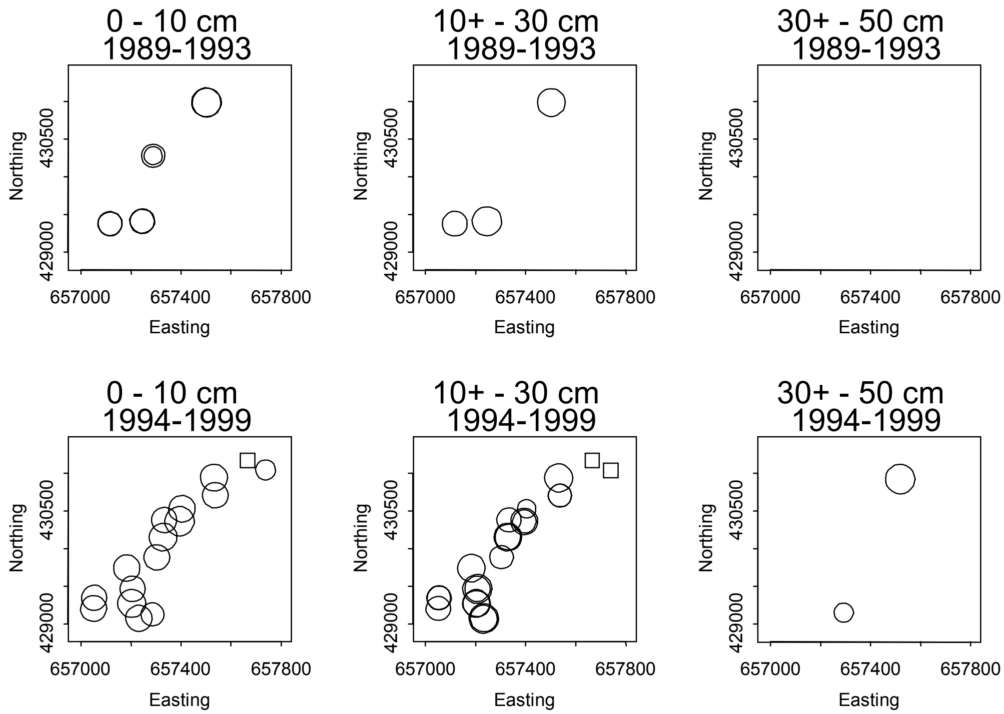

Figure A-40 Sample Locations by Northing and Easting Coordinates During 1989–1993 and 1994–1999, Depth Strata of De Pere SMU Group 6891 (0 to 50 cm)

Larger symbols indicate higher concentrations. Circles (○) indicate measured concentrations and squares (□) indicate the detection limit of concentrations below the detection limit. Coordinates are in meters.

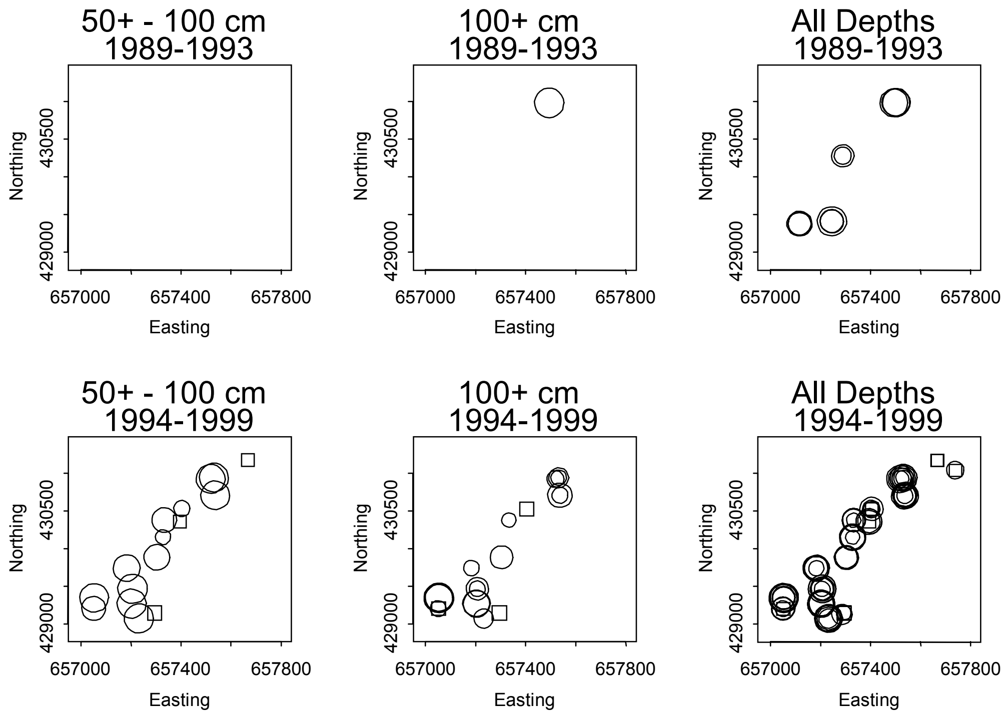

Figure A-41 Sample Locations by Northing and Easting Coordinates During 1989–1993 and 1994–1999, Depth Strata of De Pere SMU Group 6891 (50 to 100+ cm)

Larger symbols indicate higher concentrations. Circles (○) indicate measured concentrations and squares (□) indicate the detection limit of concentrations below the detection limit. Coordinates are in meters.

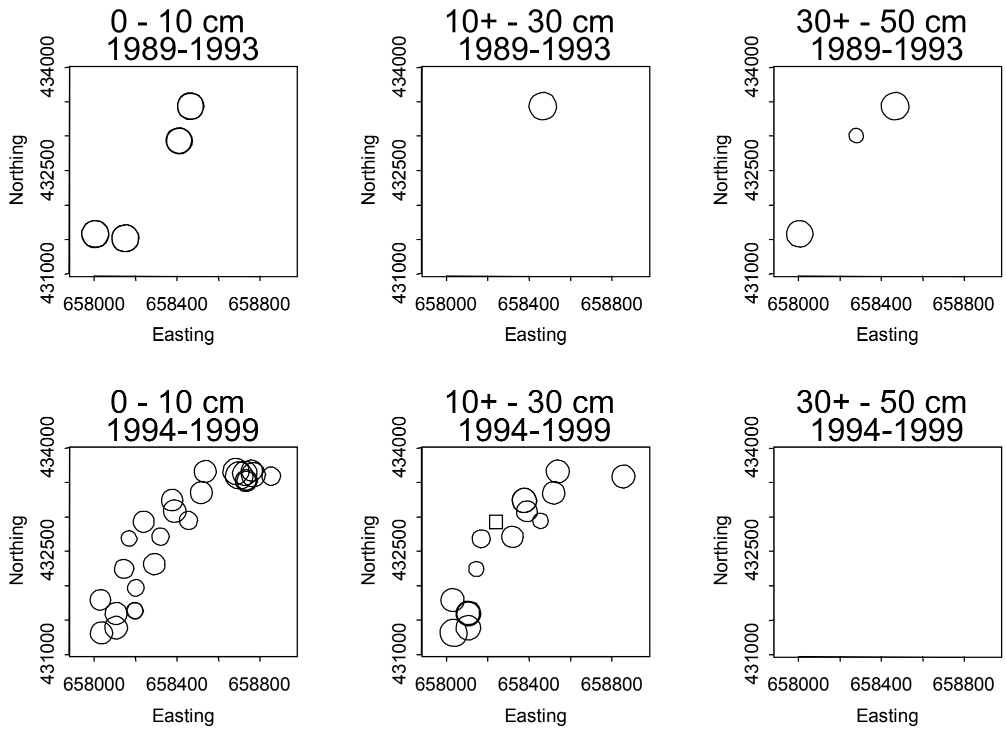

Figure A-42 Sample Locations by Northing and Easting Coordinates During 1989–1993 and 1994–1999, Depth Strata of De Pere SMU Group 92115 (0 to 50 cm)

Larger symbols indicate higher concentrations. Circles (○) indicate measured concentrations and squares (□) indicate the detection limit of concentrations below the detection limit. Coordinates are in meters.

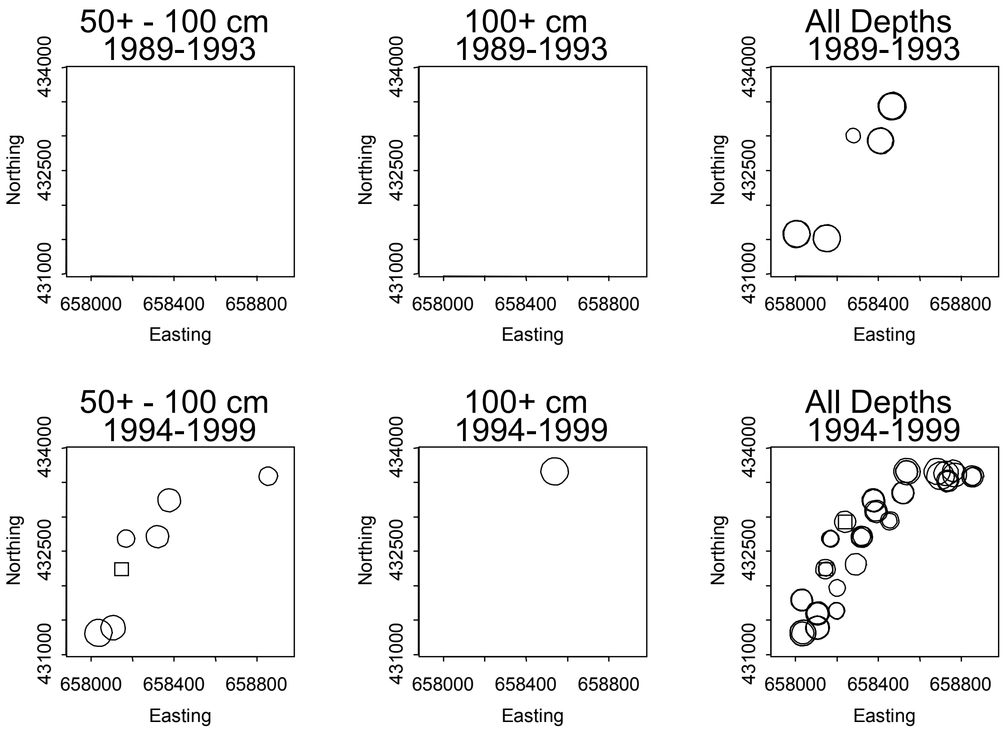

Figure A-43 Sample Locations by Northing and Easting Coordinates During 1989–1993 and 1994–1999, Depth Strata of De Pere SMU Group 92115 (50 to 100+ cm)

Larger symbols indicate higher concentrations. Circles (○) indicate measured concentrations and squares (□) indicate the detection limit of concentrations below the detection limit. Coordinates are in meters.

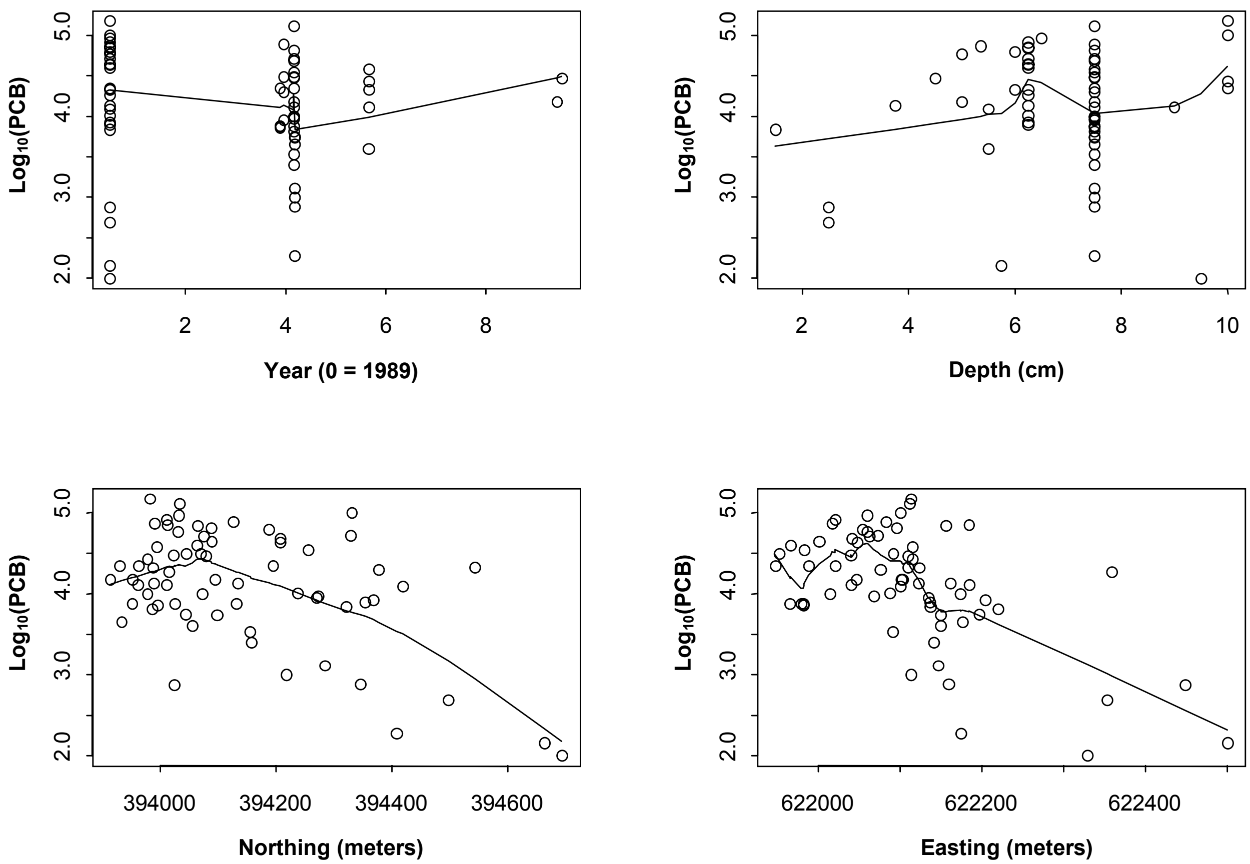

Figure A-44 Log_{10} PCB Concentration versus Time, Depth, Northing, and Easting for Little Lake Butte des Morts Deposit Group AB (0 to 10 cm) Including Fitted Smoothed Line

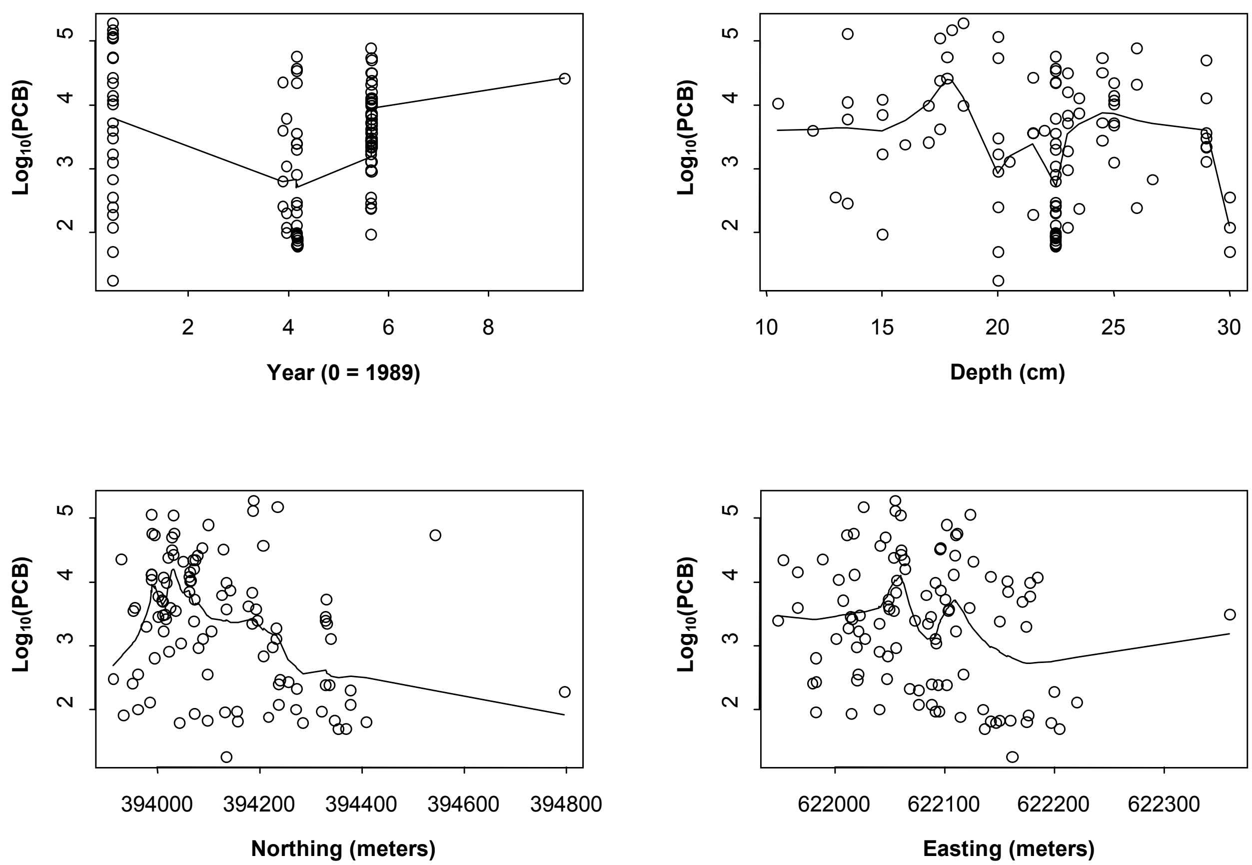

Figure A-45 Log$_{10}$ PCB Concentration versus Time, Depth, Northing, and Easting for Little Lake Butte des Morts Deposit Group AB (10 to 30 cm) Including Fitted Smoothed Line

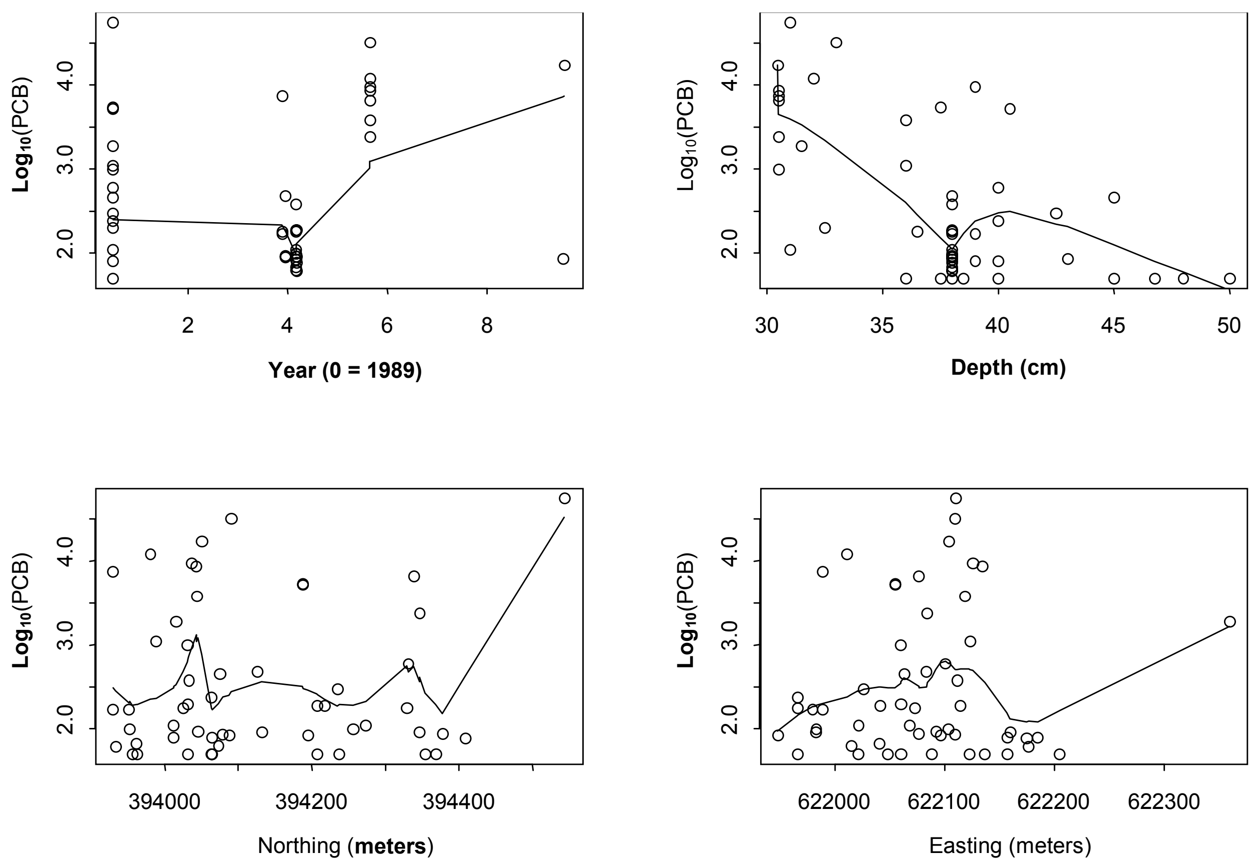

Figure A-46 Log_{10} PCB Concentration versus Time, Depth, Northing, and Easting for Little Lake Butte des Morts Deposit Group AB (30 to 50 cm) Including Fitted Smoothed Line

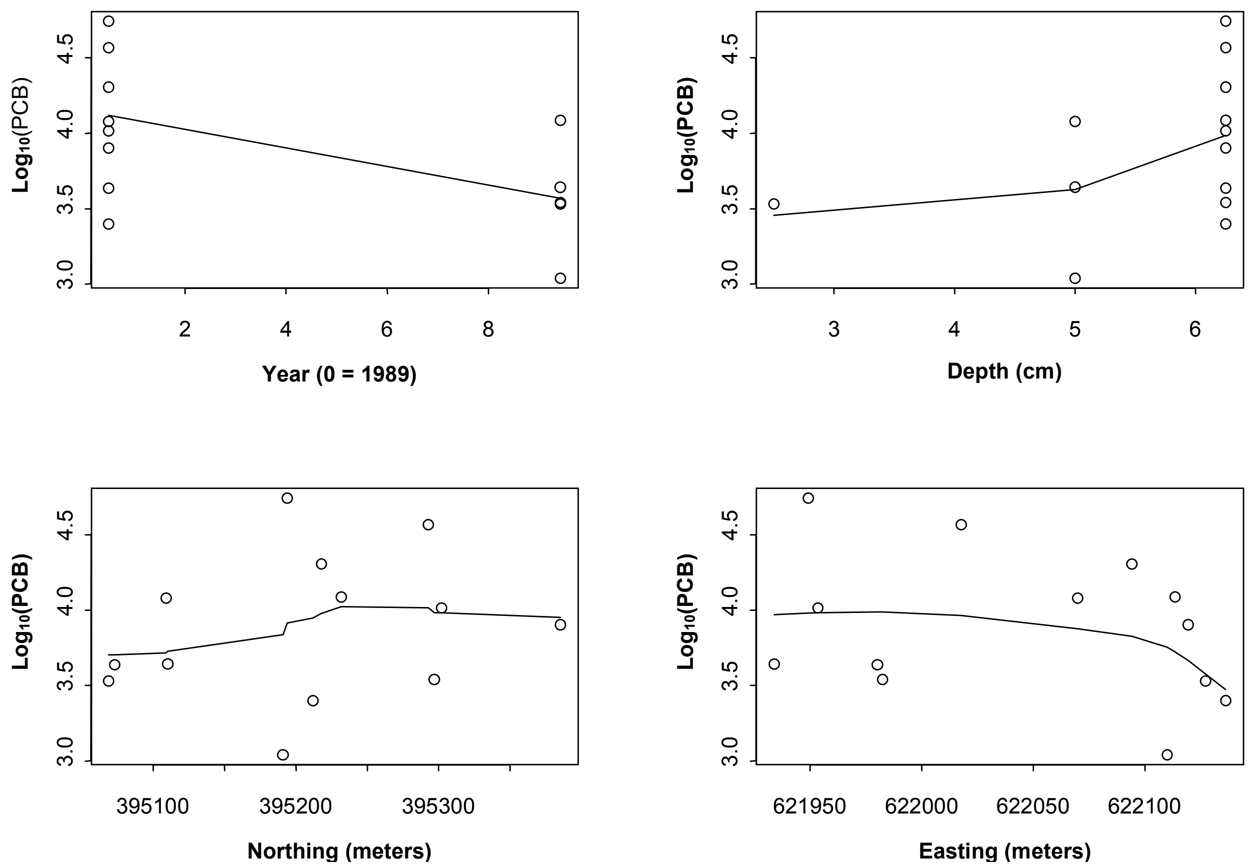

Figure A-47 Log_{10} PCB Concentration versus Time, Depth, Northing, and Easting for Little Lake Butte des Morts Deposit Group C (0 to 10 cm) Including Fitted Smoothed Line

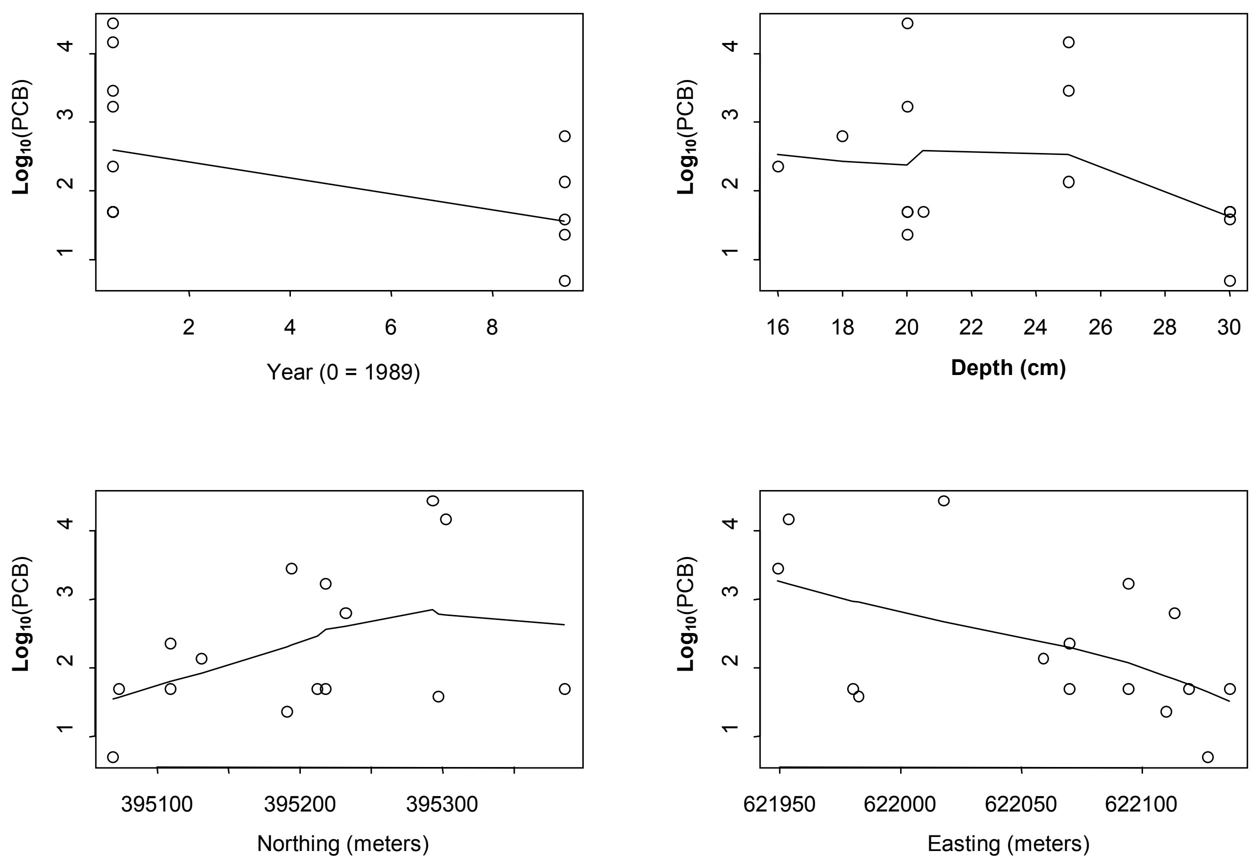

Figure A-48 Log$_{10}$ PCB Concentration versus Time, Depth, Northing, and Easting for Little Lake Butte des Morts Deposit Group C (10 to 30 cm) Including Fitted Smoothed Line

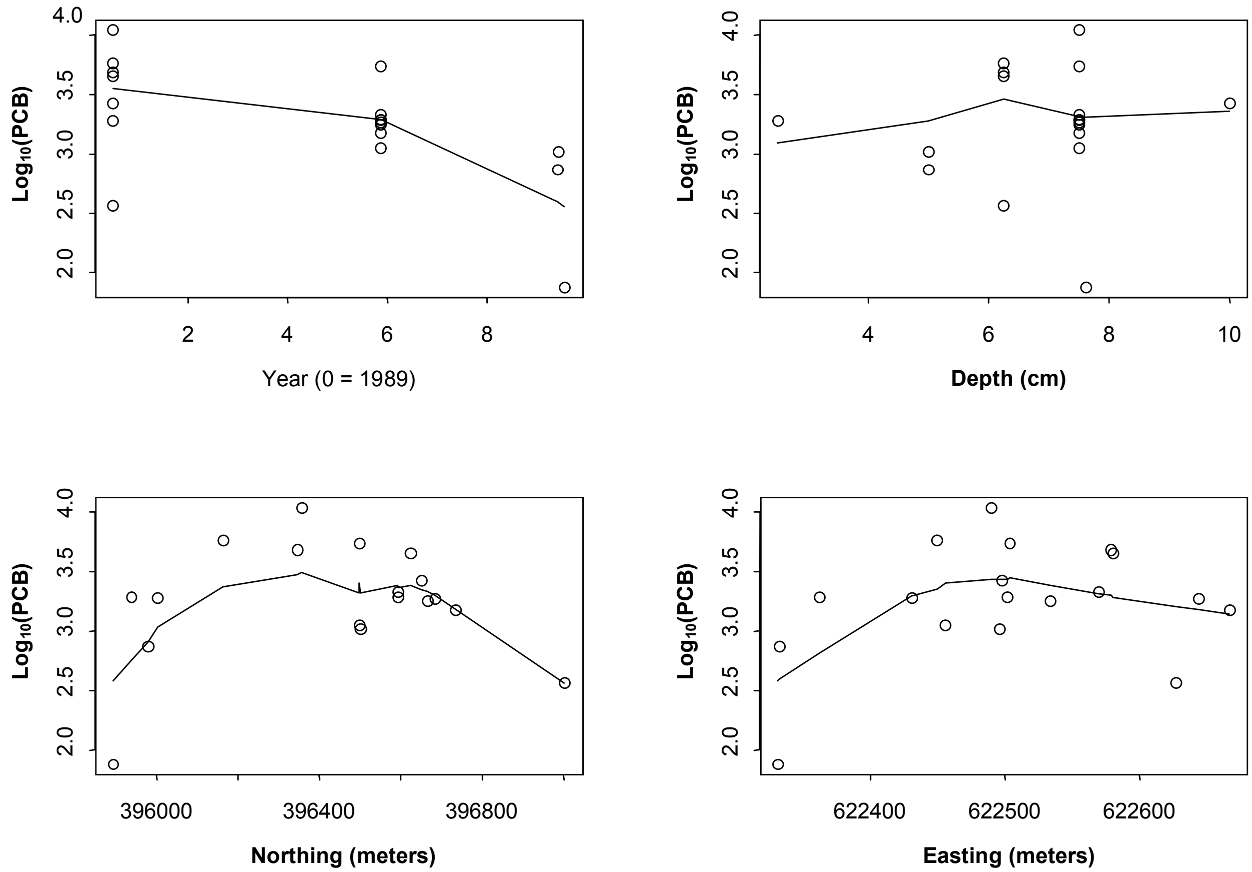

Figure A-49 Log_{10} PCB Concentration versus Time, Depth, Northing, and Easting for Little Lake Butte des Morts Deposit Group D (0 to 10 cm) Including Fitted Smoothed Line

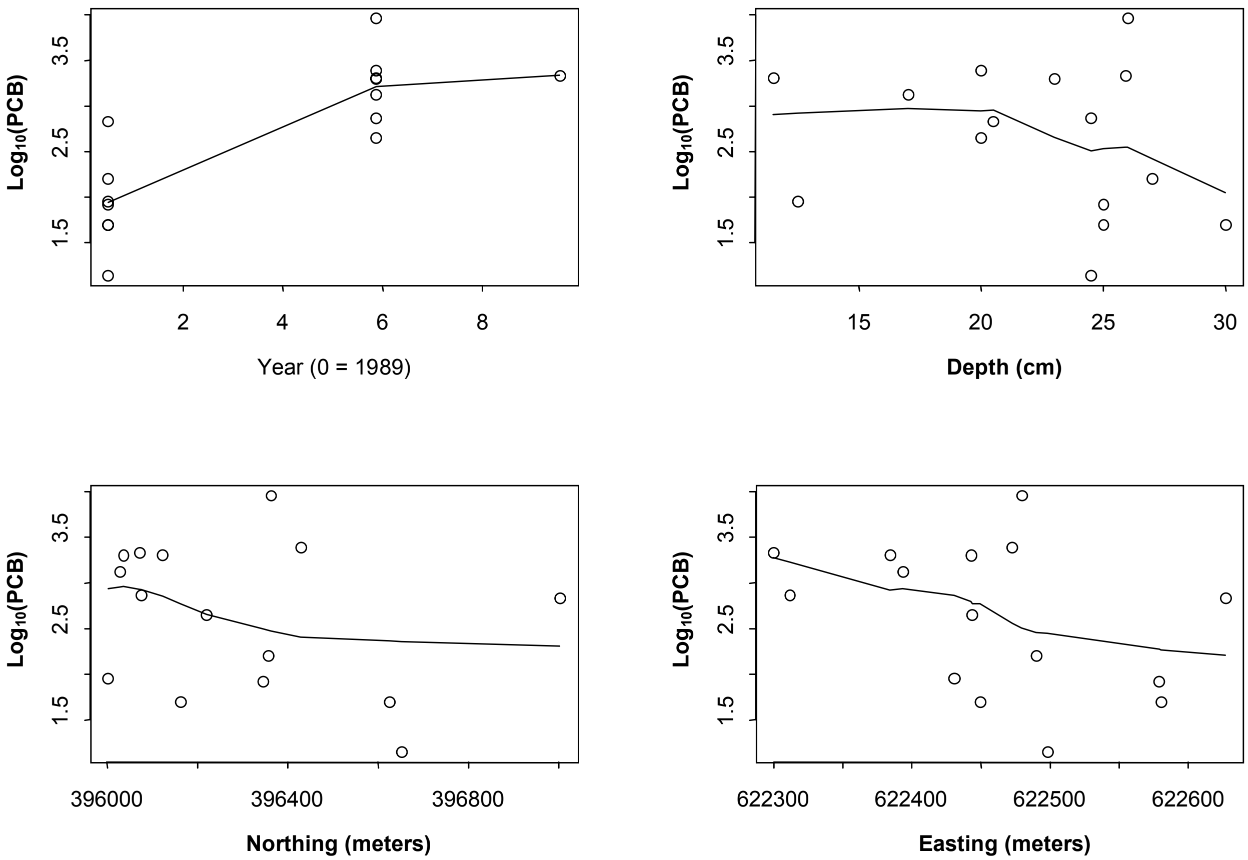

Figure A-50 Log$_{10}$ PCB Concentration versus Time, Depth, Northing, and Easting for Little Lake Butte des Morts Deposit Group D (10 to 30 cm) Including Fitted Smoothed Line

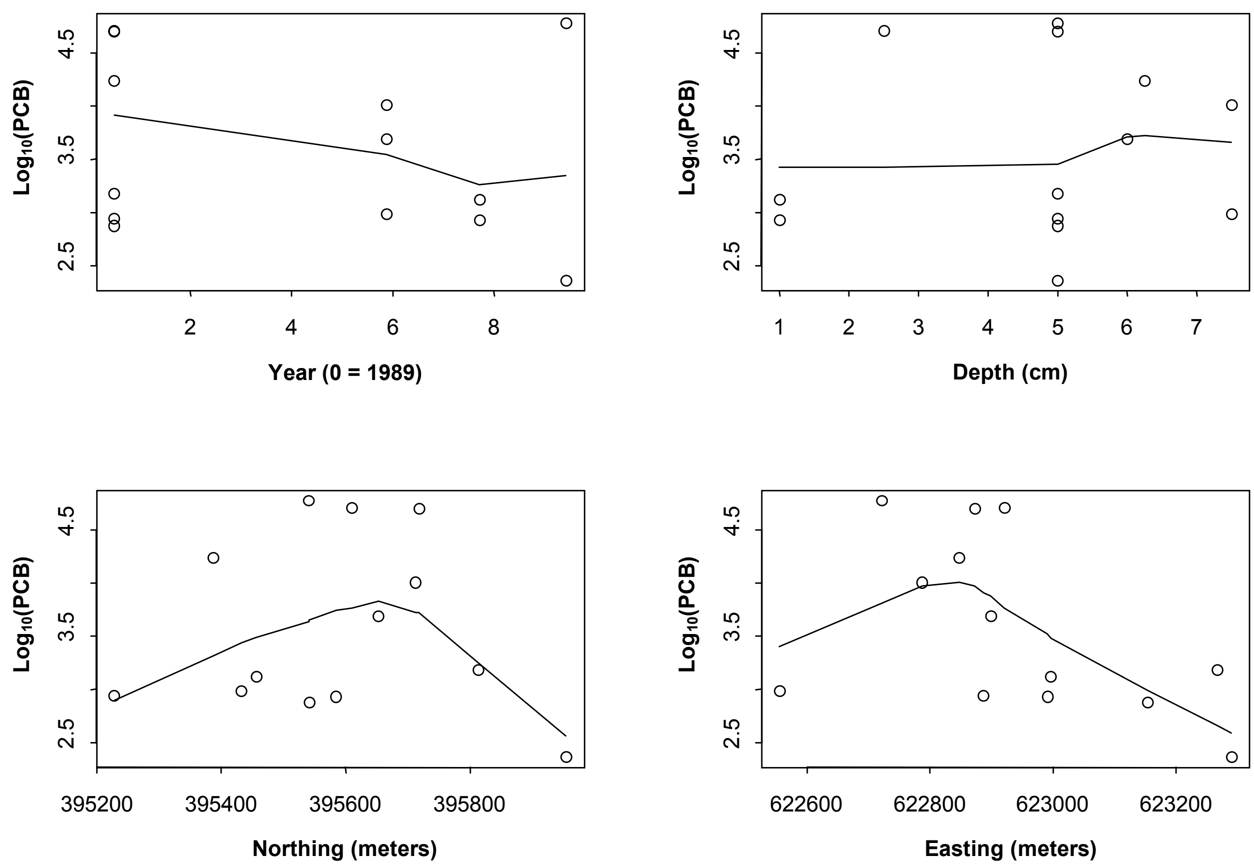

Figure A-51 Log_{10} PCB Concentration versus Time, Depth, Northing, and Easting for Little Lake Butte des Morts Deposit Group POG (0 to 10 cm) Including Fitted Smoothed Line

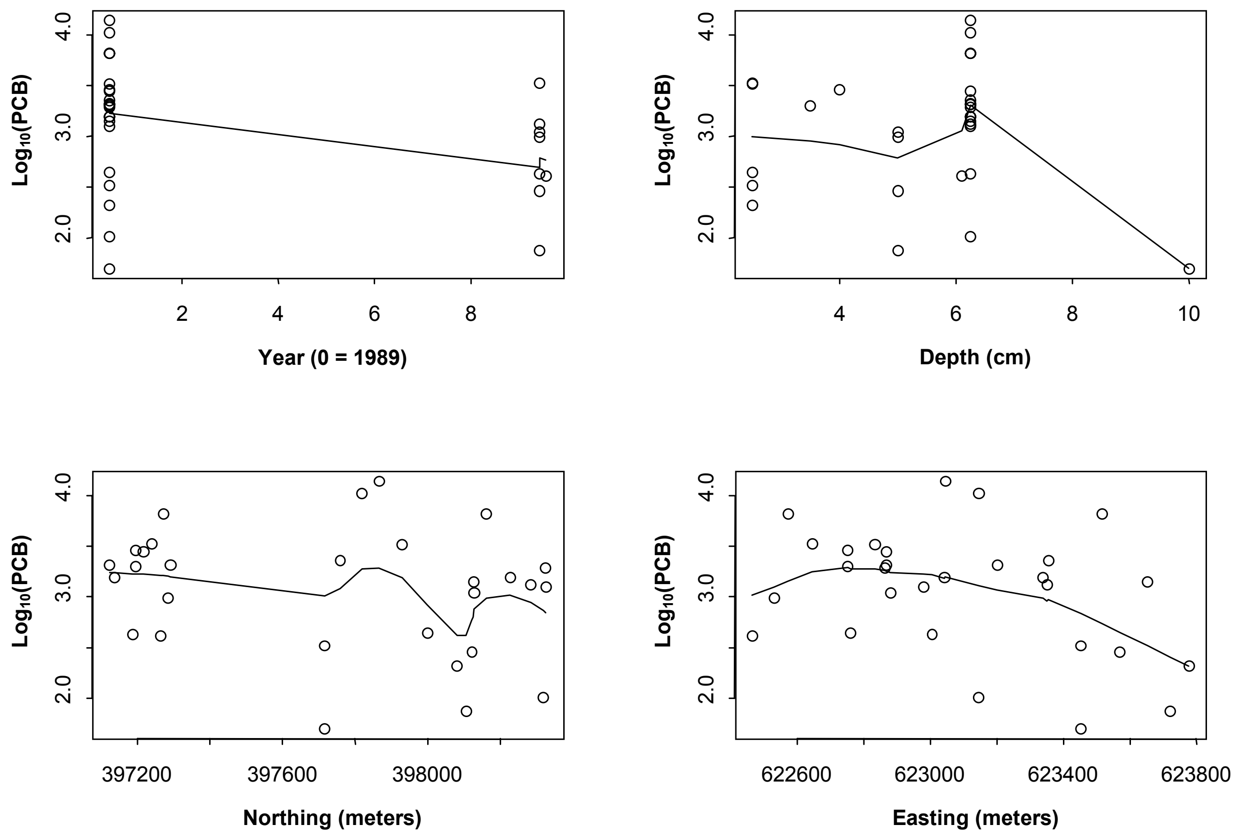

Figure A-52 Log$_{10}$ PCB Concentration versus Time, Depth, Northing, and Easting for Little Lake Butte des Morts Deposit Group F (0 to 10 cm) Including Fitted Smoothed Line

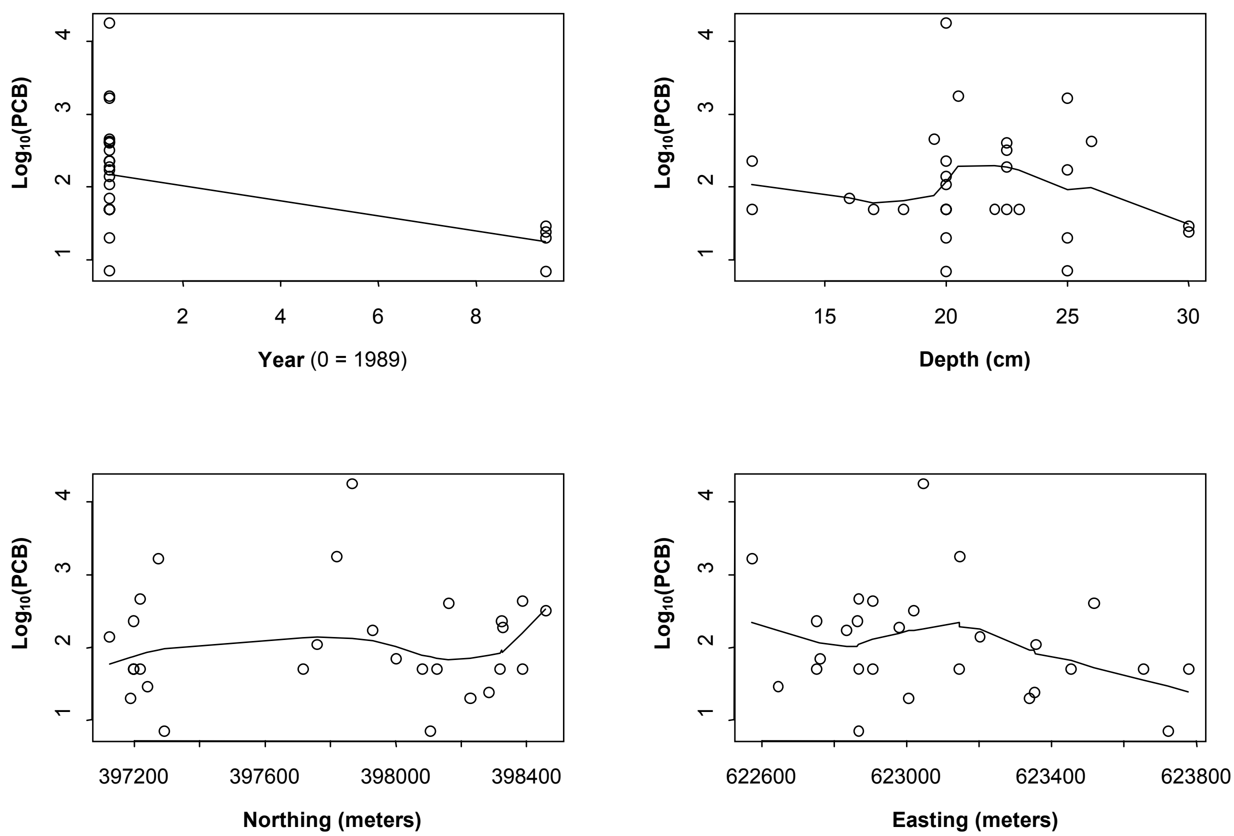

Figure A-53 Log$_{10}$ PCB Concentration versus Time, Depth, Northing, and Easting for Little Lake Butte des Morts Deposit Group F (10 to 30 cm) Including Fitted Smoothed Line

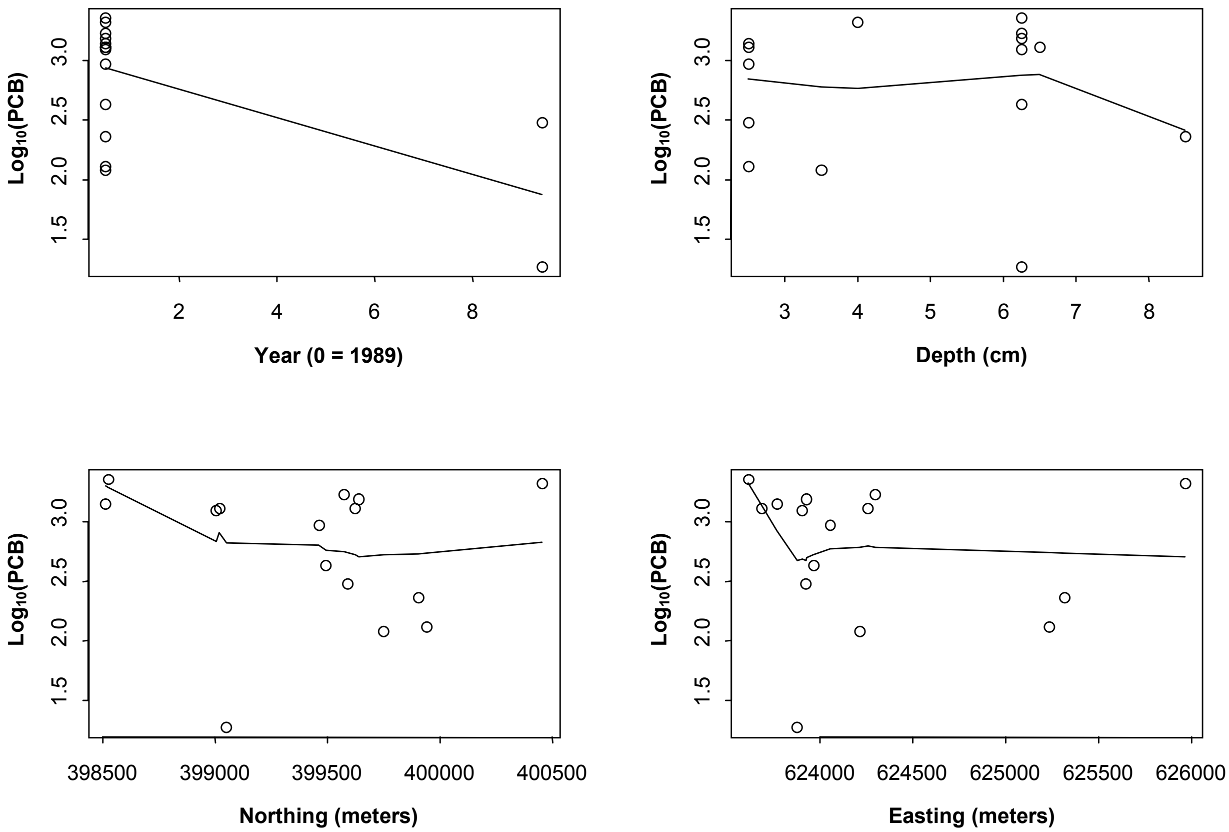

Figure A-54 Log$_{10}$ PCB Concentration versus Time, Depth, Northing, and Easting for Little Lake Butte des Morts Deposit Group GH (0 to 10 cm) Including Fitted Smoothed Line

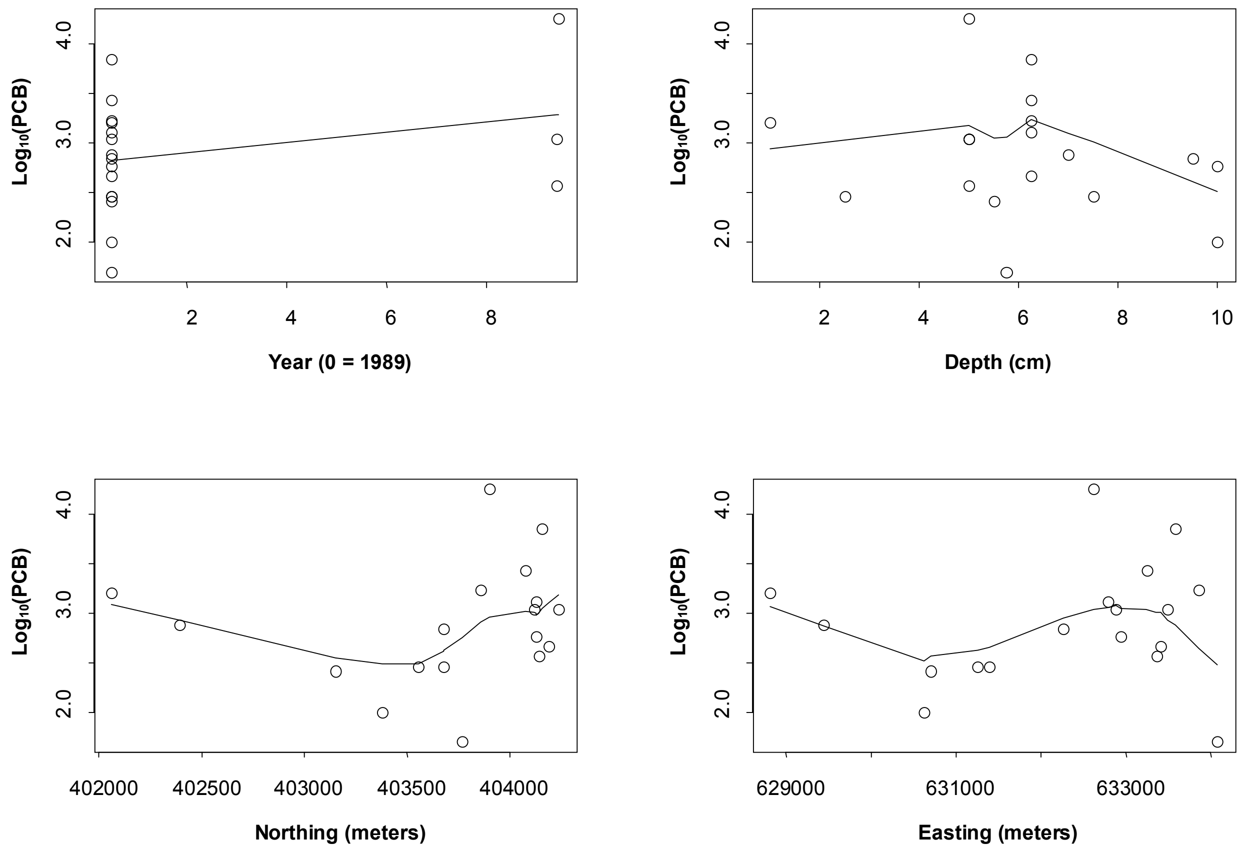

Figure A-55 Log$_{10}$ PCB Concentration versus Time, Depth, Northing, and Easting for Appleton Deposit Group IMOR (0 to 10 cm) Including Fitted Smoothed Line

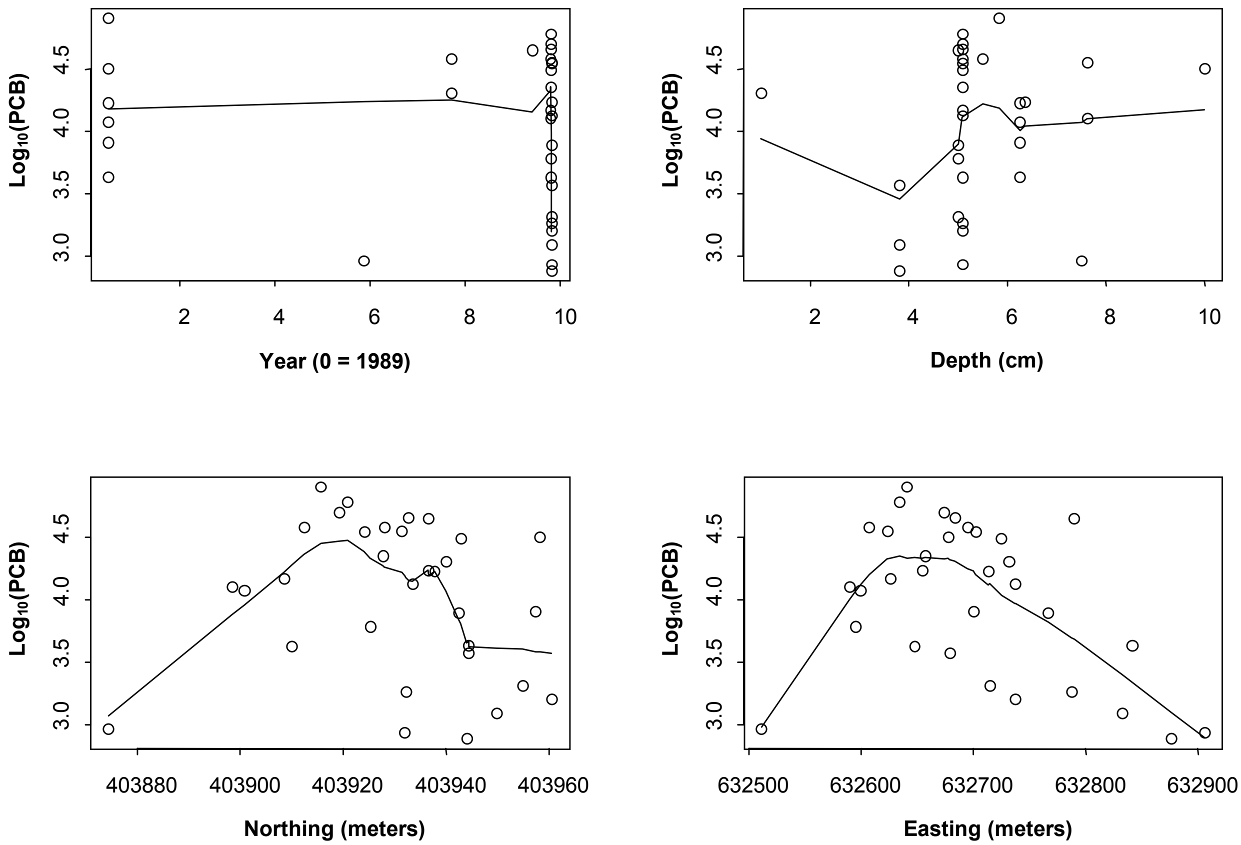

Figure A-56 Log_{10} PCB Concentration versus Time, Depth, Northing, and Easting for Appleton Deposit Group N Before Demonstration Project (0 to 10 cm) Including Fitted Smoothed Line

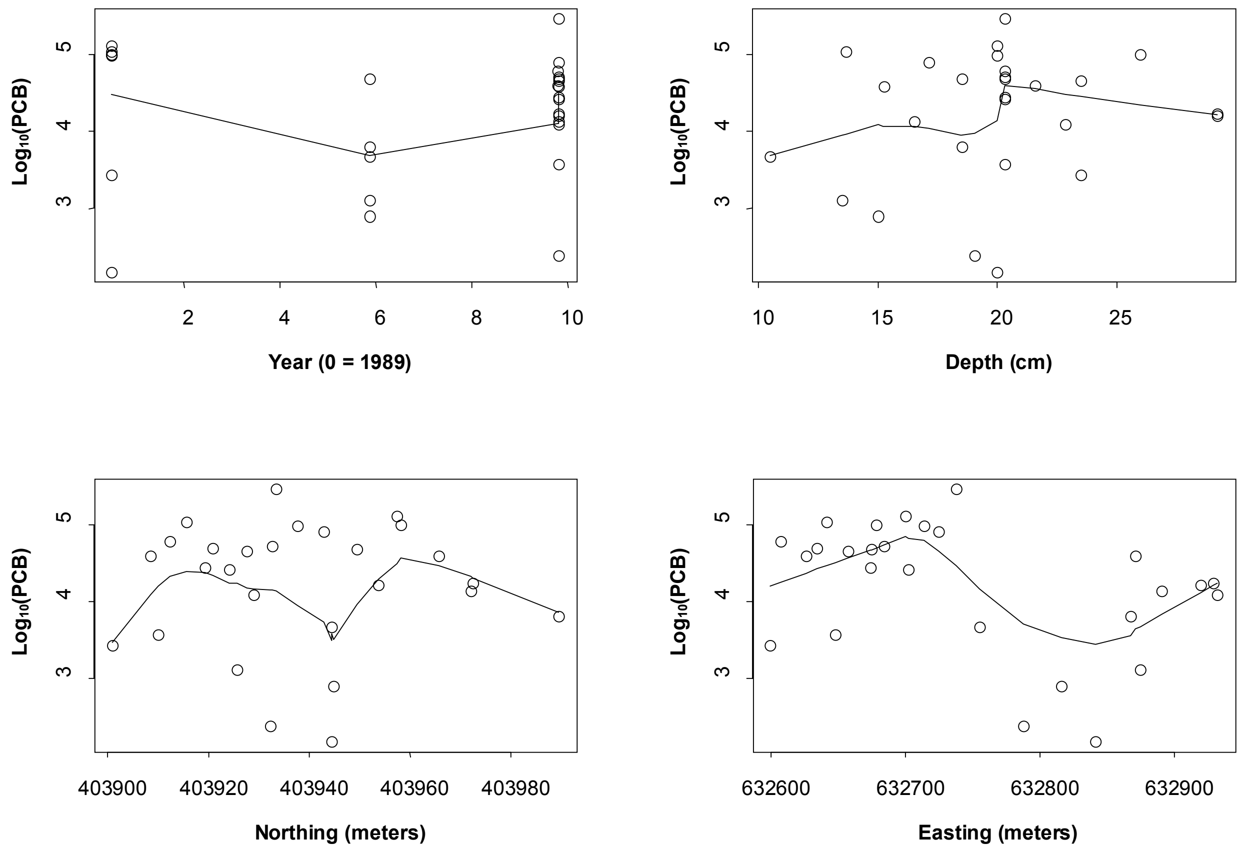

Figure A-57 Log$_{10}$ PCB Concentration versus Time, Depth, Northing, and Easting for Appleton Deposit Group N Before Demonstration Project (10 to 30 cm) Including Fitted Smoothed Line

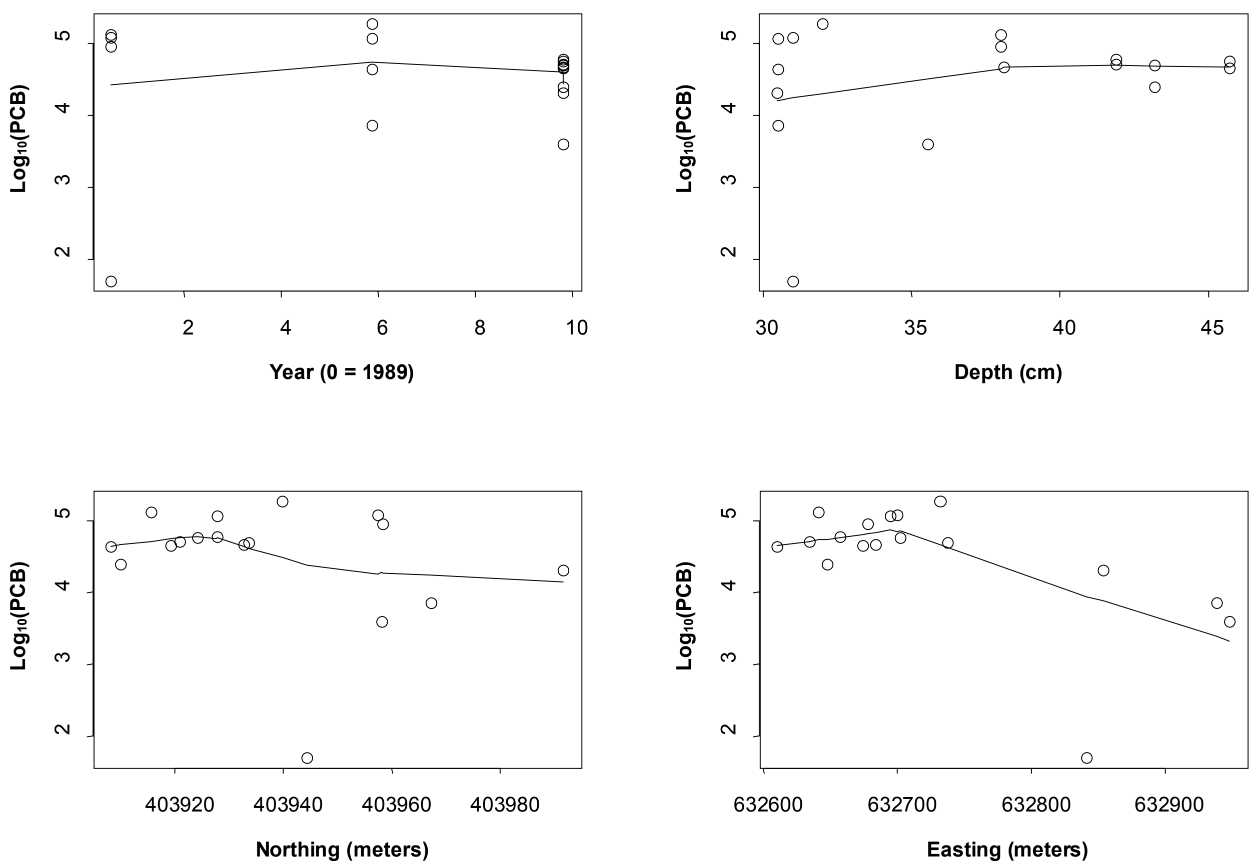

Figure A-58 Log_{10} PCB Concentration versus Time, Depth, Northing, and Easting for Appleton Deposit Group N Before Demonstration Project (30 to 50 cm) Including Fitted Smoothed Line

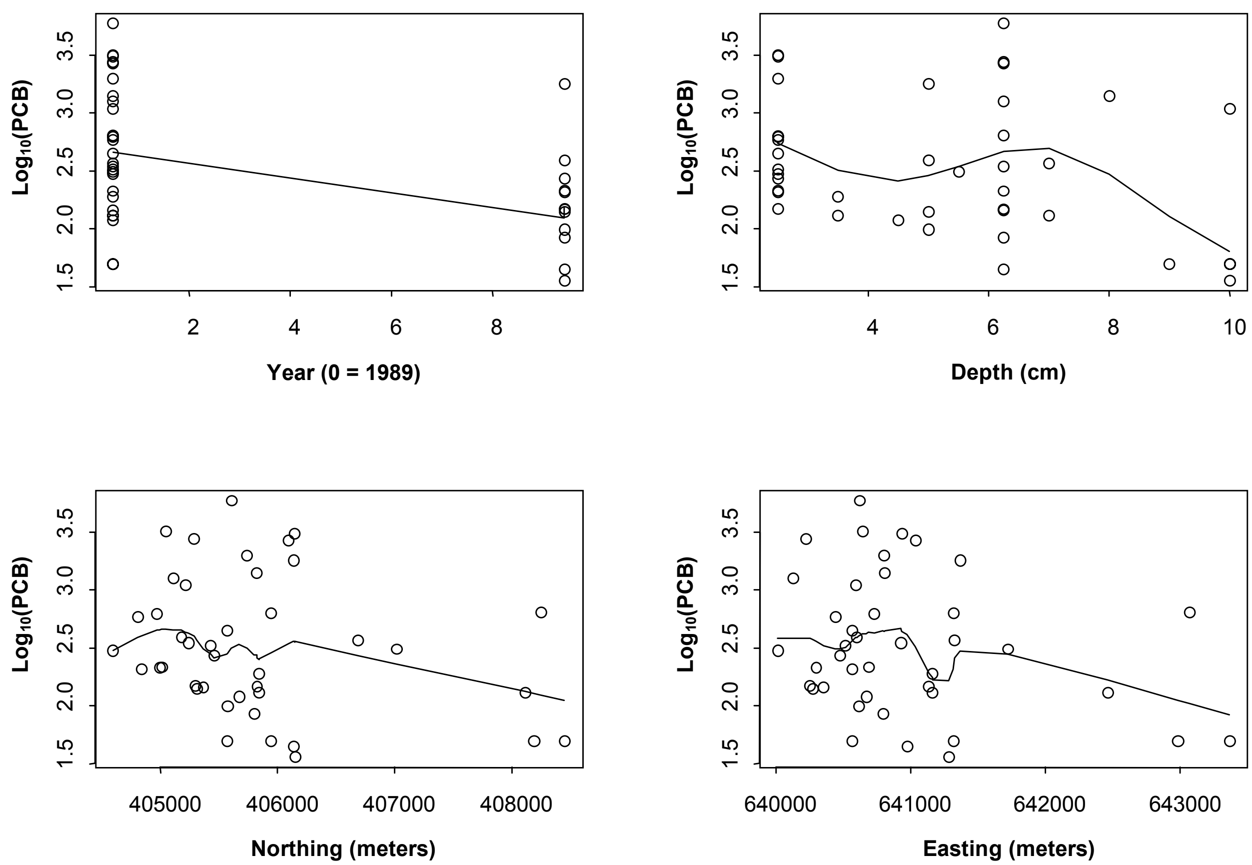

Figure A-59 Log_{10} PCB Concentration versus Time, Depth, Northing, and Easting for Appleton Deposit Group VCC (0 to 10 cm) Including Fitted Smoothed Line

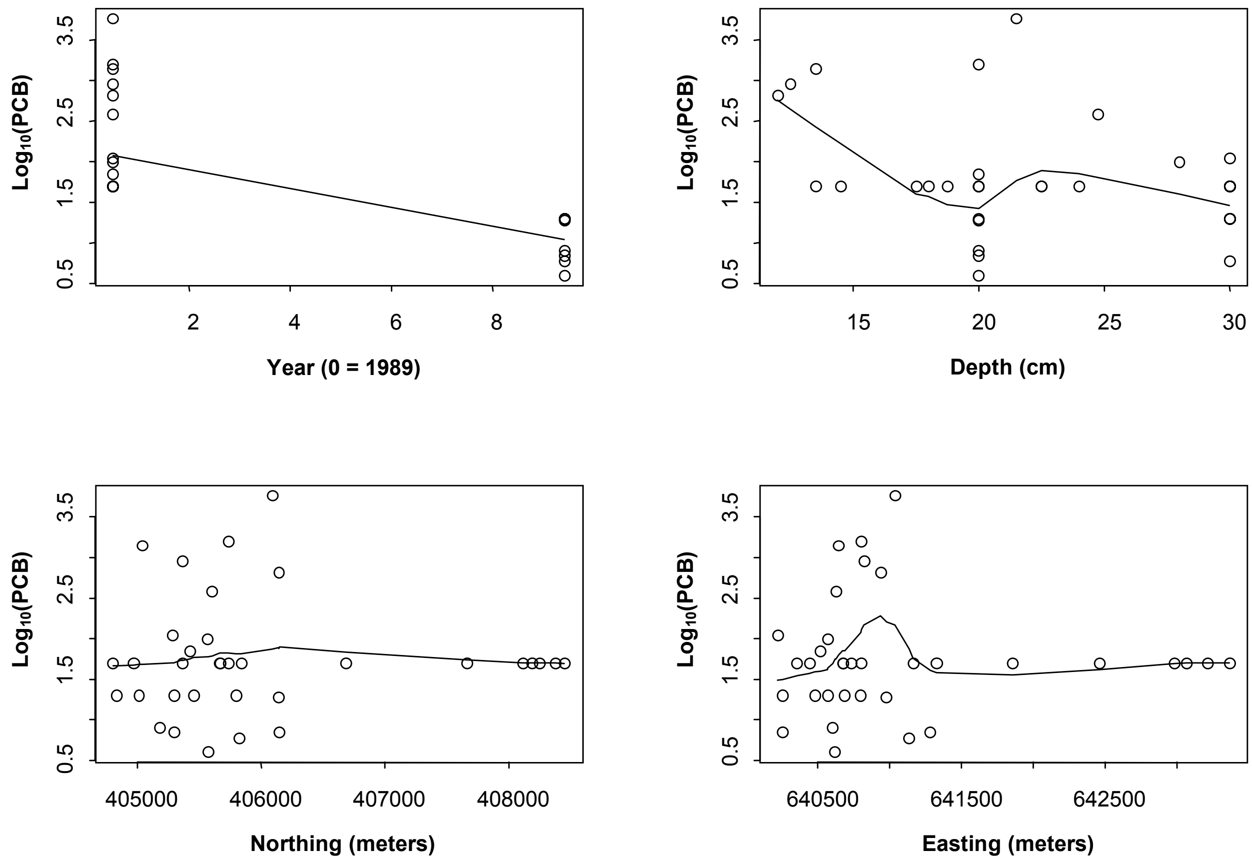

Figure A-60 Log$_{10}$ PCB Concentration versus Time, Depth, Northing, and Easting for Appleton Deposit Group VCC (10 to 30 cm) Including Fitted Smoothed Line

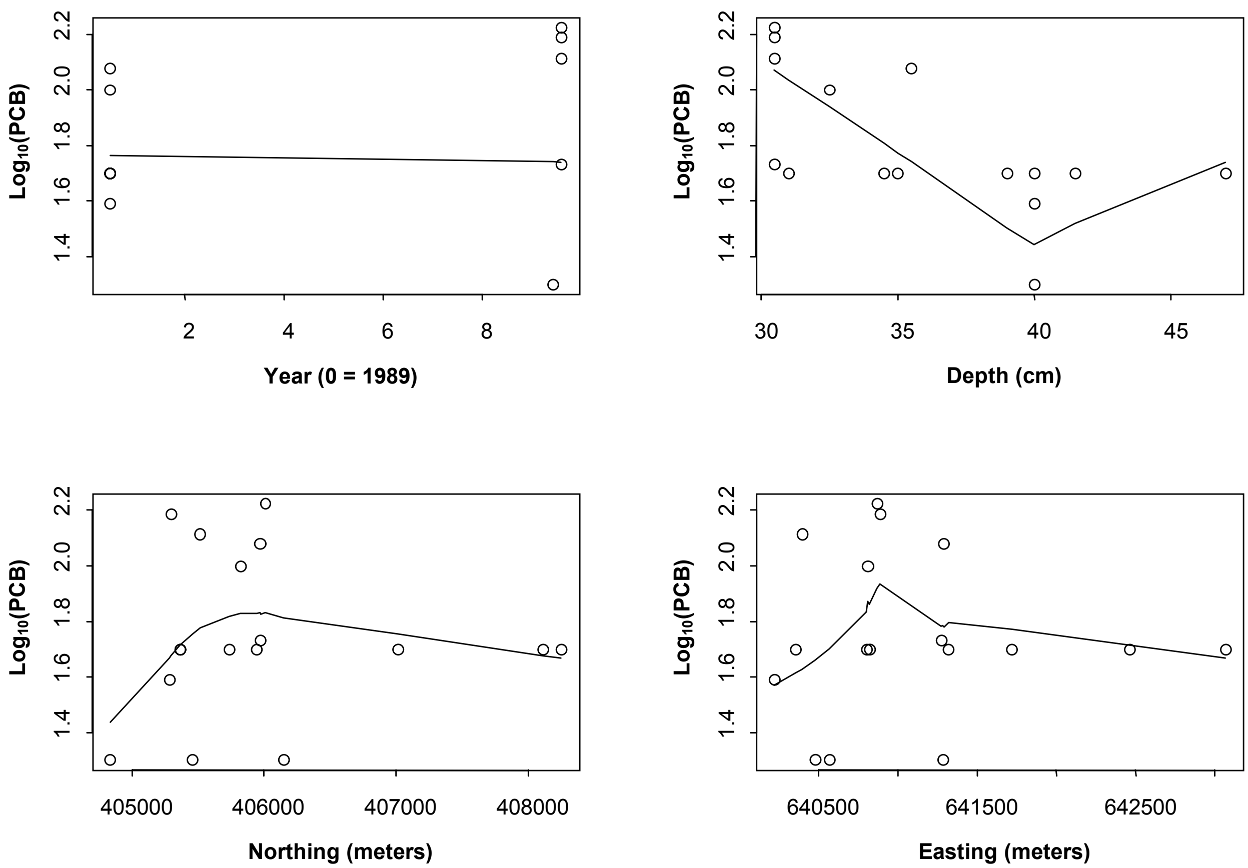

Figure A-61 Log$_{10}$ PCB Concentration versus Time, Depth, Northing, and Easting for Appleton Deposit Group VCC (30 to 50 cm) Including Fitted Smoothed Line

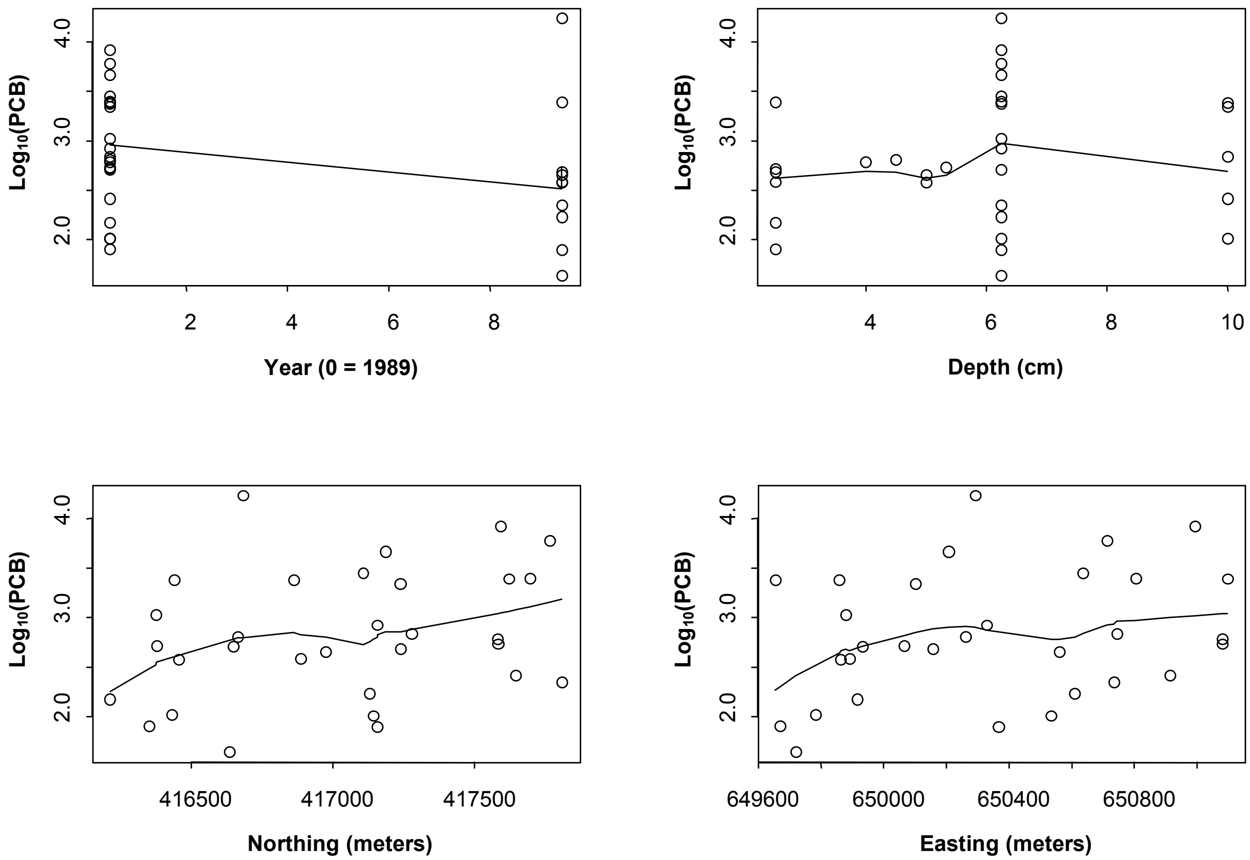

Figure A-62 Log$_{10}$ PCB Concentration versus Time, Depth, Northing, and Easting for Little Rapids Deposit Group Upper EE (0 to 10 cm) Including Fitted Smoothed Line

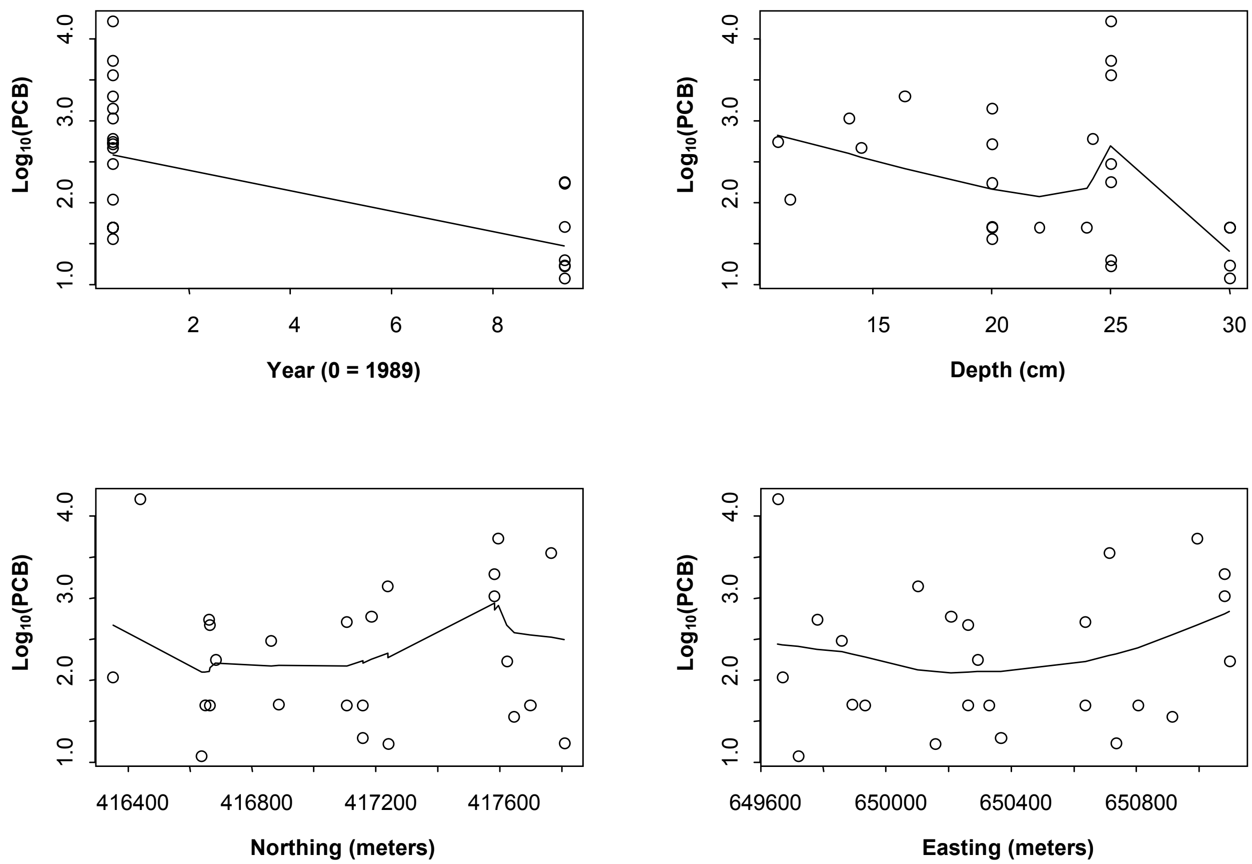

Figure A-63 Log$_{10}$ PCB Concentration versus Time, Depth, Northing, and Easting for Little Rapids Deposit Group Upper EE (10 to 30 cm) Including Fitted Smoothed Line

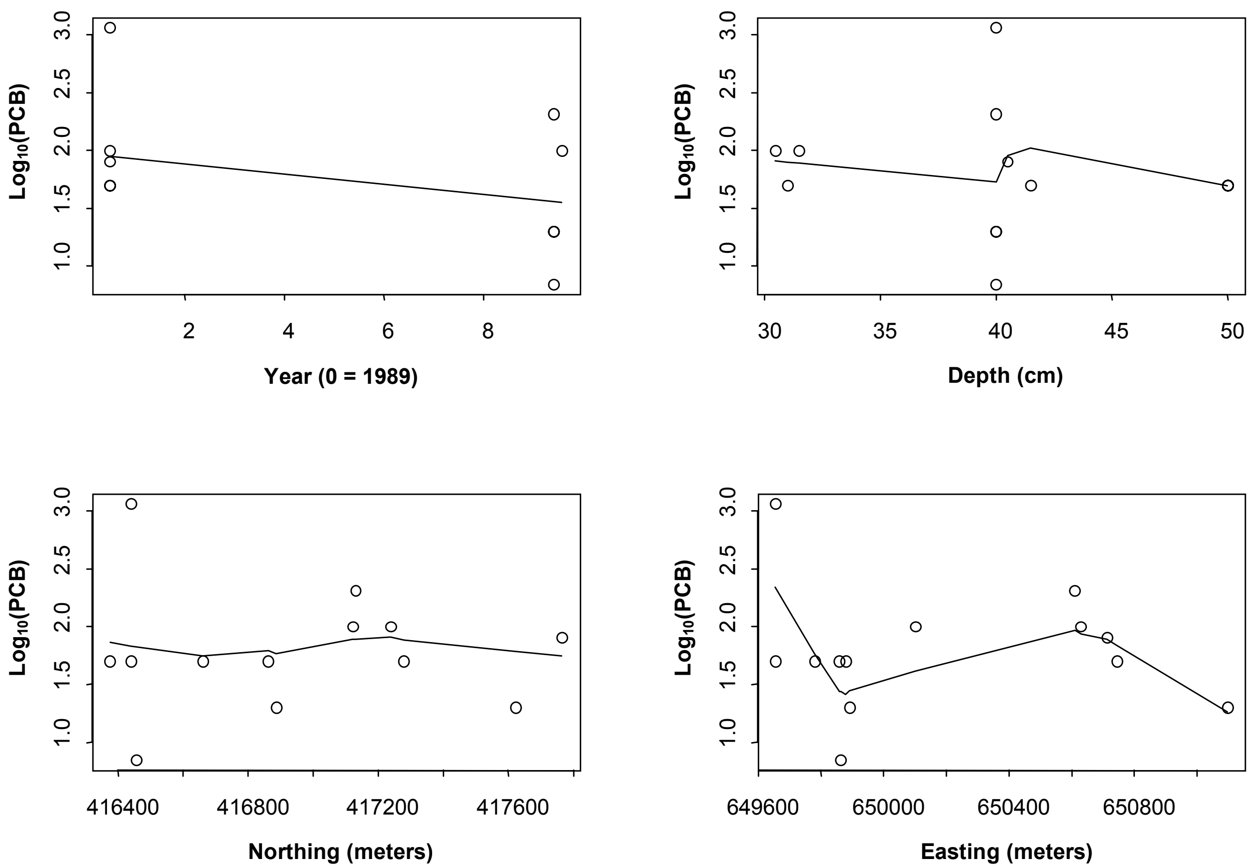

Figure A-64 Log$_{10}$ PCB Concentration versus Time, Depth, Northing, and Easting for Little Rapids Deposit Group Upper EE (30 to 50 cm) Including Fitted Smoothed Line

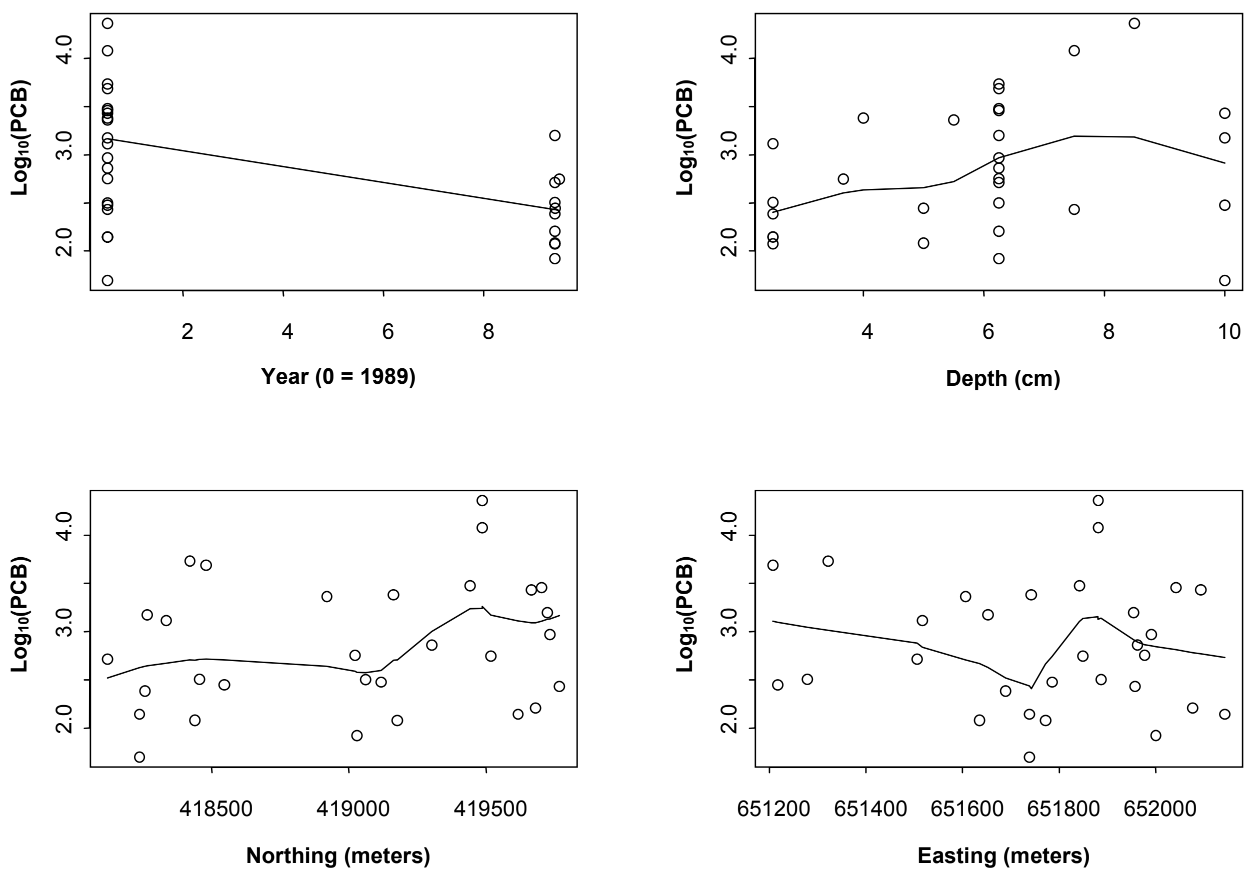

Figure A-65 Log_{10} PCB Concentration versus Time, Depth, Northing, and Easting for Little Rapids Deposit Group Lower EE (0 to 10 cm) Including Fitted Smoothed Line

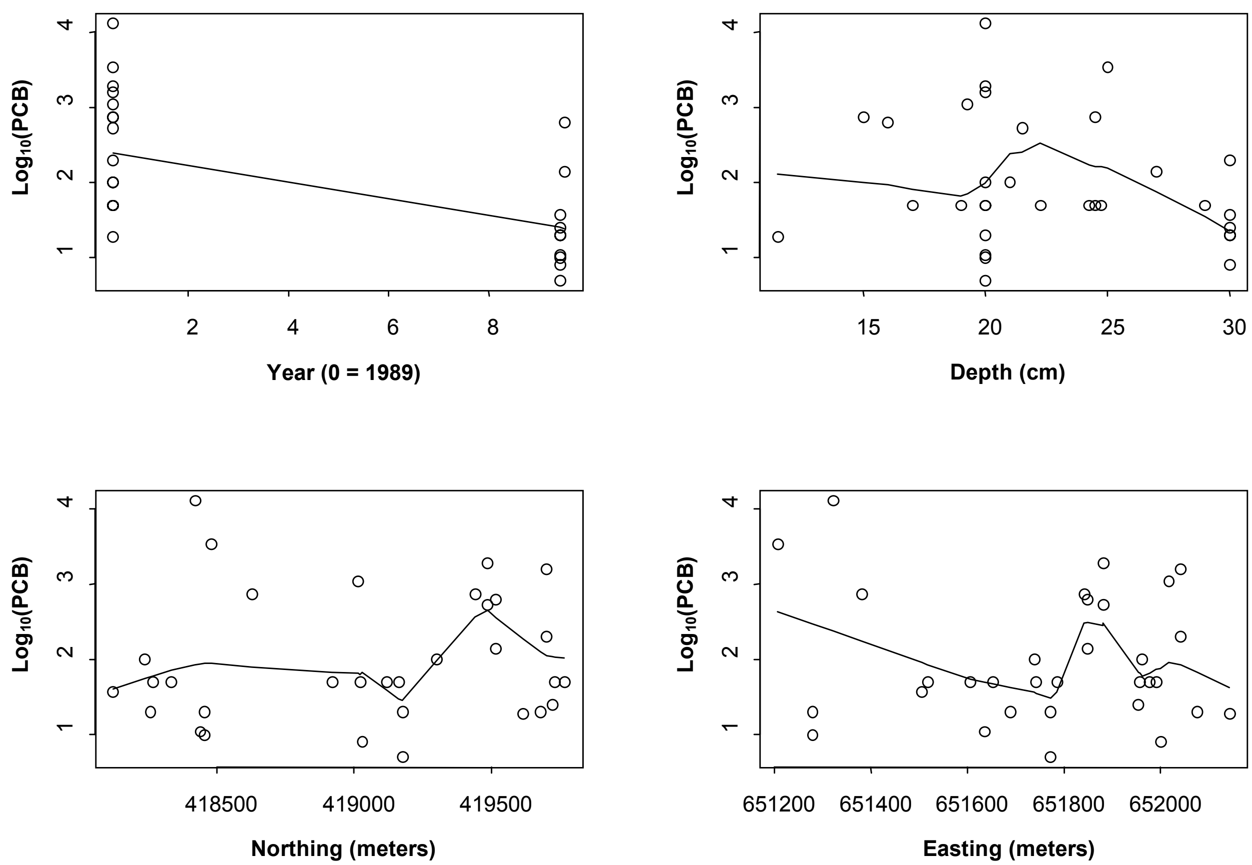

Figure A-66 Log_{10} PCB Concentration versus Time, Depth, Northing, and Easting for Little Rapids Deposit Group Lower EE (10 to 30 cm) Including Fitted Smoothed Line

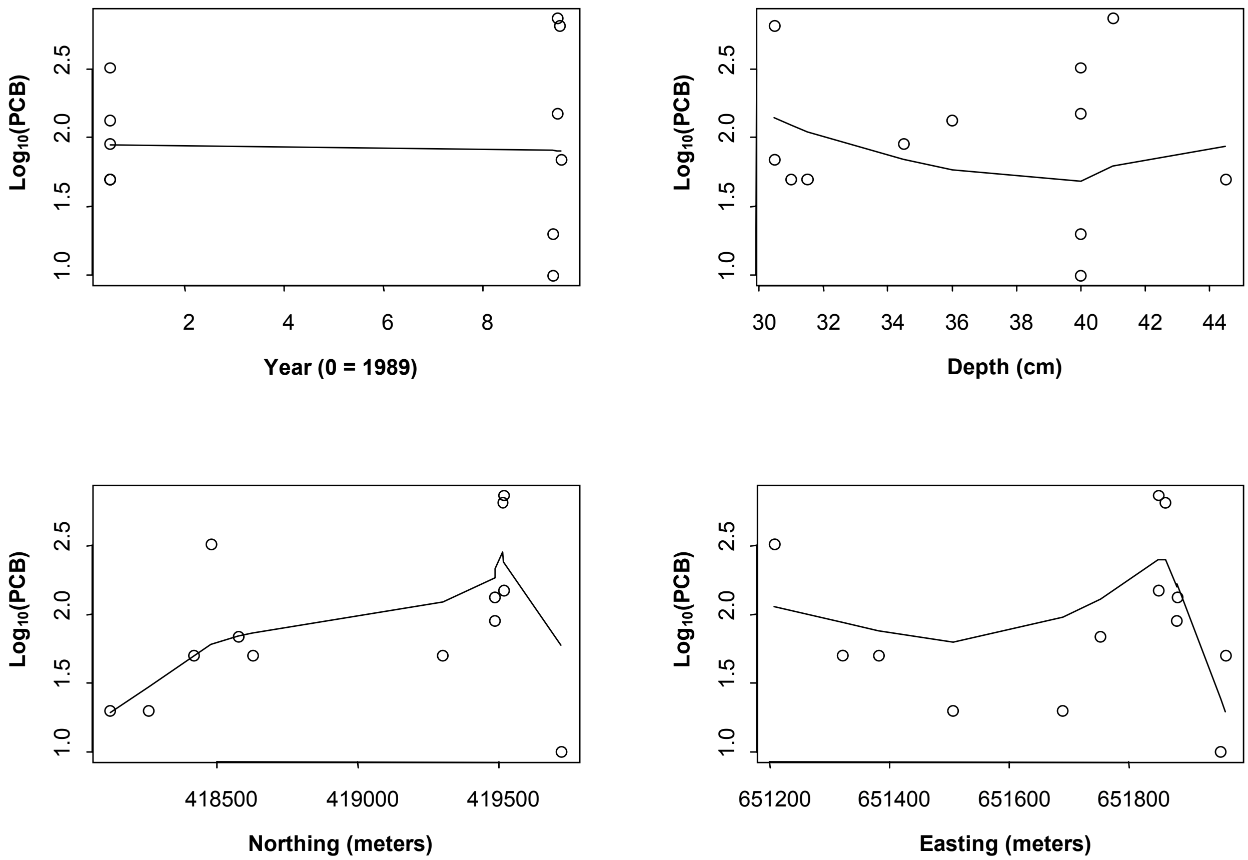

Figure A-67 Log_{10} PCB Concentration versus Time, Depth, Northing, and Easting for Little Rapids Deposit Group Lower EE (30 to 50 cm) Including Fitted Smoothed Line

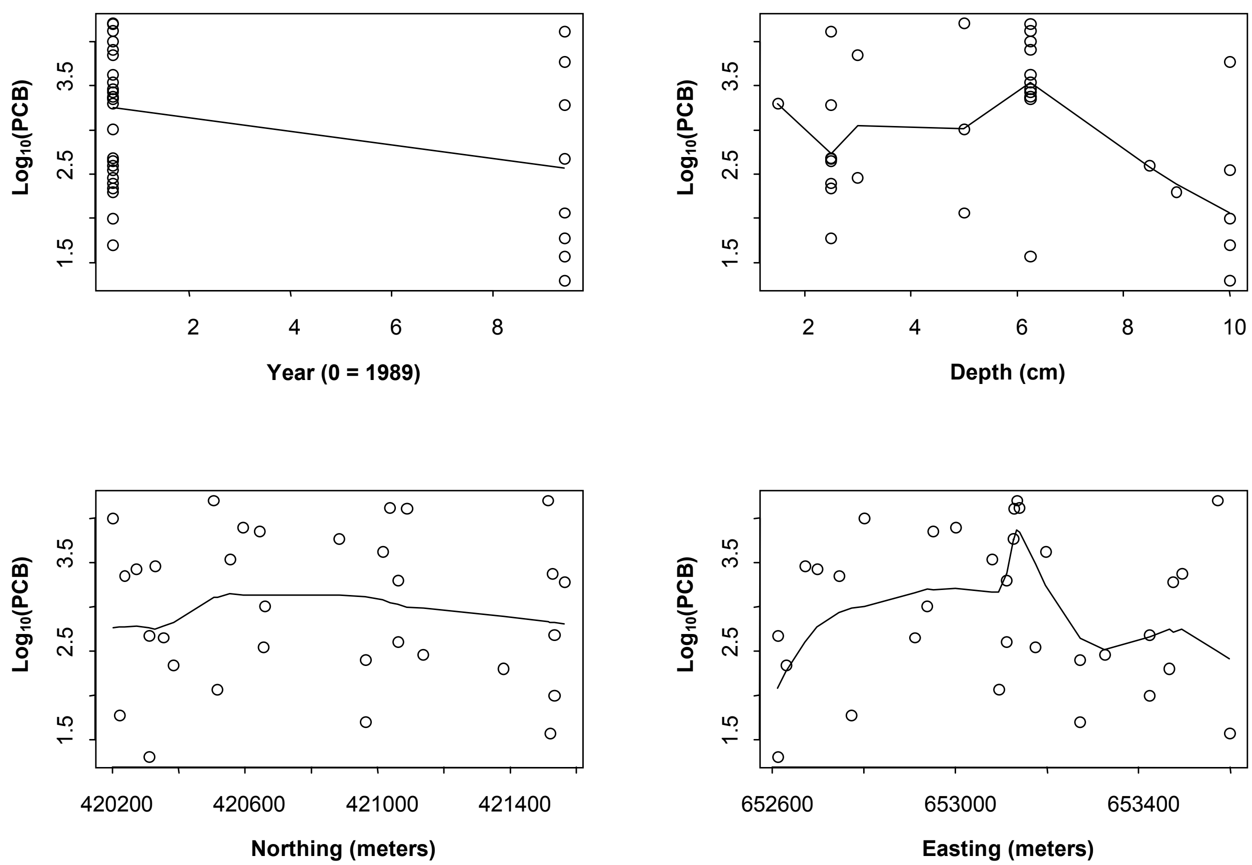

Figure A-68 Log$_{10}$ PCB Concentration versus Time, Depth, Northing, and Easting for Little Rapids Deposit Group FF (0 to 10 cm) Including Fitted Smoothed Line

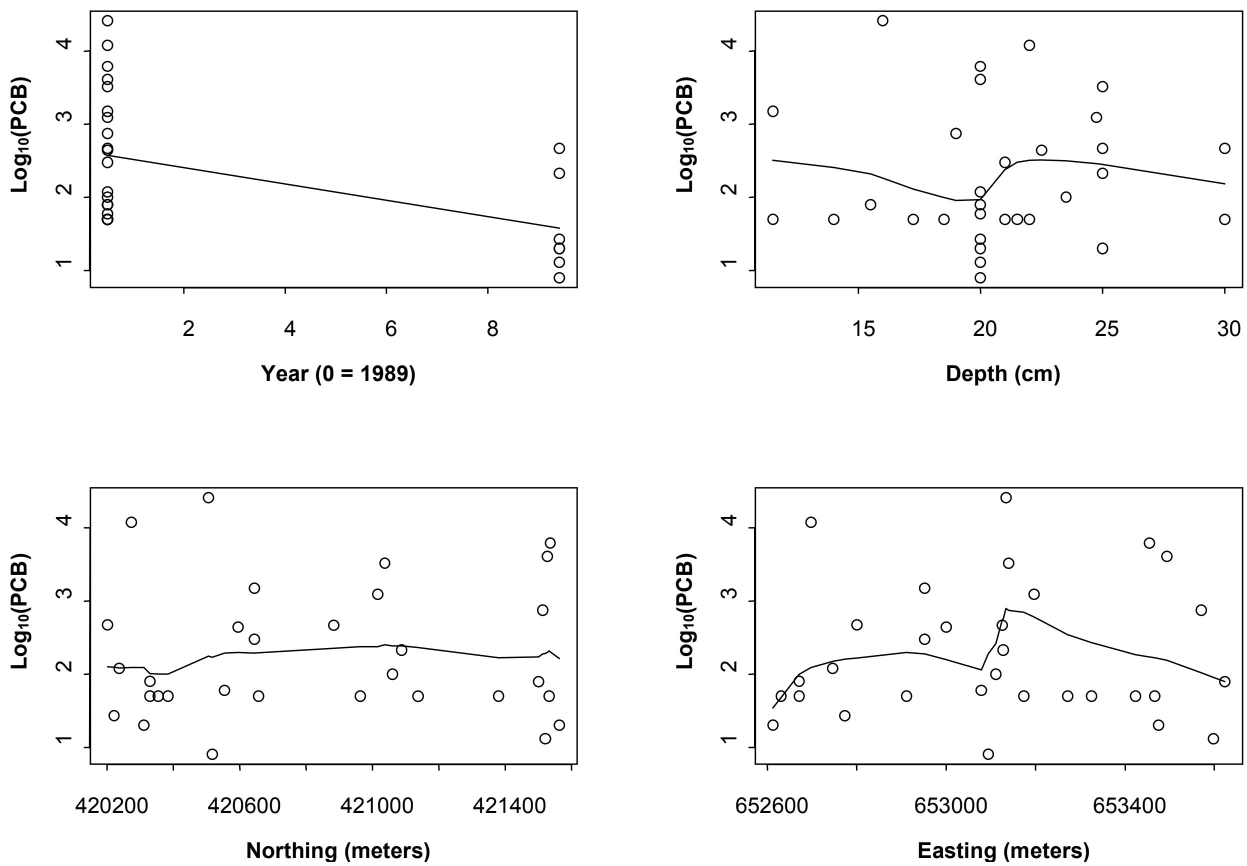

Figure A-69 Log$_{10}$ PCB Concentration versus Time, Depth, Northing, and Easting for Little Rapids Deposit Group FF (10 to 30 cm) Including Fitted Smoothed Line

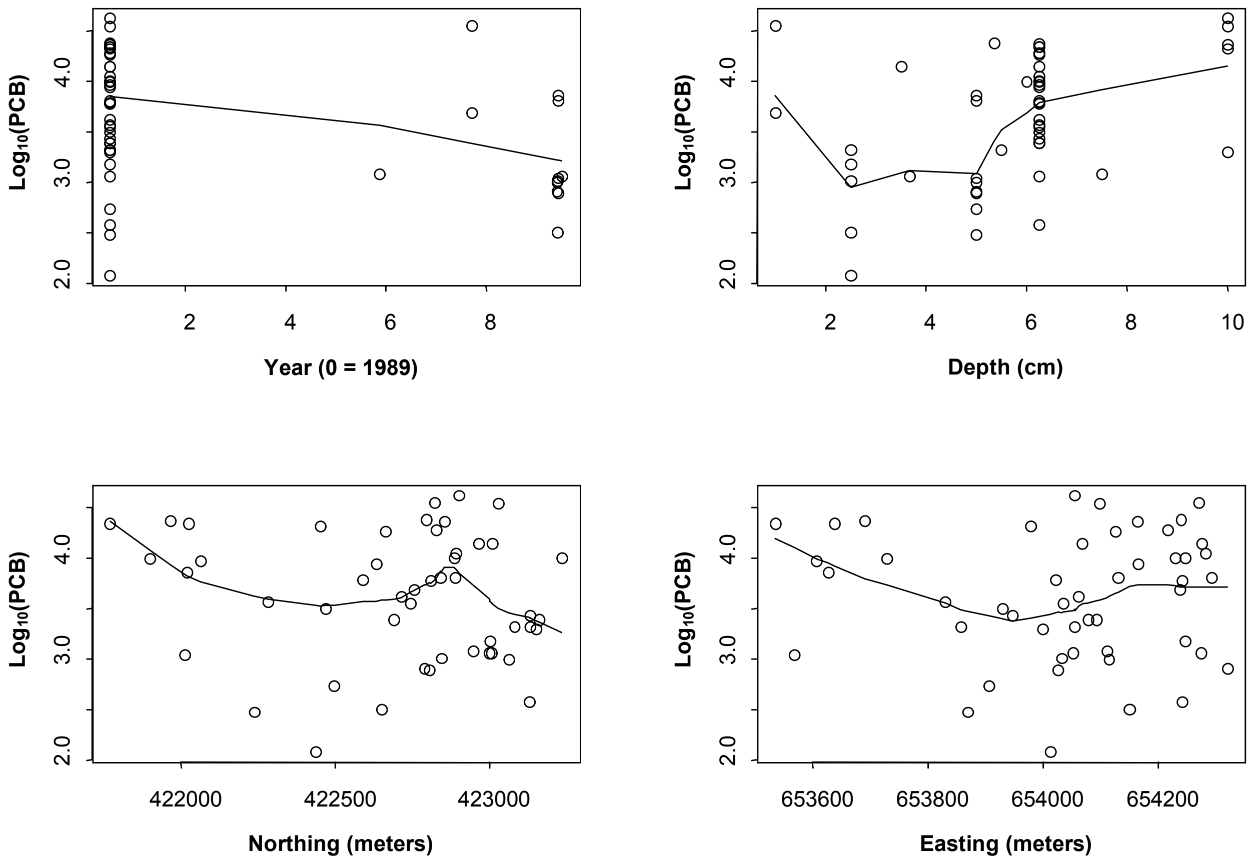

Figure A-70 Log$_{10}$ PCB Concentration versus Time, Depth, Northing, and Easting for Little Rapids Deposit Group GGHH (0 to 10 cm) Including Fitted Smoothed Line

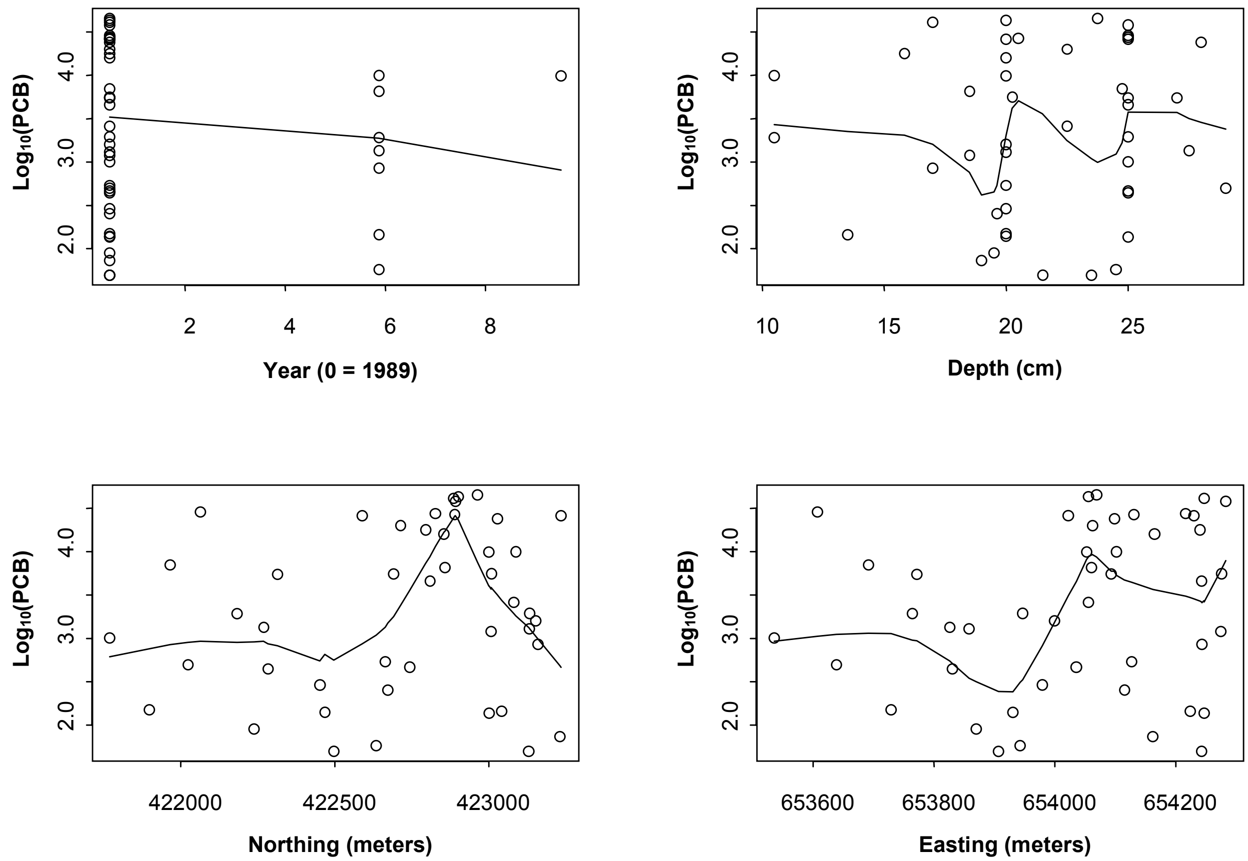

Figure A-71 Log_{10} PCB Concentration versus Time, Depth, Northing, and Easting for Little Rapids Deposit Group GGHH (10 to 30 cm) Including Fitted Smoothed Line

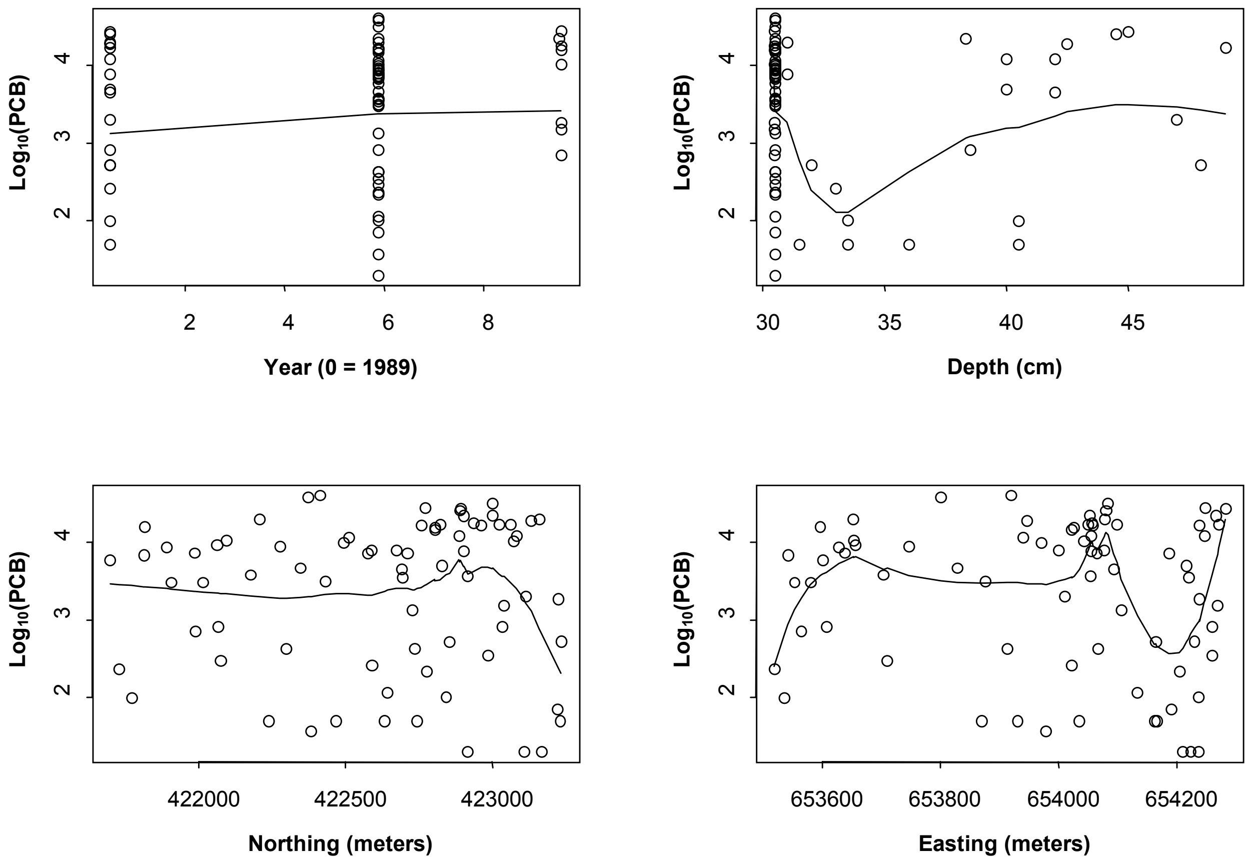

Figure A-72 Log$_{10}$ PCB Concentration versus Time, Depth, Northing, and Easting for Little Rapids Deposit Group GGHH (30 to 50 cm) Including Fitted Smoothed Line

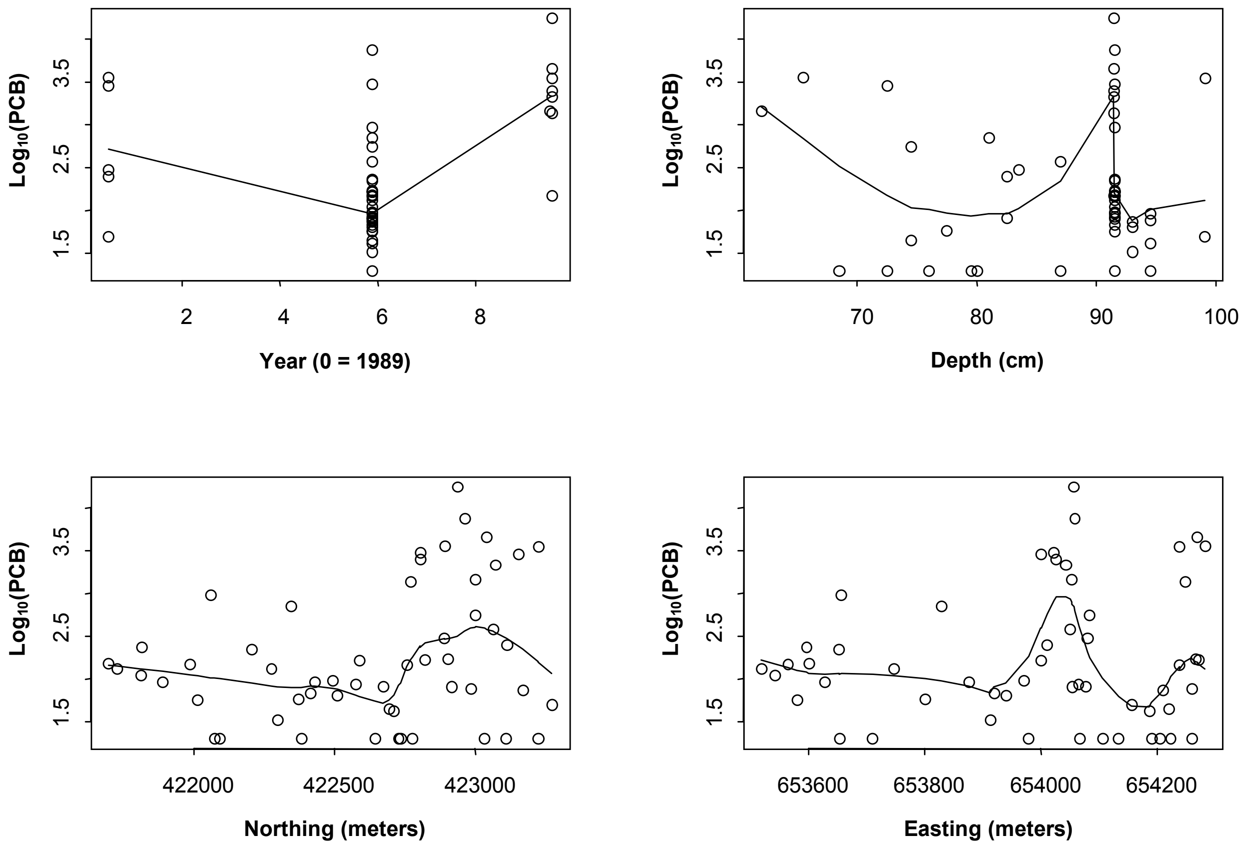

Figure A-73 Log$_{10}$ PCB Concentration versus Time, Depth, Northing, and Easting for Little Rapids Deposit Group GGHH (50 to 100 cm) Including Fitted Smoothed Line

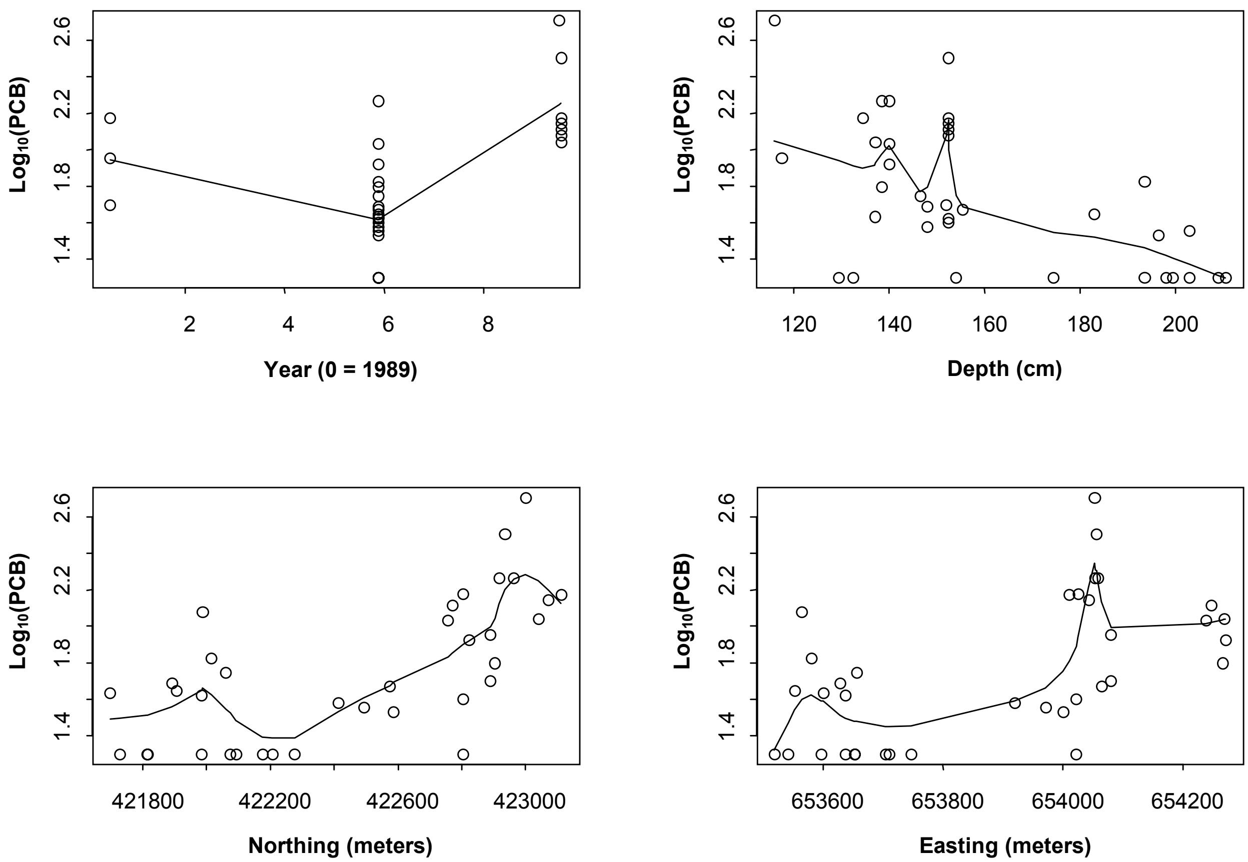

Figure A-74 Log$_{10}$ PCB Concentration versus Time, Depth, Northing, and Easting for Little Rapids Deposit Group GGHH (100+ cm) Including Fitted Smoothed Line

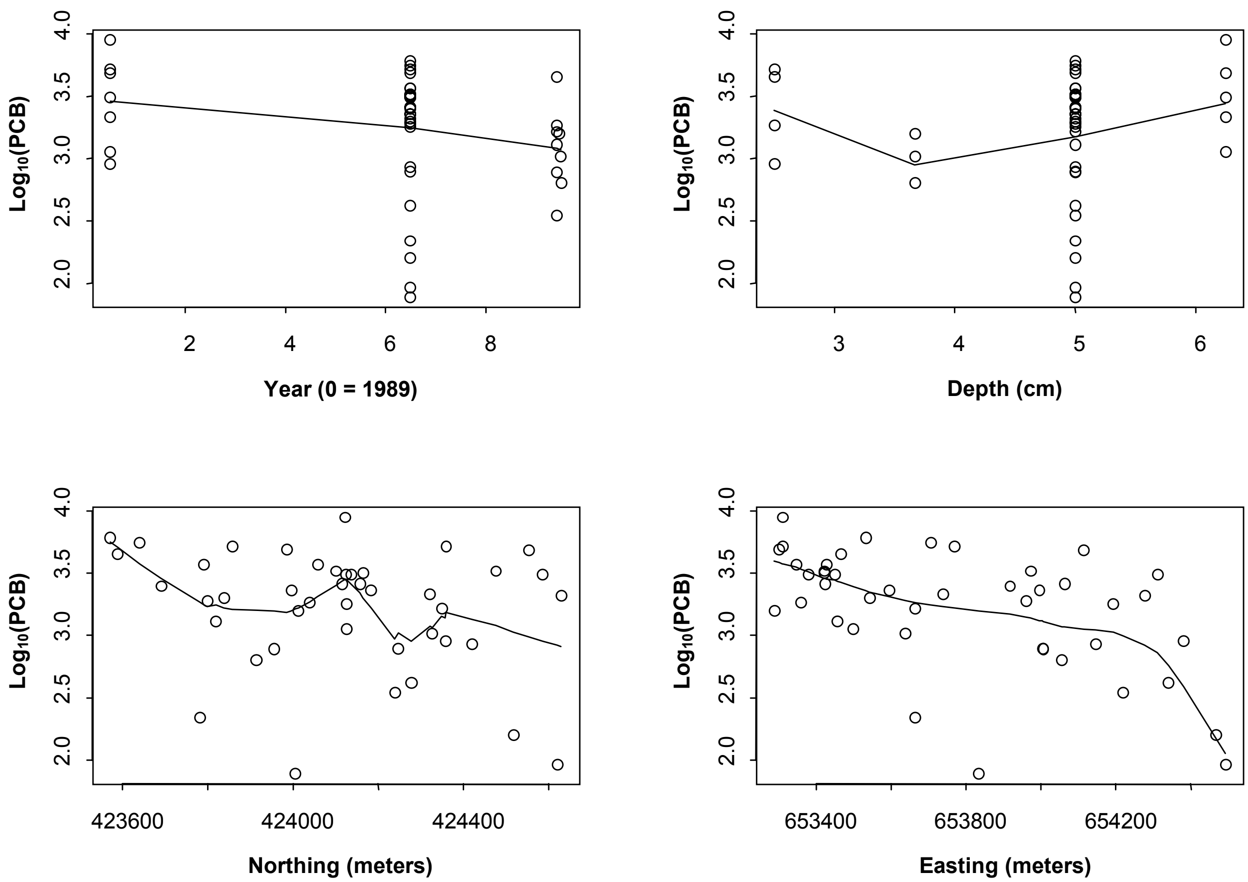

Figure A-75 Log_{10} PCB Concentration versus Time, Depth, Northing, and Easting for De Pere SMU Group 2025 (0 to 10 cm) Including Fitted Smoothed Line

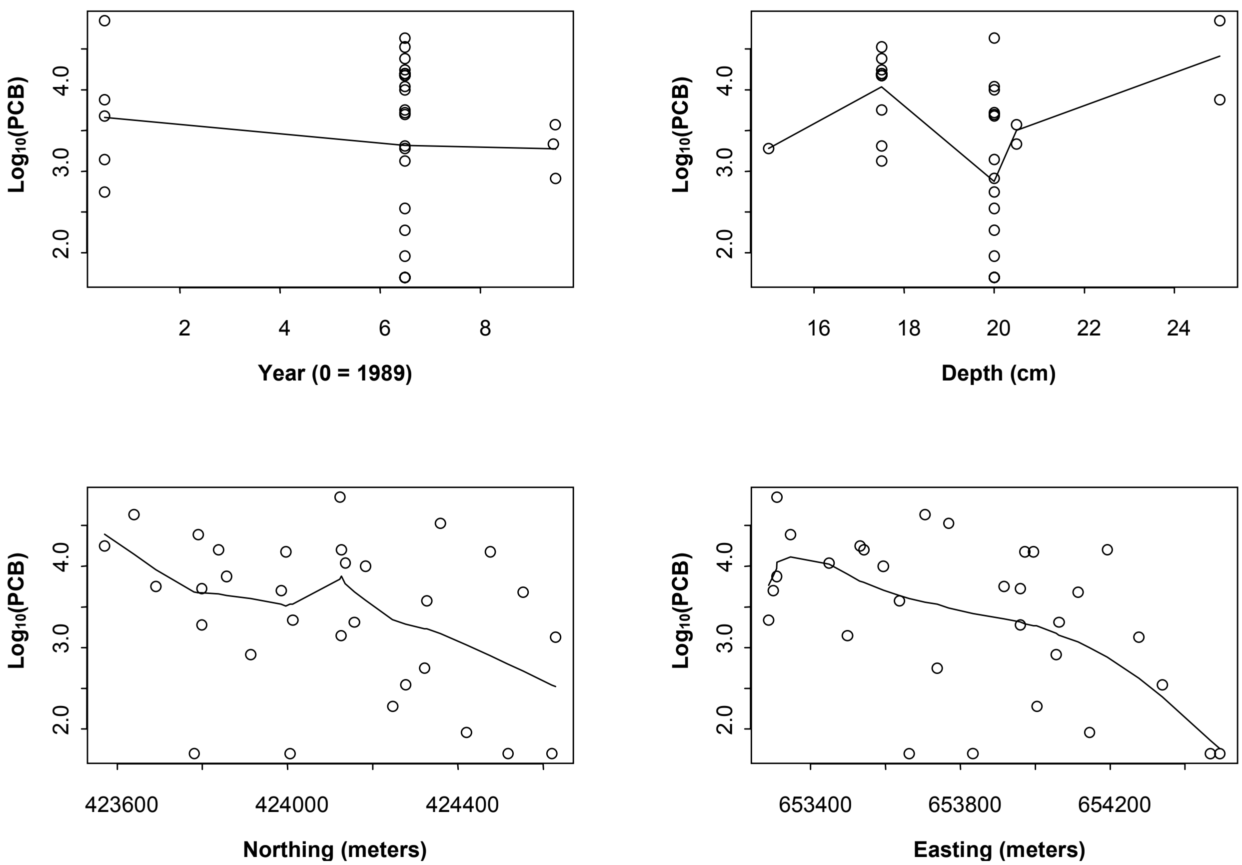

Figure A-76 Log_{10} PCB Concentration versus Time, Depth, Northing, and Easting for De Pere SMU Group 2025 (10 to 30 cm) Including Fitted Smoothed Line

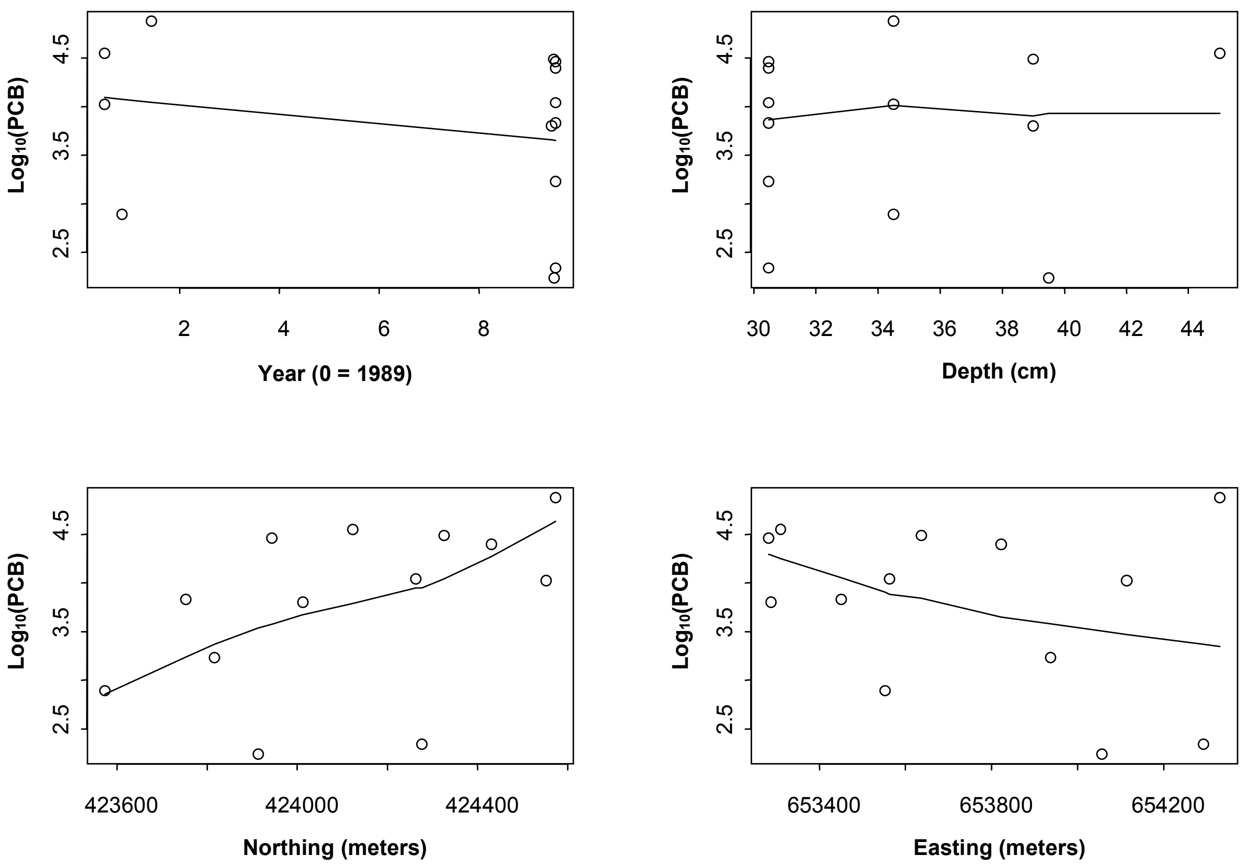

Figure A-77 Log$_{10}$ PCB Concentration versus Time, Depth, Northing, and Easting for De Pere SMU Group 2025 (30 to 50 cm) Including Fitted Smoothed Line

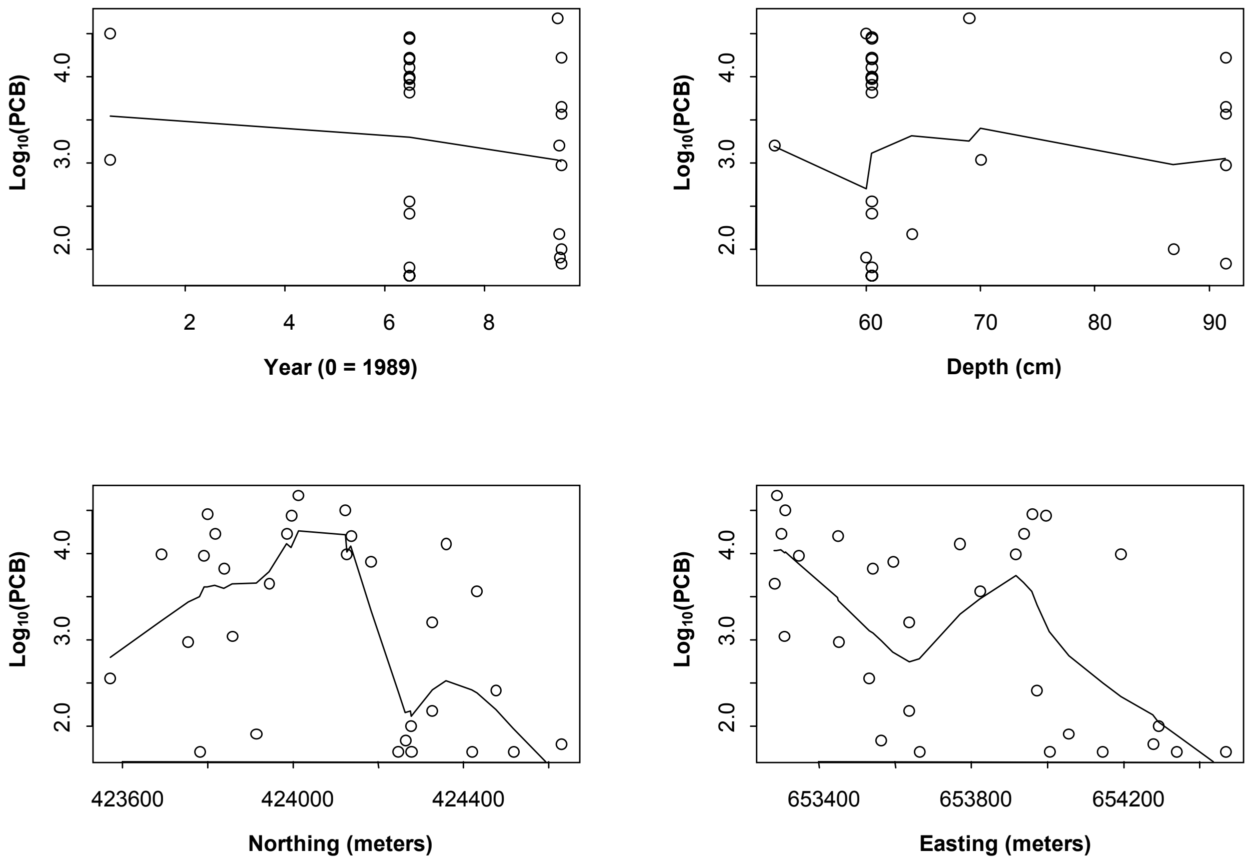

Figure A-78 Log_{10} PCB Concentration versus Time, Depth, Northing, and Easting for De Pere SMU Group 2025 (50 to 100 cm) Including Fitted Smoothed Line

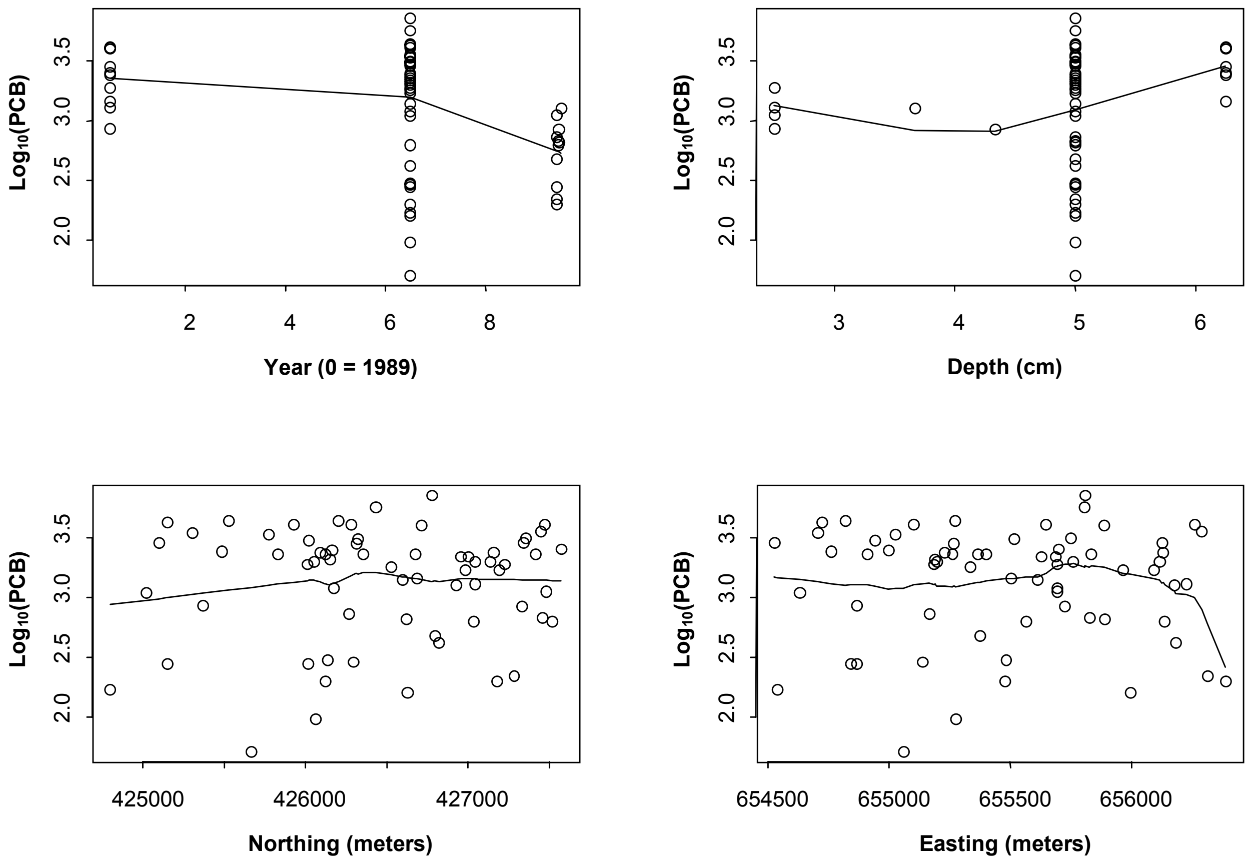

Figure A-79 Log_{10} PCB Concentration versus Time, Depth, Northing, and Easting for De Pere SMU Group 2649 (0 to 10 cm) Including Fitted Smoothed Line

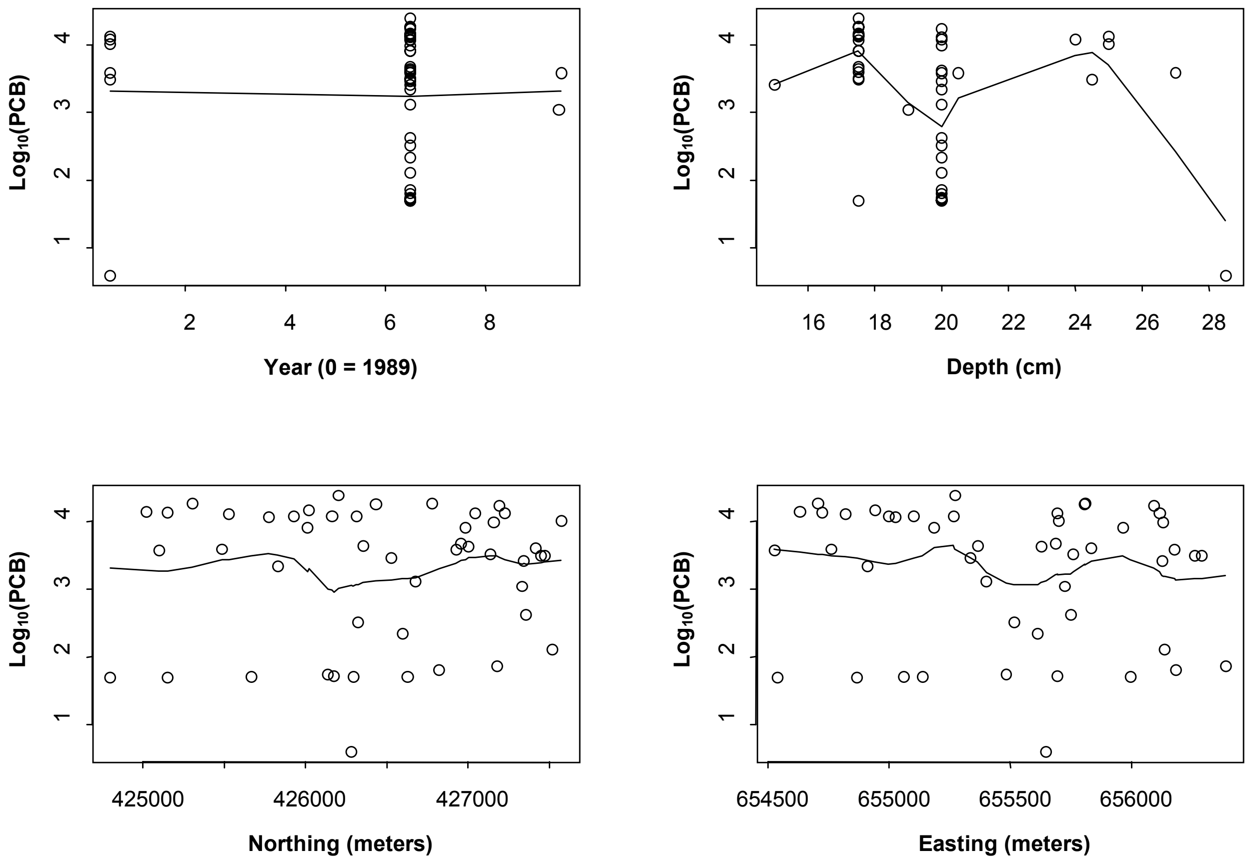

Figure A-80 Log$_{10}$ PCB Concentration versus Time, Depth, Northing, and Easting for De Pere SMU Group 2649 (10 to 30 cm) Including Fitted Smoothed Line

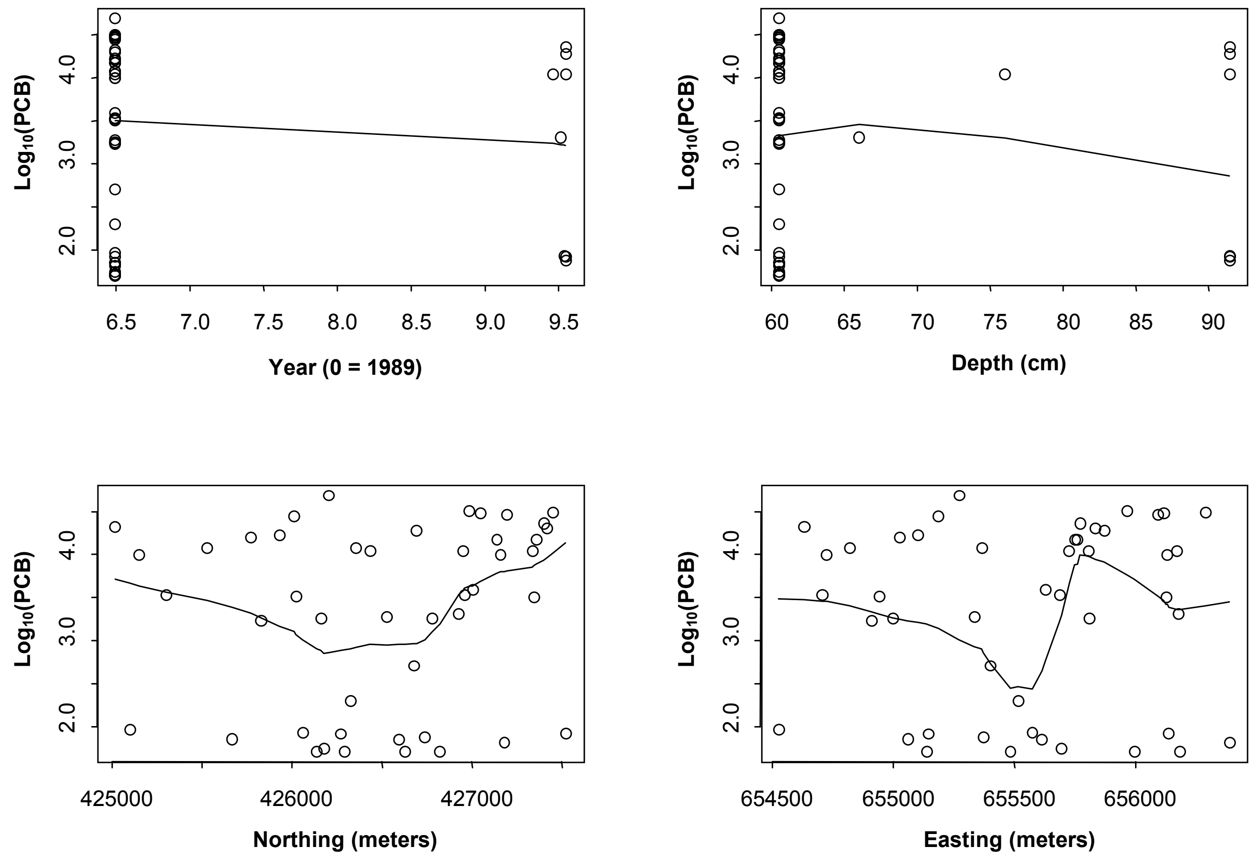

Figure A-81 Log_{10} PCB Concentration versus Time, Depth, Northing, and Easting for De Pere SMU Group 2649 (50 to 100 cm) Including Fitted Smoothed Line

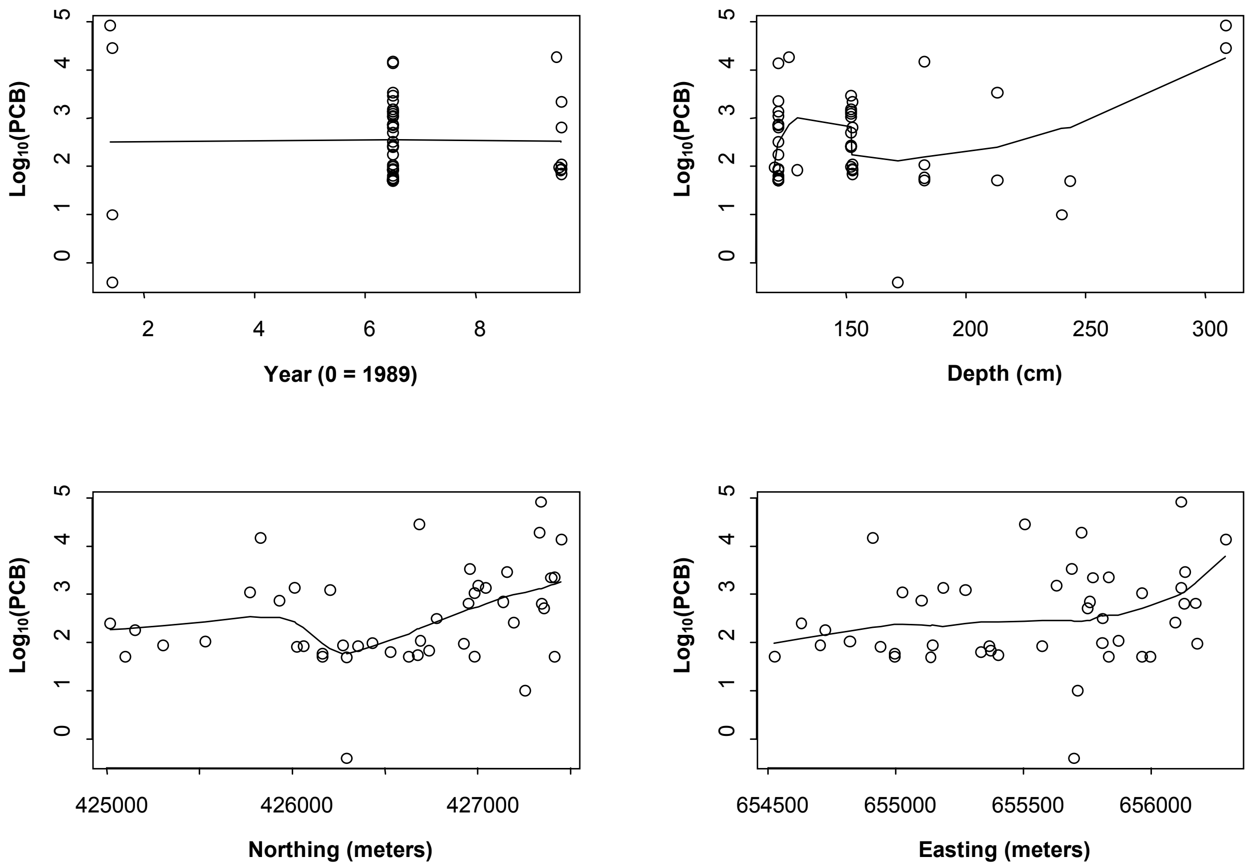

Figure A-82 Log_{10} PCB Concentration versus Time, Depth, Northing, and Easting for De Pere SMU Group 2649 (100+ cm) Including Fitted Smoothed Line

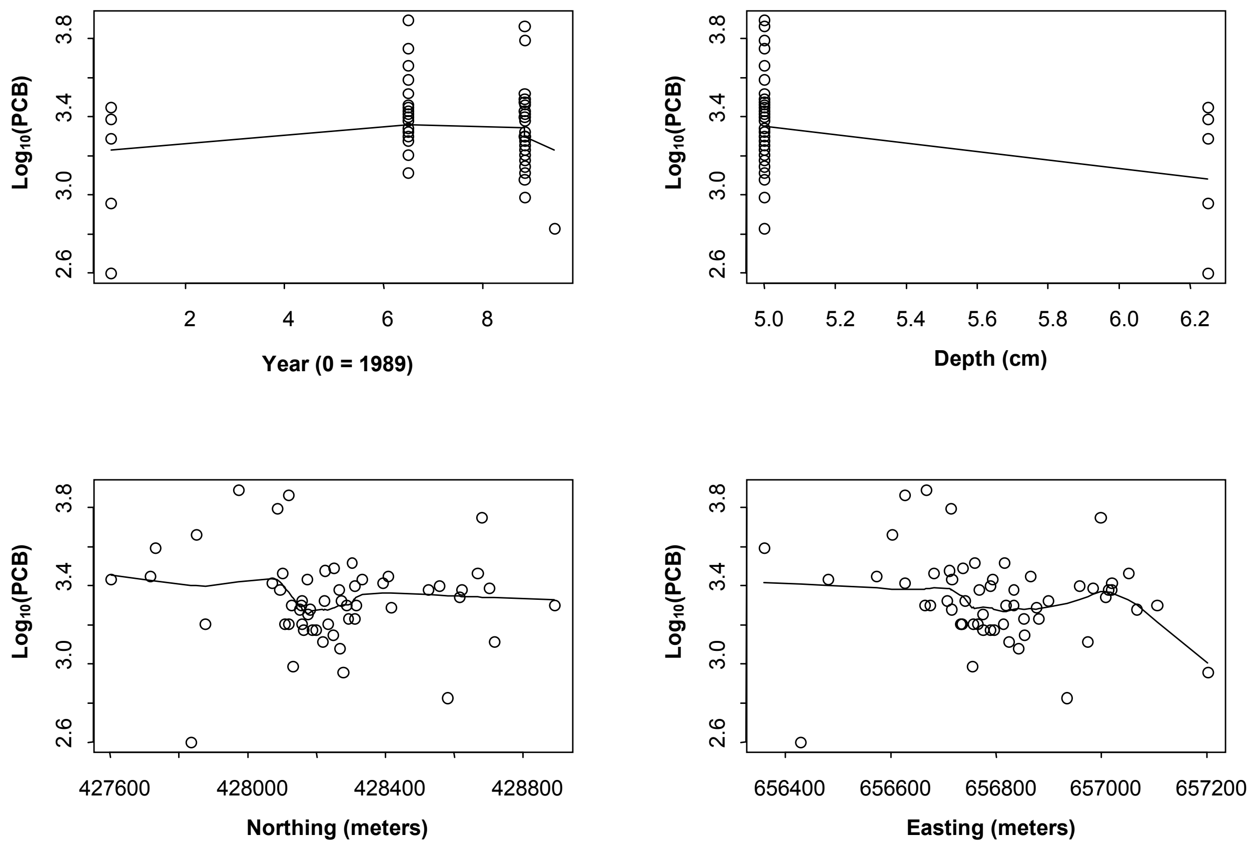

Figure A-83 Log_{10} PCB Concentration versus Time, Depth, Northing, and Easting for De Pere SMU Group 5067 (0 to 10 cm) Including Fitted Smoothed Line

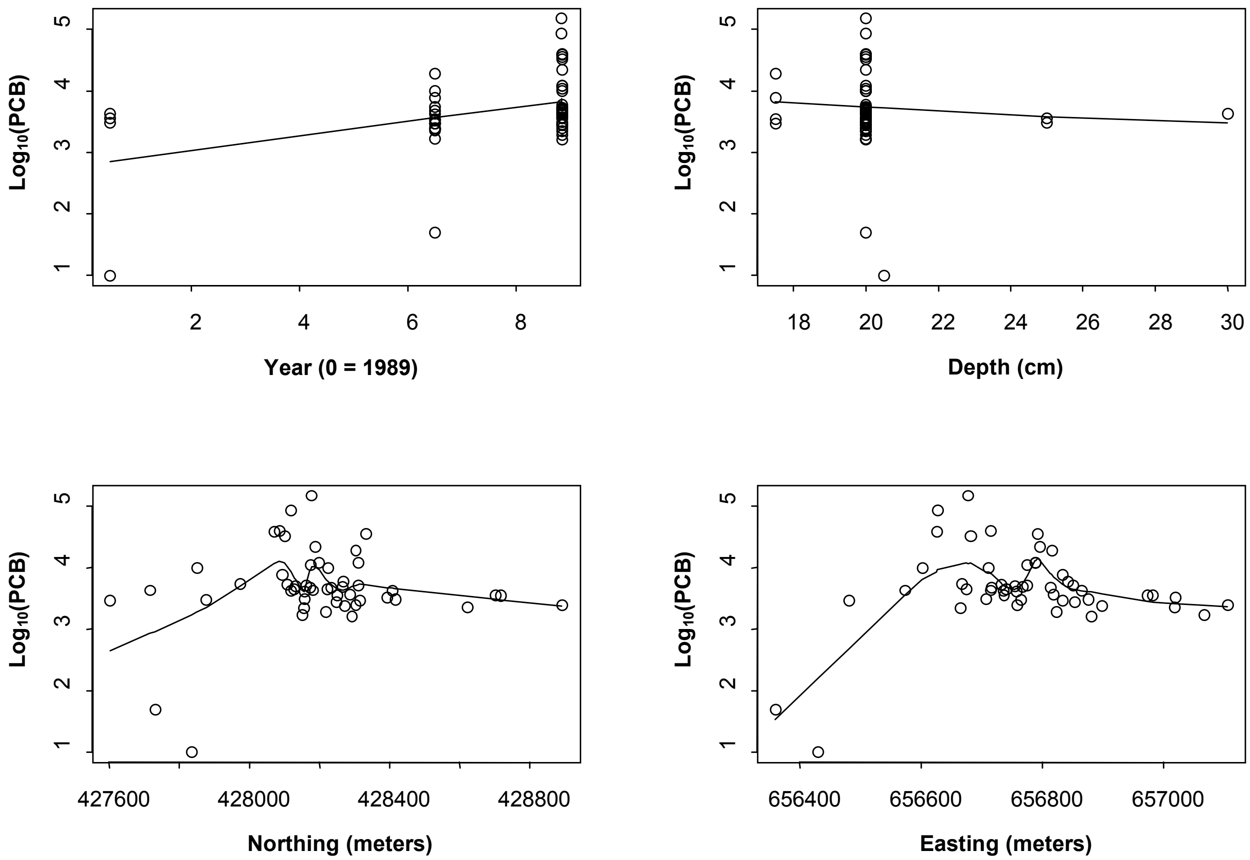

Figure A-84 Log$_{10}$ PCB Concentration versus Time, Depth, Northing, and Easting for De Pere SMU Group 5067 (10 to 30 cm) Including Fitted Smoothed Line

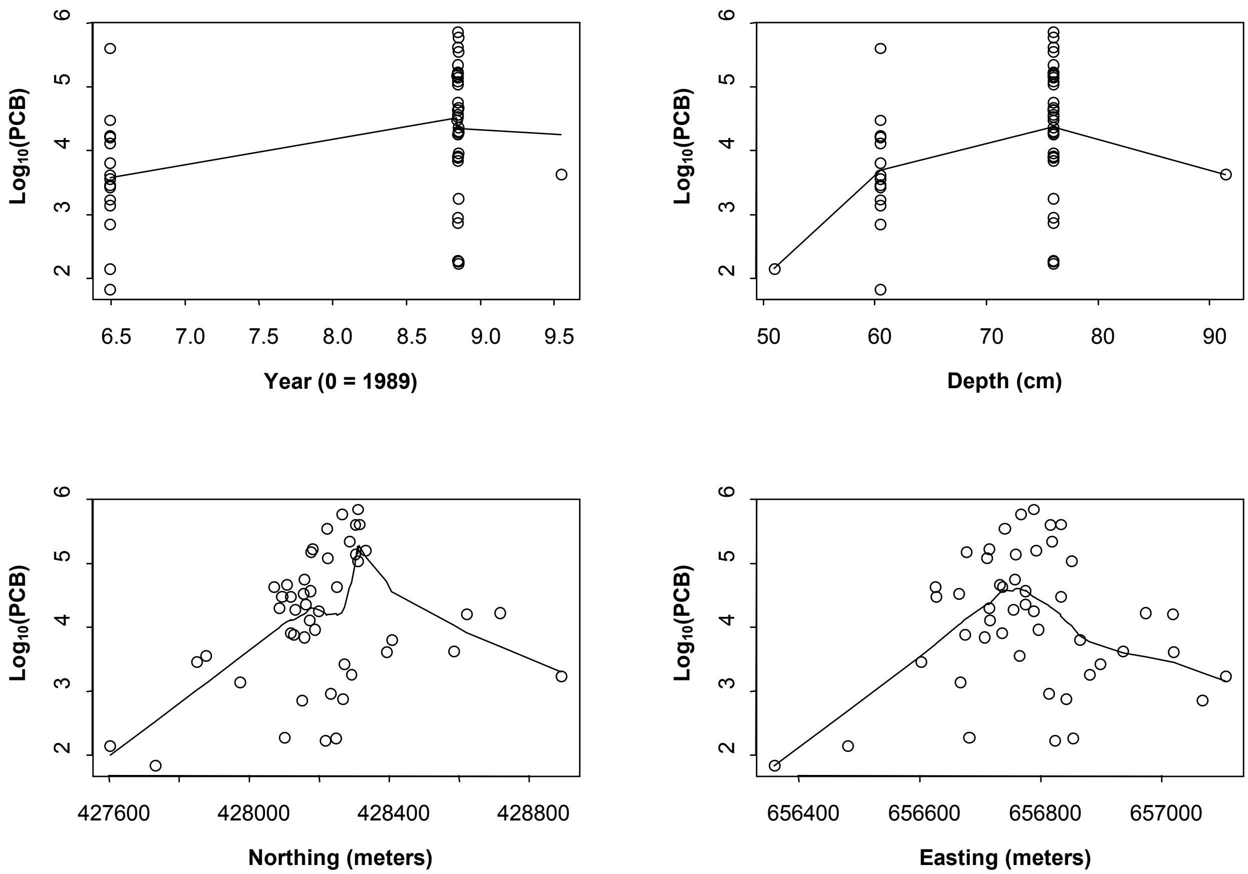

Figure A-85 Log_{10} PCB Concentration versus Time, Depth, Northing, and Easting for De Pere SMU Group 5067 (50 to 100 cm) Including Fitted Smoothed Line

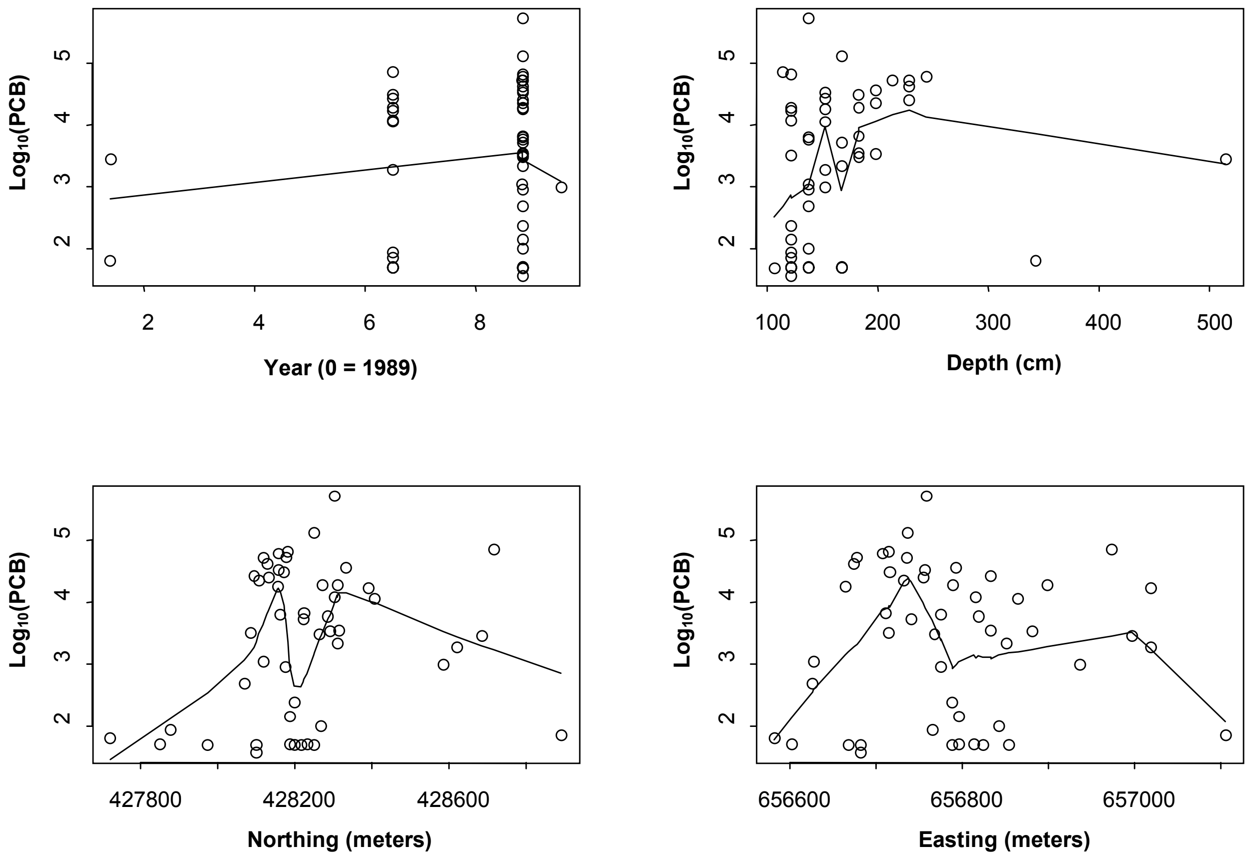

Figure A-86 Log$_{10}$ PCB Concentration versus Time, Depth, Northing, and Easting for De Pere SMU Group 5067 (100+ cm) Including Fitted Smoothed Line

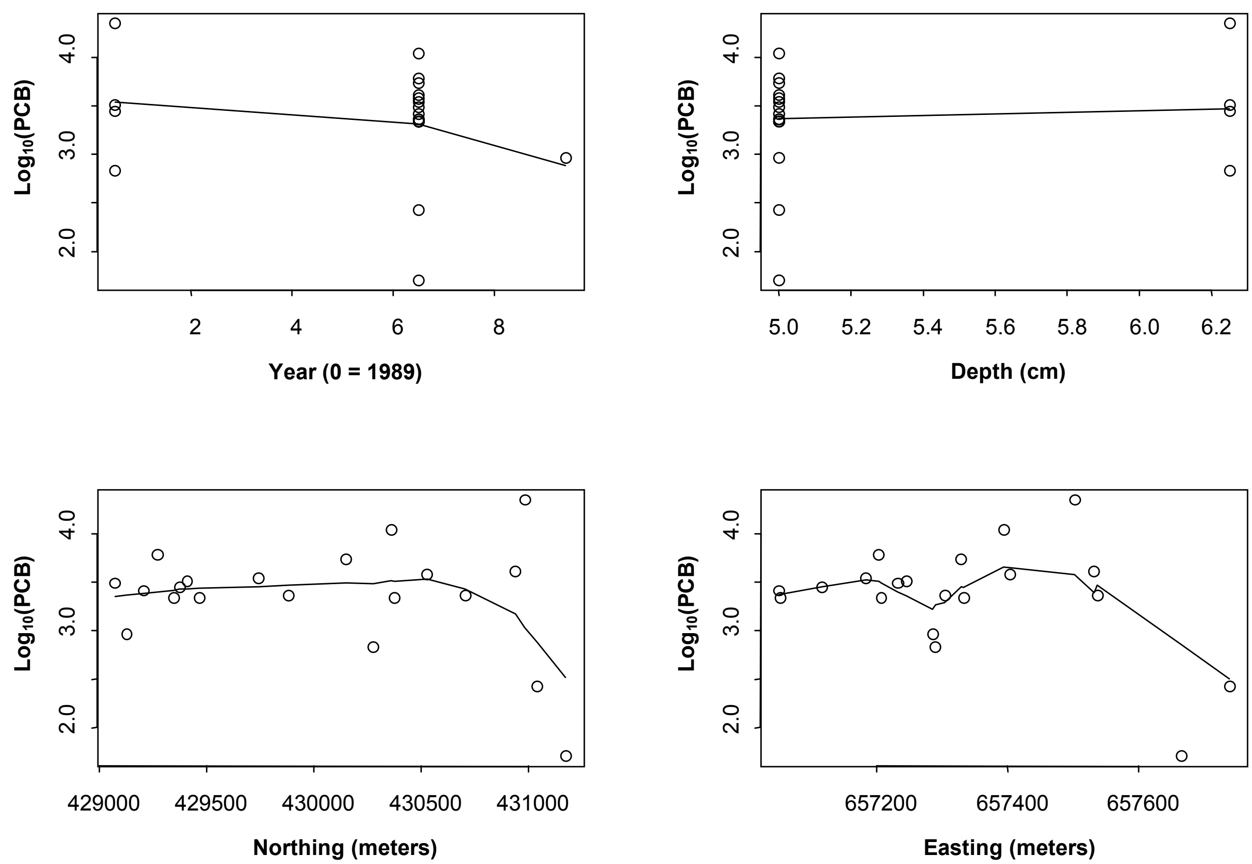

Figure A-87 Log_{10} PCB Concentration versus Time, Depth, Northing, and Easting for De Pere SMU Group 6891 (0 to 10 cm) Including Fitted Smoothed Line

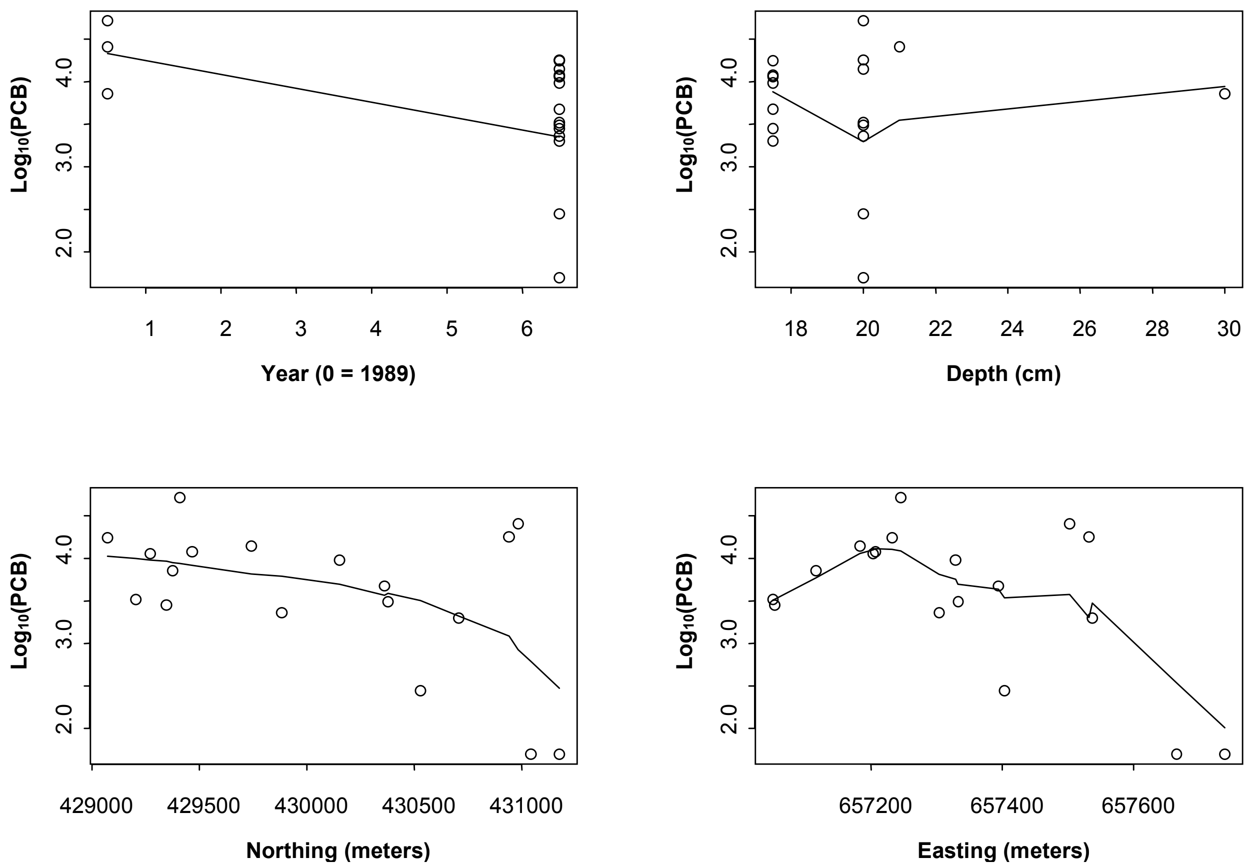

Figure A-88 Log_{10} PCB Concentration versus Time, Depth, Northing, and Easting for De Pere SMU Group 6891 (10 to 30 cm) Including Fitted Smoothed Line

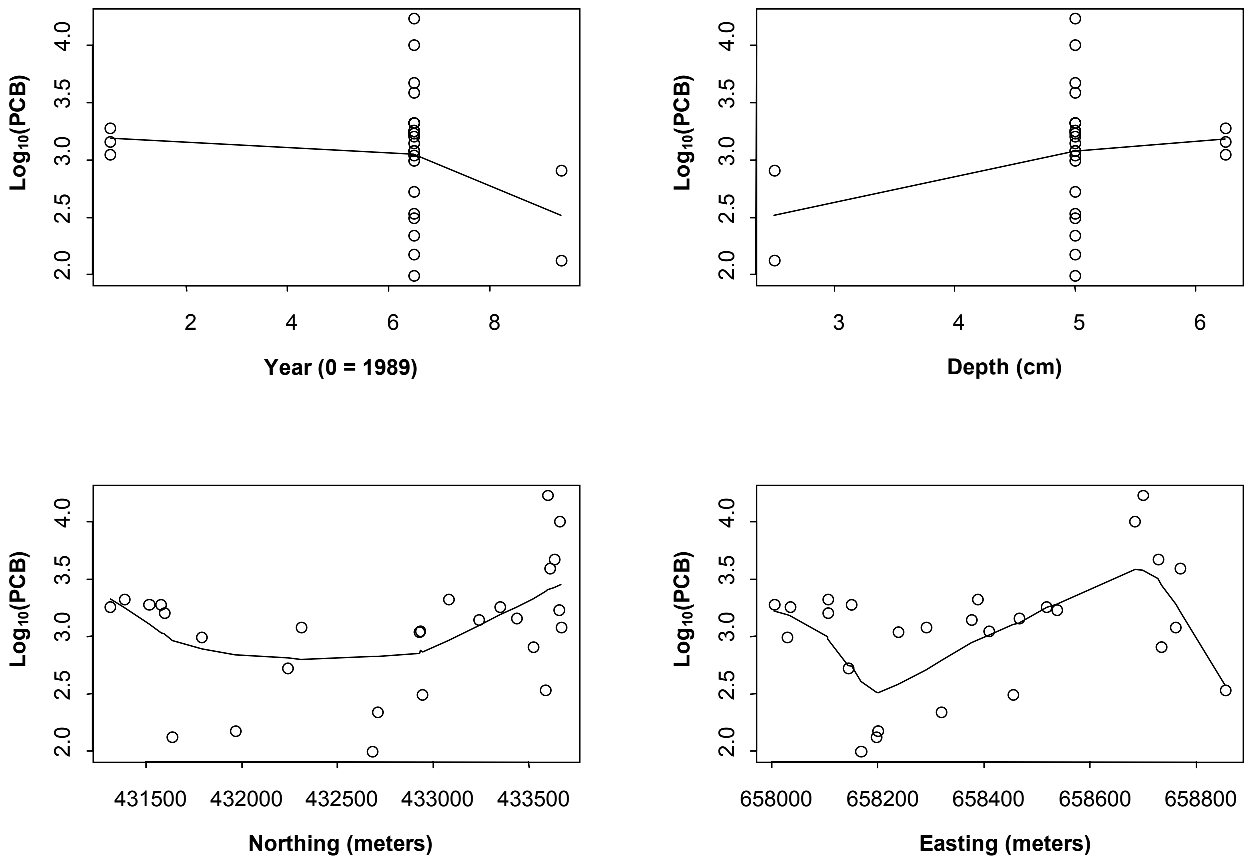

Figure A-89 Log$_{10}$ PCB Concentration versus Time, Depth, Northing, and Easting for De Pere SMU Group 92115 (0 to 10 cm) Including Fitted Smoothed Line

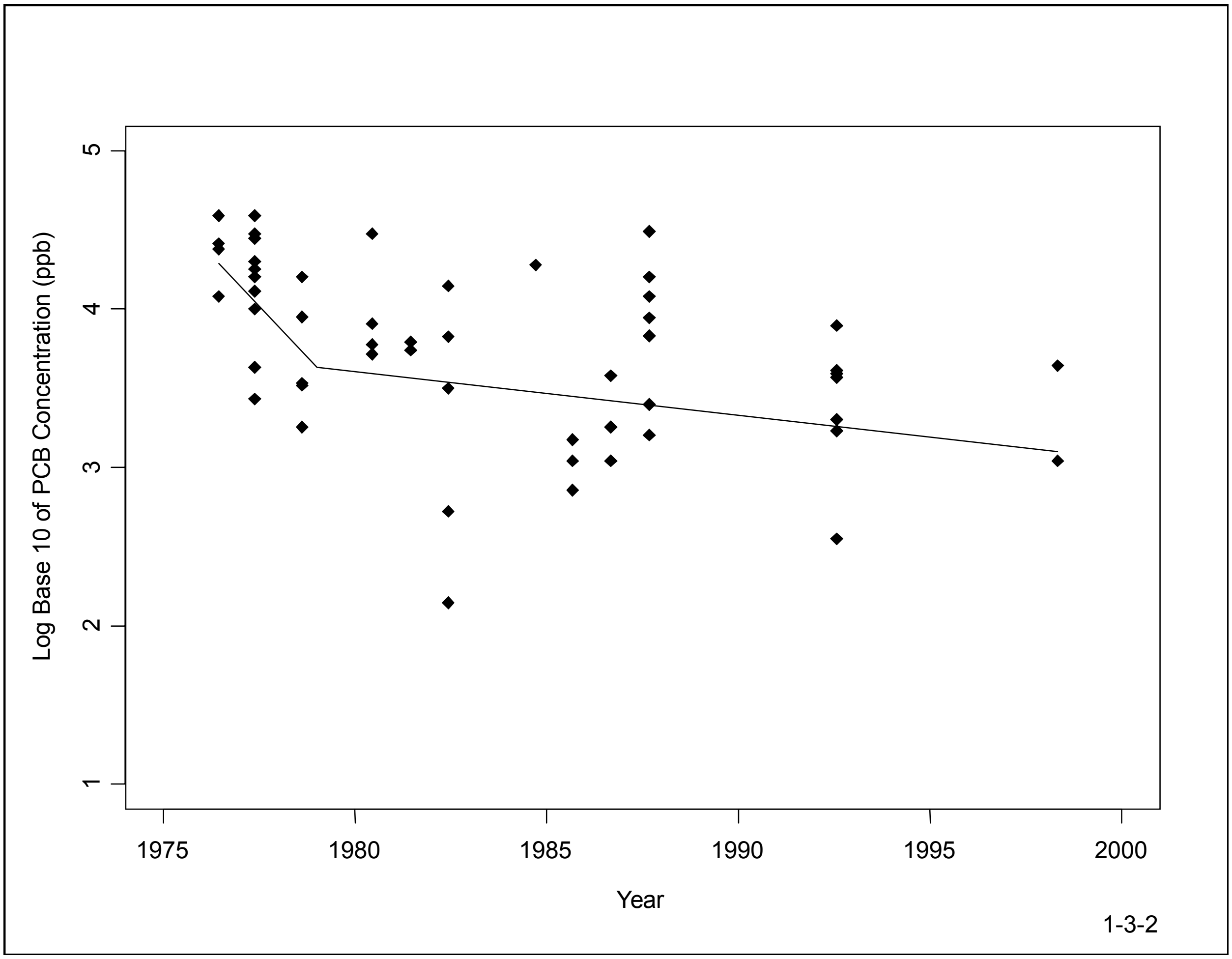

Figure A-90 Log_{10} PCB Concentration (ppb) in Little Lake Butte des Morts Carp, Skin-on Fillet, versus Time

Values at or above the detection limit are depicted as ◆.

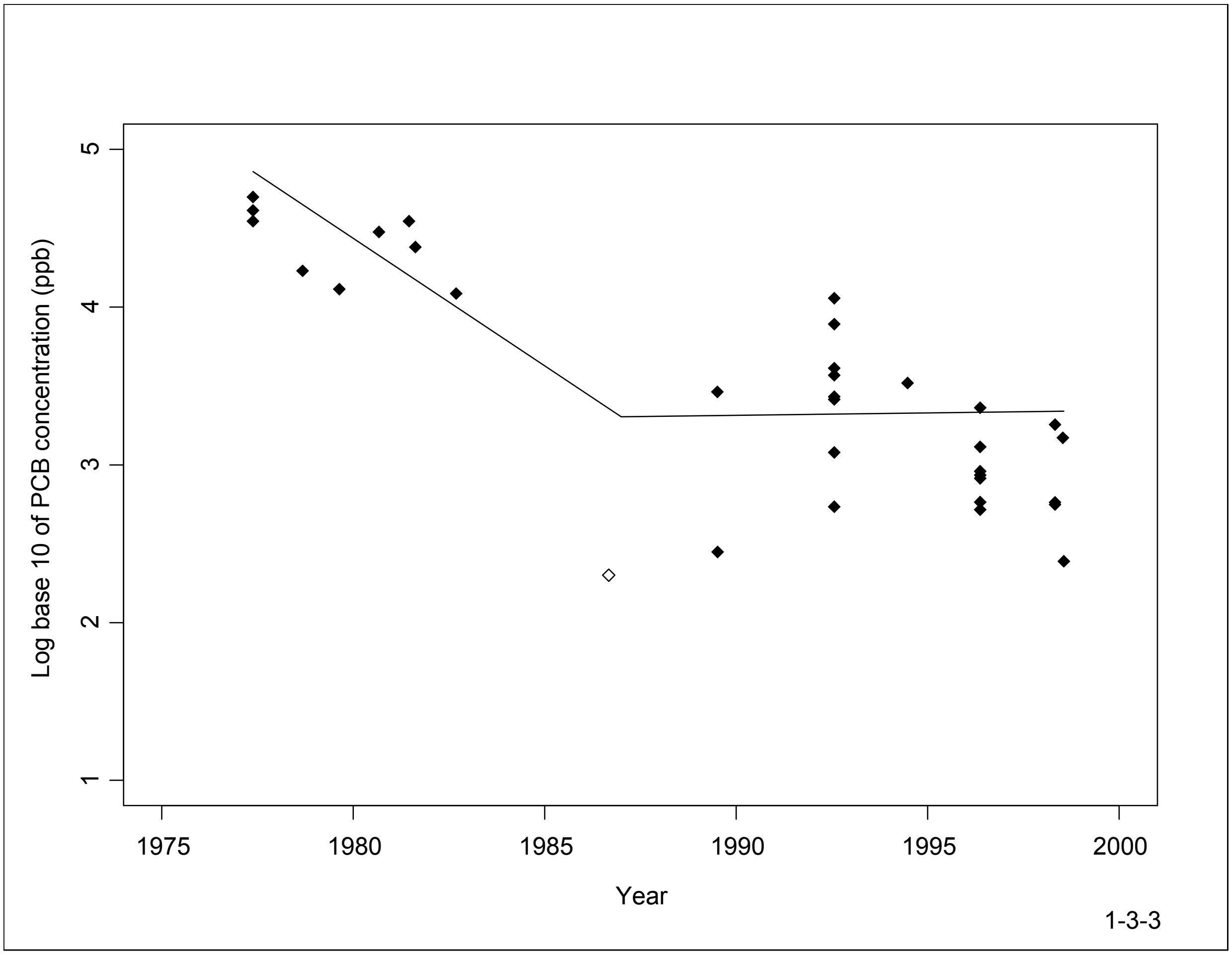

Figure A-91 Log$_{10}$ PCB Concentration (ppb) in Little Lake Butte des Morts Carp, Whole Body, versus Time

Values at or above the detection limit are depicted as ◆. Any values below detection limit are depicted as ◇.

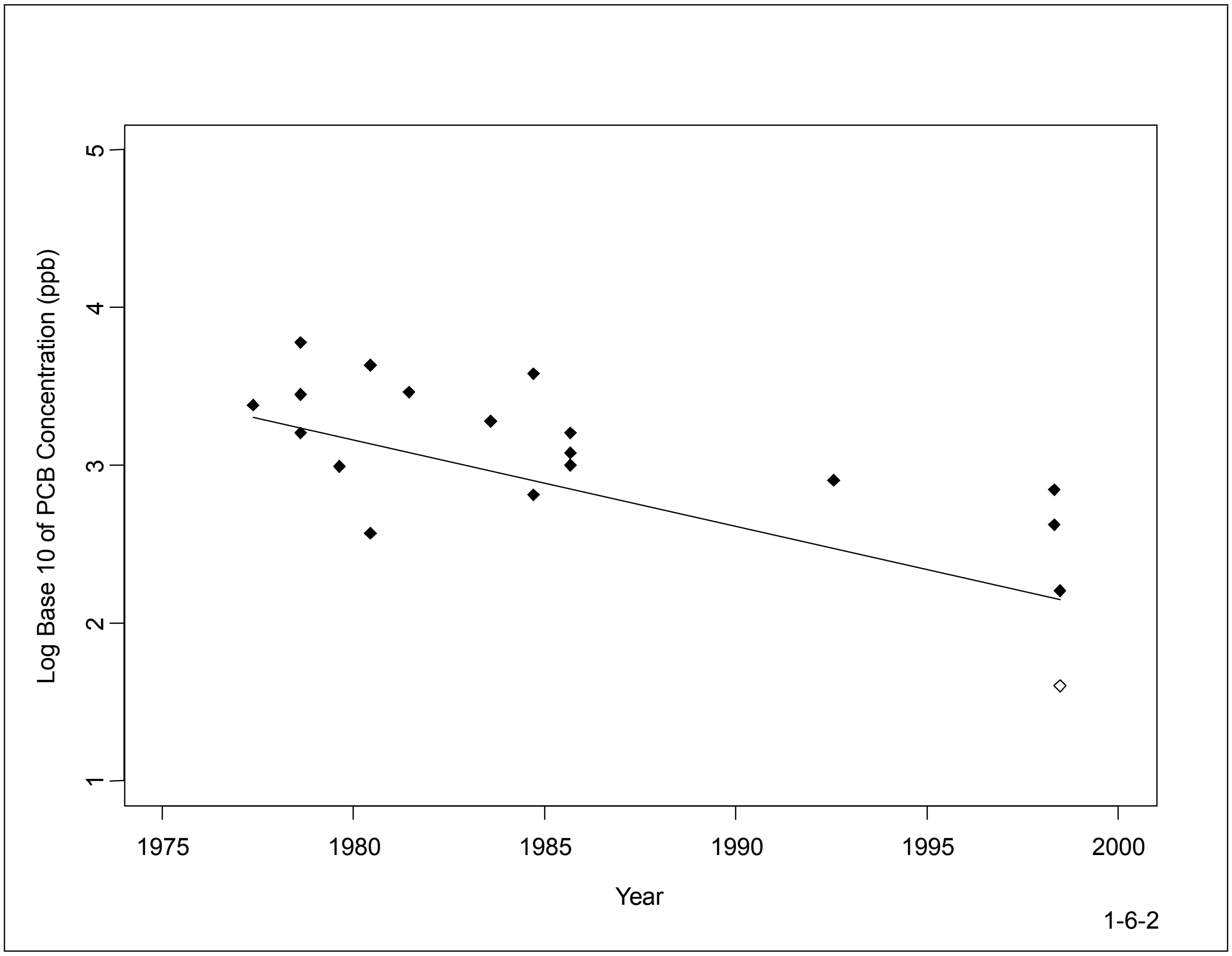

Figure A-92 Log$_{10}$ PCB Concentration (ppb) in Little Lake Butte des Morts Northern Pike, Skin-on Fillet, versus Time

Values at or above the detection limit are depicted as ◆. Any values below detection limit are depicted as ◇.

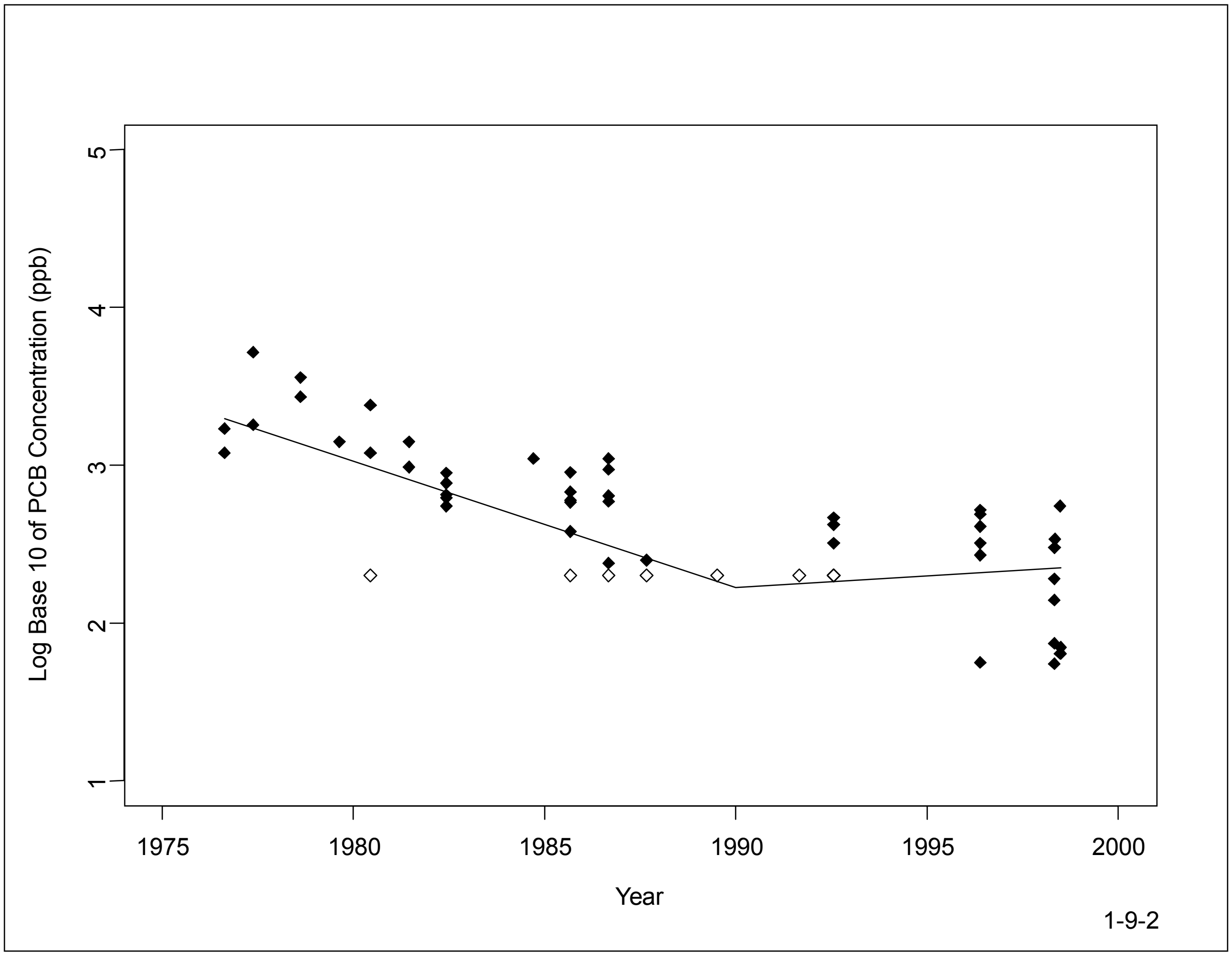

Figure A-93 Log$_{10}$ PCB Concentration (ppb) in Little Lake Butte des Morts Walleye, Skin-on Fillet, versus Time

Values at or above the detection limit are depicted as ◆. Any values below detection limit are depicted as ◇.

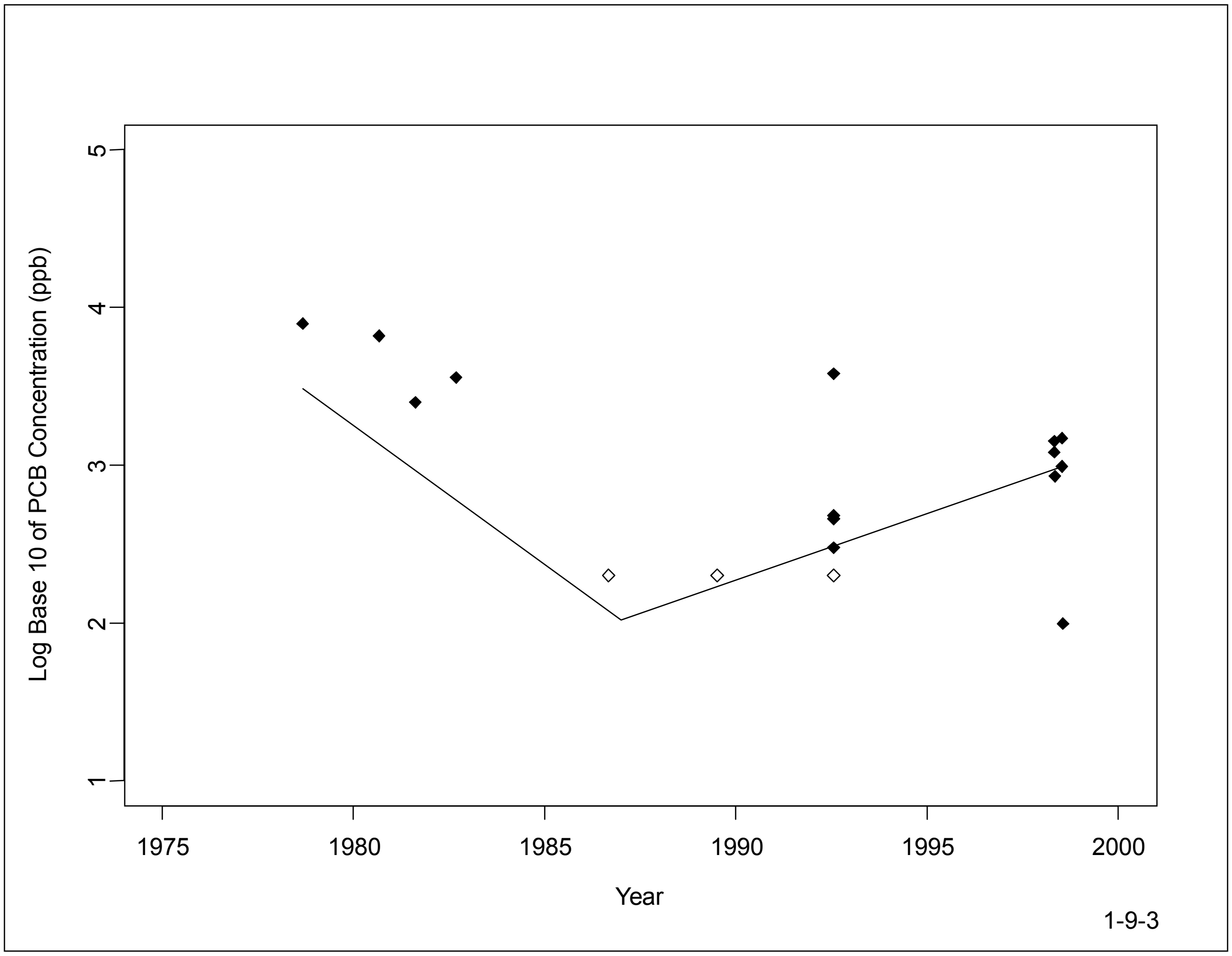

Figure A-94 Log$_{10}$ PCB Concentration (ppb) in Little Lake Butte des Morts Walleye, Whole Body, versus Time

Values at or above the detection limit are depicted as ◆. Any values below detection limit are depicted as ◇.

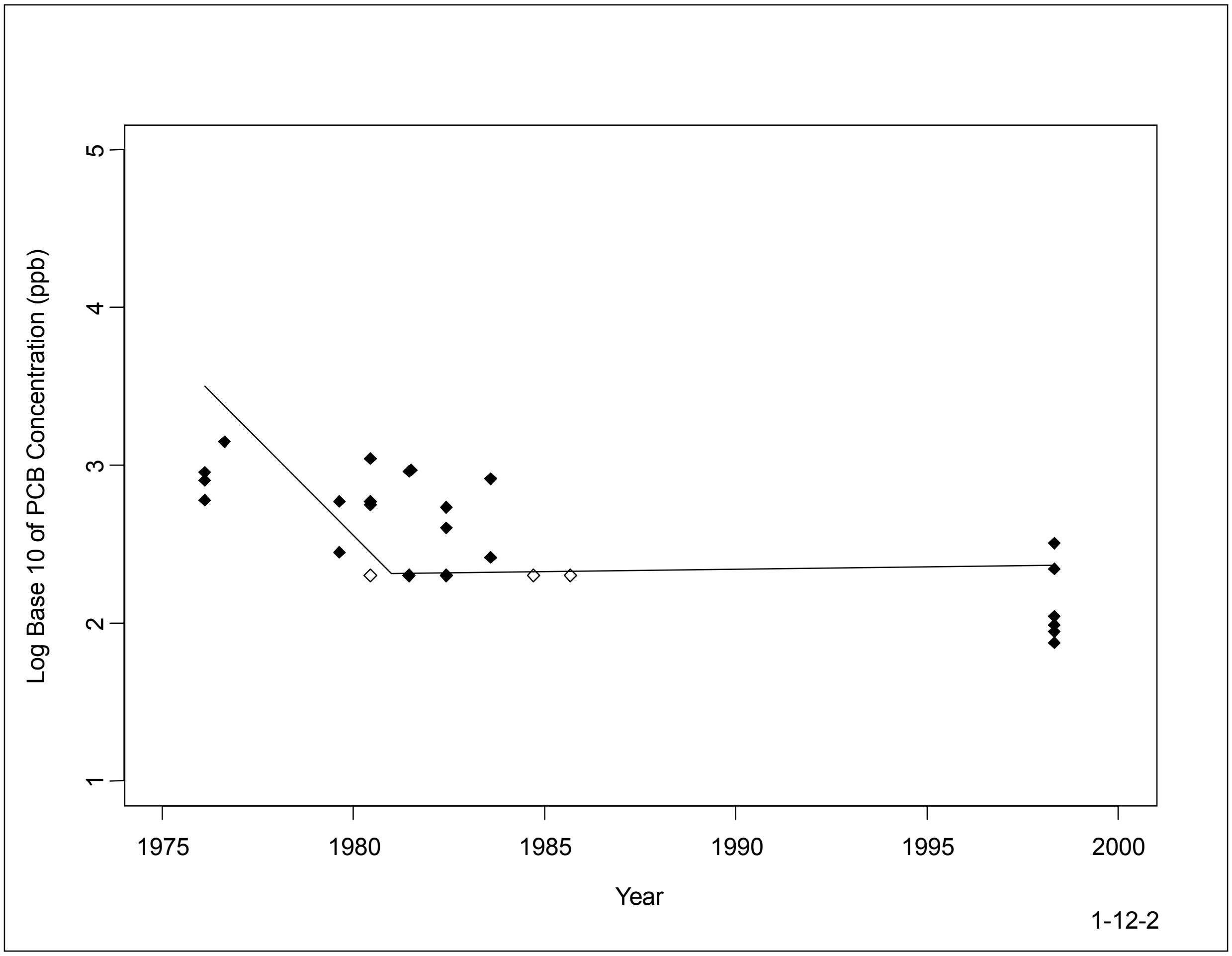

Figure A-95 Log$_{10}$ PCB Concentration (ppb) in Little Lake Butte des Morts Yellow Perch, Skin-on Fillet, versus Time

Values at or above the detection limit are depicted as ◆. Any values below detection limit are depicted as ◇.

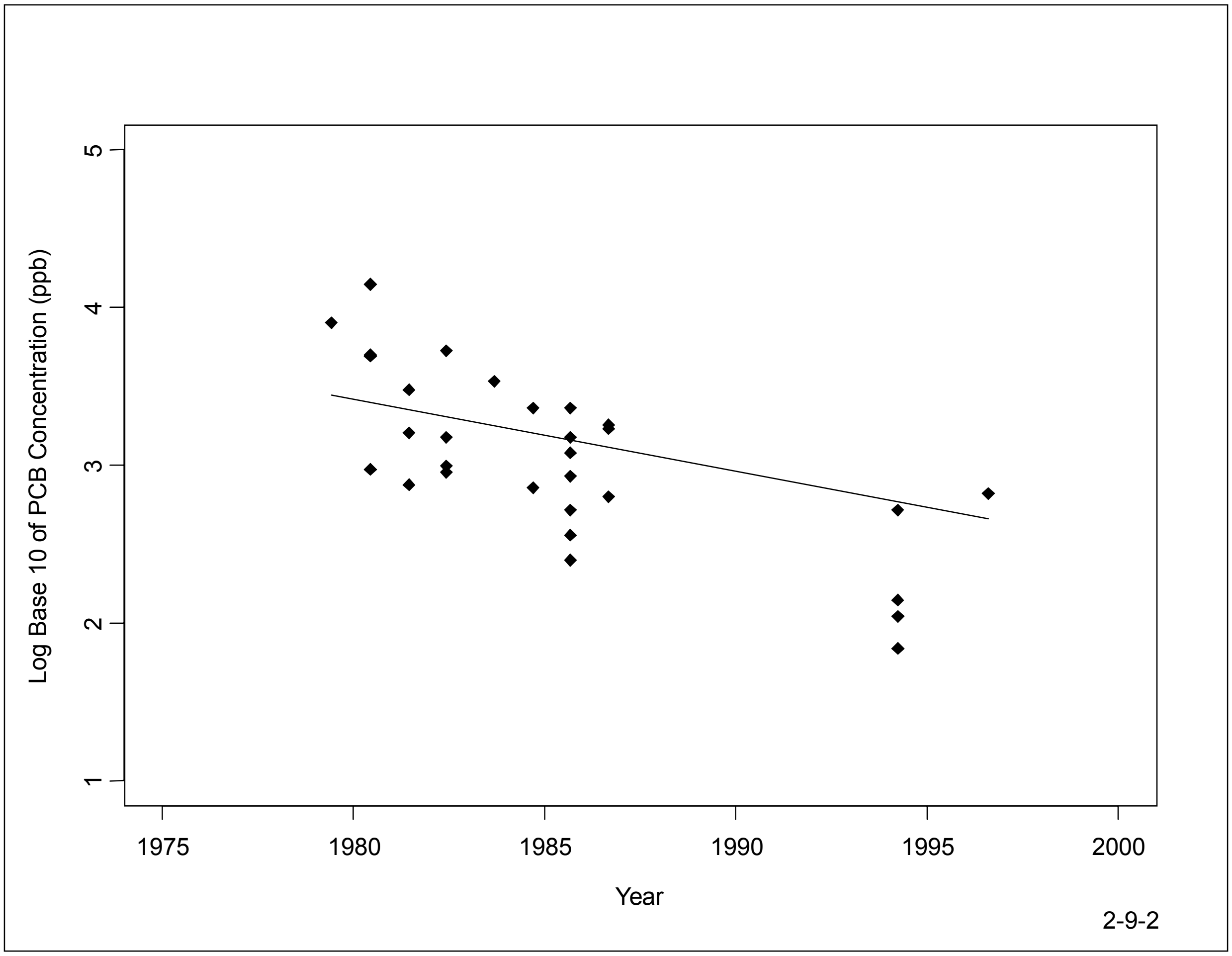

Figure A-96 Log$_{10}$ PCB Concentration (ppb) in Appleton to Little Rapids Walleye, Skin-on Fillet, versus Time

Values at or above the detection limit are depicted as ◆.

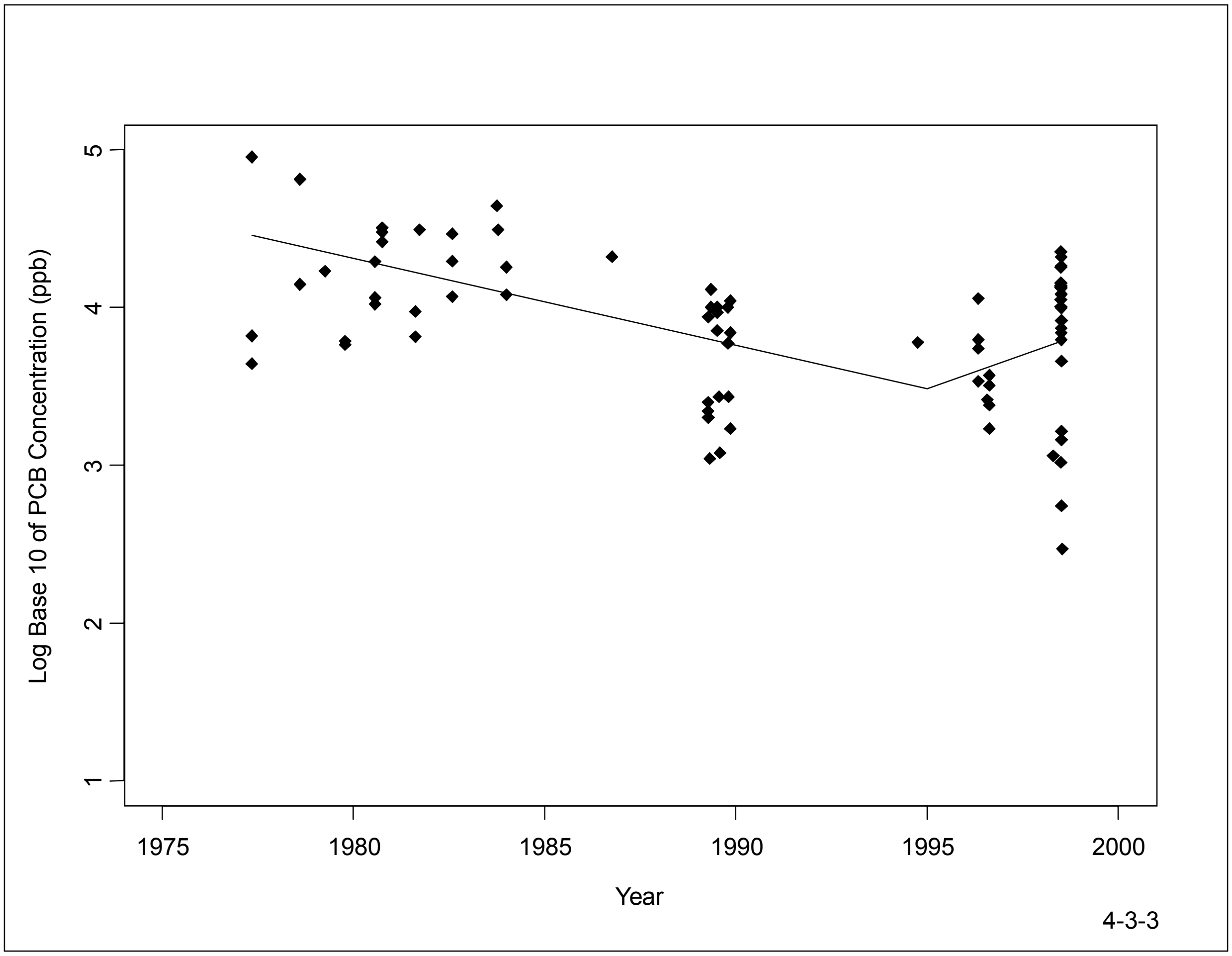

Figure A-97 Log$_{10}$ PCB Concentration (ppb) in De Pere to Green Bay Carp, Whole Body, versus Time

Values at or above the detection limit are depicted as ◆.

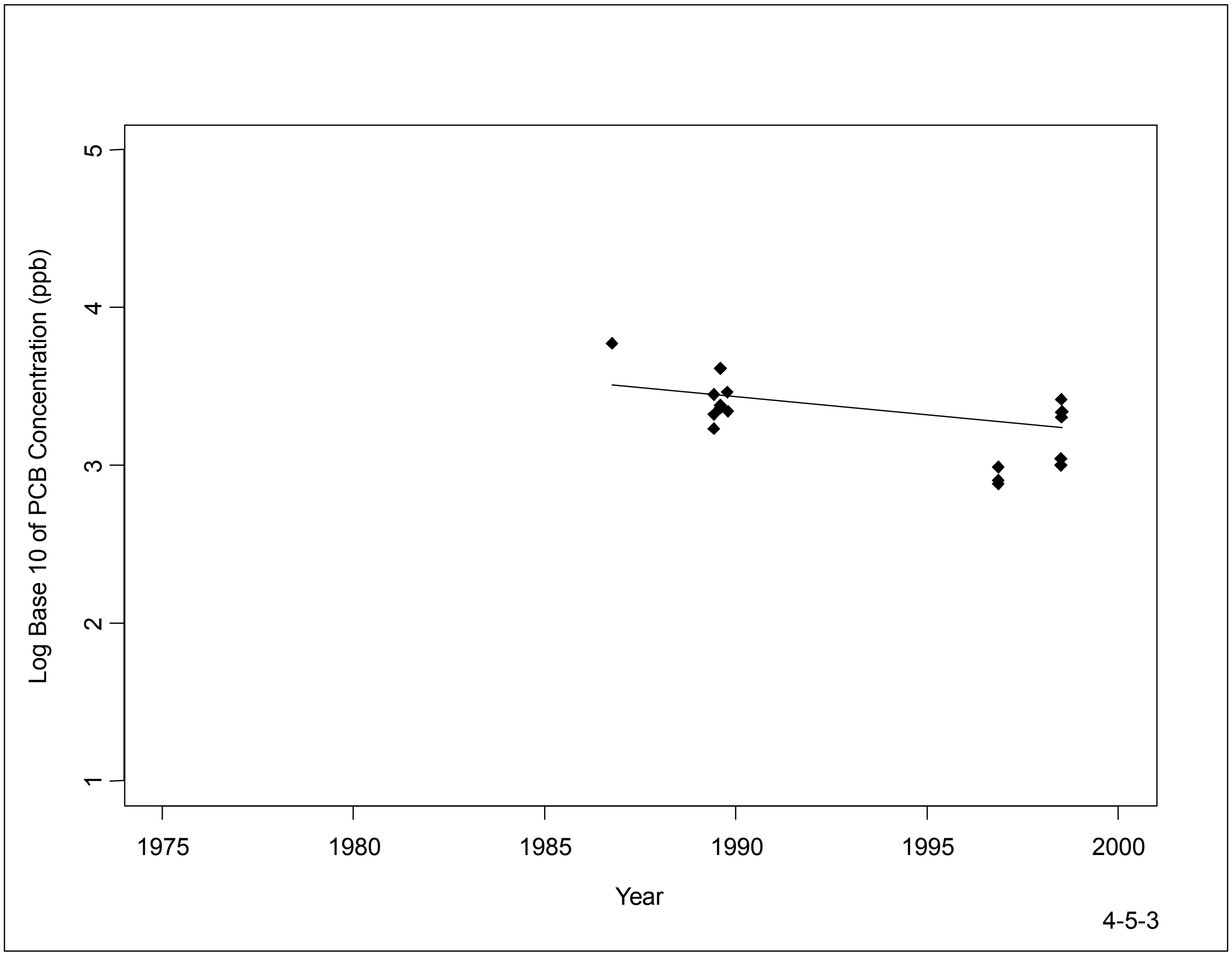

Figure A-98 Log$_{10}$ PCB Concentration (ppb) in De Pere to Green Bay Gizzard Shad, Whole Body, versus Time

Values at or above the detection limit are depicted as ◆.

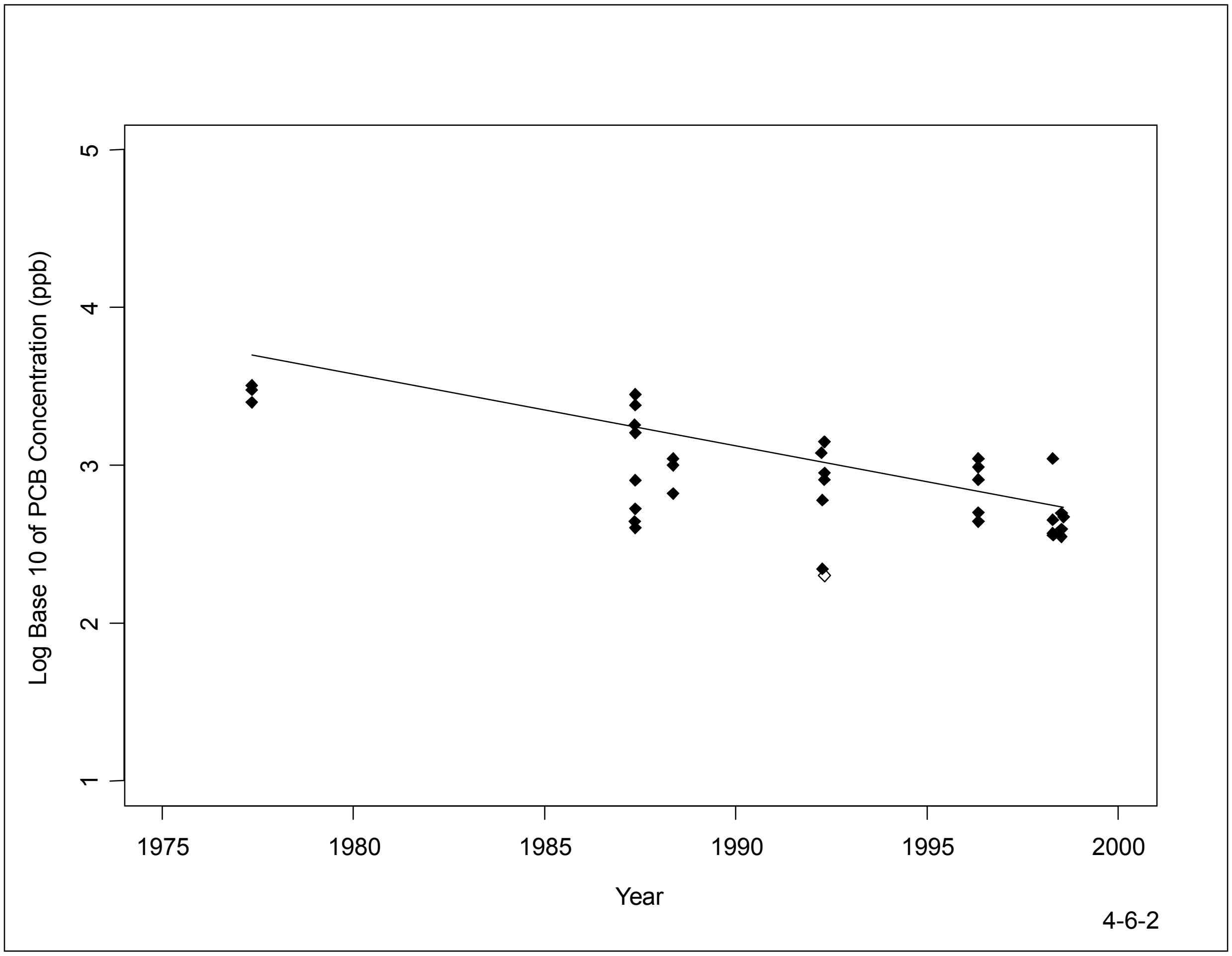

Figure A-99 Log$_{10}$ PCB Concentration (ppb) in De Pere to Green Bay Northern Pike, Skin-on Fillet, versus Time

Values at or above the detection limit are depicted as ◆. Any values below detection limit are depicted as ◇.

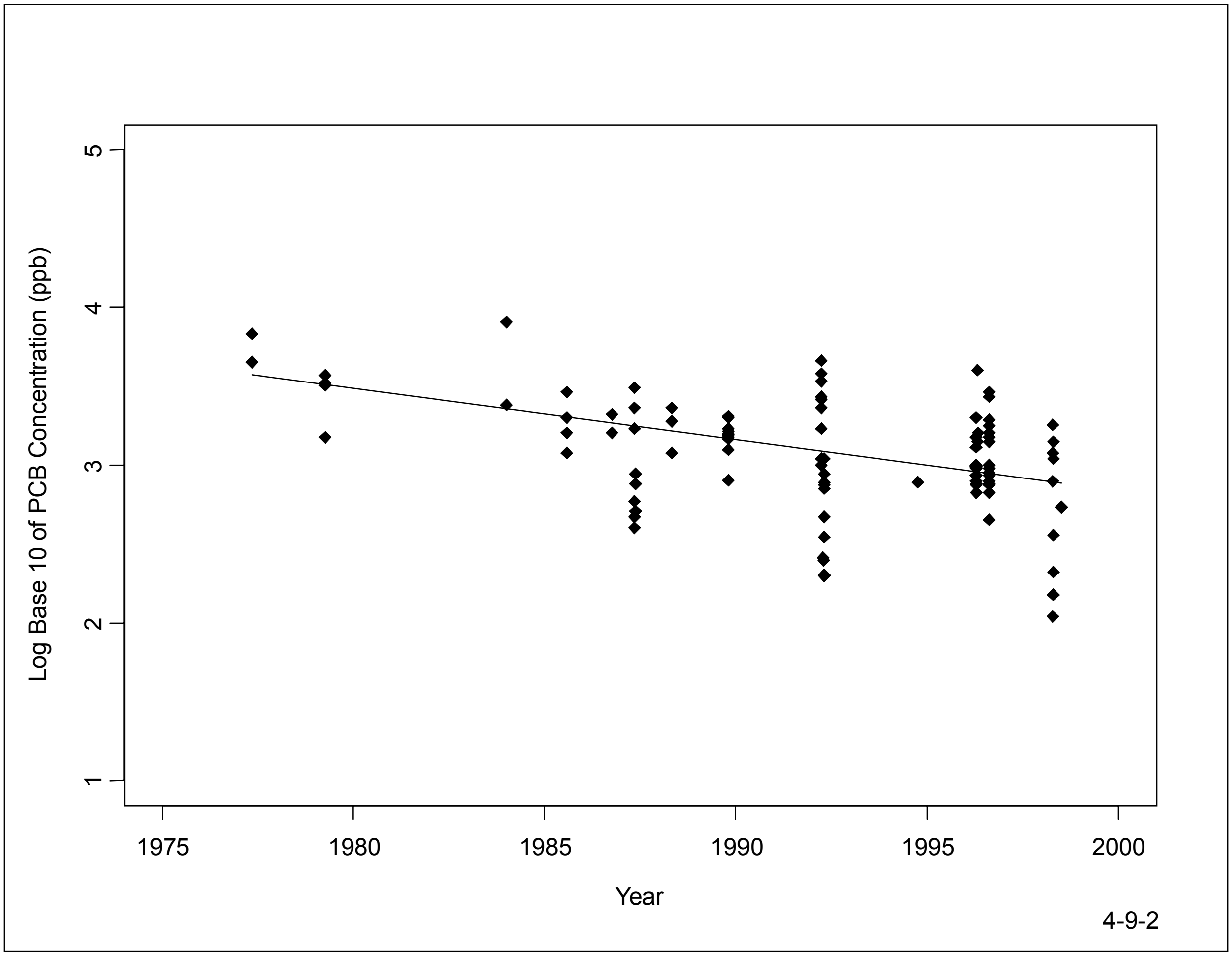

Figure A-100 Log_{10} PCB Concentration (ppb) in De Pere to Green Bay Walleye, Skin-on Fillet, versus Time

Values at or above the detection limit are depicted as ◆.

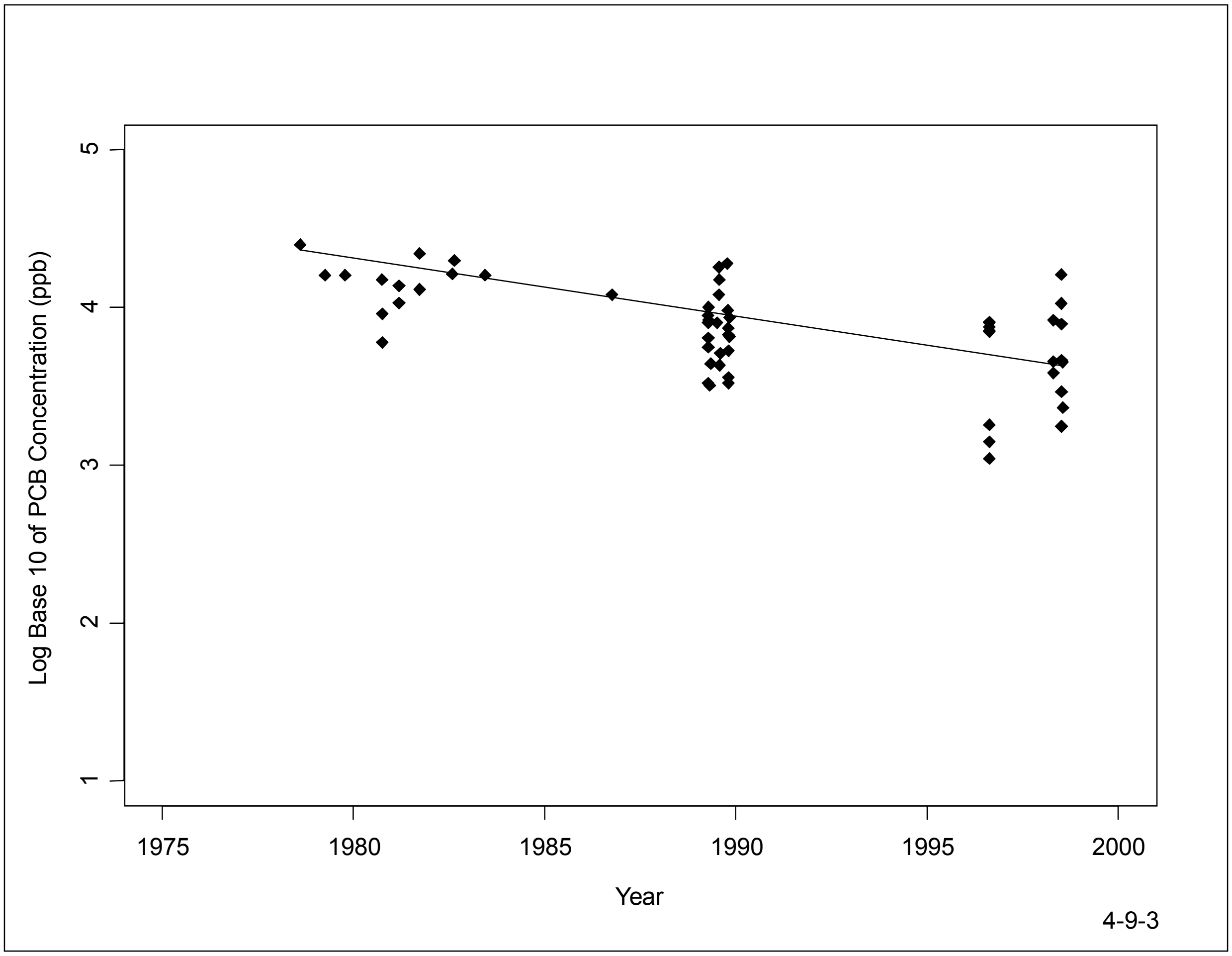

Figure A-101 Log_{10} PCB Concentration (ppb) in De Pere to Green Bay Walleye, Whole Body, versus Time

Values at or above the detection limit are depicted as ◆.

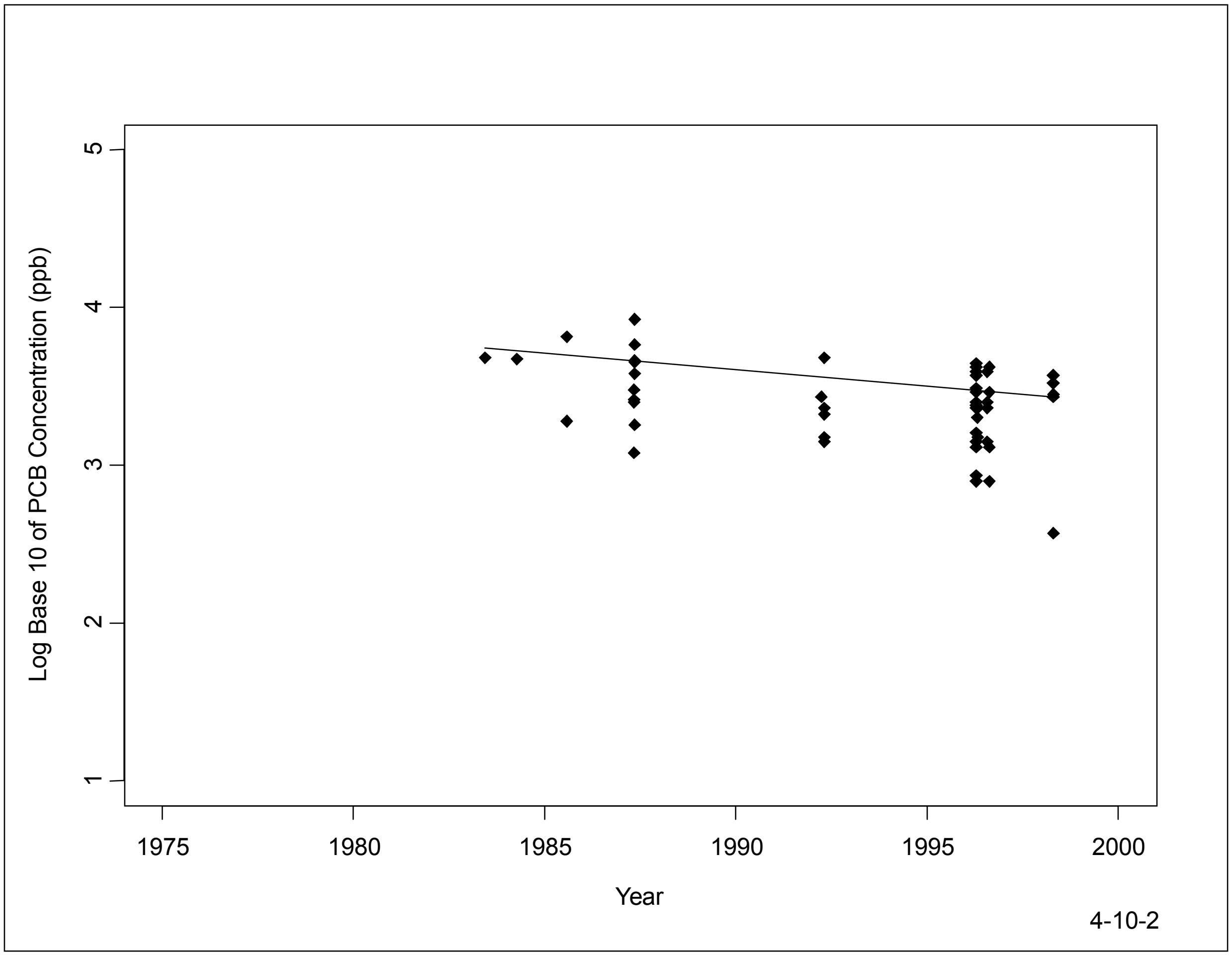

Figure A-102 Log$_{10}$ PCB Concentration (ppb) in De Pere to Green Bay White Bass, Skin-on Fillet, versus Time

Values at or above the detection limit are depicted as ◆.

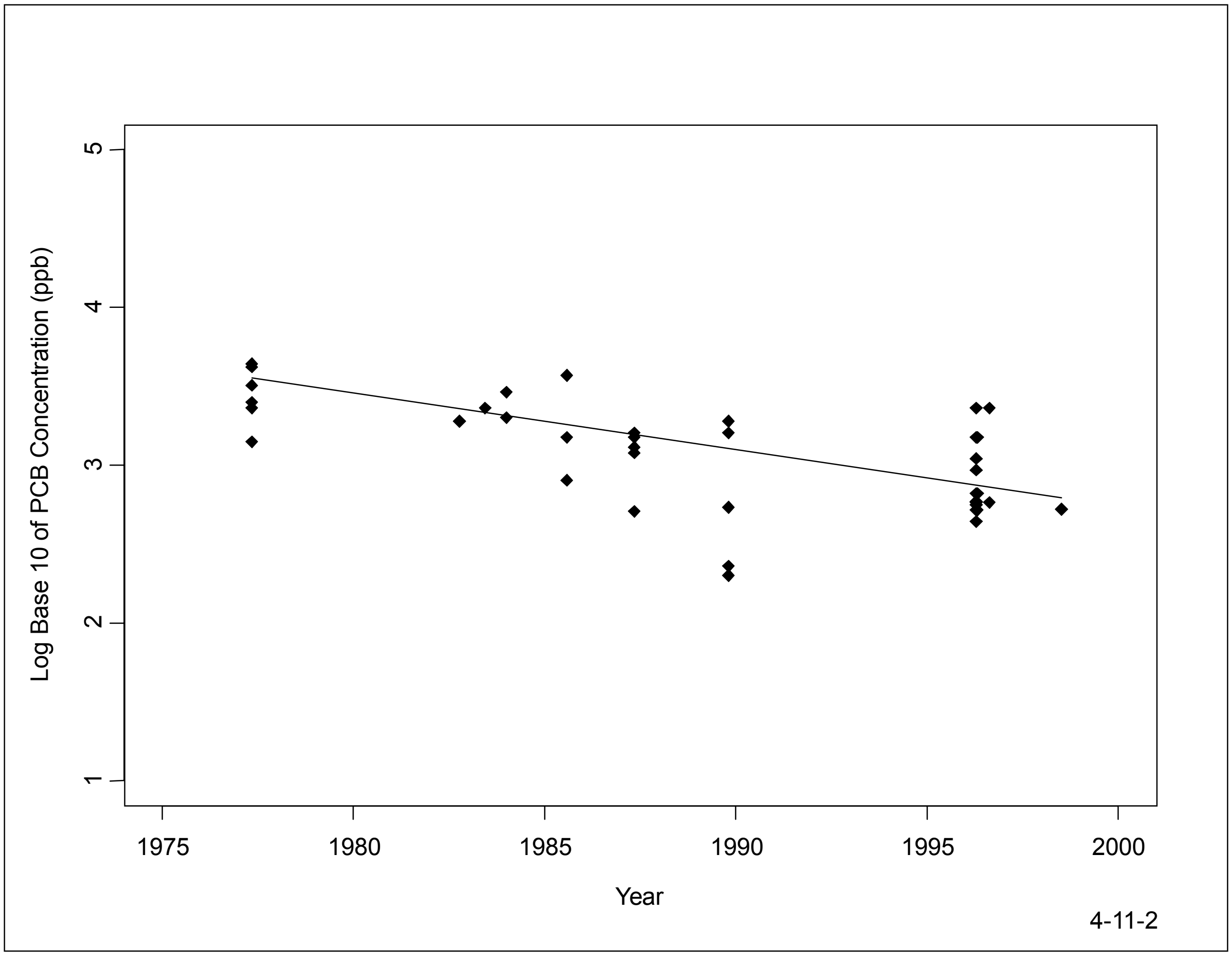

Figure A-103 Log_{10} PCB Concentration (ppb) in De Pere to Green Bay White Sucker, Skin-on Fillet, versus Time

Values at or above the detection limit are depicted as ◆.

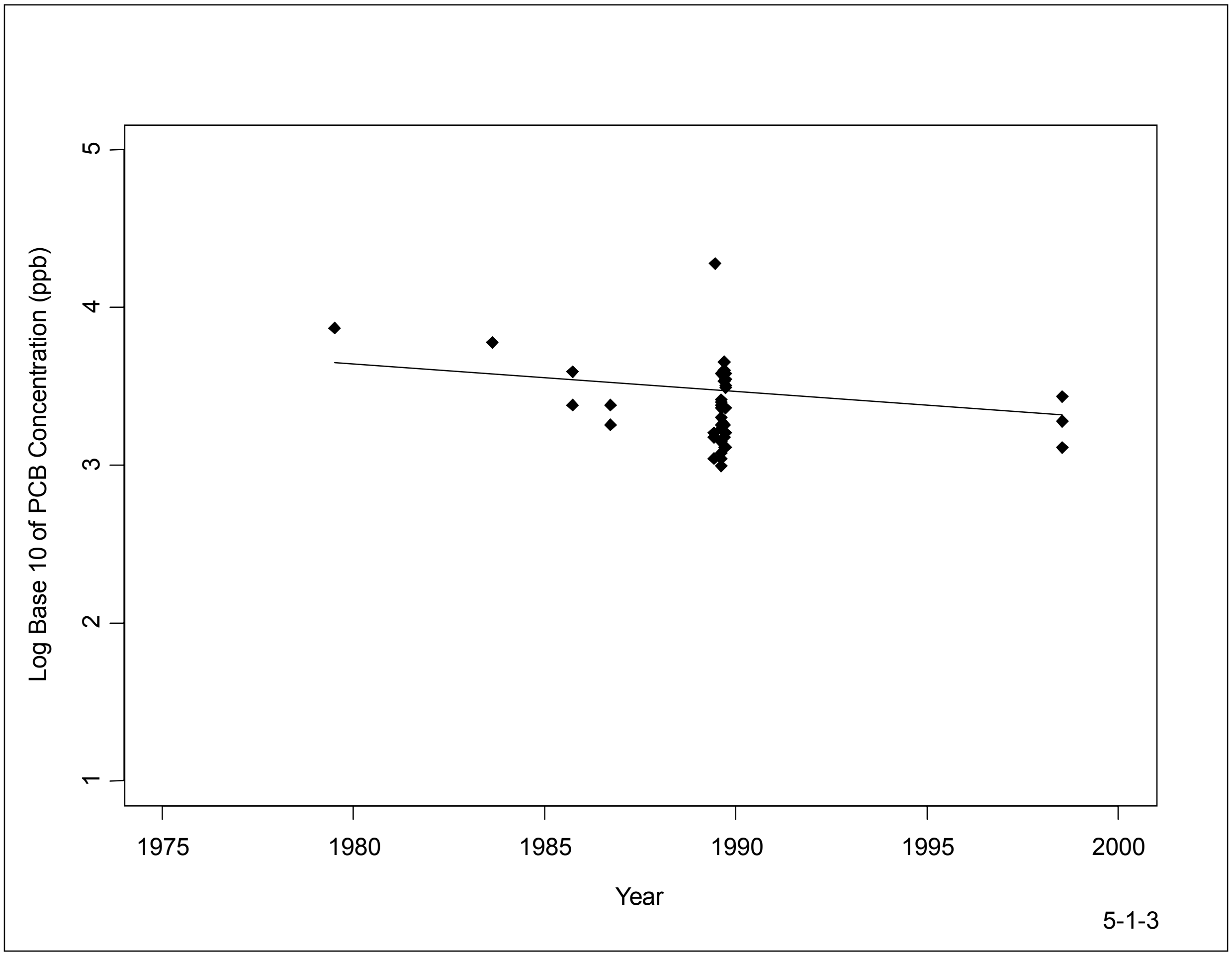

Figure A-104 Log_{10} PCB Concentration (ppb) in Green Bay Zone 2 (2A and 2B) Alewife, Skin-on Fillet, versus Time

Values at or above the detection limit are depicted as ◆.

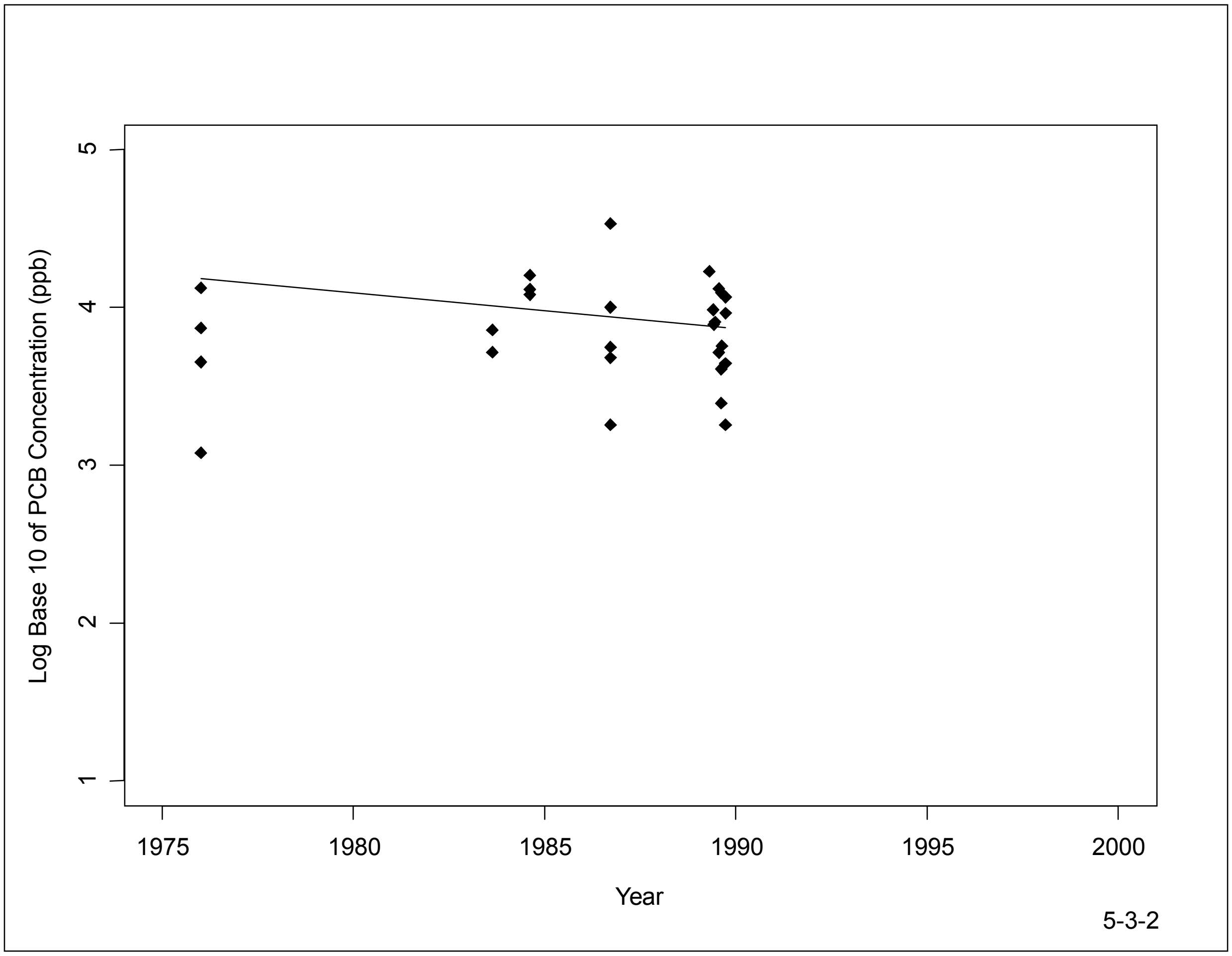

Figure A-105 Log_{10} PCB Concentration (ppb) in Green Bay Zone 2 (2A and 2B) Carp, Skin-on Fillet, versus Time

Values at or above the detection limit are depicted as ◆.

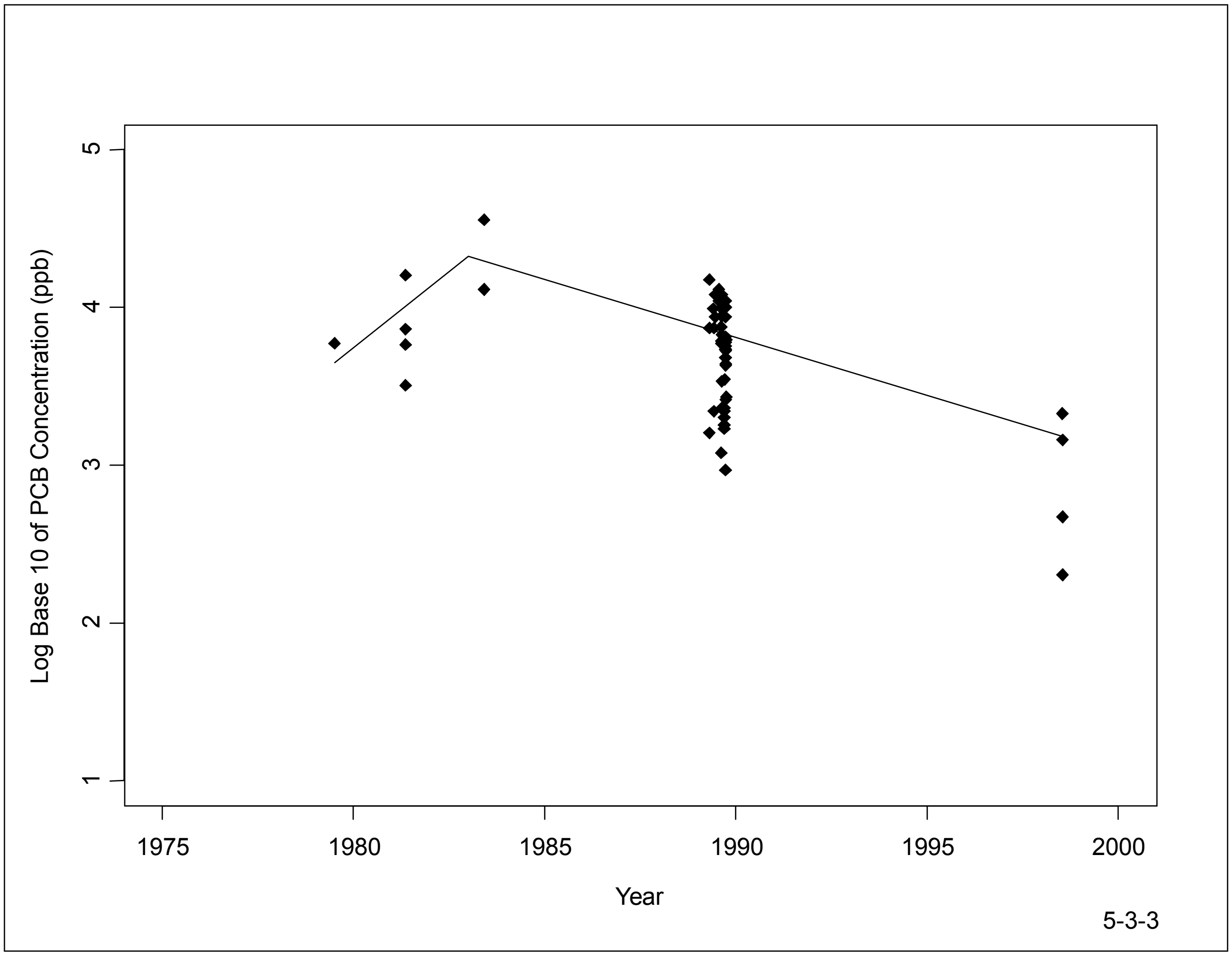

Figure A-106 Log$_{10}$ PCB Concentration (ppb) in Green Bay Zone 2 (2A and 2B) Carp, Whole Body, versus Time

Values at or above the detection limit are depicted as ◆.

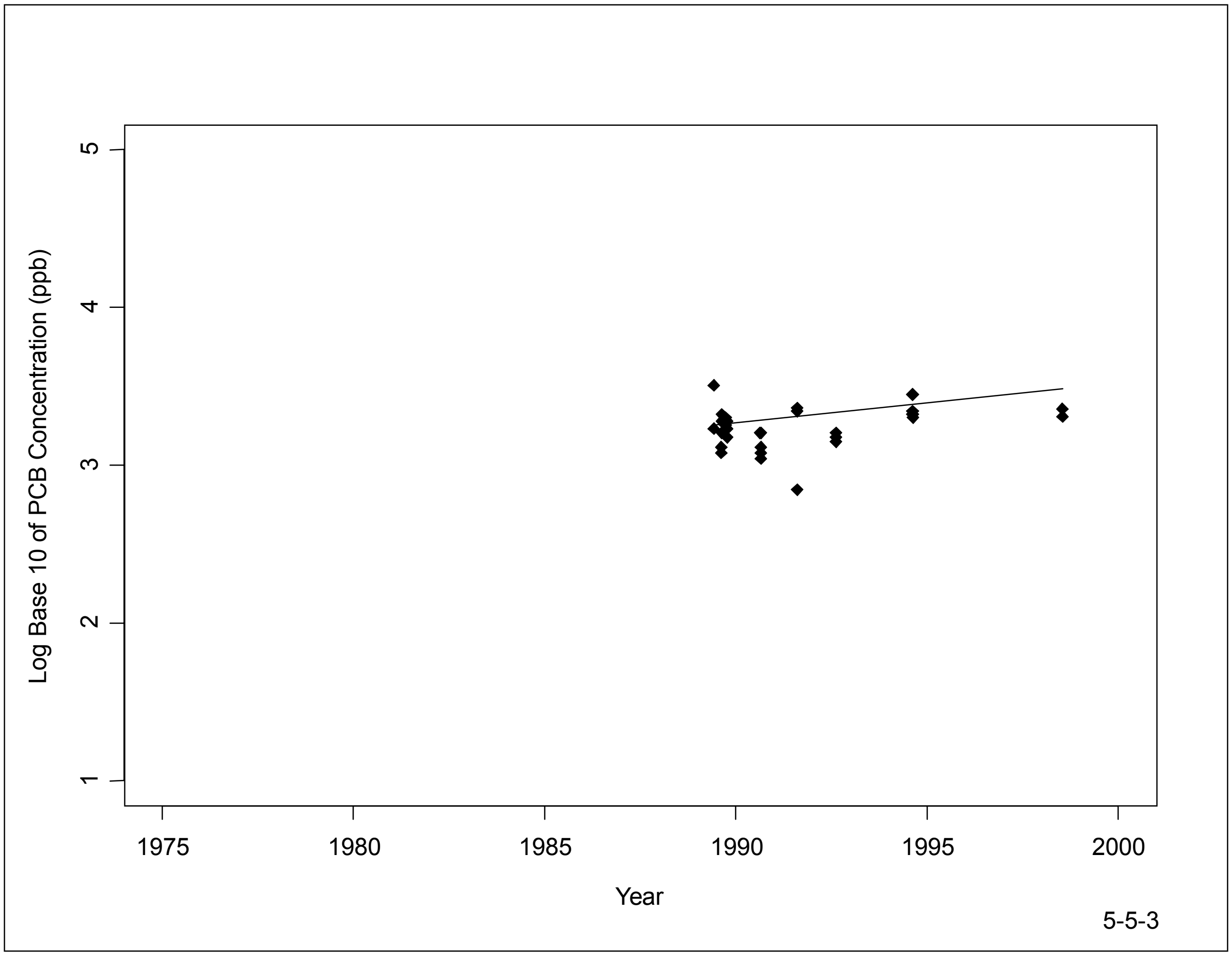

Figure A-107 Log$_{10}$ PCB Concentration (ppb) in Green Bay Zone 2 (2A and 2B) Gizzard Shad, Whole Body, versus Time

Values at or above the detection limit are depicted as ◆.

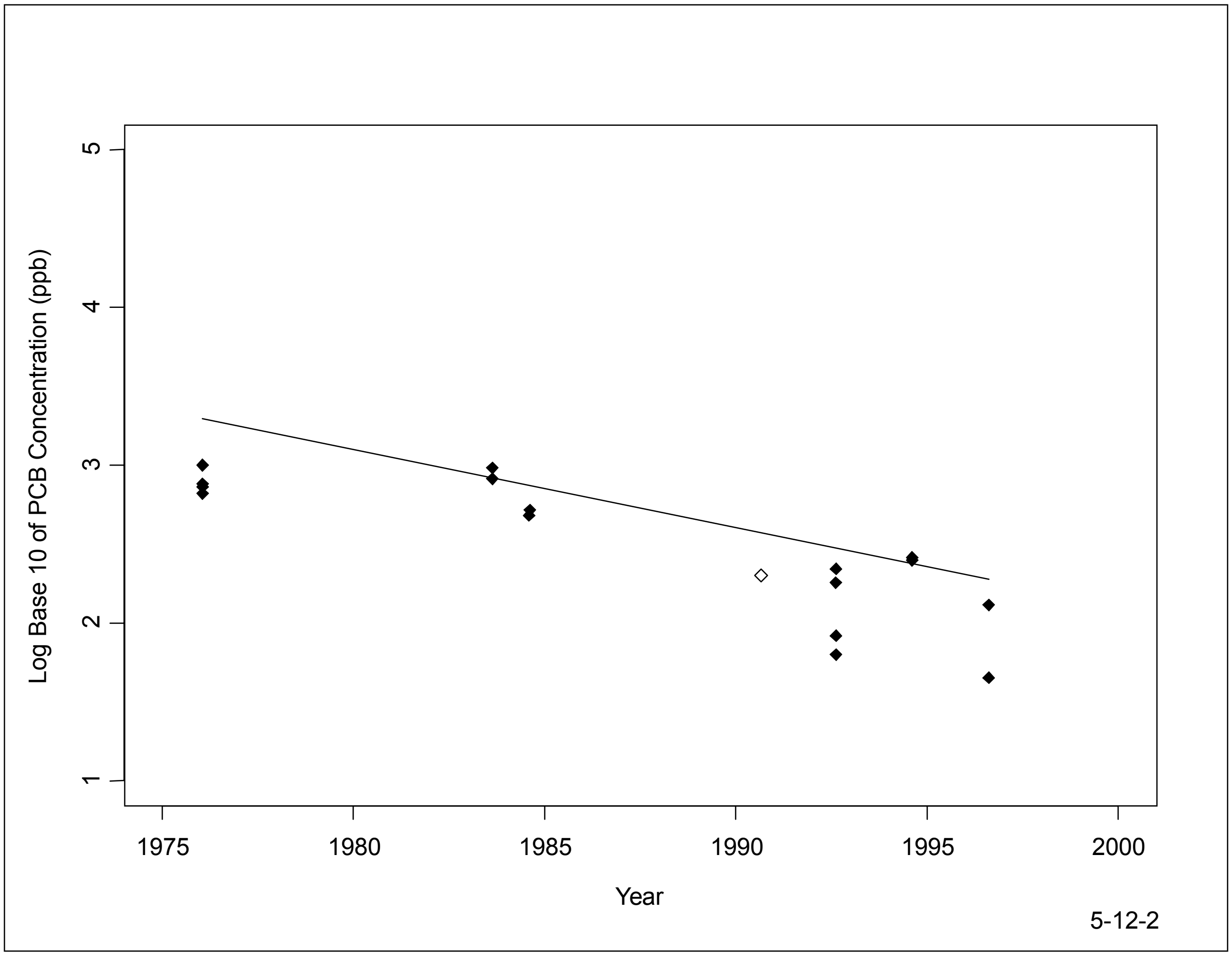

Figure A-108 Log$_{10}$ PCB Concentration (ppb) in Green Bay Zone 2 (2A and 2B) Yellow Perch, Skin-on Fillet, versus Time

Values at or above the detection limit are depicted as ◆. Any values below detection limit are depicted as ◇.

Table A-1 Details of Models Fitted to Time Trends in Sediment PCB Concentrations

Reach and Deposit Group	Depth Range (cm)	Coefficient of Log_{10}(PCB) Slope of Time Trend, Log Scale	WSEV Std. Err. of Slope	WSEV 95% Confidence Interval for Slope: Lower Limit	WSEV 95% Confidence Interval for Slope: Upper Limit	WSEV *p*-value	*p* < 0.05	Core-averaged: Sample Size	Core-averaged: # Censored	Core-averaged: % Censored	Est. Ann. % Change in PCB Conc.	Est. Ann. % Change in PCB Conc.: 95% CI Lower-bound	Est. Ann. % Change in PCB Conc.: 95% CI Upper-bound	WSEV Grid Size: Minimum (meters)	WSEV Grid Size: Northing (meters)	WSEV Grid Size: Easting (meters)	WSEV # Non-empty Grid Cells	Fitted Model Form
Little Lake Butte des Morts																		
AB	0–10	-0.0970	0.0348	-0.1708	-0.0233	0.0131	*	67	0	0	-20.0	-32.5	-5.2	110	156	110	16	quadratic
	10–30	-0.0213	0.0647	-0.1795	0.1370	0.7535		105	13	12	-4.8	-33.9	37.1	137	294	137	6	quadratic
	30–50	-0.0144	0.1113	-0.2593	0.2305	0.8995		54	28	52	-3.3	-45.0	70.0	103	153	103	11	quadratic
C	0–10	-0.0612	0.0342	-0.1563	0.0338	0.1481		13	0	0	-13.2	-30.2	8.1	101	158	101	4	quadratic
	10–30	0.0317	0.0770	-0.1820	0.2454	0.7018		15	5	33	7.6	-34.2	76.0	94	158	94	4	linear
POG	0–10	-0.0893	0.0567	-0.2467	0.0680	0.1900		13	0	0	-18.6	-43.3	16.9	363	363	367	4	quadratic
D	0–10	-0.0755	0.0317	-0.1430	-0.0080	0.0307	*	18	1	6	-16.0	-28.1	-1.8	34	111	34	15	quadratic
	10–30	0.3168	0.0454	0.2001	0.4335	0.0009	*	15	2	13	107.4	58.5	171.3	109	333	109	5	linear
F	0–10	-0.0373	0.0136	-0.0686	-0.0060	0.0252	*	29	1	3	-8.2	-14.6	-1.4	401	401	437	8	quadratic
	10–30	-0.0760	0.0749	-0.2341	0.0821	0.3246		28	9	32	-16.1	-41.7	20.8	172	191	172	17	quadratic
GH	0–10	-0.1244	0.0541	-0.2450	-0.0038	0.0443	*	15	0	0	-24.9	-43.1	-0.9	277	277	336	10	linear
Appleton																		
IMOR	0–10	0.0412	0.0255	-0.0295	0.1119	0.1810		18	1	6	9.9	-6.6	29.4	726	726	1,754	4	linear
N Pre-dredge	0–10	-0.0281	0.0065	-0.0489	-0.0072	0.0233	*	32	0	0	-6.3	-10.6	-1.7	43	43	197	3	quadratic
	10–30	0.0572	0.0440	-0.0338	0.1482	0.2061		27	1	4	14.1	-7.5	40.7	9	9	33	23	quadratic
	30–50	0.0846	0.0932	-0.1262	0.2954	0.3877		17	1	6	21.5	-25.2	97.4	17	17	68	9	quadratic
VCC	0–10	-0.0582	0.0275	-0.1287	0.0124	0.0878		41	4	10	-12.5	-25.7	2.9	1,116	1,286	1,116	5	quadratic
	10–30	-0.1537	0.0164	-0.1899	-0.1176	0.0000	*	34	21	62	-29.8	-35.4	-23.7	393	456	393	11	quadratic
	30–50	-0.0060	0.0151	-0.0396	0.0276	0.6984		17	14	82	-1.4	-8.7	6.6	285	341	285	10	linear
Little Rapids																		
Upper EE	0–10	-0.0447	0.0435	-0.1655	0.0760	0.3618		31	0	0	-9.8	-31.7	19.1	721	798	721	4	quadratic
	10–30	-0.0944	0.0429	-0.1914	0.0027	0.0554		25	6	24	-19.5	-35.6	0.6	288	291	288	9	quadratic
	30–50	-0.0712	0.0536	-0.1925	0.0502	0.2173		13	6	46	-15.1	-35.8	12.2	199	199	206	9	linear
Lower EE	0–10	-0.0682	0.0193	-0.1297	-0.0067	0.0387	*	30	2	7	-14.5	-25.8	-1.5	468	823	468	3	quadratic
	10–30	-0.0759	0.0390	-0.1585	0.0068	0.0695		33	16	48	-16.0	-30.6	1.6	104	183	104	16	quadratic
	30–50	0.0900	0.0330	0.0164	0.1635	0.0213	*	13	5	38	23.0	3.9	45.7	94	200	94	10	quadratic
FF	0–10	-0.0549	0.0557	-0.1735	0.0638	0.3400		32	4	13	-11.9	-32.9	15.8	110	151	110	15	quadratic
	10–30	-0.0962	0.0390	-0.1861	-0.0063	0.0389	*	31	12	39	-19.9	-34.9	-1.4	253	340	253	8	quadratic
GGHH	0–10	-0.0394	0.0231	-0.1036	0.0249	0.1643		49	0	0	-8.7	-21.2	5.9	392	732	392	4	quadratic
	10–30	-0.0182	0.0596	-0.1410	0.1047	0.7631		45	2	4	-4.1	-27.7	27.3	83	163	83	25	quadratic
	30–50	0.1762	0.1008	-0.0564	0.4087	0.1188		75	9	12	50.0	-12.2	156.3	191	384	191	8	quadratic
	50–100	0.1012	0.0700	-0.0417	0.2441	0.1586		54	12	22	26.2	-9.2	75.4	76	157	76	30	quadratic
	100+	0.0365	0.0249	-0.0155	0.0884	0.1587		36	16	44	8.8	-3.5	22.6	84	157	84	20	quadratic
De Pere																		
SMU Group 2025	0–10	-0.0528	0.0231	-0.1168	0.0112	0.0838		43	0	0	-11.4	-23.6	2.6	529	529	602	4	quadratic
	10–30	-0.0556	0.0750	-0.2285	0.1173	0.4796		31	5	16	-12.0	-40.9	31.0	353	353	402	8	quadratic
	30–50	-0.0580	0.0322	-0.1296	0.0137	0.1016		13	0	0	-12.5	-25.8	3.2	200	200	209	10	linear
	50–100	-0.0847	0.1058	-0.3025	0.1331	0.4306		30	9	30	-17.7	-50.2	35.9	118	118	132	25	quadratic
2649	0–10	-0.0608	0.0109	-0.0831	-0.0385	0.0000	*	66	1	2	-13.1	-17.4	-8.5	207	308	207	29	quadratic
	10–30	-0.2882	0.1440	-0.6140	0.0376	0.0764		48	5	10	-48.5	-75.7	9.0	466	694	466	9	quadratic
	50–100	0.1957	0.1419	-0.1982	0.5896	0.2399		46	8	17	56.9	-36.6	288.7	931	1,251	931	4	quadratic
	100+	0.0177	0.1548	-0.4122	0.4476	0.9146		45	10	22	4.2	-61.3	180.3	882	1,217	882	4	quadratic
5067	0–10	-0.0998	0.0345	-0.1751	-0.0245	0.0136	*	57	1	2	-20.5	-33.2	-5.5	168	258	168	12	quadratic
	10–30	0.0912	0.0649	-0.0470	0.2295	0.1800		51	1	2	23.4	-10.3	69.6	124	215	124	15	quadratic
	50–100	0.3677	0.0684	0.1918	0.5435	0.0030	*	48	0	0	133.2	55.5	249.5	248	430	248	5	quadratic
	100+	-0.1963	0.2223	-0.7402	0.3476	0.4112		50	7	14	-36.4	-81.8	122.6	174	390	174	6	quadratic
6891	0–10	-0.2208	0.0944	-0.5212	0.0796	0.1013		20	1	5	-39.9	-69.9	20.1	344	1,051	344	3	quadratic
	10–30	-0.1685	0.0765	-0.3415	0.0044	0.0550		18	2	11	-32.2	-54.4	1.0	138	420	138	9	quadratic
92115	0–10	0.0413	0.0426	-0.0502	0.1327	0.3493		27	0	0	10.0	-10.9	35.8	142	393	142	14	quadratic

Table A-1 Details of Models Fitted to Time Trends in Sediment PCB Concentrations

Reach and Deposit Group	Depth Range (cm)	R-squared			Sill Distance	Intercept Parameter Est.	WSEV Std. Err. of Intercept	Std. Err. of Intercept Based on Independence	Skewness of Untransformed PCB Conc.	Skewness of Log_{10}(PCB) Conc.	PCB Mass (kg)	Normal Scale (Std. Dev.) Est.
		Geographic Variables Only	Geographic + Time	Change Due to Time								
Little Lake Butte des Morts												
AB	0–10	0.47	0.55	0.08	25	4.4461	0.3237	0.2788	1.74	-1.13	71.7	0.465933
	10–30	0.17	0.17	0.00	25	4.0797	0.8357	0.6054	3.37	-0.09	217.7	1.02534
	30–50	0.36	0.37	0.01	0	10.4324	2.8100	2.1917	4.52	1.03	328.3	1.1568
C	0–10	0.27	0.47	0.21	25	5.2096	1.2084	1.0586	1.97	0.19	25.4	0.336235
	10–30	0.55	0.69	0.14	25	5.0070	1.4441	1.3930	2.80	0.76	14.6	0.897603
POG	0–10	0.61	0.71	0.10	75	4.4765	0.5067	0.4769	1.33	0.34	113.5	0.425786
D	0–10	0.67	0.78	0.10	0	3.8807	0.6868	0.3776	1.92	-1.18	32.1	0.2376
	10–30	0.19	0.80	0.61	0	2.2285	0.5288	0.5202	2.96	-0.25	55.5	0.397127
F	0–10	0.24	0.30	0.05	50	3.5528	0.3827	0.4099	2.40	-0.52	142.5	0.520421
	10–30	0.23	0.31	0.08	50	2.2040	1.3533	1.0844	5.15	0.97	180.1	0.789297
GH	0–10	0.02	0.61	0.59	0	3.1032	0.3153	0.3176	0.14	-1.27	15.7	0.439535
Appleton												
IMOR	0–10	0.09	0.41	0.32	0	3.1269	0.4735	0.4747	3.44	0.31	6.9	0.583018
N Pre-dredge	0–10	0.68	0.70	0.02	0	4.2292	0.4199	0.3549	1.14	-0.52	6.9	0.326511
	10–30	0.43	0.48	0.05	50	3.7450	0.6539	0.6366	2.66	-0.98	11.5	0.615759
	30–50	0.49	0.56	0.07	10	4.4070	1.5119	1.2267	1.00	-2.56	4.9	0.570745
VCC	0–10	0.14	0.31	0.17	0	3.2202	0.3490	0.2537	2.55	0.34	5.2	0.524406
	10–30	0.12	0.56	0.44	0	4.1303	0.6783	0.7806	4.76	0.99	2.9	0.734058
	30–50	0.46	0.52	0.06	0	4.4304	0.5727	0.5713	1.05	0.06	0.9	0.11942
Little Rapids												
Upper EE	0–10	0.09	0.16	0.06	0	3.2722	0.7469	0.4948	3.43	0.21	85.0	0.58418
	10–30	0.17	0.38	0.22	0	2.5703	1.1521	0.8651	4.06	0.51	46.4	0.822143
	30–50	0.03	0.24	0.22	200	4.7214	1.3448	1.7186	3.44	0.77	4.3	0.678349
Lower EE	0–10	0.36	0.52	0.16	0	2.9308	0.2663	0.3268	3.68	0.37	25.4	0.486326
	10–30	0.17	0.40	0.23	0	2.8576	0.7657	0.9180	4.97	0.80	13.2	0.96465
	30–50	0.47	0.56	0.09	0	5.0328	0.9549	1.1745	1.76	0.26	4.6	0.357574
FF	0–10	0.15	0.20	0.05	0	3.7208	0.3852	0.4231	1.52	-0.24	36.7	0.83476
	10–30	0.07	0.25	0.18	0	2.1741	1.3609	1.2502	4.02	0.77	14.6	1.12086
GGHH	0–10	0.29	0.33	0.04	0	2.8846	0.7084	0.2893	1.47	-0.38	131.6	0.50908
	10–30	0.12	0.12	0.00	0	3.3231	0.8171	0.9167	1.33	-0.22	289.6	0.91031
	30–50	0.10	0.19	0.09	0	0.0821	2.8431	1.3045	1.33	-0.74	271.4	0.964739
	50–100	0.16	0.23	0.07	0	1.4499	1.9204	1.2885	4.82	0.74	195.7	0.8449
	100+	0.62	0.72	0.09	0	2.3137	0.5420	0.4451	2.86	0.53	21.4	0.295787
De Pere												
SMU Group 2025	0–10	0.38	0.46	0.07	0	3.6631	0.4655	0.4255	1.11	-1.18	225.6	0.350891
	10–30	0.35	0.37	0.02	100	6.3342	3.4691	2.2114	2.58	-0.59	813.6	0.855251
	30–50	0.66	0.76	0.10	150	5.5480	0.9776	1.1642	1.76	-0.76	950.3	0.430459
	50–100	0.35	0.36	0.01	50	4.0031	1.1675	1.2707	1.76	-0.18	1569.3	1.13947
2649	0–10	0.06	0.17	0.11	0	3.2501	0.2065	0.4161	0.89	-1.01	356.8	0.434768
	10–30	0.31	0.43	0.12	0	10.6240	3.2452	1.9813	0.80	-0.90	1556.5	0.816451
	50–100	0.13	0.13	0.00	100	3.6653	2.3249	1.1267	1.32	-0.47	3135.5	1.07814
	100+	0.20	0.22	0.02	0	1.2186	1.9141	1.2818	5.18	0.10	1717.6	1.05288
5067	0–10	0.13	0.27	0.14	0	7.6178	1.2394	1.1333	7.47	2.40	92.4	0.186359
	10–30	0.42	0.47	0.05	0	2.4000	1.4903	1.2775	4.35	-1.43	353.7	0.472972
	50–100	0.42	0.43	0.01	0	6.5635	2.1819	1.5704	2.61	-0.36	2764.9	0.778337
	100+	0.26	0.29	0.02	0	4.9240	2.3655	1.8648	5.97	-0.22	4426.0	1.13022
6891	0–10	0.42	0.46	0.04	100	10.2963	4.2471	5.8601	3.04	-1.34	72.1	0.422776
	10–30	0.63	0.74	0.11	100	6.4202	1.3240	1.3665	2.29	-1.22	246.7	0.447153
92115	0–10	0.52	0.52	0.01	0	0.8839	0.9748	1.1169	3.37	-0.12	37.1	0.359379

Table A-1 Details of Models Fitted to Time Trends in Sediment PCB Concentrations

Reach and Deposit Group	Depth Range (cm)	Number of Samples					Mean of Within-core-avg. Sample Variances	Variance of Singleton Samples in Core-avg. Data Set	Parameter Estimates and Standard Errors					
		Single Used in Core-averaged Analyses	Core-avg. Used in Core-avg. Analyses	Total Original Single	Total in Core-avg. Analyses (mixed, single, & core-avg.)	Avg. that Ended up in a Core-avg. Sample			Intercept Estimate	WSEV Std. Err. Intercept	Independence Std. Err. Intercept	Time Estimate	WSEV Std. Err. Time	Independence Std. Err. Time
Little Lake Butte des Morts														
AB	0–10	47	20	94	67	2.4	0.0632	0.4984	4.4461	0.3237	0.2788	-0.0970	0.0348	0.0279
	10–30	87	18	134	105	2.6	0.4082	1.0782	4.0797	0.8357	0.6054	-0.0213	0.0647	0.0501
	30–50	52	2	56	54	2.0	1.4924	0.7630	10.4324	2.8100	2.1917	-0.0144	0.1113	0.0831
C	0–10	2	11	25	13	2.1	0.1032	0.0949	5.2096	1.2084	1.0586	-0.0612	0.0342	0.0272
	10–30	12	3	18	15	2.0	1.1476	0.9889	5.0070	1.4441	1.3930	0.0317	0.0770	0.0709
POG	0–10	12	1	14	13	2.0	0.0311	0.6958	4.4765	0.5067	0.4769	-0.0893	0.0567	0.0417
D	0–10	13	5	23	18	2.0	0.5476	0.2467	3.8807	0.6868	0.3776	-0.0755	0.0317	0.0267
	10–30	13	2	17	15	2.0	0.3832	0.6341	2.2285	0.5288	0.5202	0.3168	0.0454	0.0526
F	0–10	12	17	49	29	2.2	0.1923	0.3178	3.5528	0.3827	0.4099	-0.0373	0.0136	0.0266
	10–30	22	6	34	28	2.0	0.4242	0.5408	2.2040	1.3533	1.0844	-0.0760	0.0749	0.0674
GH	0–10	9	6	21	15	2.0	0.0492	0.2345	3.1032	0.3153	0.3176	-0.1244	0.0541	0.0389
Appleton														
IMOR	0–10	12	6	24	18	2.0	0.0184	0.3153	3.1269	0.4735	0.4747	0.0412	0.0255	0.0458
N Pre-dredge	0–10	26	6	42	32	2.7	0.1282	0.4005	4.2292	0.4199	0.3549	-0.0281	0.0065	0.0185
	10–30	23	4	32	27	2.3	0.0186	0.7645	3.7450	0.6539	0.6366	0.0572	0.0440	0.0334
	30–50	16	1	18	17	2.0	0.0006	0.7463	4.4070	1.5119	1.2267	0.0846	0.0932	0.0504
VCC	0–10	27	14	57	41	2.1	0.3692	0.3242	3.2202	0.3490	0.2537	-0.0582	0.0275	0.0209
	10–30	31	3	37	34	2.0	0.1965	0.5572	4.1303	0.6783	0.7806	-0.1537	0.0164	0.0420
	30–50	15	2	19	17	2.0	0.0041	0.0638	4.4304	0.5727	0.5713	-0.0060	0.0151	0.0135
Little Rapids														
Upper EE	0–10	13	18	51	31	2.1	0.2516	0.2396	3.2722	0.7469	0.4948	-0.0447	0.0435	0.0291
	10–30	15	10	36	25	2.1	0.2717	0.3608	2.5703	1.1521	0.8651	-0.0944	0.0429	0.0460
	30–50	13	0	13	13	0.0		0.2834	4.7214	1.3448	1.7186	-0.0712	0.0536	0.0659
Lower EE	0–10	15	15	49	30	2.3	0.2781	0.5693	2.9308	0.2663	0.3268	-0.0682	0.0193	0.0232
	10–30	23	10	45	33	2.2	0.4506	0.6548	2.8576	0.7657	0.9180	-0.0759	0.0390	0.0495
	30–50	11	2	15	13	2.0	0.1221	0.3792	5.0328	0.9549	1.1745	0.0900	0.0330	0.0364
FF	0–10	18	14	50	32	2.3	0.3690	0.6980	3.7208	0.3852	0.4231	-0.0549	0.0557	0.0401
	10–30	24	7	39	31	2.1	0.3304	0.9190	2.1741	1.3609	1.2502	-0.0962	0.0390	0.0606
GGHH	0–10	24	25	80	49	2.2	0.1169	0.5300	2.8846	0.7084	0.2893	-0.0394	0.0231	0.0235
	10–30	27	18	71	45	2.4	0.3074	0.9414	3.3231	0.8171	0.9167	-0.0182	0.0596	0.0665
	30–50	73	2	78	75	2.5	0.0008	0.9359	0.0821	2.8431	1.3045	0.1762	0.1008	0.0560
	50–100	51	3	57	54	2.0	0.8083	0.5186	1.4499	1.9204	1.2885	0.1012	0.0700	0.0572
	100+	33	3	39	36	2.0	0.0367	0.1512	2.3137	0.5420	0.4451	0.0365	0.0249	0.0259
De Pere														
SMU Group 2025	0–10	32	11	57	43	2.3	0.0271	0.2709	3.6631	0.4655	0.4255	-0.0528	0.0231	0.0217
	10–30	16	15	54	31	2.5	0.0886	0.9893	6.3342	3.4691	2.2114	-0.0556	0.0750	0.0726
	30–50	9	4	23	13	3.5	0.0925	0.6680	5.5480	0.9776	1.1642	-0.0580	0.0322	0.0335
	50–100	28	2	34	30	3.0	0.1551	1.1742	4.0031	1.1675	1.2707	-0.0847	0.1058	0.1163
2649	0–10	54	12	80	66	2.2	0.0153	0.2503	3.2501	0.2065	0.4161	-0.0608	0.0109	0.0211
	10–30	25	23	73	48	2.1	0.1028	1.0853	10.6240	3.2452	1.9813	-0.2882	0.1440	0.0956
	50–100	44	2	51	46	3.5	0.0433	1.1505	3.6653	2.3249	1.1267	0.1957	0.1419	0.3961
	100+	31	14	63	45	2.3	0.5315	1.0783	1.2186	1.9141	1.2818	0.0177	0.1548	0.1046
5067	0–10	53	5	63	58	2.0	0.0736	0.0919	7.6178	1.2394	1.1333	-0.0998	0.0345	0.0307
	10–30	45	6	57	51	2.0	0.2006	0.4654	2.4000	1.4903	1.2775	0.0912	0.0649	0.0465
	50–100	47	1	49	48	2.0	0.1247	1.0992	6.5635	2.1819	1.5704	0.3677	0.0684	0.4775
	100+	13	37	176	50	4.4	0.6534	1.1959	4.9240	2.3655	1.8648	-0.1963	0.2223	0.1720
6891	0–10	16	4	24	20	2.0	0.1259	0.3116	10.2963	4.2471	5.8601	-0.2208	0.0944	0.1858
	10–30	11	7	25	18	2.0	0.0973	1.0964	6.4202	1.3240	1.3665	-0.1685	0.0765	0.0689
92115	0–10	21	6	33	27	2.0	0.0284	0.3161	0.8839	0.9748	1.1169	0.0413	0.0426	0.0574

Table A-1 Details of Models Fitted to Time Trends in Sediment PCB Concentrations

Reach and Deposit Group	Depth Range (cm)	Parameter Estimates and Standard Errors														
		Depth Estimate	WSEV Std. Err. Depth	Independence Std. Err. Depth	Northing Estimate	WSEV Std. Err. Northing	Independence Std. Err. Northing	Easting Estimate	WSEV Std. Err. Easting	Independence Std. Err. Easting	Northing-squared Estimate	WSEV Std. Err. Northing-squared	Independence Std. Err. Northing-squared	Easting-squared Estimate	WSEV Std. Err. Easting-squared	Independence Std. Err. Easting-squared
Little Lake Butte des Morts																
AB	0–10	0.0127	0.0633	0.0409	-1.0975	0.4992	0.4595	-2.0095	0.9635	0.7386	-2.4494	2.1658	1.8061	-5.3925	3.5417	3.2507
	10–30	-0.0338	0.0211	0.0250	-2.9471	1.5897	0.8840	-3.2882	2.0674	1.6795	2.3822	4.8087	2.7630	-12.7711	21.9423	13.4218
	30–50	-0.2185	0.0674	0.0545	0.7990	1.5402	1.6161	3.0474	2.0452	3.0465	-6.3672	11.0640	8.3931	-20.7443	12.1952	18.3243
C	0–10	-0.1412	0.1936	0.1599	1.6869	1.2250	1.4496	-2.6324	2.2086	1.5222	-14.4039	13.6209	11.8569	-28.8072	27.5631	31.7216
	10–30	-0.1328	0.0599	0.0655	3.9183	3.9217	2.8835	-12.5252	4.3174	4.5834						
POG	0–10	-0.0434	0.1158	0.0909	2.9932	0.3684	1.0207	-3.4068	0.7446	1.1297	-1.3834	2.5588	3.4422	-6.7243	3.8221	3.0709
D	0–10	0.0016	0.0822	0.0475	-0.5055	0.9173	0.5734	0.7551	2.5966	1.9171	-3.4413	1.9010	1.1846	1.4114	15.7548	12.9109
	10–30	-0.0357	0.0227	0.0221	-0.0334	0.7334	0.6602	4.8278	2.6055	2.5146						
F	0–10	-0.0345	0.0831	0.0630	-0.0750	0.2812	0.2673	-0.5557	0.2385	0.3464	-0.2749	1.5113	0.8837	-1.0831	0.5661	0.8540
	10–30	0.0178	0.0593	0.0488	0.1980	0.3974	0.3964	-0.9190	0.7543	0.7001	-2.0705	1.5904	1.2523	-1.4047	2.0686	1.7550
GH	0–10	-0.0264	0.0497	0.0587	-0.0852	0.3564	0.3934	-0.1385	0.3700	0.3075						
Appleton																
IMOR	0–10	-0.0552	0.0659	0.0681	0.2432	1.0106	0.5859	-0.0513	0.3799	0.2284						
N Pre-dredge	0–10	0.0783	0.0842	0.0505	-13.0001	8.6265	5.7496	-1.0311	2.4778	1.5680	-576.7283	75.1630	150.1163	-28.0271	15.7291	9.8662
	10–30	-0.0098	0.0365	0.0349	38.4878	10.3435	10.4052	-10.3445	2.9457	2.3469	-633.9268	204.1228	287.0263	49.1326	30.5758	22.6896
	30–50	-0.0146	0.0374	0.0357	33.2158	21.9749	14.3060	-12.3383	7.8129	3.8360	-307.2611	243.4987	301.2426	18.4344	30.9885	18.8647
VCC	0–10	-0.0908	0.0616	0.0388	0.1753	0.2540	0.2933	-0.2587	0.3273	0.3816	-0.0144	0.1154	0.1920	-0.1078	0.1094	0.2578
	10–30	-0.0882	0.0265	0.0352	-1.0040	1.0156	1.2013	0.9931	1.0793	1.4751	-1.3033	0.7249	1.0073	0.9072	1.0233	1.3690
	30–50	-0.0829	0.0152	0.0161	0.6032	0.1695	0.2156	-0.9142	0.2435	0.2556						
Little Rapids																
Upper EE	0–10	-0.0258	0.1220	0.0572	0.3850	0.6189	0.4675	0.0762	0.5422	0.4773	-0.2680	0.0899	0.6390	-0.3970	0.3091	0.6846
	10–30	-0.0229	0.0489	0.0365	0.4099	0.6506	0.7961	-0.2514	0.5624	0.7467	-0.0198	0.7059	1.2080	1.7720	1.1293	1.1117
	30–50	-0.0745	0.0307	0.0427	-0.5189	0.9981	1.1966	0.6193	0.9395	1.2762						
Lower EE	0–10	0.0251	0.0532	0.0433	1.1109	0.2728	0.2937	-2.6603	0.4376	0.7436	0.3520	0.3646	0.4311	-1.7459	0.8458	1.4421
	10–30	-0.0552	0.0270	0.0426	0.8874	0.8233	0.6482	-1.8815	2.0380	1.4465	0.1246	1.0613	0.9360	2.6939	4.4128	3.0731
	30–50	-0.0734	0.0307	0.0313	2.4176	0.4448	0.7119	-5.1517	1.3718	1.7193	-4.0206	1.2678	1.5058	-0.6923	4.3874	4.0097
FF	0–10	-0.0864	0.0634	0.0601	0.0232	0.7702	0.9493	-0.2189	1.4350	1.5524	0.8106	1.3806	1.4371	-3.9307	3.0655	3.1191
	10–30	0.0048	0.0663	0.0572	0.5910	1.5431	1.4340	-1.2403	2.3865	2.3065	2.1896	1.1179	2.1191	-6.1569	3.0884	4.5264
GGHH	0–10	0.1141	0.0748	0.0403	-0.2046	0.3480	0.3619	1.0979	1.0084	0.7402	-0.2429	1.5891	0.8907	5.0351	2.0031	2.5160
	10–30	0.0025	0.0346	0.0387	0.7336	0.5032	0.6972	-0.7336	1.3691	1.5452	-2.6015	1.4440	1.5777	9.1624	5.6538	5.4674
	30–50	0.0818	0.0734	0.0340	0.8932	1.6858	0.7687	-3.0753	2.3031	1.3481	-2.1752	2.4315	1.1141	1.4384	7.1742	4.0281
	50–100	0.0005	0.0205	0.0153	1.7920	0.7295	0.7362	-2.4967	1.2953	1.3551	-0.1966	1.2491	1.0857	1.6211	4.4325	4.0758
	100+	-0.0063	0.0032	0.0025	0.6162	0.4661	0.4185	-0.2224	1.0309	0.8222	0.5376	0.6100	0.5136	-0.2400	2.0933	1.7928
De Pere																
SMU Group 2025	0–10	-0.0218	0.0247	0.0673	0.2322	0.1954	0.2727	-0.8168	0.2670	0.1952	1.4369	0.6614	0.6721	-0.9296	0.9774	0.5463
	10–30	-0.1353	0.1674	0.1039	0.1168	0.5505	0.7072	-1.8758	0.6483	0.6353	0.7551	2.1870	2.0435	-1.1481	2.0442	1.5719
	30–50	-0.0396	0.0231	0.0301	2.3369	0.3537	0.4625	-1.8970	0.3919	0.4047						
	50–100	0.0016	0.0198	0.0209	-0.7090	0.9904	0.9190	-1.3836	0.9355	0.8003	-4.3505	3.6551	3.2428	-2.3768	2.3783	2.3032
2649	0–10	0.0528	0.0366	0.0725	0.3481	0.1918	0.1900	-0.4861	0.2934	0.2805	-0.1224	0.1295	0.1457	0.1794	0.4357	0.3553
	10–30	-0.2963	0.1275	0.0753	1.7553	0.4476	0.4437	-2.6073	0.7299	0.6432	-0.8618	0.3015	0.3349	2.2571	0.6432	0.8075
	50–100	-0.0329	0.0535	0.0438	0.8507	1.0310	0.6052	-0.6367	1.4451	0.8173	0.8211	0.6382	0.5198	-0.4678	1.6001	1.1621
	100+	0.0044	0.0056	0.0046	0.9871	1.0713	0.6428	-0.3836	1.2383	0.8749	0.4507	0.4532	0.5315	0.5980	2.1577	1.3592
5067	0–10	-0.6896	0.2021	0.1789	0.1660	0.2830	0.1969	-0.6811	0.5147	0.3164	-0.2127	0.4270	0.3747	-0.9698	1.0473	0.8755
	10–30	0.0373	0.0522	0.0492	-0.1798	0.6369	0.5413	0.5682	1.3988	0.8701	2.2532	1.0289	1.0194	-13.8586	3.7778	3.1291
	50–100	-0.0716	0.0217	0.0660	4.1177	2.0645	1.1132	-4.8032	3.0530	1.6681	-3.1805	1.2464	1.9784	-10.7462	5.2078	5.3972
	100+	0.0019	0.0061	0.0033	5.7110	2.8462	1.8915	-6.2886	6.3528	3.3150	-7.7006	4.3032	3.9687	-4.4052	19.8825	16.6514
6891	0–10	-1.0620	0.7286	0.9291	0.2115	0.2892	0.3912	-1.3241	1.2294	1.5454	0.2611	0.2030	0.4168	-8.6671	1.3018	3.2661
	10–30	-0.0924	0.0494	0.0545	0.5512	0.5967	0.5714	-4.3170	2.3513	2.4161	0.9099	0.5955	0.5884	-17.2007	7.7080	6.1620
92115	0–10	0.2969	0.1598	0.1651	0.5306	0.4004	0.2988	-0.2891	1.1053	0.9145	0.8018	0.2686	0.2065	-1.6445	1.8395	1.6840

Table A-2 Green Bay Zones 1 and 2 Outliers

	Database ID	Reach	Fish Type	Sample Type	Total PCBs
Fish Data: Comparison of Green Bay Zones 1 and 2	WDF209006BC1	Green Bay Zone 2	alewife	whole body	19,000

Reason:

Large outlier. Other PCB values range from 990 to 4,500.

Table A-3 Detailed Data for All Fish Results

Reach	Model	Species	Sample Type	Year of Break-point	Number of Samples	Number of Samples Below Detection Limit	Standard Deviation	Chi-squared	Intercept			Final			Early		
									Intercept	Std. Err.	*p*-value	Slope	Std. Err.	*p*-value	Slope Difference	Std. Err.	*p*-value
Little Lake Butte des Morts	No Break-point	carp	skin-on fillet		55		49.63		3.3515	0.1131		-0.0456	0.0095	0.0000			
			whole body		40	1	36.67		3.6775	0.1089		-0.0750	0.0106	0.0000			
		northern pike	skin-on fillet		19	1	12.83		2.6670	0.1303	0.0000	-0.0547	0.0115	0.0003			
		walleye	skin-on fillet		63	8	42.31		2.5700	0.0737		-0.0465	0.0066	0.0000			
			whole body		18	3	26.16		2.6490	0.4089	0.0000	-0.0026	0.0429	0.9532			
		yellow perch	skin-on fillet		34	10	27.99		2.1767	0.0925		-0.0262	0.0097	0.0112			
	Best Fitting	carp	skin-on fillet	1979	55		42.91	6.72	3.3574	0.1064		-0.0276	0.0112	0.0177	-0.2280	0.0853	0.0102
			whole body	1987	40	1	29.39	7.28	3.3104	0.1645		0.0031	0.0295	0.9172	-0.1647	0.0588	0.0084
		northern pike	skin-on fillet		19	1	12.83		2.6670	0.1303	0.0000	-0.0547	0.0115	0.0003			
		walleye	skin-on fillet	1990	63	8	35.98	6.33	2.2105	0.1605		0.0147	0.0249	0.5576	-0.0945	0.0373	0.0140
			whole body	1987	18	3	16.69	9.48	2.1870	0.3811	0.0001	0.0845	0.0454	0.0874	-0.2608	0.0802	0.0069
		yellow perch	skin-on fillet	1981	34	10	17.83	10.16	2.3384	0.0908		0.0031	0.0125	0.8025	-0.2467	0.0771	0.0034
Appleton to Little Rapids	No Break-point	walleye	skin-on fillet		30		-7.15		3.0085	0.1256		-0.0456	0.0138	0.0028			
	Best Fitting	walleye	skin-on fillet		30		-7.15		3.0085	0.1256		-0.0456	0.0138	0.0028			
De Pere to Green Bay	No Break-point	carp	whole body		90		58.07		4.0144	0.0542		-0.0341	0.0055	0.0000			
		gizzard shad	whole body		19		-42.45		3.4553	0.0325		-0.0226	0.0045	0.0002			
		northern pike	skin-on fillet		40	1	-11.40		3.1688	0.0998		-0.0455	0.0073	0.0000			
		walleye	skin-on fillet		120	1	-41.16		3.1963	0.0435		-0.0324	0.0036	0.0000			
			whole body		58		-12.22		3.9812	0.0541		-0.0367	0.0054	0.0000			
		white bass	skin-on fillet		58		-41.00		3.6259	0.0678		-0.0210	0.0065	0.0020			
		white sucker	skin-on fillet		44		-3.92		3.1349	0.0762		-0.0357	0.0056	0.0000			
	Best Fitting	carp	whole body	1995	90		48.59	9.48	2.9712	0.3339	0.0000	0.0855	0.0382	0.0277	-0.1406	0.0445	0.0022
		gizzard shad	whole body		19		-42.45		3.4553	0.0325		-0.0226	0.0045	0.0002			
		northern pike	skin-on fillet		40	1	-11.40		3.1688	0.0998		-0.0455	0.0073	0.0000			
		walleye	skin-on fillet		120	1	-41.16		3.1963	0.0435		-0.0324	0.0036	0.0000			
			whole body		58		-12.22		3.9812	0.0541		-0.0367	0.0054	0.0000			
		white bass	skin-on fillet		58		-41.00		3.6259	0.0678		-0.0210	0.0065	0.0020			
		white sucker	skin-on fillet		44		-3.92		3.1349	0.0762		-0.0357	0.0056	0.0000			
Green Bay Zone 2 (2A and 2B)	No Break-point	alewife	whole body		44		-30.42		3.4844	0.0544		-0.0176	0.0087	0.0497			
		carp	skin-on fillet		28		-4.77		3.8869	0.0803		-0.0226	0.0154	0.1557			
			whole body		57		-11.66		3.7679	0.0530		-0.0414	0.0090	0.0000			
		gizzard shad	whole body		32		-51.90		3.2444	0.0535		0.0249	0.0095	0.0144			
		yellow perch	skin-on fillet		19	3	-8.96		2.6539	0.4357	0.0000	-0.0494	0.0143	0.0038			
	Best Fitting	alewife	whole body		44		-30.42		3.4844	0.0544		-0.0176	0.0087	0.0497			
		carp	skin-on fillet		28		-4.77		3.8869	0.0803		-0.0226	0.0154	0.1557			
			whole body	1983	57		-29.32	17.66	3.8825	0.0519		-0.0733	0.0104	0.0000	0.2664	0.0585	0.0000
		gizzard shad	whole body		32		-51.90		3.2444	0.0535		0.0249	0.0095	0.0144			
		yellow perch	skin-on fillet		19	3	-8.96		2.6539	0.4357	0.0000	-0.0494	0.0143	0.0038			

Note:

In the fitted models, amplitude and month of peak can be ignored if $\log_{10}$ PCB concentration estimates are needed for July 1 of any year. For other times of year, let M be the $\log_{10}$ of the estimated concentration on July 1, A = amplitude, t_{max} = ("*month of peak*" – 1)/12, and t = the specified time of year as a value between zero (1 January) and 1.0 (31 December). Define $Q(t) = -A \cdot \cos[2\pi(0.5 - t_{max})] + A \cdot \cos[2\pi(t - t_{max})]$. Then the estimated mean concentration (ppb) at time-of-year t is $M \cdot 10^{Q(t)}$.

Table A-3 Detailed Data for All Fish Results

Reach	Model	Species	Sample Type	Year of Break-point	Fat Log$_{10}$	Fat Std. Err.	Fat *p*-value	Month Peak	Amplitude	Amplitude *p*-value	Covariate Intercept Time	Mean Squared Error	Percent Change per Year	T-squared	T-squared Std. Err.	T-squared *p*-value
Little Lake Butte des Morts	No Break-point	carp	skin-on fillet		0.8927	0.1611	0.0000	1.328	0.5316	0.2260	0.0006	0.1444	-9.9650	0.00231	0.00190	0.2292
			whole body		0.8753	0.3590	0.0200	6.356	0.6174	0.0965	-0.0004	0.1374	-15.8538	0.00360	0.00229	0.1249
		northern pike	skin-on fillet		0.4469	0.2976	0.1554	1.311	0.6671	0.1594	0.0005	0.1034	-11.8315	-0.00334	0.00242	0.1904
		walleye	skin-on fillet		0.3898	0.1444	0.0091	1.558	0.1861	0.6458	0.0001	0.0934	-10.1572	0.00285	0.00123	0.0241
			whole body		0.9062	0.4038	0.0429	12.515	0.9205	0.4523	-0.0156	0.2303	-0.5888	0.00789	0.00327	0.0329
		yellow perch	skin-on fillet		0.3972	0.2323	0.0980	1.338	0.3079	0.1117	0.0001	0.0955	-5.8564	0.00609	0.00210	0.0071
	Best Fitting	carp	skin-on fillet	1979	0.8675	0.1519	0.0000	12.904	0.3939	0.0078	0.0006	0.1277	-6.1477	-0.00137	0.00236	0.5645
			whole body	1987	0.8626	0.3293	0.0131	7.013	0.8307	0.0025	-0.0039	0.1156	0.7139	-0.01442	0.00670	0.0388
		northern pike	skin-on fillet		0.4469	0.2976	0.1554	1.311	0.6671	0.1594	0.0005	0.1034	-11.8315	-0.00334	0.00242	0.1904
		walleye	skin-on fillet	1990	0.5012	0.1455	0.0011	11.638	0.2005	0.0273	-0.0034	0.0857	3.4395	-0.00949	0.00939	0.3167
			whole body	1987	0.9858	0.3619	0.0185	11.562	0.4627	0.0040	-0.0157	0.1410	21.4715	-0.02024	0.01008	0.0698
		yellow perch	skin-on fillet	1981	0.4946	0.2067	0.0236	7.033	0.2185	0.0007	0.0005	0.0719	0.7276	-0.00211	0.00587	0.7217
Appleton to Little Rapids	No Break-point	walleye	skin-on fillet		1.0801	0.1555	0.0000	8.121	0.4280	0.0010	0.0015	0.0461	-9.9680	-0.00472	0.00405	0.2554
	Best Fitting	walleye	skin-on fillet		1.0801	0.1555	0.0000	8.121	0.4280	0.0010	0.0015	0.0461	-9.9680	-0.00472	0.00405	0.2554
De Pere to Green Bay	No Break-point	carp	whole body		0.8225	0.1180	0.0000	6.889	0.1825	0.0471	-0.0001	0.1116	-7.5413	0.00214	0.00103	0.0411
		gizzard shad	whole body		0.5055	0.0897	0.0001	8.558	0.5814	0.0000	-0.0001	0.0063	-5.0657	0.00318	0.00289	0.2902
		northern pike	skin-on fillet		0.7224	0.1664	0.0001	10.122	0.1730	0.3531	-0.0004	0.0407	-9.9517	0.00093	0.00079	0.2489
		walleye	skin-on fillet		0.8509	0.0673		9.454	0.0172	0.7566	-0.0001	0.0406	-7.1920	-0.00051	0.00062	0.4177
			whole body		0.4449	0.1231	0.0007	6.973	0.1190	0.2038	-0.0001	0.0474	-8.1055	-0.00003	0.00082	0.9712
		white bass	skin-on fillet		0.8170	0.1134	0.0000	6.750	0.3258	0.1043	0.0001	0.0289	-4.7229	0.00152	0.00183	0.4104
		white sucker	skin-on fillet		0.4255	0.1496	0.0071	6.923	0.0827	0.5528	0.0000	0.0536	-7.8956	0.00110	0.00104	0.2996
	Best Fitting	carp	whole body	1995	0.7871	0.1125	0.0000	6.657	0.0642	0.0004	-0.0126	0.1005	21.7626	0.01676	0.03616	0.6442
		gizzard shad	whole body		0.5055	0.0897	0.0001	8.558	0.5814	0.0000	-0.0001	0.0063	-5.0657	0.00318	0.00289	0.2902
		northern pike	skin-on fillet		0.7224	0.1664	0.0001	10.122	0.1730	0.3531	-0.0004	0.0407	-9.9517	0.00093	0.00079	0.2489
		walleye	skin-on fillet		0.8509	0.0673		9.454	0.0172	0.7566	-0.0001	0.0406	-7.1920	-0.00051	0.00062	0.4177
			whole body		0.4449	0.1231	0.0007	6.973	0.1190	0.2038	-0.0001	0.0474	-8.1055	-0.00003	0.00082	0.9712
		white bass	skin-on fillet		0.8170	0.1134	0.0000	6.750	0.3258	0.1043	0.0001	0.0289	-4.7229	0.00152	0.00183	0.4104
		white sucker	skin-on fillet		0.4255	0.1496	0.0071	6.923	0.0827	0.5528	0.0000	0.0536	-7.8956	0.00110	0.00104	0.2996
Green Bay Zone 2 (2A and 2B)	No Break-point	alewife	whole body		0.9126	0.1409	0.0000	6.054	0.1664	0.0335	-0.0001	0.0293	-3.9623	0.00191	0.00113	0.0992
		carp	skin-on fillet		0.7643	0.1515	0.0000	3.941	0.2377	0.0288	-0.0001	0.0494	-5.0631	-0.00608	0.00349	0.0956
			whole body		0.9578	0.1099	0.0000	6.794	0.1308	0.2408	0.0000	0.0477	-9.1004	-0.00275	0.00118	0.0238
		gizzard shad	whole body		-0.1295	0.1177	0.2811	2.645	0.3356	0.0300	-0.0002	0.0116	5.9098	-0.00074	0.00319	0.8176
		yellow perch	skin-on fillet		1.0912	0.4683	0.0353	4.726	0.4459	0.5489	-0.0020	0.0316	-10.7477	0.01258	0.00339	0.0026
	Best Fitting	alewife	whole body		0.9126	0.1409	0.0000	6.054	0.1664	0.0335	-0.0001	0.0293	-3.9623	0.00191	0.00113	0.0992
		carp	skin-on fillet		0.7643	0.1515	0.0000	3.941	0.2377	0.0288	-0.0001	0.0494	-5.0631	-0.00608	0.00349	0.0956
			whole body	1983	0.8981	0.0950	0.0000	6.864	0.2382	0.0000	-0.0002	0.0350	-15.5359	0.00335	0.00175	0.0616
		gizzard shad	whole body		-0.1295	0.1177	0.2811	2.645	0.3356	0.0300	-0.0002	0.0116	5.9098	-0.00074	0.00319	0.8176
		yellow perch	skin-on fillet		1.0912	0.4683	0.0353	4.726	0.4459	0.5489	-0.0020	0.0316	-10.7477	0.01258	0.00339	0.0026

Note:

In the fitted models, amplitude and month of peak can be ignored if $\log_{10}$ PCB concentration estimates are needed for July 1 of any year. For other times of year, let M be the $\log_{10}$ of the estima concentration on July 1, A = amplitude, t_{max} = ("*month of peak*" – 1)/12, and t = the specified time of year as a value between zero (1 January) and 1.0 (31 December). Define $Q(t) = -A \cdot \cos[2\pi(0.5 - t_{max})] + A \cdot \cos[2\pi(t - t_{max})]$. Then the estimated mean concentration (ppb) at time-of-year t is $M \cdot 10^{Q(t)}$.

Table A-4 Testing the Null Hypothesis that a Straight Line Fits As Well As a Spline Model with a Breakpoint

Reach	Species	Sample Type	Year of Best-fitting Breakpoint	Sample Size	*p*-value for Breakpoint	*p* < 0.05	Final (post-break) Slope	*p*-value for Final Slope	Pre-break Slope Minus Final Slope	*p*-value for Slope Difference	Pre-break Slope
Little Lake Butte des Morts	Carp	skin-on fillet	1979	55	0.0347	*	-0.028	0.0177	-0.228	0.0102	-0.256
		whole body	1987	40	0.0263	*	0.003	0.9172	-0.165	0.0084	-0.162
	Northern Pike	skin-on fillet	1996	19	0.2723		-0.325	0.0685	0.301	0.1214	-0.024
	Walleye	skin-on fillet	1990	63	0.0423	*	0.015	0.5576	-0.095	0.0140	-0.080
		whole body	1987	18	0.0088	*	0.084	0.0874	-0.261	0.0069	-0.176
	Yellow Perch	skin-on fillet	1981	34	0.0062	*	0.003	0.8025	-0.247	0.0034	-0.244
	Combined++			**229**	**0.0000**	*****					
Appleton to Little Rapids	Walleye	skin-on fillet	1983	30	0.4526		-0.056	0.0015	0.103	0.2142	0.047
De Pere to Green Bay	Carp	whole body	1995	90	0.0087	*	0.086	0.0277	-0.141	0.0022	-0.055
	Gizzard Shad	whole body	1990	19	0.4672		-0.020	0.0018	-0.042	0.2303	-0.062
	Northern Pike	skin-on fillet	1996	40	0.1421		0.060	0.2616	-0.117	0.0514	-0.056
	Walleye	skin-on fillet	1993	120	0.5680		-0.046	0.0006	0.019	0.2885	-0.027
		whole body	1996	58	0.5550		0.010	0.8196	-0.052	0.2805	-0.042
	White Bass	skin-on fillet	1996	58	0.6059		0.019	0.6373	-0.045	0.3193	-0.025
	White Sucker	skin-on fillet	1990	44	0.1986		-0.006	0.7235	-0.049	0.0749	-0.055
	Combined++			**429**	**0.0906**						
Green Bay Zone 2 (2A and 2B)	Alewife	whole body	1986	44	0.0863		-0.001	0.9394	-0.076	0.0285	-0.077
	Carp	skin-on fillet	1985	28	0.1811		-0.063	0.0226	0.105	0.0698	0.042
		whole body	1983	57	0.0001	*	-0.073	0.0000	0.266	0.0000	0.193
	Gizzard Shad	whole body	1996	32	0.6655		-0.014	0.7556	0.047	0.3721	0.033
	Yellow Perch	skin-on fillet	1986	19	0.0008	*	0.062	0.0325	-0.573	0.0004	-0.511
	Combined++			**180**	**0.0000**	*****					

Note:

++ Indicates *p*-value for the test that all fish categories in a reach do not have a breakpoint.

Table A-5 Breakpoint, Final Slope, and Percent Change per Year of PCB Concentration from Best-fitting Model

Reach	Species	Sample Type	Year of Breakpoint	Number of Samples	Final (post-break) Slope	*p*-value for Final Slope (versus zero)	Percent per Year
Little Lake Butte des Morts	Carp	skin-on fillet	1979	55	-0.028	0.0177	-6.1
		whole body	1987	40	0.003	0.9172	0.7
	Northern Pike	skin-on fillet	0	19	-0.055	0.0003	-11.8
	Walleye	skin-on fillet	1990	63	0.015	0.5576	3.4
		whole body	1987	18	0.084	0.0874	21.5
	Yellow Perch	skin-on fillet	1981	34	0.003	0.8025	0.7
Appleton to Little Rapids	Walleye	skin-on fillet	0	30	-0.046	0.0028	-10.0
De Pere to Green Bay	Carp	whole body	1995	90	0.086	0.0277	21.8
	Gizzard Shad	whole body	0	19	-0.023	0.0002	-5.1
	Northern Pike	skin-on fillet	0	40	-0.046	0.0000	-10.0
	Walleye	skin-on fillet	0	120	-0.032	0.0000	-7.2
		whole body	0	58	-0.037	0.0000	-8.1
	White Bass	skin-on fillet	0	58	-0.021	0.0020	-4.7
	White Sucker	skin-on fillet	0	44	-0.036	0.0000	-7.9
Green Bay Zone 2 (2A and 2B)	Alewife	whole body	0	44	-0.018	0.0497	-4.0
	Carp	skin-on fillet	0	28	-0.023	0.1557	-5.1
		whole body	1983	57	-0.073	0.0000	-15.5
	Gizzard Shad	whole body	0	32	0.025	0.0144	5.9
	Yellow Perch	skin-on fillet	0	19	-0.049	0.0038	-10.7

Table A-6 Model Parameters and Other Statistics for the Best-fitting Model

Reach	Species	Sample Type	Year of Breakpoint	Number of Samples			Final (post-break) Slope	
				n	Intercept	Standard Error	Final	Standard Error
Little Lake Butte des Morts	Carp	skin-on fillet	1979	55	3.36	0.11	-0.028	0.011
		whole body	1987	40	3.31	0.16	0.003	0.030
	Northern Pike	skin-on fillet	0	19	2.67	0.13	-0.055	0.011
	Walleye	skin-on fillet	1990	63	2.21	0.16	0.015	0.025
		whole body	1987	18	2.19	0.38	0.084	0.045
	Yellow Perch	skin-on fillet	1981	34	2.34	0.09	0.003	0.012
Appleton to Little Rapids	Walleye	skin-on fillet	0	30	3.01	0.13	-0.046	0.014
De Pere to Green Bay	Carp	whole body	1995	90	2.97	0.33	0.086	0.038
	Gizzard Shad	whole body	0	19	3.46	0.03	-0.023	0.005
	Northern Pike	skin-on fillet	0	40	3.17	0.10	-0.046	0.007
	Walleye	skin-on fillet	0	120	3.20	0.04	-0.032	0.004
		whole body	0	58	3.98	0.05	-0.037	0.005
	White Bass	skin-on fillet	0	58	3.63	0.07	-0.021	0.006
	White Sucker	skin-on fillet	0	44	3.13	0.08	-0.036	0.006
Green Bay Zone 2 (2A and 2B)	Alewife	whole body	0	44	3.48	0.05	-0.018	0.009
	Carp	skin-on fillet	0	28	3.89	0.08	-0.023	0.015
		whole body	1983	57	3.88	0.05	-0.073	0.010
	Gizzard Shad	whole body	0	32	3.24	0.05	0.025	0.010
	Yellow Perch	skin-on fillet	0	19	2.65	0.44	-0.049	0.014

Notes:

MSE - Mean square error.

* An estimate of the residual variance.

** An estimate of residual standard deviation.

Table A-6 Model Parameters and Other Statistics for the Best-fitting Model

Reach	Species	Sample Type	Year of Breakpoint	*p*-value for Final Slope				*p*-value for Early Slope Difference		
				p-value	Percent per Year	Pre-break Slope Minus Final Slope	Standard Error	*p*-value	Coefficient of Log(% lipid)	Standard Error
Little Lake Butte des Morts	Carp	skin-on fillet	1979	0.0177	-6.1	-0.228	0.085	0.0102	0.87	0.15
		whole body	1987	0.9172	0.7	-0.165	0.059	0.0084	0.86	0.33
	Northern Pike	skin-on fillet	0	0.0003	-11.8				0.45	0.30
	Walleye	skin-on fillet	1990	0.5576	3.4	-0.095	0.037	0.0140	0.50	0.15
		whole body	1987	0.0874	21.5	-0.261	0.080	0.0069	0.99	0.36
	Yellow Perch	skin-on fillet	1981	0.8025	0.7	-0.247	0.077	0.0034	0.49	0.21
Appleton to Little Rapids	Walleye	skin-on fillet	0	0.0028	-10.0				1.08	0.16
De Pere to Green Bay	Carp	whole body	1995	0.0277	21.8	-0.141	0.044	0.0022	0.79	0.11
	Gizzard Shad	whole body	0	0.0002	-5.1				0.51	0.09
	Northern Pike	skin-on fillet	0	0.0000	-10.0				0.72	0.17
	Walleye	skin-on fillet	0	0.0000	-7.2				0.85	0.07
		whole body	0	0.0000	-8.1				0.44	0.12
	White Bass	skin-on fillet	0	0.0020	-4.7				0.82	0.11
	White Sucker	skin-on fillet	0	0.0000	-7.9				0.43	0.15
Green Bay Zone 2 (2A and 2B)	Alewife	whole body	0	0.0497	-4.0				0.91	0.14
	Carp	skin-on fillet	0	0.1557	-5.1				0.76	0.15
		whole body	1983	0.0000	-15.5	0.266	0.059	0.0000	0.90	0.10
	Gizzard Shad	whole body	0	0.0144	5.9				-0.13	0.12
	Yellow Perch	skin-on fillet	0	0.0038	-10.7				1.09	0.47

Notes:

MSE - Mean square error.

* An estimate of the residual variance.

** An estimate of residual standard deviation.

Table A-6 Model Parameters and Other Statistics for the Best-fitting Model

Reach	Species	Sample Type	Year of Breakpoint	*p*-value for Log(% lipid)	Month of Seasonal Peak	Amplitude of Seasonal Peak	*p*-value for Seasonal Effect	Mean Square Error*	Square Root of MSE**
Little Lake Butte des Morts	Carp	skin-on fillet	1979	0.0000	12.9	0.39	0.0078	0.128	0.357
		whole body	1987	0.0131	7.0	0.83	0.0025	0.116	0.340
	Northern Pike	skin-on fillet	0	0.1554	1.3	0.67	0.1594	0.103	0.322
	Walleye	skin-on fillet	1990	0.0011	11.6	0.20	0.0273	0.086	0.293
		whole body	1987	0.0185	11.6	0.46	0.0040	0.141	0.376
	Yellow Perch	skin-on fillet	1981	0.0236	7.0	0.22	0.0007	0.072	0.268
Appleton to Little Rapids	Walleye	skin-on fillet	0	0.0000	8.1	0.43	0.0010	0.046	0.215
De Pere to Green Bay	Carp	whole body	1995	0.0000	6.7	0.06	0.0004	0.100	0.317
	Gizzard Shad	whole body	0	0.0001	8.6	0.58	0.0000	0.006	0.079
	Northern Pike	skin-on fillet	0	0.0001	10.1	0.17	0.3531	0.041	0.202
	Walleye	skin-on fillet	0	0.0000	9.5	0.02	0.7566	0.041	0.201
		whole body	0	0.0007	7.0	0.12	0.2038	0.047	0.218
	White Bass	skin-on fillet	0	0.0000	6.7	0.33	0.1043	0.029	0.170
	White Sucker	skin-on fillet	0	0.0071	6.9	0.08	0.5528	0.054	0.231
Green Bay Zone 2 (2A and 2B)	Alewife	whole body	0	0.0000	6.1	0.17	0.0335	0.029	0.171
	Carp	skin-on fillet	0	0.0000	3.9	0.24	0.0288	0.049	0.222
		whole body	1983	0.0000	6.9	0.24	0.0000	0.035	0.187
	Gizzard Shad	whole body	0	0.2811	2.6	0.34	0.0300	0.012	0.108
	Yellow Perch	skin-on fillet	0	0.0353	4.7	0.45	0.5489	0.032	0.178

Notes:

MSE - Mean square error.

* An estimate of the residual variance.

** An estimate of residual standard deviation.

Table A-7 Final Slope and Percent Change per Year for Best-fitting Model, and Sensitivity Analysis

Reach	Species	Sample Type	Sample Size	Year of Breakpoint—Best Model			Year of Breakpoint—Earliest			Year of Breakpoint—Latest			Year of Breakpoint—1985		
				Year	Percent Change per Year	*p*-value (for % = 0)	Year	Percent Change per Year	*p*-value (for % = 0)	Year	Percent Change per Year	*p*-value (for % = 0)	Year	Percent Change per Year	*p*-value*
Little Lake Butte des Morts	Carp	skin-on fillet	55	1979	-6.15	0.0177	1979	-6.15	0.0177	1985	-1.56	0.7419	1985	-1.56	0.7419
		whole body	40	1987	0.71	0.9172	1985	-4.04	0.5264	1990	-0.25	0.9765	1985	-4.04	0.5264
	Northern Pike	skin-on fillet	19	0	-11.83	0.0003									
	Walleye	skin-on fillet	63	1990	3.44	0.5576	1979	-8.37	0.0000	1994	8.82	0.4482	1985	-5.83	0.0379
		whole body	18	1987	21.47	0.0874	1984	15.10	0.2024	1990	21.11	0.1324	1985	18.49	0.1285
	Yellow Perch	skin-on fillet	34	1981	0.73	0.8025	1979	0.27	0.9252	1996	333.61	0.0122	1985	4.33	0.3297
	Combined				**-4.86**	**0.0055**									
Appleton to Little Rapids	Walleye	skin-on fillet	30	0	-9.97	0.0028									
De Pere to Green Bay	Carp	whole body	90	1995	21.76	0.0277	1990	-0.69	0.8232	1996	29.80	0.0191	1985	-5.63	0.0238
	Gizzard Shad	whole body	19	0	-5.07	0.0002									
	Northern Pike	skin-on fillet	40	0	-9.95	0.0000									
	Walleye	skin-on fillet	120	0	-7.19	0.0000									
		whole body	58	0	-8.11	0.0000									
	White Bass	skin-on fillet	58	0	-4.72	0.0020									
	White Sucker	skin-on fillet	44	0	-7.90	0.0000									
	Combined				**-6.89**	**0.0000**								**-6.92**	**0.0000**
Green Bay Zone 2 (2A and 2B)	Alewife	whole body	44	0	-3.96	0.0497									
	Carp	skin-on fillet	28	0	-5.06	0.1557									
		whole body	57	1983	-15.54	0.0000	1983	-15.54	0.0000	1984	-16.15	0.0000	1985	-15.90	0.0000
	Gizzard Shad	whole body	32	0	5.91	0.0144									
	Yellow Perch	skin-on fillet	19	0	-10.75	0.0038									
	Combined				**-5.11**	**0.0000**								**-5.99**	**0**

Note:

* For testing whether percent change per year is different from zero.

Table A-8 Computing Whole Body PCB Concentrations*

Species	Convert	Modify PCB Target by this Factor
Carp	0.59	1.69
Northern Pike	0.1	10.00
Walleye	0.1	10.00
White Bass	0.43	2.33
White Sucker	0.59	1.69
Yellow Perch	0.04	25.00

Note:

* Based on fillet-to-whole body conversion factors. These conversion factors were used to multiply specified skin-on fillet PCB concentrations to yield the corresponding expected concentration in a whole-body sample—used in analyses of time to reach specified PCB concentrations.